Validation of p75ECD and Edaravone as neuroprotective drug candidates for neurodegenerative diseases

A Thesis Submitted in Total Fulfilment of the Requirements for the Degree of

DOCTOR OF PHILOSOPHY

IN

PHARMACOLOGICAL SCIENCES

By

SALLY KELLINY

Master of Pharmacological Sciences

Bachelor of Pharmaceutical Sciences



University of South Australia

Clinical and Health Sciences, School of Pharmacy and Medical Sciences, Neuroregeneration Laboratory

Adelaide, South Australia

May 2021

To my best friend and beloved husband Shaheer, who has always been there for me and supported me at my highest and lowest points in life, and to my beautiful strong children Nadine and Jonathan, who endured my deficiencies and who always remind me that life is beautiful. To my devoted parents, Hamdy and Nahed, who constantly encouraged me and helped me to achieve my goals, and to my siblings Joseph and Maria who always supported me, and to my lovely Uncle who passed away after suffering Alzheimer's disease.

ACKNOWLEDGEMENTS

This work would not have been possible without the financial support provided by the Commonwealth through the Australian Government Research Training Program (RTP) Scholarship, support given by the School of Pharmacy and Medical Sciences during my PhD at the University of South Australia and the support of the Cultural Affairs, Egyptian Ministry of Higher Education.

I would like to express my sincere gratitude, appreciation and very special thanks to Prof. Xin-Fu Zhou, for his constructive supervision, scientific guidance, encouragement and for exerting much of his time and effort for the fine adjustment, monitoring, and guiding my efforts in all steps in this thesis with his creative valuable advice and instructions. Without his generous advice and encouragement, this work would not have come to light. Really, I greatly respect his scientific thinking and creative mentality. His generosity, kindness and humanity are unique and everlasting.

I am deeply grateful to my co-supervisor Associate Prof. Larisa Bobrovskaya for her scientific guidance, encouragement, and moral support. She kindly exerted much of her time and effort to teach me and help me improve my laboratory techniques, interpret results logically, and troubleshoot experimental errors. I appreciate her time and dedication in drafting my thesis chapters and her tremendous help to improve my writing skills and reasoning. Without her supervision, I would not have been able to complete my work.

I would like to offer my special thanks to Prof. Yan-Jiang Wang, my co-supervisor in China for helping me draft my thesis chapter of one of the proposed projects. Although I was unlucky to get the opportunity to work in his laboratory due to family commitments, I hope I can work in his lab one day and meet his wonderful team of young and expert scientists, and his team of medical doctors and professionals.

I would like to express my sincere gratitude to Prof. Richard Upton for scientific guiding and assistance to draft the second chapter of my thesis that was published as two research papers. I appreciate his time, effort and dedication for teaching me pharmacokinetic modelling methods of drug development, which I was not very specialized in.

I would also like to thank every kind hand in the Core Animal Facility that gave me the chance to complete this study. I would like to thank Jess Parken, Kelly Wicks and Alysha Servin who have helped me in breeding and generating the animals for my projects. I am really grateful to

Becky Nitschke and Claire Whelan for teaching me many techniques and for technical assistance in my experiments. Special thanks to Dr. Lewis Vaughan, the Animal Welfare Officer for technical guidance and assistance. I also thank Ms. Ruth Brogan for her assistance in writing animal ethics and annual reports.

I am deeply grateful to Mr. Andrew Beck for his guidance and great help in immunohistochemistry technique and microscopy. His advice on tissue processing, staining and acquiring images helped me a lot to improve my figures. He has also been a kind person and a friend to me during my PhD. I would also like to thank Mrs. Rupal Pradhan, Mrs. Carolyn Streckbein and Mrs. Karen Teague for their technical assistance in the laboratory.

My special thanks are extended to the administrative staff of the School of Pharmacy and Medical Science, Mrs. Evonne MacMaster, Mrs. Hattie Li and Dr. Kirsty Turner for their consistent thought regarding my PhD and progress.

I would like to thank the members of the Neuroregeneration Laboratory for their kind assistance. My colleagues have been so wonderful, kind and demonstrated diverse skills and capabilities. Thank you!

Finally, I cannot find the words to express my great thankfulness to my family, my husband and my kids who gave me plenty of love, support and kindness and have been always with me through this journey. God bless them all and convey upon them peace and happiness.

Lastly, all praise is to God for granting me the power and will, relieving me during hard times, and helping me throughout my whole life.



Sally Kelliny

TABLE OF CONTENTS

Title page ..... **i**

Dedication ..... **iii**

Acknowledgements ..... **v**

List of Figures ..... **xv**

List of Tables ..... **xx**

List of Schemes and Diagrams ..... **xxi**

Abbreviations ..... **xxii**

Thesis Summary ..... **xxvii**

Declaration ..... **xxix**

Chapter 1: Introduction **1**

1. Alzheimer's Disease (AD) and Frontotemporal Dementia (FTD): Epidemiology and Risk Factors **2**

2. Neuropathological Hallmarks **3**

2.1. Neuropathological hallmarks of AD and mechanisms of the disease 3

2.2. Genetics and Neuropathology of FTD 15

3. AD hypotheses **18**

3.1. Amyloid cascade hypothesis 18

3.2. Tau hypothesis 20

3.3. Neurotrophin Hypothesis 22

3.4. Mitochondrial dysfunction and Oxidative stress hypothesis 31

3.5. The inflammation hypothesis 33

4. Current and Novel Therapeutic Strategies **34**

4.1. Currently approved therapies for AD and FTD 34

4.2. Novel therapeutic strategies 34

4.2.1. Therapies targeting Aβ production, accumulation, and clearance 34

4.2.2. AD therapies based on neurotrophins 36

4.2.3. Therapies based on reducing Tau phosphorylation and misfolding in AD and FTD-Tau 39

4.2.4. Oxidative stress-based therapies, anti-inflammatory and neuroprotective approaches 40

5. Animal models of Alzheimer's disease and Frontotemporal dementia with Tau pathology **43**

6. Hypotheses and Aims 48

Chapter 2: Pharmacokinetics of p75ECD-Fc 74

Preclinical Study of the Pharmacokinetics of p75ECD-Fc, a Novel Human Recombinant Protein for Treatment of Alzheimer's Disease, in Sprague Dawley Rats 77

1. Introduction 77

2. Materials and Methods 78

2.1. Materials 78

2.2. Animal Procedures and Tissue Sampling 78

2.3. Serum, Tissues, CSF and Urine Samples Collection 78

2.4. Frozen and Fixed Tissue Preparation 79

2.5. In-vitro Stability of p75ECD-Fc in Human Plasma 79

2.6. Development of Standard curves for p75ECD-Fc in Sandwich ELISA 79

2.7. Sera, Urine, CSF and Tissue Samples Analysis 79

2.8. Immunofluorescent Analysis of p75ECD-Fc in Tissues 79

2.9. Non-Compartmental Pharmacokinetic Analysis (NCA) 80

2.10. Statistical Analysis 80

3. Results **80**

3.1. Non-Compartmental Pharmacokinetic Analysis 80

3.2. Distribution of p75ECD-Fc in Different Tissues 81

3.3. Immunofluorescence Staining of p75ECD-Fc in Tissues 81

3.4. In-vitro Stability of p75ECD-Fc in Human Plasma 81

4. Discussion **83**

Pharmacokinetic Modelling of Human Recombinant Protein, p75ECD-Fc: A Novel Therapeutic Approach for Treatment of Alzheimer's Disease, in Serum and Tissue of Sprague Dawley Rats **88**

1. Introduction 89

2. Methods 90

2.1. Data Set and General Modeling Methods 90

2.2. Compartmental Model Development 90

2.2.1. Intravenous Model 90

2.2.2. Intravenous and Subcutaneous Model 90

2.2.3. Model Refinements 91

2.3. Semi-Physiological Tissue Models 91

2.4. Model Selection 91

2.5. Model Evaluation 91
3. Results **91**
3.1. Description of the Observed Data 91
3.2. Compartment Models 92
3.2.1. Intravenous Model 92
3.2.2. Intravenous and subcutaneous Model 92
3.2.3. Model Refinements 92
3.2.4. Model Evaluation 93
3.3. Semi-Physiological Tissue Models 94
4. Discussion 96
5. Conclusion 99
Supplementary Material 102

Chapter 3: The Effect of Intravenous Injection of The Extracellular Domain of p75^{NTR} On the Cognitive Deficits and Amyloid Plaque Load In APP/PS1 Alzheimer's Disease Transgenic Mice 110
1. Introduction **111**
2. Review of Literature **113**
3. Materials and methods **119**
3.1. Materials 119
3.2. Animals 119
3.3. Treatment protocol 120
3.4. Behavioral Tests 120
3.4.1. Morris Water Maze 120
3.4.2. Open field test 121
3.4.3. Novel Object Recognition test (NORT) 121
3.4.4. Y maze novel arm and Y maze spontaneous alternation tests 122
3.5. Immunohistochemical (IHC) and TUNEL staining 122
3.6. Congo Red stain 123
3.7. Golgi-cox Stain 124
3.8. Western Blotting 124
3.9. Analysis of antibodies against p75ECD using ELISA 125
3.10. Statistical analysis 125

4. Results **126**
4.1. Effect of p75ECD-Fc on the cognitive deficits in APP/PS1 AD mice 126
4.1.1. Morris Water Maze (MWM) 126
4.1.2. Open field test 128
4.1.3. Y maze and NORT 128
4.2. Effect of p75ECD-Fc on Amyloid beta plaque load in APP/PS1 mice 130
4.3. Effect of p75ECD-Fc on neuroinflammation in APP/PS1 mice 134
4.4. Effect of p75ECD-Fc treatment on the levels of synaptic proteins and synaptic plasticity in APP/PS1 mice 136
4.5. Effect of p75ECD-Fc treatment on apoptosis and neuron viability in APP/PS1 mice 138
4.6. Effect of p75ECD-Fc on Tau phosphorylation and kinases involved in Aβ and Tau accumulation 141
4.7. p75ECD-Fc did not generate significant increase in the endogenous antibodies 143
5. Discussion **144**
6. Conclusion **147**

Chapter 4: A Novel Oral Edaravone formulation partially alleviates Tau pathology and motor deficits in an animal model of Frontotemporal Dementia **157**
1. Introduction **160**
2. Materials and methods **161**
2.1. Materials 161
2.2. Animals 161
2.3. Treatment Protocol 161
2.4. Behavioral Tests 162
2.4.1. Morris Water Maze (MWM) 162
2.4.2. Open field test and elevated plus maze test 162
2.4.3. Novel Object Recognition Test (NORT) 162
2.4.4. Y maze spontaneous alternation and Y maze novel arm 162
2.4.5. Hind Limb Clasping Test 163
2.5. Immunohistochemical analysis (IHC) 163
2.6. Western Blotting analysis 163
2.7. Statistical analysis 164

3. Results **164**
3.1. Edaravone improved spatial learning memory of P301L mice in MWM test 164
3.2. Edaravone altered the exploratory behavior of P301L mice in open field and elevated plus maze tests 164
3.3. Edaravone did not affect the working memory in Y maze novel arm test and spontaneous alternation test 165
3.4. EDR improved the recognition memory in P301L mice 165
3.5. EDR attenuated motor deficits in P301L mice 166
3.6. Effect of EDR on phosphorylated Tau protein levels in P301L mice 166
3.7. EDR treatment altered GSK-mediated Tau phosphorylation 166
3.8. EDR treatment reduced neuroinflammation in the brains of P301L mice 167
3.9. EDR treatment attenuates loss of synaptic plasticity and protected neurons in the brain of P301L mice 167
3.10. EDR alleviates oxidative stress in P301L mice 167
4. Discussion **167**
5. Conclusion 170
6. Supplementary Material **186**

Chapter 5: A New Approach to Model Sporadic Alzheimer's Disease by Intracerebroventricular Streptozotocin Injection in APP/PS1 Mice 207
1. Introduction **210**
2. Materials and Methods 211
2.1. Chemicals and Antibodies 211
2.2. Animals 211
2.3. The Experimental Protocol 211
2.4. Behavioral Tests 213
2.4.1. Morris Water Maze 213
2.4.2. Open Field Test 213
2.4.3. Novel Object Recognition Test 213
2.4.4. Y Maze Spontaneous Alternation and Y Maze Novel Arm 214
2.5. Immunohistochemical and TUNEL Staining 214
2.6. Congo Red Staining 214
2.7. Golgi Staining 214
2.8. Western Blot Analysis 214

2.9. Statistical Analysis 215
3. Results **215**
3.1. Effect of STZ on Body Weight and Mortality 215
3.2. STZ Exacerbates the Cognitive Decline in APP/PS1 Mice 215
3.2.1. Spatial Reference Memory (MWM) 215
3.2.2. Anxiety, Locomotor and Exploratory Behavior (Open Field Test) 215
3.2.3. Working Memory (Y-Maze Novel Arm and Spontaneous Alternation) 215
3.2.4. Recognition Memory (NORT) 215
3.3. STZ Increases Aβ Plaques in APP/PS1 Mice 216
3.4. STZ Increases Tau Phosphorylation in AD and WT Mice 218
3.5. STZ Promotes Neuroinflammation in APP/PS1 and WT Mice 219
3.6. STZ Induces Oxidative Stress and Triggers Apoptotic Cell Death in APP/PS1 and WT Mice 219
3.7. STZ Alters Synaptic Proteins and Reduces Spine Density and Length in Hippocampus in AD and WT Mice 220
3.8. STZ Dysregulates Pathways Involved in Brain Insulin Signaling in APP/PS1 and WT Mice 222
4. Discussion **222**
5. Conclusion **226**

Chapter 6: General Discussion and Future Directions 231

1. Discussion **232**
2. Conclusions **236**
3. Future directions **236**
Appendices **244**
Publications arising from this thesis **244**
Other publications **244**
Conference Abstracts **244**
Awards and Scholarships **244**

LIST OF FIGURES

Chapter 1

Figure 1 The proteolytic cleavage of the amyloid precursor protein (APP) by the non-amyloidogenic (left) and amyloidogenic (right) processing pathways 6

Figure 2 Tau-mediated neurodegeneration 9

Figure 3 Tau isoforms and MAPT mutations in frontotemporal dementia and parkinsonism linked to chromosome 17 (FTDP-17) 17

Figure 4 The sequence of major pathogenic events leading to AD proposed by the amyloid cascade hypothesis 21

Figure 5 Models of Trk and p75 receptor activation 25

Figure 6 Neurotrophin receptor signalling 26

Figure 7 Schematic representation of the various interactors of $p75^{NTR}$ 30

Figure 8 The interplay between oxidative stress and Alzheimer's Disease (AD) 32

Figure 9 Chemical structure of Edaravone 41

Figure 10 Mechanism of STZ-induced neurotoxicity and AD pathology 47

Chapter 2

Preclinical Study of the Pharmacokinetics of p75ECD-Fc, a Novel Human Recombinant Protein for Treatment of Alzheimer's Disease, in Sprague Dawley Rats.

Figure 1 Standard curve of p75ECD-Fc is generated using sandwich ELISA technique . 79

Figure 2 (A) and (B) Concentration-time curves of p75ECD-Fc after single IV (black squares) and SC (red circles) injection of 3mg/kg in SD rats 80

Figure 3 Double-label immunofluorescence showing the in-vivo colocalization of p75ECD-Fc (red) in CD11b-positive cells of the liver, lung, Iba-1 positive cells in the skin and S100-positive cells in the brain (green) 83

Figure 4 Drug concentration-time curve of plasma incubation of p75ECDFc 84

Figure 5 Representative diagram illustrating the proposed mechanism of action of p75ECD-Fc in AD 84

Pharmacokinetic Modelling of Human Recombinant Protein, p75ECD-Fc: A Novel Therapeutic Approach for Treatment of Alzheimer's Disease, in Serum and Tissue of Sprague Dawley Rats

Figure 1 Representative structure of p75ECD-Fc 90

Figure 2 a, b Observed serum concentration-time curve and the logarithmic scale of p75ECD-Fc in 12 male and female Sprague Dawley rats after i.v. (dashed line) and s.c. (solid line). c Graphical plot showing the detection of ADAs in the 42-day time point serum of the marked rats 93

Figure 3 Structural illustration of a population pharmacokinetic model of serum p75ECD-Fc concentration profile 95

Figure 4 Key diagnostic plots for p75ECD-Fc given by two routes (i.v., s.c.) comparing observed concentrations with individual- and population-predicted concentrations 95

Figure 5 Goodness-of-fit plots for p75ECD-Fc given by two routes (i.v. and s.c.) at a single dose of 3 mg/kg in 12 SD rats 96

Figure 6 Visual predictive check (VPC) 97

Figure 7 Tissue plasma partition coefficient (R) of p75ECD-Fc after single i.v. and s.c. injection of 3 mg/kg in SD rats 97

Figure 8 Scheme for a single tissue model to characterize the biodistribution of p75ECD-Fc in various tissues 98

Figure 9 p75ECD-Fc concentration–time profiles in multiple tissues 99

Supplementary Figure 1: Key Diagnostic plots for weighted residual of Base model over the range of predicted concentrations with the inclusion of zero order loss parameter from the central compartment 107

Supplementary Figure 2: Key Diagnostic plots for weighted residual of Base model over the range of predicted concentrations with the inclusion of first order loss parameter from the peripheral compartment 108

Chapter 3

Figure 1 Neurotrophins, their receptors and signaling pathways 115

Figure 2 Illustration of functions of $p75^{NTR}$ in Aβ metabolism 116

Figure 3 Acquisition and learning in the Morris water maze 127

Figure 4 Open Field Test 129

Figure 5 Novel Object Recognition and Y maze tasks 130

Figure 6 Effect of p75ECD-Fc treatment on the amyloid plaque pathology in APP/PS1 mice 133
Figure 7 Effect of p75ECD-Fc treatment on neuroinflammation in APP/PS1 mice 135
Figure 8 Effect of p75ECD-Fc on synaptic dysfunction in APP/PS1 mice 137
Figure 9 Effect of p75ECD-Fc on neuronal apoptosis in APP/PS1 mice 139
Figure 10 Effect of p75ECD-Fc treatment on apoptosis 140
Figure 11 Effect of p75ECD-Fc treatment on Tau phosphorylation and expression levels of kinases involved in Aβ and phosphorylated Tau accumulation 142
Figure 12 Comparison of serum antibodies to p75ECD-Fc among the WT, Saline treated APP/PS1 and p75ECD-Fc treated mice 143

Chapter 4

Figure 1 Acquisition learning and Probe trial in MWM test 177
Figure 2 Open field and Elevated plus maze task 178
Figure 3 Y maze spontaneous alternation and Y maze novel arm tasks 180
Figure 4 Effect of EDR on the recognition memory and motor function of P301L mice 181
Figure 5 Immunostaining of coronal brain section from vehicle (Soluplus) and EDR-treated P301L mice (age = 14 months old) with anti-pS396 and anti-GFAP 182
Figure 6 Western blot and their quantitative analysis of total brain homogenates of P301L mice at 14 months old 183
Figure 7 Immunostaining of coronal brain section from vehicle (Soluplus) and EDR-treated P301L mice (age = 25 months old) with anti-pS396, anti-GFAP and anti-CD45 184
Figure 8 Western blot and their quantitative analysis of total brain homogenates of P301L mice at 25 months old 185
Supp. Figure 1 Morris Water Maze Test 187
Suppl. Figure 2 Effect of EDR on neuronal viability against oxidative neurotoxicity in P301L mice at 25 months age 188
Suppl. Figure 3 Western blot of total brain homogenates of P301L mice at 14 months old probed with antibody against pS396 Tau and AT8 189
Suppl. Figure 4 Western blot of total brain homogenates of P301L mice at 14 months old probed with antibody against total human Tau, mouse Tau 5 and Synaptophysin 190
Suppl. Figure 5 The Whole Western blot of total brain homogenates of WT and P301L mice at 14 months old probed with antibody against GFAP and Iba-1 191

Suppl. Figure 6 The whole Western blot of total brain homogenates of WT and P301L mice at 14 months old probed with antibody against GSK-3β and its phosphorylated form pS9 192
Suppl. Figure 7 The whole Western blot of total brain homogenates of WT and P301L mice at 14 months old probed with antibody against PSD-95, NeuN and VAMP-2 193
Suppl. Figure 8 Western blot of total brain homogenates of P301L mice at 14 months old probed with antibody against 4-HNE 194
Suppl. Figure 9 Western blot of total brain homogenates of P301L mice at 25 months old probed with antibody against total human Tau, mouse Tau 5, pS396 and AT8 phosphorylated Tau 195
Suppl. Figure 10 The whole Western blot of total brain homogenates of WT and P301L mice at 25 months old probed with antibody against GFAP and Iba-1 196
Suppl. Figure 11 The whole Western blot of total brain homogenates of WT and P301L mice at 25 months old probed with antibody against GSK-3β and its phosphorylated form pS9 197
Suppl. Figure 12 Western blot of total brain homogenates of WT and P301L mice at 25 months old probed with antibody against PSD-95, VAMP-2 and Synaptophysin 198
Suppl. Figure 13 Western blot of total brain homogenates of P301L mice at 25 months old probed with antibody against 4-HNE and 3-NT 199
Suppl. Figure 14 Western blot of total brain homogenates of P301L mice at 14 and 25 months old probed with antibody against Total Human Tau7 and Mouse tau 5 200
Suppl. Figure 15 Western blot of total brain homogenates of P301L mice at 14 and 25 months old probed with antibody against phosphorylated Tau pS396 201
Suppl. Figure 16 Western blot of total brain homogenates of P301L mice at 14 and 25 months old probed with antibody against phosphorylated Tau AT8 202
Suppl. Figure 17 Western blot of total brain homogenates of P301L mice at 14 and 25 months old probed with antibody against PSD-95 203
Suppl. Figure 18 Western blot of total brain homogenates of P301L mice at 14 and 25 months old probed with antibody against Synaptophysin 204
Suppl. Figure 19 Western blot of total brain homogenates of P301L mice at 14 and 25 months old probed with antibody against GSK-3β and its phosphorylated form pS9 205

Chapter 5

Figure 1 Representative diagram of the study design 213
Figure 2 Morris water maze 216
Figure 3 Open field test, Y maze task, and novel object recognition test 217
Figure 4 STZ exacerbates the amyloid pathology in APP/PS1 mice 218
Figure 5 STZ ICV induces tau hyperphosphorylation in the brains of WT and APP/PS1mice 219
Figure 6 STZ ICV promotes severe neuroinflammation in WT and APP/PS1 mice 220
Figure 7 STZ ICV induces neuronal apoptosis in WT and APP/PS1 mice 221
Figure 8 STZ ICV induces oxidative stress and reduces synaptic plasticity in WT and APP/PS1 mice 223
Figure 9 Effects of ICV STZ on the expression levels of kinases involved in insulin signaling pathways and JNK phosphorylation in the WT and APP/PS1 mouse brain 5 weeks after injection 224

LIST OF TABLES

Chapter 2

Preclinical Study of the Pharmacokinetics of p75ECD-Fc, a Novel Human Recombinant Protein for Treatment of Alzheimer's Disease, in Sprague Dawley Rats……

Table 1 Noncompartmental pharmacokinetics of p75ECD-Fc after single IV and SC injection of 3mg/kg to SD rats 81

Table 2 Tissue, urine and CSF concentration of p75ECD-Fc after single IV and SC injection of 3mg/kg in SD rats 82

Table 3 Concentrations of p75ECD-Fc in human plasma at different incubation times .. 82

Pharmacokinetic Modelling of Human Recombinant Protein, p75ECD-Fc: A Novel Therapeutic Approach for Treatment of Alzheimer's Disease, in Serum and Tissue of Sprague Dawley Rats

Table 1 Final estimates of population pharmacokinetic parameters obtained by fitting the i.v. data to a 2-compartment model with linear elimination kinetics in the terminal phase 94

Table 2 Population parameters for the 2-compartment base model and final model 94

Table 3 Estimated values for p75ECD-Fc tissue-plasma partition coefficient (R) and the apparent ratio of tissue-plasma flow to tissue volume (QV) 98

Chapter 3

Supplementary Table 1 Primary antibodies used..... 149

Chapter 5

Table 1 Primary antibodies used 212

LIST OF SCHEMES AND DIAGRAMS

Chapter 2

Scheme 1 Schematic illustration of different steps of the study starting with IV and SC injection of p75ECD-Fc into Sprague Dawley rats followed by samples collection, histochemical and pharmacokinetics analysis 78

Chapter 4

Scheme 1 Schematic illustration of the study design showing animal groups, behavioral tests performed and different biochemical and immunohistochemical analysis 176

Chapter 6

Diagram 1: A summary of the findings obtained throughout different chapters 240

LIST OF ABBREVIATIONS

AAV	Adeno-associated viruses
Aβ	Amyloid beta
ABC	Avidin biotin complex
ACh	Acetylcholine
AD	Alzheimer's disease
ADAs	Antidrug antibodies
ADAM	A Disintegrin And Metalloprotease
AGEs	Advanced glycation end products
AICD	APP intracellular domain
Akt	Protein kinase B
ALP	Autophagy-lysosomal pathway
ALS	Amyotrophic lateral sclerosis
AMPA	α-amino-3-hydroxy-5-methyl-4-isoxazole propionic acid
ANOVA	Analysis of variance
ApoE4	Apolipoprotein-E4
APP	Amyloid precursor protein
APPfl	Amyloid precursor protein full length
ASOs	Antisense oligonucleotides
AUC	Area under the curve
AUMCinf	Area under the first moment curve
BACE	beta site amyloid precursor protein cleaving enzyme
Bax	Bcl-2-associated X protein
BBB	Blood brain barrier
BCA	Bicinchoninic acid assay
Bcl-2	B-cell lymphoma 2
BDNF	Brain derived neurotrophic factor
BFCN	Basal forebrain cholinergic neurons
Bim	Bcl-2 interacting mediator of cell death
BSA	Bovine Serum Albumin
CA	Capture antibody
CAA	Cerebral amyloid angiopathy
cAMP	Cyclic adenosine monophosphate
CBD	Corticobasal degeneration
CD11b and CD45	name of proteins expressed on surface of macrophages
CD33	a Protein Coding gene
Cdk	Cyclin-dependent kinase
CHO	Chinese Hamster Ovary
CI	Confidence interval
CL	Clearance
CLt	Total body clearance
Cmax	Peak plasma concentration
CNS	Central nervous system
CoQ10	Coenzyme Q10
COX	Cytochrome *c* oxidase
Cp	Plasma concentration
CSF	Cerebrospinal fluid

CTF	Carboxy terminal fragment
CTFα or C83	Carboxy terminal fragment alpha of Amyloid precursor protein
CTFβ or C99	Carboxy terminal fragment beta of Amyloid precursor protein
CWRES	Conditional weighted residuals
cy2 and cy3	Cyanine dyes
DAB	Diaminobenzidine
DAPI	4′,6-diamidino-2-phenylindole
DG	Dentate gyrus
DI	Discrimination index
DNPH	2,4-Dinitrophenyl hydrazine
DTT	Dithiothreitol
ECD	Extracellular domain
EDR	Edaravone
EDTA	Ethylenediaminetetraacetic acid
ELISA	Enzyme-linked immunosorbent assay
EOAD	Early onset Alzheimer's disease
ERK	Extracellular regulated kinase
F	Bioavailability
FAD	Familial Alzheimer's Disease
FOCE-I	First-order conditional estimation method with interaction
FPR	Formyl peptide receptors (a chemotactic receptor)
FTD	Frontotemporal dementia
FTLD	Frontotemporal lobar degeneration
FTDP-17	Frontotemporal dementia with parkinsonism linked to chromosome 17
GAPDH	Glyceraldehyde-3-phosphate dehydrogenase
GFAP	Glial fibrillary acidic protein
GGA proteins	Golgi-localized γ-ear containing ADP ribosylation factor-binding
GSK-3β	Glycogen synthase kinase 3 beta
GWAS	Genome-wide associated studies
H_2O_2	Hydrogen peroxide
HC	Hippocampus
HCl	Hydrochloric acid
HI	Hypoxic-ischemic
HK	Humanely killed
4-HNE	4-hydroxy nonenal
HPCs	High pathology controls
HRP	Horseradish peroxidase
HTRF	Homogeneous time-resolved fluorescence assay
Iba-1	Ionized calcium binding adaptor molecule 1 (a microglia/macrophage-specific calcium-binding protein)
ICV	Intracerebroventricular
IDE	Insulin-degrading enzyme
IGF	Insulin like growth factor
IgG	Immunoglobulin G
IL-1β	Interleukin-1β
IP	Intraperitoneal
IV or i.v.	Intravenous

IgG	Immunoglobulin G
IHC	Immunohistochemical
IPRED	Individual predicted
IRDye	Infrared dye
IRs	Insulin receptors
IRS	Insulin receptor substrate
IRAK-1	Interleukin-1 receptor associated kinase
JNK	c-Jun N-terminal kinase
ka	Absorption rate constant
kDa	Kilodalton
Kel (λz)	Elimination rate constant
LINGO-1	leucine-rich repeat and immunoglobulin domain-containing 1
LOAD	Late onset Alzheimer's disease
LTD	Long-term depression
LTP	Long-term potentiation
mAb	Monoclonal antibody
MAG	Myelin-associated glycoprotein
MAPK	Mitogen-activated protein kinase
MAPT	Microtubule associated protein tau
MCI	Mild cognitive impairment
MMP	Matrix metalloproteinase
MRT	Mean residence time
MWM	Morris Water Maze
nAChR	Nicotinic acetylcholine receptors
NaCl	Sodium Chloride
NADE	neurotrophin receptor-associated cell death executor
NaOH	Sodium Hydroxide
NC	Neocortex
NCA	Non-compartmental pharmacokinetic analysis
NEP	Neprilysin
NeuN	Neuronal nuclei antigen
NF-κB	Nuclear factor kappa B
NFTs	Neurofibrillary tangles
NGF	Nerve growth factor
NgR	Nogo receptor
NHS	Normal horse serum
NMDA	N-methyl-D-aspartate
NO	Nitric Oxide
NORT	Novel Object Recognition Test
NRAGE	neurotrophin receptor-interacting MAGE homolog
Nrf2/HO-1	Nuclear factor erythroid 2-related factor/ hemeoxygenase-1
NRIF	neurotrophin receptor interacting factor
NSAIDs	Non-steroidal anti-inflammatory drugs
NT-3, NT-4/5	Neurotrophins 3 and Neurotrophin 4/5
NT	Neuropil threads
3-NT	3-nitrotyrosine
OBS	Observed
OCT	Optimal cutting temperature compound

OFT	Open Field Test
OFV	Objective function value
OMgP	Oligodendrocyte myelin glycoprotein
OS	Oxidative stress
PAGE	Polyacrylamide gels
p75ECD	p75 extracellular domain
p75ECD-Fc	A human recombinant fusion protein of p75 extracellular domain and Fc of human IgG
p75FL	p75 neurotrophin receptor full length
$p75^{NTR}$	p75 neurotrophin receptor
p75ICD	p75 Intracellular domain
PBS	Phosphate-buffered saline
PBPK	Physiologically based pharmacokinetic
PDK1	Phosphoinositide-dependent protein kinase 1
PHF	Paired helical filaments
PI3K	Phosphatidylinositol-3-kinase
PiD	Pick's disease
PK	Pharmacokinetics
PKA	Protein kinase A
PLCγ	Phospholipase C gamma
PP	Protein phosphatase
PPARγ	Peroxisome proliferators activated receptor gamma
PRED	Predicted
PSD-95	Postsynaptic density-95 protein
PSEN	Presenilin
PSP	Progressive supranuclear palsy
PUMA	p53 upregulated-modulator of apoptosis
Q	Intercompartmental transit rates
QV	Apparent ratio of tissue-plasma flow to volume (describing the rate of equilibration of the tissue with the plasma
R	Partition coefficient between tissue and plasma
RAGE	Receptor for advanced glycation end products
RI	Recognition index
RIPA	Radioimmunoprecipitation assay
RIP2	Receptor-interacting protein 2
ROCK	Rho-associated protein kinase
RNS	Reactive nitrogen species
ROS	Reactive oxygen species
RT	Room Temperature
S-100	name of proteins expressed on surface of astrocytes
SAPK/JNK	Stress-activated protein kinase/c-Jun N-terminal kinase
sAPPα	Soluble ectodomain region cleaved by α-secretases
sAPPβ	Soluble ectodomain region of APP cleaved by BACE1
SAD	Sporadic Alzheimer's disease
SDS	Sodium Dodecyl Sulphate
S.D.	Standard deviation
S.E.	Standard error
siRNAs	small interfering RNAs

SNAP25	Synaptosomal-associated protein-25
SC-1	Schwann cell factor 1
SC or s.c.	Subcutaneous
STZ	Streptozotocin
t1/2	Elimination half-life
TACE	TNF-α-converting enzyme
TAFD	Time after dose
TAOKs	Thousand-and-One Amino Acid Kinases
TBS	Tris-buffered saline
TDP-43	TAR DNA-binding protein-43
TGN	Trans-golgi network
TMB	Tetramethylbenzidine
TNF-α	Tumor Necrosis Factor alpha
tPA	Tissue plasminogen activator
TRAF-6	Tumor necrosis factor receptor-associated factor-6
TREM2	Triggering Receptor Expressed On Myeloid Cells 2
Tris	(2-amino-2-hydroxymethylpropane-1,3-diol (systematic), tris(hydroxymethyl) aminomethane (manufacturer)
Trk	Tropomyosin kinase receptor
TUNEL	Terminal deoxynucleotidyl transferase mediated dUTP Nick End Labeling
UPS	Ubiquitin proteasome system
V	Volume of distribution
VAMP2	Vesicle-associated membrane protein-2
VPC	Visual predictive check
Vss	Volume of distribution at steady-state
WB	Western blot
WT	Wild type

Validation of p75ECD and Edaravone as neuroprotective drug candidates for neurodegenerative diseases

THESIS SUMMARY

Alzheimer's disease (AD) is a devastating form of dementia with the number of affected individuals rising sharply. The main hallmarks of the disease include amyloid beta (Aβ) plaque deposits and neurofibrillary tangles consisting of hyperphosphorylated Tau protein, besides other pathological features that contribute to the disease complexity. Current approved medications are symptomatic and, no disease modifying therapy is available to halt the disease progression. The causes of sporadic AD are multifactorial and mostly age-related and involve risk factors such as Diabetes, cardiovascular or cerebrovascular disorders. Therefore, development of multi-targeted therapeutic approach could hold promise for treatment of AD and other neurodegenerative disorders such as tauopathies.

Recent studies provided the evidence that neurotrophin imbalance during aging represents the initial trigger for AD. $p75^{NTR}$ death receptor is upregulated in AD, while the shedding of its extracellular binding domain (p75ECD) is switched off. $p75^{NTR}$ induces amyloidosis and mediates Aβ induced neurotoxicity, while its ECD exerts neuroprotection through scavenging Aβ and enhancing its clearance. Therefore, in chapter 2 and 3, we aimed to study the effect of intravenous administration of p75ECD-Fc, a human fusion recombinant protein of p75ECD and Fc part of human IgG on cognitive deficits and amyloid plaque load in AD mice. We also performed pharmacokinetic analysis and modelling in rats to study its stability, distribution and to understand its possible mechanism of action. Results indicated that p75ECD-Fc did improve the spatial and recognition memory in AD mice and reduced plaque load, besides, it improved synaptic plasticity, but no effect on Tau phosphorylation was found. We also found that the p75ECD-Fc is mainly localized in resident macrophages in peripheral organs specifically liver and kidney, while little is detected in the brain and CSF indicating a limited ability to cross the BBB. The results suggest that p75ECD-Fc may enhance peripheral Aβ clearance which would promote the protein efflux form the brain according to the "peripheral sink mechanism". We also assumed that p75ECD-Fc may also act centrally to antagonize the toxic effects of Aβ and proneurotrophins mediated by $p75^{NTR}$ through scavenging these ligands and enhancing their phagocytic clearance through its Fc tail.

Oxidative stress (OS) is main factor contributing to AD. OS can induce a vicious cycle of apoptosis that involves Aβ and Tau accumulation. Therefore, targeting oxidative stress could provide promising results. In chapter 4, we aimed to investigate the effect of Edaravone on P301L mice, an animal model of Frontotemporal dementia with parkinsonism (FTDP-17) that expresses Tau pathology in the brain. Edaravone is a potent antioxidant that is approved for treatment of acute ischemic stroke and Amyotrophic lateral sclerosis. It displays anti-inflammatory and neuroprotective effects. Results showed that Edaravone oral formulation improved cognitive and motor deficits and produced comparable effects on Tau pathology and neuroinflammation and alleviated oxidative stress in the brain of P301L mice.

In chapter 5, we aimed to produce an animal model that can recapitulate many features of sporadic AD. Transgenic animal models represent the genetic aspect of the disease (familial type) which only accounts for 1-5% of cases. The inconsistency between the pathology in animal models and that in humans may explain the failure of many drugs in clinical trials while proved to be effective in animal studies. Streptozotocin (STZ), when injected into the brain, can induce a number of sequential events that are very close to sporadic AD and could represent the insulin resistance brain state observed in aged and AD patients. Results showed that STZ brain injection induced severe cognitive deficits in young AD mice and robust Tau phosphorylation, inflammation, and oxidative stress, besides increase in Aβ plaque load and dysregulation of insulin signaling in the brain. These results indicated that this approach is successful and shows many pathological features of sporadic AD and thus could be a useful model to test novel therapeutic strategies.

Taken together, p75ECD-Fc and Edaravone are potential candidates for treatment of AD and tauopathies. STZ animal model is a successful approach to model sporadic AD and for successful clinical drug development.

DECLARATION

I declare that:

This thesis presents work carried out by myself and does not incorporate without acknowledgment any material previously submitted for a degree or diploma in any university; to the best of my knowledge, it does not contain any materials previously published or written by another person except where due reference is made in the text; and all substantive contributions by others to the work presented, including jointly authored publications, is clearly acknowledged.



Sally Kelliny

Signed: 30th April 2021

CHAPTER 1: INTRODUCTION

1. Alzheimer's Disease and Frontotemporal Dementia: Epidemiology and Risk Factors

Alzheimer's disease (AD) is a severe neurodegenerative disorder characterized by gradual and progressive deficits in more than one domain of cognition including learning and memory, attention, language, and deterioration of social skills [1]. It accounts for about 80% of dementia cases and is considered the 7th leading cause of death in the United States [2]. In 2018 in Australia, dementia including AD was the leading cause of death among females [3]. AD is classified, based on the age of onset, into two categories: late onset AD (LOAD) or sporadic that accounts for >95% of AD cases, and early onset or familial (EOAD) which accounts for 1-5% of AD cases [4]. Familial or EOAD is mostly caused by genetic mutation in three autosomal dominant genes which are amyloid-β precursor protein (*APP*), presenilin-1 (*PSEN1*) or presenilin-2 (*PSEN2*). *APP* is the gene coding for the sequence of amyloid beta (Aβ) whereas *PSEN1* and *PSEN2* are involved in APP processing and Aβ generation [5]. While sporadic AD that accounts for majority of cases is multifactorial. The exact causes of the disease are not yet recognized. Aging is considered the main risk factor, other non-genetic risk factors may include cardiovascular disease, diabetes, lifestyle, or cerebrovascular disease [4]. Apolipoprotein (apo) *E4*, referred to as allele ε4 (*APOEε4*) gene, which encodes ApoE4 lipid carrier (involved in Aβ binding and clearance) has been genetically linked to late onset AD [6]. Carriers of one or two alleles of *APOε4* have ~ 3.5-10 times increased risk of developing the disease, respectively [7,8].

Other common causes of dementia, in addition to AD, include Frontotemporal dementia (FTD) and Lewy body dementia [9]. FTD is a spectrum of clinical syndromes characterized by progressive decline in behaviour and personality (the behavioural variant) and/or speech/language (the language variant; primary progressive aphasia (PPA)) with relative

preservation of memory and with or without related features of motor neuron disease or parkinsonism [10]. It is associated with neurodegeneration of the frontal and anterior temporal lobes [11-13]. FTD is considered the second most common cause of dementia in the younger population after AD and 3rd among older population [12]. In FTD, 30-50% of cases are familial and have a strong family history of dementia, while the remaining cases are sporadic [14]. Familial cases are caused by mutations in Microtubule-associated protein Tau (MAPT) [15], Chromosome 9 open reading frame 72 [16], Progranulin [17], Valosin-containing protein [18] or Chromatin-modifying protein 2B [19]. 44 different mutations of Tau on chromosome 17 have been identified in number of families with frontotemporal dementia and parkinsonism (FTDP-17) [20]. The Progranulin gene mutation was identified in 2006 as the second FTD-related gene on chromosome 17 and is responsible for even a larger proportion of FTD. Much less common mutations associated with Valosin-containing protein gene and cause a rare familial syndrome of inclusion body myopathy with Paget disease of bone and FTD. Another rare mutation in the gene for Chromatin-modifying protein 2B is found in a large Danish FTD lineage. A recent discovery of the mutation in the Chromosome 9 open reading frame 72 has identified the most genetic cause of FTD/amyotrophic lateral sclerosis (ALS) combination found in several families. Head trauma and thyroid disease were identified as non-genetic risk factors of FTD and are associated with a 3.3-fold and a 2.5-fold higher risk, respectively [12,13].

2. Neuropathological Hallmarks of AD and FTD

2.1. Neuropathological hallmarks of AD and mechanisms of the disease

Alzheimer's disease is characterized by accumulation of cerebral plaques loaded with β-amyloid peptide (Aβ) and dystrophic neuritis distributed throughout the cortical layer, as well as intracellular neurofibrillary tangles composed of hyperphosphorylated tau protein in the medial temporal-lobe structures [21,22]. Extensive neuron loss, cerebral amyloid angiopathy

(CAA), inflammation, synaptic failure and oxidative damage are also core features of AD [23]. An early and massive loss of basal forebrain cholinergic neurons (BFCN) is also a key base for cognitive impairment in AD, which has inspired the concept of the old cholinergic hypothesis of AD [24].

Amyloid plaques. Amyloid beta (Aβ) peptides, consisting of 36 to 43 amino acids, are naturally derived from amyloid precursor protein (APP), a type I transmembrane protein, after sequential cleavage by beta-site amyloid precursor protein-cleaving enzyme 1 (BACE-1); β-secretase and γ-secretase which is a protein complex with presenilin 1 at its catalytic core [25]. The amyloidogenic pathway of APP is favoured in acidic compartments such as endosomes, where reinternalized APP is first cleaved by β-secretase to produce sAPPβ and 99-residue carboxy terminal fragment (APP-CT, C99), and that is further cleaved by γ-secretase to generate Aβ and the APP intracellular domain (AICD). APP, anchored to the plasma membrane, may undergo non-amyloidogenic cleavage by α-secretase within the Aβ region generating soluble sAPPα and C83, the latter of which is further processed by γ-secretase to yield P3 and AICD [26].

$A\beta_{40}$ monomers are more dominant than the toxic and more hydrophobic $A\beta_{42}$ species that shows higher tendency of aggregation [23]. The exact function of Aβ is still controversial, but several reports suggested that at physiological levels, Aβ may play a role in modulation of synaptic plasticity [27,28]. An imbalance between production and clearance of Aβ can drive its aggregation and this could be the initiating factor in AD. This theory is referred to as "amyloid cascade hypothesis" that could explain the genetic forms of AD [29] and the amyloid pathology in Down's syndrome [30]. Aβ spontaneously self-aggregates into soluble oligomers and other intermediate assemblies, that are synaptotoxic, which can also grow into fibrils and self-arranged into β-pleated sheets to form the dense-core plaques (primarily $A\beta_{42}$) and CAA (mainly $A\beta_{40}$) [22,23]. Severity of cognitive impairment in AD patients correlates with the

levels of the soluble oligomers in the brain, particularly $A\beta_{40}$, rather than the total plaque load [31]. Several lines of evidence indicated that increased levels of Aβ oligomers might initiate the synaptic damage and be responsible for neurodegeneration in AD [32-36]. Aβ is physiologically secreted from synapses, upon neuronal activation, in a process related to normal release of neurotransmitters [23]. In vitro studies showed that excessive Aβ release might dampen neuronal excitatory transmission [37], damage synapses, and interfere with activity-regulated cytoskeleton associated protein (Arc) distribution [32]. Therefore, synaptic function is the best indicator of the extent of cognitive impairment in AD patients and perfectly correlates with the levels of cerebral Aβ oligomers.

Steady-state levels of Aβ are regulated by proteases neprilysin and insulin-degrading enzyme (IDE). Neprilysin (NEP) is a membrane-anchored zinc endopeptidase that is capable of degrading Aβ monomers as well as oligomers [38], while Insulin-degrading enzyme, a thiol metalloendopeptidase, degrades small peptides such as insulin and Aβ monomers [39]. Animal studies showed that overexpression of these enzymes prevents plaque formation [40]. In contrast, deletion of IDE or reduction of neprilysin reduces Aβ degradation by more than 50% and drives its accumulation [41,42]. However, analysis of NEP and IDE levels and activity in post-mortem frontal cortex from sporadic AD patients at different ages showed that reduction of NEP and IDE is not a primary cause of Aβ accumulation, but these changes only occur in late stages of the disease secondary to neurodegeneration [43].

Cerebral amyloid angiopathy (CAA). CAA is caused by deposits of Aβ (mainly $A\beta_{40}$) in the arteries and cortical capillaries especially in the posterior parts of the brain that weaken the vessel wall and can lead to life-threatening lobar haemorrhages [22].

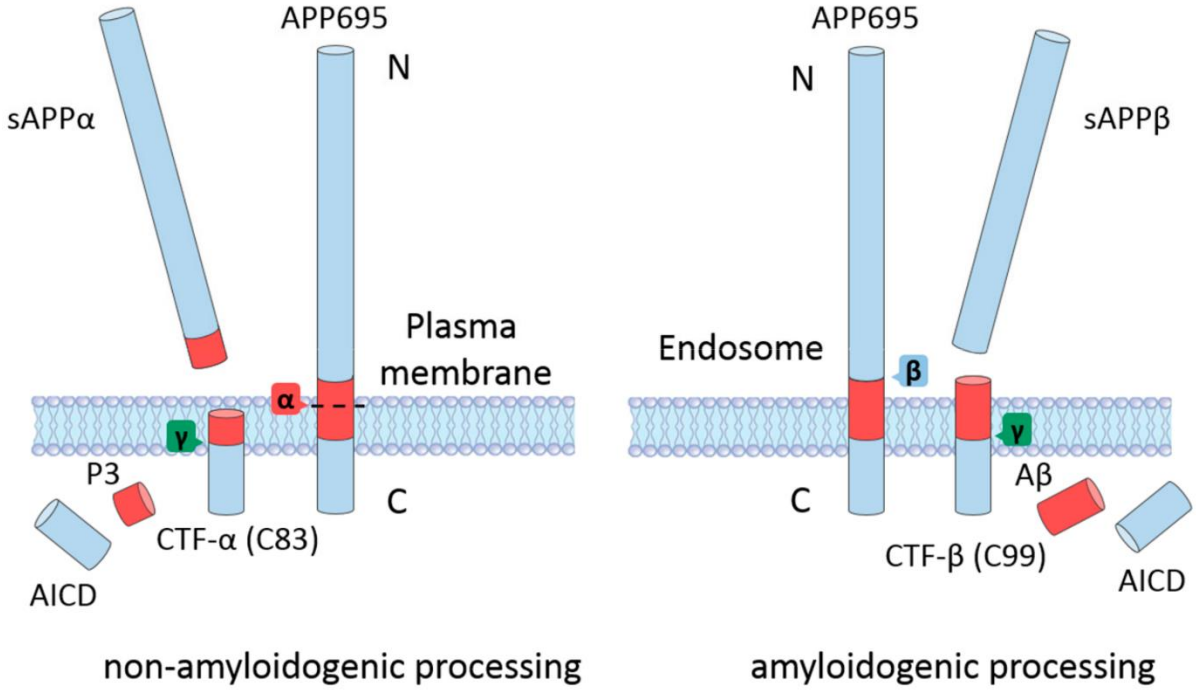


Figure 1 The proteolytic cleavage of the amyloid precursor protein (APP) by the non-amyloidogenic (left) and amyloidogenic (right) processing pathways. In the non-amyloidogenic pathway, mature APP anchored to the plasma membrane is processed by α-secretase within the amyloid-β (Aβ) region (shown in red) and releases soluble APPα (sAPPα) and the C-terminal fragment-α (CTF-α). The CTF-α is further processed by γ-secretase to generate P3 and the APP intracellular domain (AICD). In the amyloidogenic pathway, which preferentially occurs in acidic environments such as endosomes, reinternalized APP is consecutively cleaved by β- and γ-secretase to produce soluble APPβ (sAPPβ), Aβ, and AICD. The C-terminal fragment-β (CTF-β) is an intermediate product of the β-secretase cleavage. Reproduced with permission form Zhang et al. 2019 [26].

Neurofibrillary tangles (NFTs). NFTs are filamentous inclusions of hyperphosphorylated and misfolded Tau protein within the pyramidal neurons and occur in AD and tauopathies [44,23]. NFTs are accompanied by neuropil threads (NT) which result from the breakdown of dendrites and axons of the tangle-bearing neurons [22]. In contrast to amyloid deposits, NFTs exhibit a characteristic distribution pattern and spatiotemporal progression that correlates with the severity and duration of AD [22,45-47]. In 1991, Braak H. and Braak E. developed a qualitative evaluation method that allowed the differentiation of neuropathological stages of AD based on the changes in the distribution pattern of NFT and NT [48].

Tau is a highly soluble cytoplasmic protein that promotes axonal transport through bindings to tubulin during its polymerization into microtubules promoting its assembly and stabilization. Tau also functions in neurite outgrowth and acts act as postsynaptic scaffolding protein, modulating the activity of Src tyrosine kinases in actin remodelling, [49,50] and facilitates the postsynaptic trafficking of Fyn to PSD-95/NMDA (N-methyl-D-aspartate) glutamate receptors signaling complex [51]. In pathologic conditions, Tau undergoes aberrant phosphorylation and misfolding that leads to its dissociation from microtubules and makes it prone to self-assembly and aggregation to paired helical filaments (PHF) and NFT. Accumulation of tau causes disruption of cytoskeleton and axonal transport, interferes with mitochondrial dynamics [52] and makes neurons more susceptible to oxidative stress damage and thereby accelerates degeneration [53]. Similar to Aβ oligomers, intermediate tau aggregates are cytotoxic and impair cognition, because they can bind to healthy tau promoting its detachment from microtubules [54]. In contrast, NFT filaments are believed to be the inert form that the neurons are packaging Tau into as a protective response to sequester the toxic intermediate Tau species [55,56]. What controls the extent of Tau phosphorylation is the balance between the activity of tau kinases and phosphatases, mainly protein phosphatase 2A (PP2A), as well as Tau conformation that affects its interaction with these enzymes [55]. Glycogen synthase kinase (GSK-3), cyclin dependent protein kinase-5 (Cdk-5), protein kinase A (PKA), mitogen activated protein (MAP) kinase ERK1/2, and stress-activated protein kinases (C-Jun amino-terminal kinase (JNK) are the main kinases implicated in abnormal Tau phosphorylation [55]. Studies also showed that caspase-mediated cleavage of Tau at the carboxy-terminus, likely by caspase-3 [57], alters tau conformation facilitating its hyperphosphorylation and fibrillization, and hence is considered a key pathway in tangle formation [58-60]. Interestingly, studies showed that Aβ induces caspase activation and the subsequent truncation of Tau, [59,57] in addition to activating GSK-3 and Cdk Tau kinases [61-65], thus, driving the tau pathology.

Evidence from in vitro and in vivo experimental studies indicated that Aβ precedes and drives tau aggregation [66-68]. Furthermore, it was shown that Tau is necessary for Aβ-induced neurotoxicity in cultured hippocampal neurons and cognitive deficits in AD mice, and that targeting tau pathology could block Aβ-induced neurotoxicity [69,70]. These findings provide a mechanistic link between Aβ and Tau in AD. In addition, oxidative stress, impaired protein-folding function of the endoplasmic reticulum and deficient proteasome-mediated and autophagic-mediated clearance of damaged proteins are all associated with aging and accelerate the accumulation of amyloid and tau proteins in AD [71,72].

It is worth to mention that some patients with no overt symptoms of dementia antemortem show profuse Aβ plaques in the brain similar to AD patients (referred to as high pathology controls; HPCs). But levels of soluble Aβ, the presence of CAA, NFT and neuropil threads surrounding the amyloid core, besides, inflammation, only could distinguish HPC from AD patients [31,73].

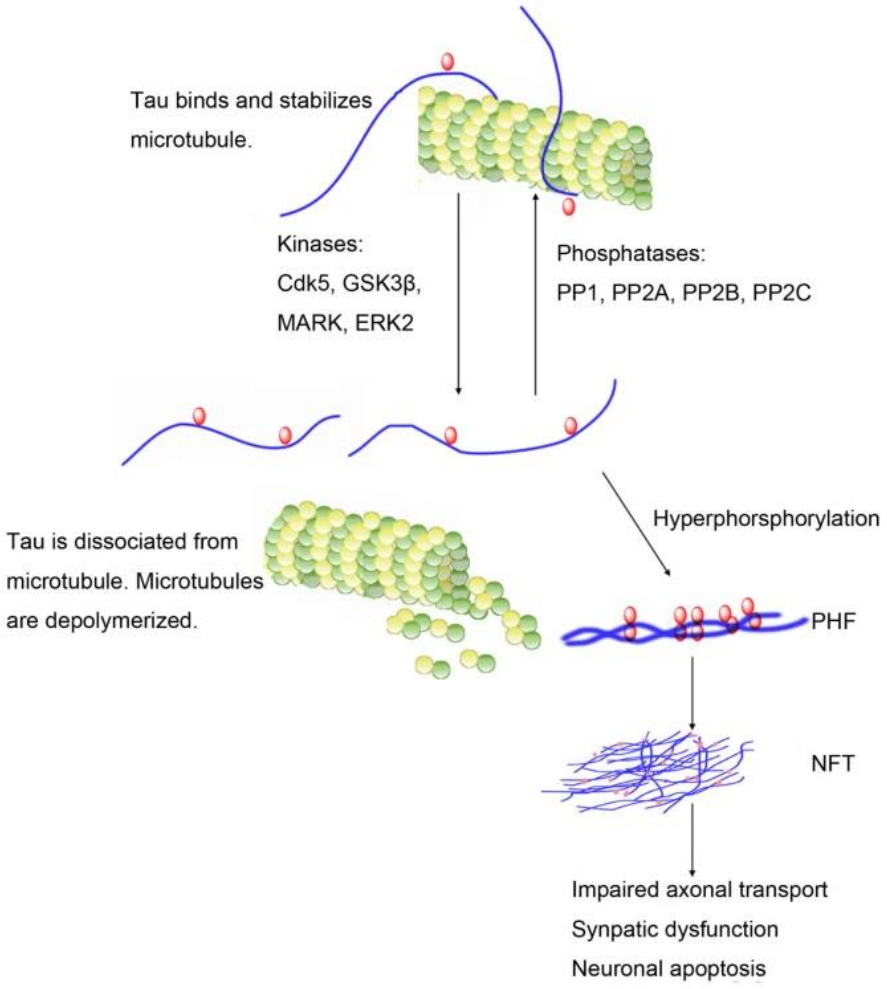


Figure 2 Tau-mediated neurodegeneration. Physiologically tau protein can bind and thereby stabilize microtubules (MTs). The attachment of tau to MT is regulated by its phosphorylation level. Phosphorylation of tau mediated by kinase (Cdk5, GSK3β, MARK and ERK2) may lead to the detachment of tau from MT and hereby cause MT depolymerization. Conversely, phosphatase (PP1, PP2A, PP2B and PP2C) will reduce the phosphorylation level of tau and restore the binding ability of tau for MT. Such equilibrium between the roles of kinases and phosphatases is disrupted under pathological condition and increase in the kinase activity and decrease in the phosphatase activity will cause tau hyperphosphorylation. Hyperphosphorylated tau protein is misfolded, and forms β-sheet-containing structure paired helical filaments (PHFs). These structure transitions will lead to more organized aggregates, and eventually develop neurofibrillary tangles (NFT) inside neurons. NFT will impair normal axonal transport, disrupt synaptic plasticity, and finally induce cell loss. Reproduced with permission from Duan et al 2012 [74].

Synaptic Failure. AD is primarily identified as a disorder of synaptic failure [23,75]. Synapse loss contributes to the cortical atrophy of the AD brain [22] and is the best correlate with the degree of dementia [76]. Hippocampal synapses start to decline in patients with mild cognitive impairment (MCI), while their remaining synapses increase in size (become enlarged) as a compensation to reduced synaptic density/number [77]. The expression levels of presynaptic protein synaptophysin is reduced by 25% in mild (early) AD [78]. With disease progressing, synaptic loss can surpass neuron loss and both synapse number and size decline [76].

Aging itself induces synaptic failure [79]. Intraneuronal soluble Aβ oligomers can also trigger neuronal injury and synaptic deficits. Chen et al. showed that applying $A\beta_{42}$ peptides to rat hippocampal slices inhibited long term potentiation (LTP) through calcineurin-dependent mechanisms shifting the balance towards depression [80]. Aβ-induced spine loss is believed to be mediated through acting on NMDA glutamate receptors causing disruption of calcium influx thus mimicking a state of partial NMDAR blockage [81,31]. This induces LTD that is associated with synaptic shrinkage and retraction [82]. Aβ also triggers endocytosis of NMDA [83] and postsynaptic AMPA (α-amino-3-hydroxy-5-methyl-4-isoxazole propionic acid) glutamate surface receptors [84], the latter of which induces a prolonged depression following LTP-inducing stimulus train. Similar to Aβ, aging impairs basal synaptic transmission and

induces NMDAR-dependent inhibition of LTP by disrupting intracellular Ca^{2+} signalling [85]. Therefore, it is tempting to say that Aβ may exacerbate aging-related Ca^{2+} dysregulation and synaptic dysfunction [80]. Moreover, Aβ also binds to p75 neurotrophin receptor and tyrosine kinase B receptor (TrkB, a receptor for brain derived neurotrophic factor: BDNF) in synapse terminals provoking a situation in which levels of BDNF and nerve growth factor (NGF) are already suppressed while the levels of proneurotrophins are increased leading to neurodegeneration. Aβ may also bind to nicotinic acetylcholine receptors (nAChR) suppressing cholinergic transmission and the ACh release from the presynaptic terminal [23].

Evidence indicated that $Aβ_{42}$ may disturb intracellular calcium homeostasis by forming ion channel-like structures in the lipid bilayer membrane of Neuro-2a (N2A) mouse neuroblastoma cells causing increase in calcium influx and intraneuronal calcium levels, thereby activating signal transduction pathways leading to neurotoxicity and degeneration [86].

On the other hand, accumulation of phosphorylated Tau at synaptic terminals and its relocation to dendritic spines is also synaptotoxic. It may interact with PSD-95/NMDAR complex and enhance calcium influx and may impair the synaptic trafficking and anchoring of glutamate receptors [87]. It may lead to tau oligomer deposition and disruption of synaptic ubiquitin-proteasome system [88]. Also, misfolded Tau may propagate to neighbouring neurons along synaptic networks [89-92] via “prion-like” and seeding mechanisms [93], and such transmission is accelerated by Aβ [94].

Neuroinflammation. Neuritic plaques, NFT and injured neurons may all provoke inflammation in AD brain. Activated microglia and astrocytes cluster in the vicinity of neuritic plaques and their biochemical markers are elevated in the brains of AD patients [95]. Aging can augment the inflammatory response in the brain and render it vulnerable to Aβ neurotoxicity [96,97]. Streit et al. first demonstrated that aged and AD brains show senescent

and dystrophic microglia and suggested that this morphological changes make it dysfunctional and fail to clear Aβ [98]. Aβ is one of the potent triggers for inflammation in AD [99]. In vitro studies demonstrated that Aβ and APP could initiate inflammation by inducing glia activation and the subsequent release of a variety of inflammatory mediators as interleukin-1β (IL-1β) and tumor necrosis factor- α (TNF-α) as well as free radicles such as nitric oxide (NO) [100]. The release of such proteins and oxidants enhances Aβ-induced glial activation [101], amplifies the inflammatory response and inhibits the microglial phagocytosis of Aβ peptides [102]. Therefore, this sate of chronic activation creates a continuous cycle of detrimental inflammatory stimuli that lead to neurotoxicity [103,99]. Hyperactive microglial state combined with ineffective phagocytic ability may lead to aggregation of Aβ from diffuse to neuritic plaques and inefficient clearance of damaged neurites creating a focal spot for accumulation of aggregation-prone peptides. Cell culture studies revealed that Aβ could stimulate glia by activating NF-κB (nuclear factor Kappa B), a transcription factor implicated in the induction of genes including cytokines and immunoreceptors [103]. Activation of NF-κB by Aβ possibly occurs via binding to RAGE, the receptor for advanced glycation end products [104] or through Aβ's chemokine-like activity acting at formyl chemotactic receptors (FPR) [105].

Mitochondrial Dysfunction and Oxidative stress. Mitochondrial dysfunction and oxidative stress (OS) have been associated with the pathogenesis of AD and occur early prior to the appearance of plaque pathology [106-108]. Aβ itself is a mitochondria poison. Several studies showed that Aβ and APP may accumulate inside the mitochondria [109] and across its import channels [110] causing morphological changes including swelling and disruption of its function. Aβ may inhibit the respiratory chain complex IV (cytochrome *c* oxidase, COX) and key Krebs-cycle enzymes (α-ketoglutarate and pyruvate dehydrogenase) leading to impaired oxygen consumption and energy production and result in generation of free radicles and

reactive oxygen species (ROS) [111]. Aβ may also induce loss of mitochondrial membrane potential and opening of the permeability-transition pores (ψm) that is exacerbated by the presence of pathogenic Tau [112]. These defects could result in mitochondrial fragmentation [113], provoke oxidative stress and trigger apoptotic signaling pathways [114]. In fact, AD and normal aging brains gradually accumulate mitochondrial DNA mutations due to sustaining high levels of oxidative damage which likely contribute to mitochondrial defects in AD [115].

In addition, compiling evidence suggests a possible role of Tau in mitochondrial dysfunction and OS. Transgenic mice bearing human pathogenic mutation P301L of tau, a model of Frontotemporal dementia with Parkinsonism-17 (FTDP-17), exhibited mitochondrial dysfunction and impaired energy production associated with accumulation of ROS with aging. Phosphorylated Tau specifically affects the activity of complex I [116] and hinders axonal trafficking of mitochondria and their synaptic docking due to microtubule destabilization [117,118]. Mitochondrial dysfunction can also cause Tau hyperphosphorylation. Besides, P301L tau mitochondria were vulnerable toward Aβ-induced neurotoxic insult. These findings suggest a synergistic action of Tau and Aβ pathology on the mitochondrial dysfunction, OS and synaptic plasticity [119].

Dysfunctional mitochondria in AD are the major source of OS. Besides, advanced glycation end products (AGEs), formed from non-enzymatic reaction of sugar ketone or aldehyde with protein, can induce OS through acting on RAGE receptor, in the same way as Aβ, and modulating gene transcription involved in inflammation through NF-κB. Accumulation of AGEs is a feature of aging [120] and age-related diseases such as diabetes mellitus [121]. Also, stimulated microglia release reactive oxygen (ROS)/reactive nitrogen species (RNS) as a response mechanism for attacking opsonized targets. These oxidants bind with membrane lipids and several proteins inducing damage to several molecular targets [122].

OS can upregulate Tau phosphorylation in AD through activation of kinases as GSK3β and mitogen-activated protein kinases (MAPKs) [123] including JNK; a stress-activated protein kinase (SAPK) that amplifies stress signals to the nucleus [124]. Oxidants such as 4-hydroxy-2-nonenal (4-HNE) and carbonyls modify Tau protein rendering it more prone to aggregate and polymerize [125]. SAPK/JNK induced by OS is also involved in Aβ deposition through provoking APP phosphorylation at Threonine 668 favouring its amyloidogenic processing [126,127]. OS induced by hydrogen peroxide may potentiate BACE1 gene expression and activity and enhances Aβ formation [128]. In turn, Aβ may trigger JNK activation leading to neuron death [129]. Therefore, it is suggested that OS plays a major role to induce Tau and Aβ accumulation in AD through upregulation of upstream signaling pathways, and, in positive feedback loop, Aβ and Tau aggravate the inflammatory and oxidative stress cellular responses leading to neurotoxicity [122]. These findings strongly suggest that targeting OS and the mitochondria could be a successful strategy for AD therapeutics.

Neuronal Loss. Massive neuronal loss is a main pathological feature in the hippocampus and cerebral cortex of AD patients. Evidence of neuronal apoptosis is observed in sporadic and familial AD brains. Collapse of the mitochondrial membrane potential and opening of the permeability-transition pores activates caspase-3 initiating cell lysis and proteolysis. In addition, Aβ is a key mediator of degeneration not only in neurons but also in cerebral endothelia cells and astrocytes that constitute the BBB [130]. Aβ activates stress-activated protein kinases p38 MAPK and JNK/c-Jun pathway as well as the mitochondrial regulatory protein p53 and triggers apoptotic signaling through p53 upregulated-modulator of apoptosis (PUMA) and proapoptotic protein Bim (Bcl-2 interacting mediator of cell death) and Bax [23,131]. Furthermore, *in vitro* studies showed that Aβ triggers a rapid and sustained downregulation of a key anti-apoptotic protein, Bcl-2, in human neuron primary culture while it increases levels of Bax, therefore, enhancing neuron vulnerability to age-related stresses such

as OS [132]. Interestingly, Tamagno et al. showed that all these biological events induced by Aβ were simulated by oxidative stress reactive intermediates and were significantly prevented or blocked when cells are pre-treated with antioxidants or by specific SAPKs inhibitors suggesting a direct involvement of OS in Aβ induced apoptotic signaling [133].

Insulin resistance. A strong association was found between AD and cerebral insulin resistance. Disturbance in brain insulin signaling might be an early contributing factor to late onset AD [134]. Type 2 diabetes is also associated with an increased risk of dementia. Factors related to metabolic syndrome such as hyperlipidaemia and hypertension are linked to Diabetes and may contribute to dementia [135]. Patients of advanced AD may present with high plasma insulin levels, low CSF insulin levels and reduced CSF/plasma insulin ratio compared to healthy age matched adults [136], reflecting a progressive peripheral insulin resistance. In addition, impaired insulin transduction mechanism and loss of tyrosine kinase activity were reported in AD brains with compensatory increase in number of insulin receptors (IRs) compared to age matched controls. However, the number of brain IRs in aged and AD patients is significantly less than healthy adults (<65 years old) [137]. In addition, the expression levels of several components of the insulin signaling pathway were found to be altered in brains of AD patients. In this regard, levels of insulin like growth factor IGF (I and II), their corresponding receptors and mRNA levels of insulin receptor substrate (IRS) are reduced. This is associated with reduced levels of phosphatidylinositol 3-kinase (PI3K) and phospho-Akt/Protein Kinase B (the active form), while enhanced GSK-3β activity (reduced phosphorylated GSK-3β levels) as well as increased APP mRNA expression [138]. These changes were also observed in age-matched healthy controls (age > 60), which means that aberrant insulin signaling is age-related and can precede or accompany the initial stages of cognitive decline [139]. Brain insulin resistance reduces neuronal energy/glucose metabolism and will eventually induce defects in synaptic integrity and render the neurons susceptible to other cellular insults such as inflammation, OS,

and mitochondrial dysfunction. Zhao et al. showed that Aβ oligomers induced a rapid and substantial loss of neuronal surface IRs in hippocampal neurons in vitro specifically on dendrites and inhibited insulin receptor signaling [140]. Aβ oligomers caused persistent increase in Akt phosphorylation at Ser473 which is a main component in the negative feedback loop on PI3K and IRs that contributes to insulin resistance in AD brain [141]. Therefore, the term "type 3 diabetes" has been proposed to describe the pathophysiology of insulin resistance brain state of sporadic AD [138].

2.2. Genetics and Neuropathology of FTD

In FTD or referred to as frontotemporal lobar degeneration (FTLD), astrogliosis and neuron loss are observed in the cortices of the affected frontal and temporal lobes. Oxidative stress is another component of the pathology of FTD especially in subtypes associated with Tau accumulation. FTLD is characterized by intracellular accumulation of abnormal protein inclusion in cytoplasm or nuclei of neuronal and glial cells. Based on the constituent of these inclusions, FTLD was divided into subcategories [142,143]. Initially, the first group was identified by accumulation of hyperphosphorylated tau protein and referred to FTLD-tau including Pick's disease (~40% of FTD cases) [144]. Later another type of inclusion, found in >50% of patients, is tau-negative and ubiquitin-positive staining inclusions. These inclusions were recognized later to be formed of transactive response (TAR) DNA-binding protein-43 (TDP-43), thus referred to as FTLD-TDP [145,146]. Majority of the remaining cases are TDP43-negative cases and associated with inclusions of fusedin-sarcoma protein (FUS), thus referred to as FTLD-FUS, which is the cause of familial amyotrophic lateral sclerosis (ALS) type 6 [143]. Yet, some patients show protein inclusions that remain unknown till today, referred to as FTLD-ubiquitin proteasome system (FTLD-UPS) [10,147]. In the following few sentences, we will focus on mutations in MAPT gene, the Tau gene, that account for 5% of FTD cases and frequently associated with parkinsonism (FTDP-17).

Several studies showed that MAPT mutations, including R5L, K257T, I260V, G272V, DK280, P301L, P301S, Q336R, V337M and R406W may promote Tau filament formation, reduce binding of mutant Tau to protein phosphatase 2A (PP2A), reduce Tau binding to microtubules and enhance Tau hyperphosphorylation [20]. These pathogenic Tau mutations may either affect mRNA splicing of exon 10 or they are missense mutations located inside or outside exon 10. Most coding region mutations in exon 10 (N279K, L284L, DN296, N296N, N296H, S305N and S305S) enhance splicing of exon 10, thus shifting the ratio between three- and four-repeat isoforms. These mutations lead to the formation of wide twisted ribbon-like filaments that consist only of four-repeat tau isoforms [148]. On the other hand, some Tau mutations on exon 10 do not affect mRNA splicing, such as the P301L mutation, that is relatively common in FTDP-17 families. Isolated Tau filaments from patients are of narrow twisted ribbon-like morphology predominantly consisting of four-repeat mutant tau isoforms. The aforementioned Tau mutations are present widespread in both nerve cells and glial cells. [149]. This contrasts with AD in which paired helical tau filaments (PHF) only present within nerve cells and consist of all six Tau isoforms [150]. Other mutations were found in exons 9-13 with the resultant Tau pathology varies in filamentous morphology and isoform composition according to the position and the nature of the mutation and resembles that of sporadic tauopathies such as progressive supranuclear palsy (PSP), corticobasal degeneration (CBD), AD or Pick's disease (PiD) [20].

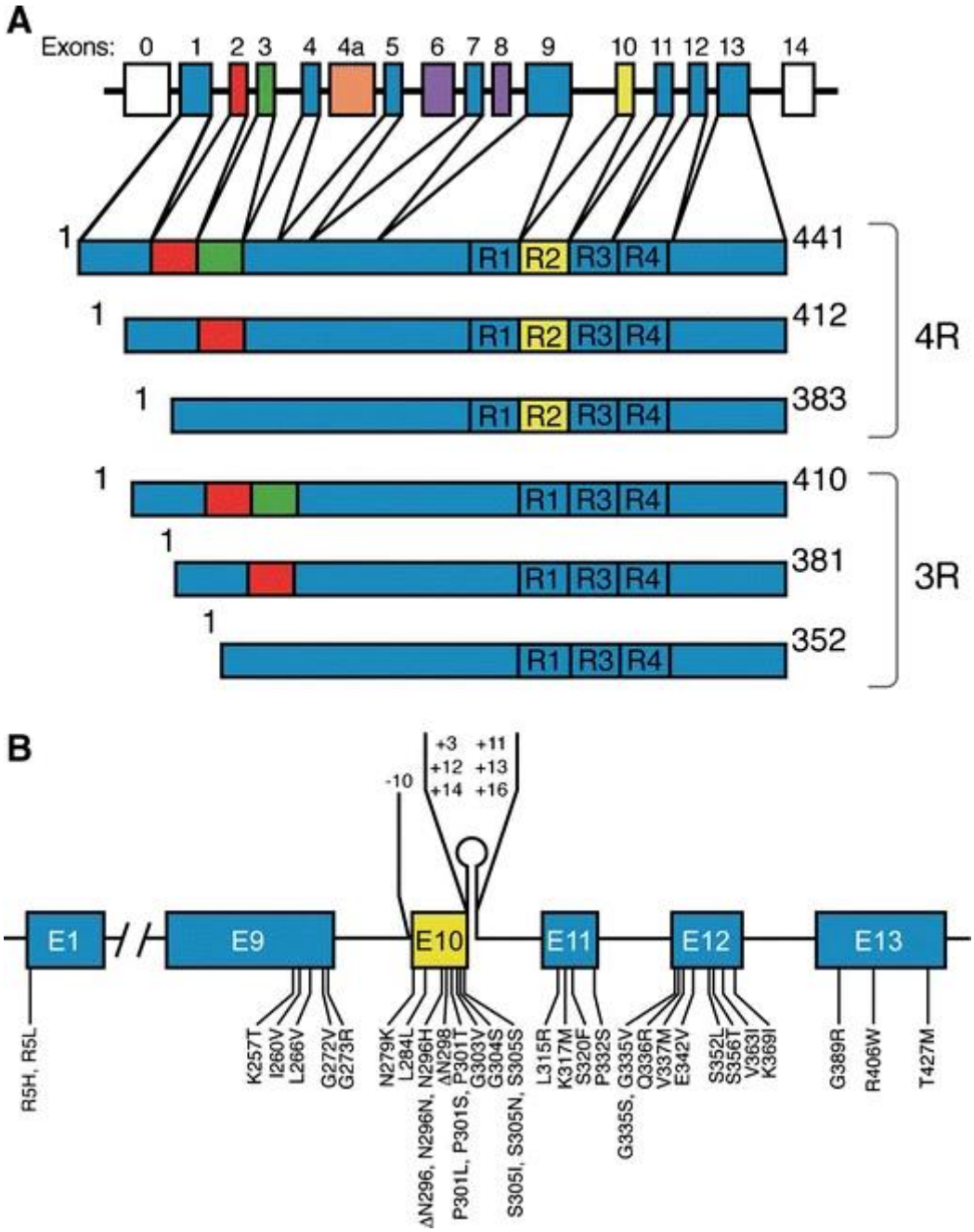


Figure 3 Tau isoforms and MAPT mutations in frontotemporal dementia and parkinsonism linked to chromosome 17 (FTDP-17). A MAPT and the six tau isoforms expressed in adult human brain. MAPT consists of 16 exons (E). Alternative mRNA splicing of E2 (red), E3 (green) and E10 (yellow) gives rise to the six tau isoforms (352–441 amino acids). The constitutively spliced exons (E1, E4, E5, E7, E9, E11, E12 and E13) are indicated in blue. E0, which is part of the promoter, and E14 are non-coding (white). E6 and E8 (violet) are not transcribed in human brain. E4a (orange) is only expressed in the peripheral nervous system. The repeats of tau (R1–R4) are shown, with three isoforms having four repeats each (4R) and three isoforms having three repeats each (3R). Each repeat is 31 or 32 amino acids in length. The exons and introns are not drawn to scale. **B Mutations in MAPT in frontotemporal dementia and parkinsonism linked to chromosome 17 (FTDP-17).** Thirty-seven coding region mutations in E1, E9, E10, E11, E12 and E13 of MAPT and seven intronic mutations flanking E10 are shown. Reproduced with permission form Goedert 2011 [150].

3. AD hypotheses

3.1. Amyloid cascade hypothesis

The amyloid cascade hypothesis, postulated in 1992 by Hardy and Higgins, assumes that "Aβ disposition is a central event and causative agent of the AD pathogenic cascade and that Tau tangles, cell loss, vascular damage and dementia follow as a direct result of this disposition" [151,152]. It combines histopathological and genetic material and suggests that the deposition of the Aβ peptides in the brain parenchyma, due to imbalance between Aβ production and clearance [153], initiates a series of events that eventually lead to AD dementia [154]. Support for this hypothesis came from autosomal-dominant familial AD cases which ultimately originates from aberrant Aβ production and aggregation due to *APP*, *PSEN1* or *PSEN2* gene mutations [155-157] or due to defects in Aβ clearance as a result of the presence of *APOE4* allele in late onset AD [158,159]. However, therapeutic approaches centred on Aβ have failed in phase III clinical trials. Also, it becomes evident that there is no linear correlation between cognitive alterations in dementia and Aβ plaques in humans. In particular, this hypothesis did not explain the driving force for amyloidosis in sporadic AD, which is actually a consequence of ageing, and not linked to genetic risk factors. This calls upon reconsidering and modifying the amyloid cascade hypothesis. However, Selkoe and Hardy believe that the discovery of various genetic risk loci for late onset AD through the genome-wide association (GWA) studies such as *TREM2* and *CD33*, although very rare, could support the amyloid cascade hypothesis [153]. Such risk genes are involved in processes regulating cholesterol/sterol metabolism, modulating the inflammatory response of microglia to Aβ and the brain's innate immune system, and endosomal vesicle recycling. These processes might be addressed with available drugs such as statins or anti-inflammatory agents [160,161].

Also, this theory could not describe the relationship between Aβ and Tau [162,154]. In sporadic AD, Tau pathology may precede amyloid beta [163,164]. In sporadic AD, Aβ and Tau may

evolve separately, however, both interact reciprocally and synergistically in mediating neurodegeneration [165,166]. While Aβ is essential to trigger Tau pathology, it does not correlate with cell loss or dementia. Aβ plaque pathology starts to appear in regions such as the precuneus and frontal lobes that are anatomically disconnected from those showing extensive neuron loss (hippocampus and entorhinal cortex). This is opposite to Tau which follows a regular spatiotemporal progression that clearly correlates with neuronal loss, cerebral atrophy and dementia [154]. It is thus assumed that Aβ initiates a neurotoxic complex process through inducing early Tau phosphorylation, then Tau mediates the downstream signaling of degeneration [167,168]. In other words, Tau is essential for Aβ-induced neurotoxicity [70]. A scenario by Karran et al. suggested that once this pathogenic cascade starts, it becomes self-sustaining, more complex and irrelevant to Aβ [154]. Therefore, Aβ-targeted therapeutic approaches could be beneficial provided if administered early in the disease course. This conclusion was supported from findings of clinical trials of Aβ antibodies showing that they have slowed the cognitive decline in mild AD patients, but showed no benefit in moderate cases while their brains still showing heavy distribution of Tau pathology across the cortex [153]. In line with these findings, a study found that suppression of endogenous wild type Tau prevented cognitive deficits in AD mouse model expressing human mutant APP without detectable changes in plaque pathology [169]. Also, targeting both Aβ and Tau, not only Aβ, by passive immunotherapy was able to ameliorate cognitive deficits in 3×Tg AD animal model [170,171]. In addition, GSk-3β inhibitors reduced Aβ-induced cell death in hippocampal neurons following nerve growth factor (NGF) withdrawal [167].

The Amyloid cascade hypothesis was further modified to point out the early and toxic effects of Aβ oligomers [172] and considers synapses as early targets for these toxic species [75]. However, the negative results and adverse effects of Aβ immunization in clinicals studies called for reconsidering the whole hypothesis.

In 2008, Small and Duff hypothesized that “common upstream drivers cause both elevation in Aβ and tau hyperphosphorylation through independent but parallel mechanisms”. This hypothesis referred to as “dual hit”, and authors believe that this theory might explain the molecular mechanisms in late onset AD [173]. But this theory again failed to explain the relationship between APP/Aβ and Tau.

Musiek et al. [174] assumed that Aβ is likely a key initiator of a complex pathogenic cascade which causes AD, thus supporting the Amyloid cascade Hypothesis in general. However, Aβ may not act chiefly to trigger other downstream processes. Thus, Aβ seems to be necessary but not sufficient to cause AD. Instead, a complex network of pathologic processes including age-related stressors such as oxidative stress congregate to produce the neuropathologic and clinical features of AD.

3.2. Tau hypothesis

Recent reports suggest that Tau may be the initiating factor in sporadic AD as early tau inclusion may develop decades before Aβ plaques according to Braak staging [175]. It is hypothesized that calcium dysregulation may drive Tau phosphorylation in aging due to loss of phosphodiesterase (PDE4) activity, which catabolizes cyclic adenosine monophosphate (cAMP). This results in activation of cAMP/Protein kinase A (PKA) signaling that causes calcium leakage to cytosol and primes Tau for subsequent phosphorylation by GSK3β. Also, it is suggested that Tau fibrils may trap endosomes containing APP and increase APP and BACE accumulation through disrupting microtubule transport so leading to amplification of Aβ production. This may create a vicious cycle where pathologic Tau induces Aβ production and Aβ then induces further Tau phosphorylation [164]. However, some argue against this hypothesis referring to FTD-Tau cases that do not have amyloid plaque pathology.

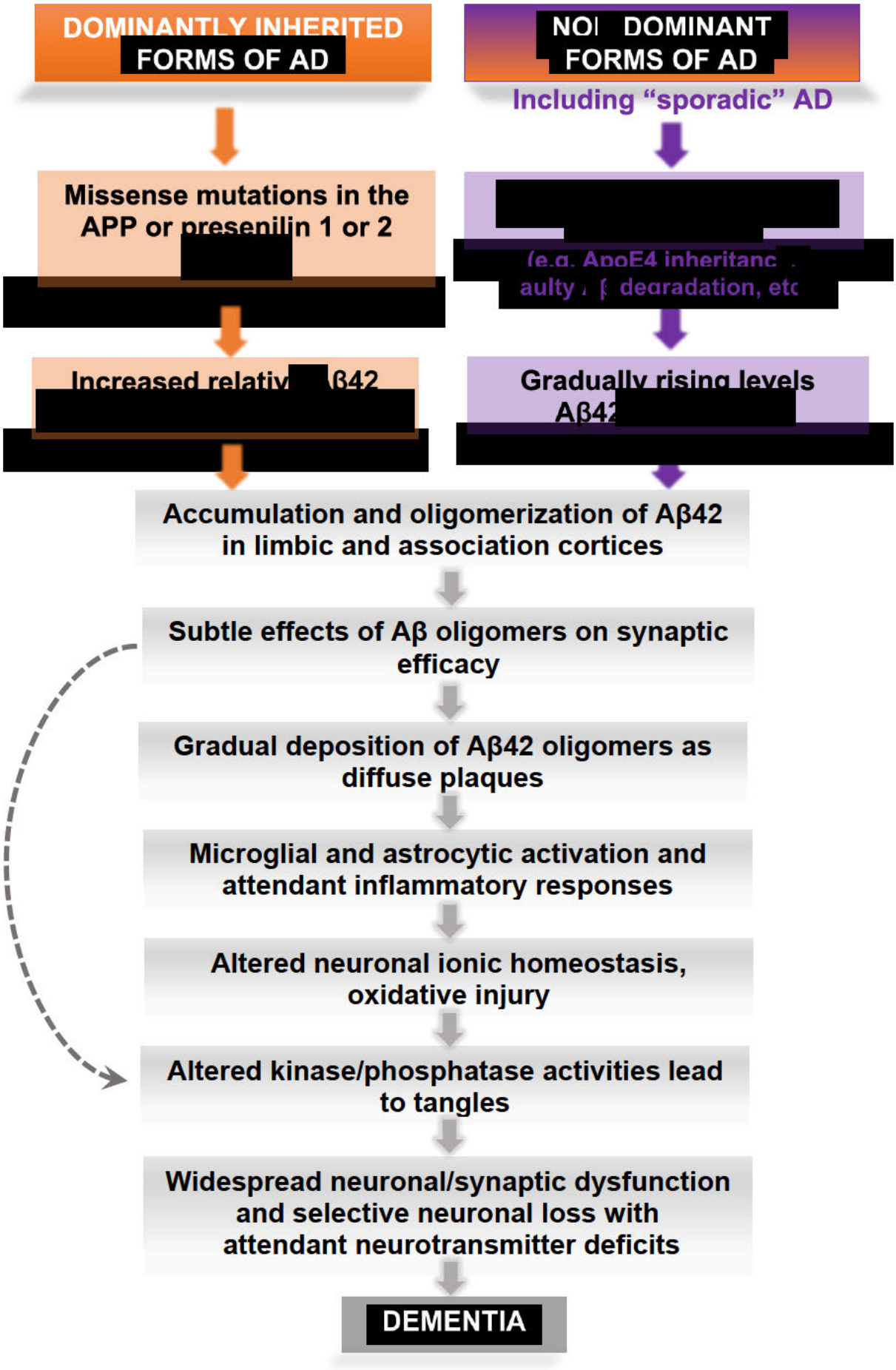

DOMINANTLY INHERITED FORMS OF AD
NOI DOMINANT FORMS OF AD
Including "sporadic" AD
Missense mutations in the APP or presenilin 1 or 2
(e.g. ApoE4 inheritanc
aulty , β degradation, etc
Increased relativ β42
Gradually rising levels Aβ42
Accumulation and oligomerization of Aβ42 in limbic and association cortices
Subtle effects of Aβ oligomers on synaptic efficacy
Gradual deposition of Aβ42 oligomers as diffuse plaques
Microglial and astrocytic activation and attendant inflammatory responses
Altered neuronal ionic homeostasis, oxidative injury
Altered kinase/phosphatase activities lead to tangles
Widespread neuronal/synaptic dysfunction and selective neuronal loss with attendant neurotransmitter deficits
DEMENTIA

Figure 4 The sequence of major pathogenic events leading to AD proposed by the amyloid cascade hypothesis. The curved grey arrow indicates that Aβ oligomers may directly injure the synapses and neurites of brain neurons, in addition to activating microglia and astrocytes. Adopted from Selkoe and Hardy 2016 [153].

3.3. Neurotrophin Hypothesis

According to neurotrophin hypothesis, imbalance of neurotrophins and their receptors during aging plays a critical role in abnormal Aβ accumulation, cholinergic and synaptic dysfunction, and hence, neurodegeneration in sporadic AD [176-178]. Cattaneo group was the first to provide evidence that neurotrophic deficits are the upstream driver, by developing comprehensive AD-like neurodegeneration in anti-NGF (nerve growth factor) AD11 mouse [178,179], which was reversed by early NGF delivery through an olfactory route [180]. Earlier study by Costantini et al. [181] suggested that the expression of TrkA tyrosine kinase receptor predominates in younger age mediating neuron survival. While during aging, a switch from TrkA to p75 neurotrophin receptor ($p75^{NTR}$), a death receptor, occurs that promotes APP processing, stabilizes BACE1 expression and enhances Aβ production. In a positive feedback loop, Aβ binds to $p75^{NTR}$ with high affinity and activates receptor signaling including MAPKs, JNK, p53 and NF-κB translocation leading to caspase-3 activation and apoptotic cell death. Therefore, $p75^{NTR}$ plays a crucial role in Aβ accumulation and in mediating Aβ-induced neurotoxicity in aging [181-185].

Neurotrophin signaling. Neurotrophins including brain derived neurotrophic factor (BDNF), nerve growth factor (NGF), neurotrophin-3 (NT-3), and NT-4/5 are trophic factors known to regulate several aspects of neuronal functions during development and in adult nervous system by maintaining neuron survival, differentiation, axonal growth, myelination, expression of ion channels and neurotransmitters and synaptogenesis [186]. They have been implicated in the pathophysiology of a several neurodegenerative and neuropsychiatric disorder such as AD and depression. Neurotrophins activate two different types of receptors: the Trk (tropomyosin-

related kinase), a tyrosine kinase receptor family and $p75^{NTR}$, a 75KDa type I transmembrane protein that belongs to the TNF (tumor necrosis factor) receptor superfamily together with sortilin which is a neuronal type-1 VPS10-domain receptor, a Golgi sorting protein and the co-receptor with $p75^{NTR}$ for proneurotrophins. Through Trks and $p75^{NTR}$, neurotrophins activate many signaling pathways, including those mediated by Ras and the mitogen-activated protein kinases (MAPK)/extracellular signal-regulated kinases (Erk), phospholipase Cγ (PLCγ), PI3k/Akt, NF-κB, RhoA and JNK cascades [187,188].

The mature neurotrophins are cleaved from proneurotrophins by intracellular furin, extracellular tPA (tissue plasminogen activator) or matrix metalloproteinases (MMP) [189]. Proneurotrophins exert opposite effects to the mature ones, through binding to different receptor complexes. Proneurotrophins favour to interact with $p75^{NTR}$/sortilin more potently than mature neurotrophins and mediate apoptotic signals. While mature neurotrophins selectively bind to Trk receptors and mediate neuronal survival and regeneration. Studies showed that whilst BDNF can promote learning and memory through activating TrkB, facilitating LTP in the hippocampus [190]. In contrast, proBDNF interacts preferentially with $p75^{NTR}$ together with the trafficking protein sortilin and can induce LTD and marked reduction in synaptic transmission in hippocampal slices. The effect of proBDNF likely involves enhancement of the expression of NR2B subunit of the NMDA receptor [191,192]. Similarly, proNGF induces neuron death through binding with high affinity to $p75^{NTR}$-sortilin receptor complex which subsequently activates a small GTPase; Rac, and the proapoptotic JNK signaling cascade [193-195]. Conversely, NGF selectively binds to $p75^{NTR}$/TrkA and activates Ras/Erk1/2 [196] and NF-κB-mediated transcriptional mechanisms, inducing cell survival signaling [197]. However, in the absence of TrkA, NGF/$p75^{NTR}$ mostly mediates apoptotic pathways. $p75^{NTR}$ signaling recruits various adaptor proteins such as NADE (neurotrophin receptor-associated cell death executor), NRIF (neurotrophin receptor interacting factor) and

NRAGE (neurotrophin receptor-interacting MAGE homolog) that are associated with apoptosis, or RIP2 (receptor-interacting protein 2), IL-1 receptor associated kinase (IRAK) and TRAF-6 (tumor necrosis factor receptor-associated factor-6) that promote survival, therefore, providing a bifunctional switch for cell survival or death [198-200].

$p75^{NTR}$ may also associate with Nogo-66 receptor (NgR) and LINGO-1 (leucine-rich repeat and immunoglobulin domain-containing 1), and this receptor complex, when activated by myelin proteins such as myelin-associated glycoprotein (MAG), oligodendrocyte myelin glycoprotein (OMgP), and Nogo-66, inhibits axonal growth and prevents regeneration of injured nerve fibres through activation of the small GTPase RhoA [201,202].

$p75^{NTR}$ can interact with all three types of Trk receptors and modulate Trks' ligand-binding affinity presumably by conformational change [203]. The binding of $p75^{NTR}$ with TrkA promotes its autophosphorylation and enhances its binding affinity for NGF [204], supporting the NGF/TrkA neuron survival through PI3K/Akt, NF-κB pathways, and antiapoptotic Bcl-2 expression [205]. However, $p75^{NTR}$ may have opposite or negative effect on TrkB and C by reducing autophosphorylation of TrkB in response to BDNF or NT-4 [206]. Activation of $p75^{NTR}$-Trk receptor complex with mature neurotrophins promotes cell survival and antagonizes the proapoptotic signaling cascade mediated by $p75^{NTR}$-sortilin complex and proneurotrophins [207]. $p75^{NTR}$ may also promote retrograde transport of neurotrophins [208]. Therefore, $p75^{NTR}$ is considered a main regulator of cell survival and differentiation and can mediate either survival or degeneration depending on the ligand and pathway activated [209].

$p75^{NTR}$ is primarily cleaved in endosomal membranes by TNF-α-secretase cleaving enzyme (TACE, also known as ADAM17) generating the soluble extracellular domain (p75ECD) which is the ligand binding site, followed by γ-secretase to release its intracellular domain (p75ICD) [210]. The metalloprotease-mediated shedding of $p75^{NTR}$ can be regulated by

TrkA/NGF signaling and TrkB [211,212]. The p75ICD consists of a chopper domain and TNF-like death domain and is thought to mediate neural apoptotic signals [213,214,188].

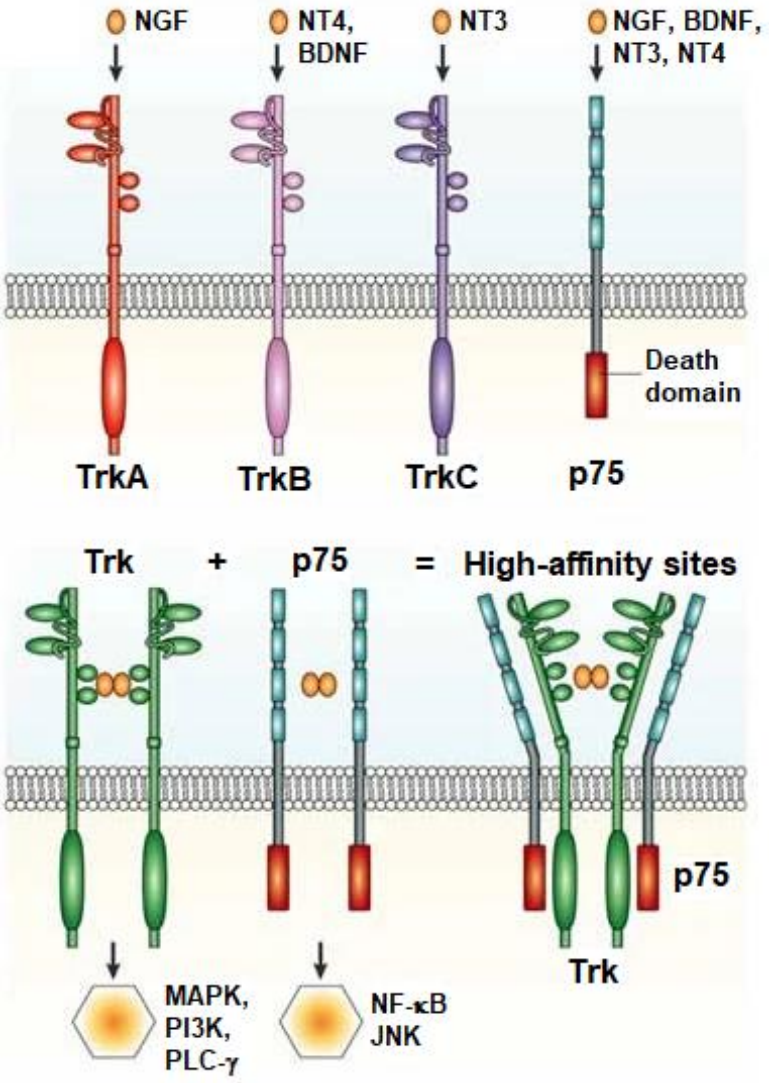


Figure 5 Models of Trk and p75 receptor activation. Neurotrophin binding results in dimerization of each receptor. Neurotrophins bind selectively to specific Trk receptors, whereas all neurotrophins bind to p75. Trk receptors contain extracellular immunoglobulin G (IgG) domains for ligand binding and a catalytic tyrosine kinase sequence in the intracellular domain. Each receptor activates several signal transduction pathways. The extracellular portion of p75 contains four cysteine-rich repeats, and the intracellular part contains a death domain. Neurotrophin binding to the p75 receptor mediates survival, cell migration and myelination through several signalling pathways. Interactions between Trk and p75 receptors can lead to changes in the binding affinity for neurotrophins. BDNF, brain-derived neurotrophic factor; JNK, Jun N-terminal kinase; MAPK, mitogen-activated protein kinase; NGF, nerve growth factor; NT, neurotrophin; PI3K, phosphatidylinositol 3-kinase; PLC-γ, phospholipase Cγ. Reproduced with permission from Chao 2003 [186].

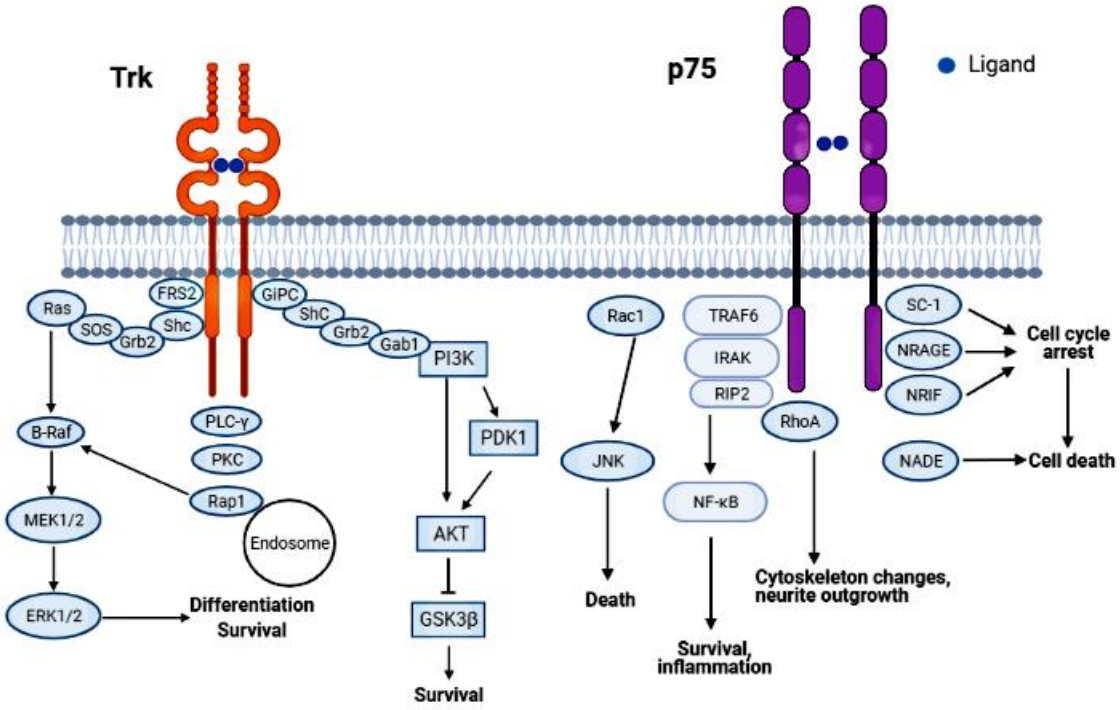


Figure 6 Neurotrophin receptor signalling. Trk receptors mediate differentiation and survival signalling through extracellular signal-regulated kinase (ERK), phosphatidylinositol 3-kinase (PI3K) and phospholipase Cγ (PLC-γ) pathways. Trk family members recruit and increase the phosphorylation of PLC-γ and Src homologous and collagen-like adaptor protein (Shc), which leads to activation of PI3K and ERK. Rap1 exerts its actions from an endosomal location. The p75 receptor predominantly signals to activate NF-κB and Jun N-terminal kinase (JNK) and modulates RhoA activity. These responses are mediated through adaptor proteins that bind to the cytoplasmic domain of p75, including neurotrophin-receptor interacting factor (NRIF), neurotrophin associated cell death executor (NADE), neurotrophin-receptor-interacting MAGE homologue (NRAGE), Schwann cell 1 (SC1) and receptor-interacting protein 2 (RIP2), which can exert effects on apoptosis, survival, neurite elongation and growth arrest. Akt, protein kinase B; FRS2, fibroblast growth factor receptor substrate 2; Gab1, Grb2-associated binder-1; Grb2, growth factor receptor-bound protein 2; GIPC, GAIP interacting protein, C terminus; MEK, mitogen-activated protein kinase (MAPK)/ERK kinase; PDK1, phosphoinositide-dependent kinase 1; SH2B, Src homology 2-B; SOS, Son of Sevenless; TRAF6, tumour necrosis factor receptor-associated factor 6. Adopted from Chao 2003 [186].

Neurotrophins in AD. Post-mortem studies in AD revealed severe reduction in the expression levels of BDNF [215] and TrkA and B, upregulation of proNGF (due to decrease of proteolytic conversion) and sortilin [216] and failure of retrograde transport of NGF signal in cholinergic neurons [203,217]. Interruption of NGF and BDNF signaling activates amyloidogenesis and favours apoptotic cell death via proNGF/$p75^{NTR}$ signaling in hippocampal neurons [218,219]. NGF controls both APP phosphorylation at T668 as well as subcellular trafficking and localization of APP and BACE1. NGF inhibits JNK-mediated phosphorylation of APP at T668, which in turn favours TrkA interaction with APP. This interaction favours α-secretase cleavage of APP and induces its trafficking to the Golgi where APP-BACE interaction and cleavage is inhibited [220]. The potential significance of NGF in amyloidosis rises from the fact that TrkA fails to interact with phosphorylated APP T668. In AD, these events are severely disrupted where pAPP T668 highly accumulates in dystrophic neurites and plaques and APP-TrkA interaction is inhibited. In a positive feedback loop, Aβ may aggravate and participate in neurotoxicity induced by neurotrophin imbalance. Aβ could inhibit TrkA phosphorylation and ubiquitination and disrupt its association with $p75^{NTR}$ and NGF, hence inhibits TrkA neuron survival signaling pathways [221]. Tiernan et al. provided evidence for link between pre-tangle pathology and neurotrophin imbalance within the cholinergic nucleus basalis neurons. Disrupted neurotrophin signaling contributes and coincides with the progression of NFT pathology in AD patients [222], and in turn, phosphorylated Tau (pS422+ neurons) may impair NGF retrograde transport [223] and inhibit TrkA expression and therefore supports the shift from pro-survival to pro-apoptotic signaling [222].

$p75^{NTR}$ in AD. $p75^{NTR}$ pan receptor is a member of TNF superfamily that is mainly expressed in the BFCN, dorsal root ganglion and sympathetic neurons. It is upregulated in aging and in response to stress conditions such as OS, inflammation and brain injury altering the ratio of $p75^{NTR}$ to Trk in favour of $p75^{NTR}$ [224]. $p75^{NTR}$ has diverse roles and activates three main

pathways including neuronal growth, apoptosis, and synaptic plasticity [225]. It is also involved in neuronal cell cycle re-entry, which is believed to be a key pathological mechanism underlying the development of AD and other neurodegenerative diseases [226].

Several studies proved that $p75^{NTR}$ mediates Aβ-induced neurotoxicity [182,183] and Tau hyperphosphorylation [227] and regulates Aβ deposition and metabolism in the brain [228]. Similar to proneurotrophins, Aβ (both soluble oligomeric and aggregated) can bind to $p75^{NTR}$ inducing apoptotic signals and neurite collapse through upregulation of JNK expression and phosphorylation [184], caspases as well as through RhoA/ROCK pathway triggering spine loss [229]. However, low concentration of Aβ (in the nanomolar to picomolar range) can mediate $p75^{NTR}$-induced neurite growth, like NGF, through induction of Ras-Erk pathway [230]. Aβ can upregulate $p75^{NTR}$ [231] and sortilin expression, through $p75^{NTR}$/RhoA signaling pathways [232]. Activation of $p75^{NTR}$ and sortilin pathways enhances BACE1 expression and trafficking [233] and induces APP phosphorylation and localization into endosomes, through JNK activation thereby, maintaining a vicious cycle of amyloidosis and neurodegeneration [234,235]. Matrone et al. showed that accumulation of Aβ in AD, due to failure of NGF signal, may induce TrkA phosphorylation and interaction with $p75^{NTR}$ and PS1 shifting the neurotrophic signal of TrkA to apoptotic signal of $p75^{NTR}$ via the activation of phospholipase Cγ (PLCγ) and catalysed by Src and CDK5 kinases [236]. $p75^{NTR}$ also plays a major role in Aβ uptake and clearance through inducing lysosomal internalization and degradation of Aβ-$p75^{NTR}$ complex in the BFCN [237], however, this process may be impaired in degenerated neurites. Wang et al. showed that deletion of $p75^{NTR}$ in APP/PS1 AD mice reduced soluble Aβ levels in the brain and serum but increased plaque accumulation [228]. While delivery of p75ECD-Fc recombinant protein into the hippocampus of AD mice suppressed plaque aggregation, attenuated synthetic $Aβ_{42}$ peptide oligomerization and fibrillation, and solubilizes fibrilized Aβ in vitro [238,228]. These findings indicated that $p75^{NTR}$ plays a critical role in Aβ production

possibly via NGF/$p75^{NTR}$ signaling pathway [177]. Moreover, the findings of this study highlighted the possible role of p75 extracellular domain in sequestering Aβ, reducing its aggregation and promoting its clearance, in a way, similar to that of anti-Aβ antibodies. Therefore, $p75^{NTR}$ plays two opposing roles in Aβ homeostasis in the brain. On one side, $p75^{NTR}$ signaling may increase Aβ production and maintain steady-state levels of Aβ. On the other side, p75ECD after shedding from the membrane may bind and sequester Aβ, thus suppressing its aggregation in the brain and enhancing its clearance across the blood brain barrier (BBB).

In this respect, Yao et al. found that the levels of p75ECD is reduced dramatically in the brain and CSF in AD, while the levels of p75 full-length increased, which is possibly due to the Aβ-induced reduction in the expression and activity of the cleaving enzyme TACE [238]. Petri et al. suggested that Aβ dose dependently inhibits TACE through the activation of PDK1 (3-phosphoinositide-dependent kinase-1) signalling pathway, which triggers TACE internalization and reduces the cell-surface activity of TACE [239]. TACE inhibition reduces the shedding of p75 extracellular domain and accumulates the full-length receptor (p75 fl), leading to aggravation of the apoptotic $p75^{NTR}$ signaling pathway mediated by Aβ and proneurotrophins. Consequently, restoration of p75ECD levels could sequester Aβ, inhibit its aggregation and may serve as a competitive antagonist on $p75^{NTR}$ full-length by antagonizing the binding of Aβ with $p75^{NTR}$. Treatment of AD transgenic mice with AAVECD-Fc administered either in one of the lateral ventricles or peripherally improved learning and memory and reduced AD pathologies including amyloid plaques, tau phosphorylation, cell death, synaptic degeneration and neuroinflammation [238,240]. Similarly, p75ECD-Fc suppressed Aβ-induced neurotoxicity and Tau phosphorylation in P301L mice, a model of frontotemporal dementia [241,227]. Therefore, p75ECD is considered a potential diagnostic biomarker and novel therapeutic approach for treatment of AD and tauopathies [242].

Conversely, the levels of p75ECD increase in the blood of AD patients and could differentiate AD from cognitively normal subjects [243]. The source of p75ECD in the blood is still elusive since p75 mRNA levels in peripheral blood cells are not altered between the two groups [244].

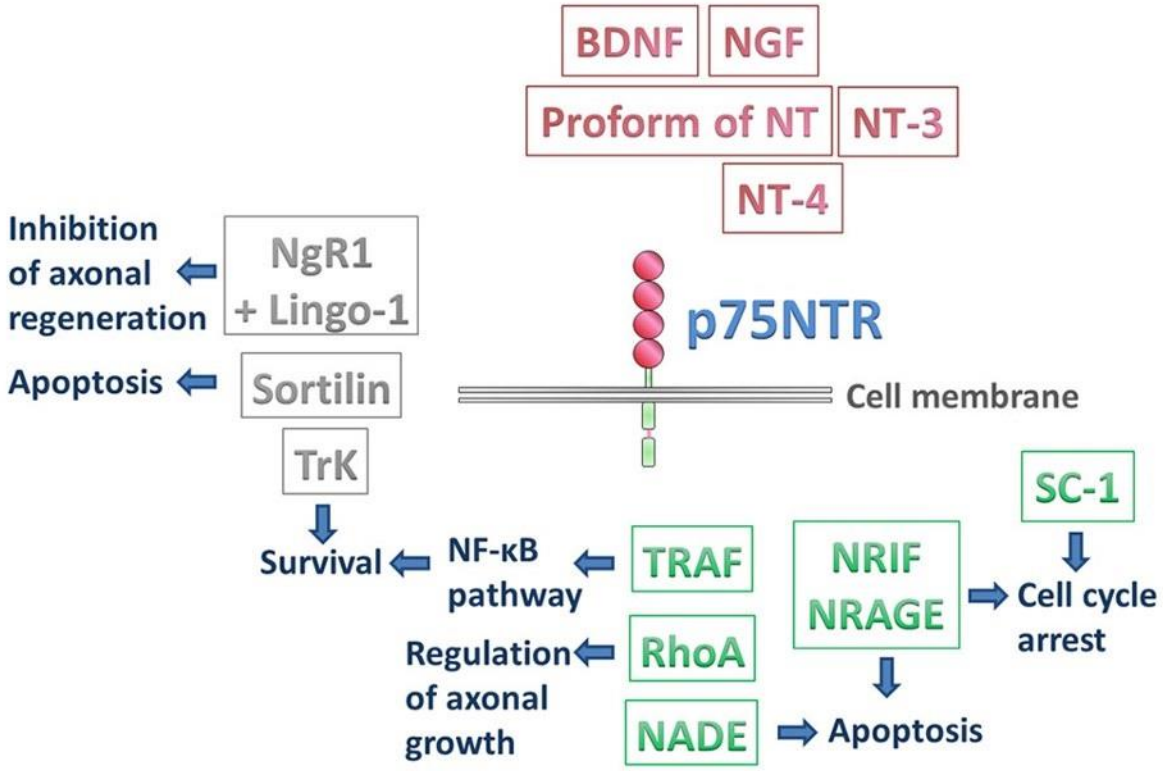


Figure 7 Schematic representation of the various interactors of p75^{NTR}. The extracellular domain binds neurotrophins as well as their respective proforms (red). Interaction with other receptors (gray) influences the outcome of p75NTR activation. As the intracellular domain lacks catalytic activity, the signaling of p75NTR is partially carried out by interactors of the intracellular domain (green), which also accounts for the different effects of p75NTR stimulation. BDNF, brain-derived neurotrophic factor; Lingo-1, immunoglobulin-like domain-containing nogo receptor interacting protein 1; NADE, p75NTR-associated cell death executor; NGF, nerve growth factor; NgR1, Nogo-66 receptor 1; NRAGE, neurotrophin receptor-interacting melanoma antigen homolog; NRIF, neurotrophin receptor interacting factor; NT, neurotrophin; RhoA, ras homolog gene family, member A; SC-1, Schwann cell factor 1; TRAF, TNF receptor–associated factor; Trk, tyrosine receptor kinase. Reproduced with permission from Becker et al. 2018 [245].

3.4. Mitochondrial dysfunction and Oxidative stress hypothesis

Oxidative stress has been identified as a contributing factor in aging and in the progression of several neurodegenerative diseases including AD [118], FTD-Tau [246,247] and amyotrophic lateral sclerosis [248]. Evidence from studies on iPSC-derived early sporadic AD patient neuronal cells showed increased production of ROS and dysfunction of the mitochondrial respiratory chain prior to Aβ and Tau accumulation [249]. Oxidative damage has also been found to underlie different subtypes of FTD but more prominently in FTD-tau cases [246]. Kamat et al. in 2014 suggested that "oxidative stress mediated through NMDAR and their interaction with other molecules might be a driving force for tau hyperphosphorylation and synapse dysfunction" [250].

Mitochondria are considered the main source of intracellular oxidant production [251]. Accordingly, Swerdlow et al. suggested the mitochondrial cascade hypothesis which states that "in sporadic, late-onset AD, loss of mitochondrial function associated with age affects the expression and processing of APP initiating Aβ accumulation" [252,253].

Increased production of reactive oxygen species (ROS) and reactive nitrogen species (RNS) due to aging and disease-dependent mitochondrial dysfunction as well as insufficient antioxidant defences induce synaptic damage and neurotoxicity. Oxidative damage to cellular components including nuclear and mitochondrial DNA, lipids and proteins likely result in abnormal metabolism and metal ion homeostasis, activation of caspases and stress-activated protein kinases, and main tau kinases as GSK-3β, inhibition of phosphatases and inflammation [254]. These events could represent the initial trigger that could enhance the production and accumulation of Aβ and hyperphosphorylated Tau. In a positive feedback loop, Aβ and Tau could independently exacerbate mitochondrial dysfunction and OS, therefore contributing to a vicious cycle that exacerbates with time leading to neuronal death [118,255,256]. Tau oligomers may interfere with the autophagy-lysosomal pathway (ALP) which plays a role in

clearance of misfolded proteins [257,258] and degradation of impaired mitochondria, and conversely, mitochondrial dysfunction aggravates ALP impairment and contributes to Tau protein accumulation in AD and FTD-tau [259,258].

According to Fade et al. “aging-dependent oxidative stress represents a crucial initiator of neurodegeneration, causing covalent modification of different molecules, enhancing the expression of proNGF and other key regulators of the cell cycle as well as of $p75^{NTR}$ that forces cell cycle re-entry and neuronal tetraploidization and eventually lead to microglial and/or astrocytic activation and setting the cell to stress response” [226]. The presence of polyploid cells have been detected in the frontal cortex of both control and in AD brains but increased in AD brains [260,261].

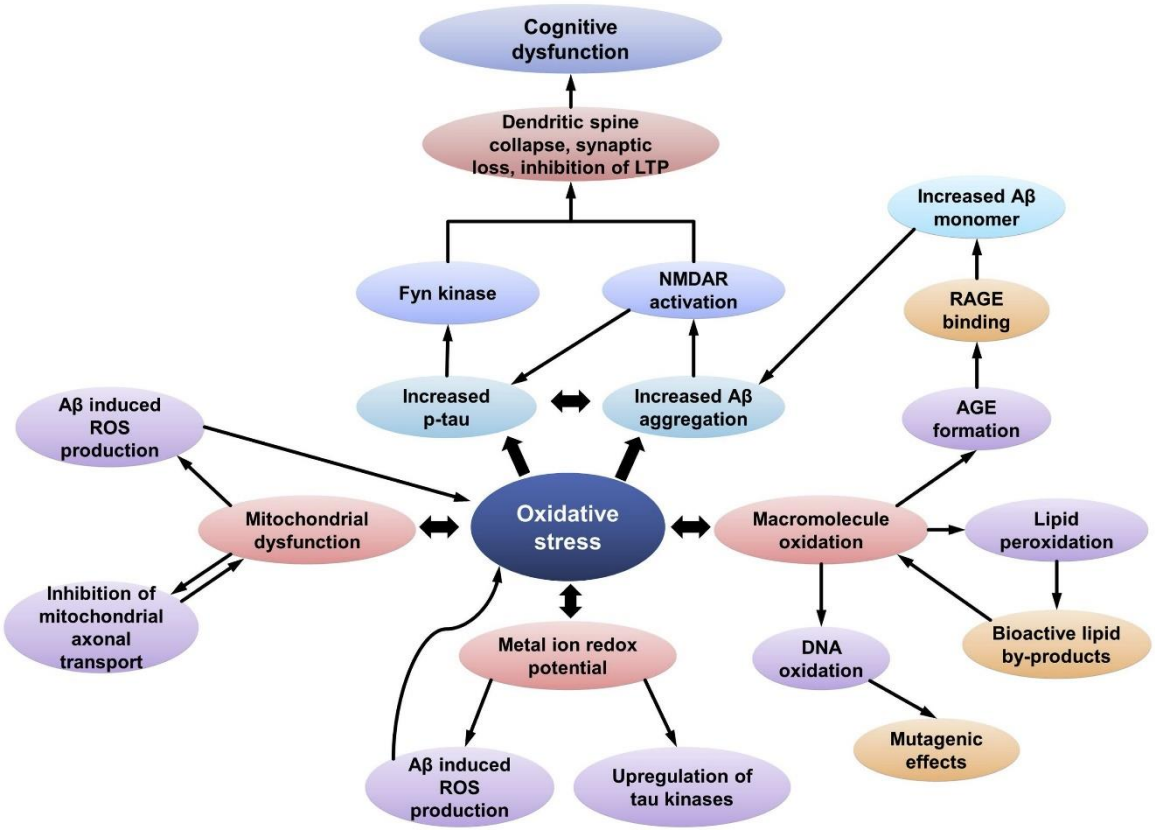


Figure 8 The interplay between oxidative stress and Alzheimer’s Disease (AD). Oxidative stress contributes to AD pathophysiology by causing dysfunction of neuronal mitochondria, the oxidation of macromolecules, the generation of ROS by the binding of metal ions to Aβ plaques and the upregulation of p-tau and Aβ synthesis. The result of this is activation of Fyn kinase causing activation of a pathway leading to the death of dendritic spines, loss of synapses,

and inhibition of LTP, causing cognitive dysfunction. ROS – reactive oxygen species, p-tau – hyperphosphorylated tau protein, Aβ – amyloid beta, AGE – advanced glycated end products, RAGE – receptor for advanced glycated end products, NMDAR - N-methyl-d-aspartate receptors, LTP – long-term potentiation. Reproduced with permission from Cassidy et al. 2020 [262].

3.5. The inflammation hypothesis

Krstic et al. suggested that inflammation represents a major trigger to neuropathology of sporadic AD, referred to as "the inflammation hypothesis of AD" [263]. Chronic inflammation and cellular stress to neurons during aging caused by disease (i.e., Diabetes) or age-related changes induce Tau phosphorylation and misfolding that result in impairing axonal transport. Such changes might hinder protein extrusion mechanisms and induce focal axonal swellings and blockage with concomitant accumulation of mitochondria, leading to disturbed energy metabolism and ultimately axonal leakage and loss of synaptic connections. This state of chronic inflammation and defective axonal transport will promote APP accumulation and amyloidogenic processing, which subsequently induces priming and recruitment of microglia and astrocytes to the degenerating neurons. Microglia and astrocytes become over-activated and release inflammatory mediators that will eventually extend to the nearby neurons. This hypothesis is supported by the observations of Braak and colleagues who recently reported that tau-related neuronal changes appeared quite before than did amyloid deposits, and that in more than half of investigated cases, abnormal tau protein occurred without the presence of Aβ deposits [175]. These findings indicate that formation of hyperphosphorylated Tau induced by inflammatory states and leading to impairments in neuronal integrity could represent an early neuropathological event that precedes deposition of the classical AD hallmarks [263].

4. Current and Novel Therapeutic Strategies

4.1. Currently approved therapies for AD and FTD

Current symptomatic treatments for AD include the acetylcholinesterase inhibitors; donepezil, galantamine, rivastigmine and tacrine, and a low-affinity NMDA receptor antagonist; memantine for moderate to severe AD. The acetylcholinesterase inhibitors mediate their effects by partially alleviating the cholinergic deficit in AD [264], whereas the precise mechanism of action of memantine remains elusive, but it is thought to interfere with neurotoxic effects of Aβ mediated on NMDA receptor [265]. Generally, the effects of these drugs are quite limited as they somewhat improve some of the symptoms but do not treat the underlying causes of the disease [154].

To date, only one disease-modifying treatment approved in USA for FTD is Riluzole. Current symptomatic treatments include antidepressants such as selective serotonin reuptake inhibitors and trazodone and neuroleptics such as olanzapine, risperidone and aripiprazole to treat aggression, agitation and psychosis. Unfortunately, so far no treatment proved to be safe and effective is available to alleviate motor symptoms that associate FTD with parkinsonism (FTDP-17) [14].

4.2. Novel therapeutic strategies

4.2.1 Therapies targeting Aβ production, accumulation, and clearance.

So far, nearly all Aβ-targeted phase III clinical trials in AD have not shown statistically significant benefits on its clinical endpoints and they were discontinued due to side effects that are most likely not target-related [153,21,154].

Modulation of β- and γ-secretases' activity

Clinical trials are carried out to investigate the safety and efficacy of selective BACE1 inhibitors. However, clinical development of almost all these compounds such as Verubecestat,

Atabecestat, Umibecestat and Elenbecestat have been terminated due to severe adverse events and lack of significant improvement on cognition scores [266].

Similarly, the clinical development of various γ-secretase inhibitors such as Semagacestat and Avagacestat was discontinued as they were neither effective nor safe due to severe adverse events that might be caused by lack of selectivity to APP and Notch [267,268].

Aβ vaccination and Anti-Aβ Antibodies (immunization therapies)

Aβ vaccination (AN1792) and anti-Aβ antibodies (bapineuzumab, solanezumab, Aducanumab and ponezumab) were developed as a potential therapeutic approach for reducing levels of brain Aβ. Antibodies were designed to target the mid-region of Aβ and bind primarily to monomers and low-n oligomers. They may act through two basic mechanisms. First mechanism assumes that the antibodies in the periphery capture Aβ and inhibit its uptake to the brain which will consequently accelerate Aβ efflux from the brain and promote deposited plaque dissociation [269,270]. Second mechanism is that antibodies cross the BBB and sequester Aβ in the brain and enhance the phagocytosis of Aβ/antibody complex by microglia through opsonization [271,272]. Both active and passive vaccination were successful in AD animal models. However, the clinical development of most of Aβ immunotherapies was halted due to severe immune response such as meningoencephalitis, microhemorrhage and vasogenic edema. These adverse effects might be due to the direct interaction of antibodies with Aβ in the brain rather than in the periphery which might hinder the efflux of this complex to the blood and be trapped in brain vascular wall inducing inflammatory responses and resulting in accumulation of multimeric toxic Aβ species in the brain [273]. Also, autoimmune meningoencephalitis might be caused by the abnormal infiltration of T lymphocytes into the brain activated by the T cell-activating domain of Aβ vaccine [274].

4.2.2 AD therapies based on neurotrophins.

NGF gene delivery

According to the neurotrophin hypothesis for AD, therapies aimed at restoring the homeostatic balance between ligands and receptors of the neurotrophin pathway appear to have a truly disease modifying efficacy [178]. However, therapeutic application of neurotrophins has been limited so far owing to their poor plasma stability (half-life of few minutes or less) and oral bioavailability and restricted ability to penetrate the BBB. Besides, their pleiotropic actions, triggered by acting on a complex receptor signaling network, could lead to adverse effects such as hyperalgesia with NGF treatment [275]. For example, stereotaxic gene delivery of NGF proved to be effective and well-tolerated in phase I clinical trial [276]. But the invasiveness of the procedure and adverse events encountered by participants such as severe back pain and weight loss have limited its clinical development [276-278].

Small molecule neurotrophin ligands

A recent approach developed by Longo et al. involves the use of small molecule ligands that "may bind to receptors at sites that would otherwise be occupied by only one of the several domains within a bound protein ligand" [275]. Such binding may or may not result in substantial displacement of the native ligand from the receptor and may promote conformational changes that activate the receptor. These ligands focused on the modelling of binding domains within NGF, BDNF or NT3. Examples of small molecule ligands are 7,8 dihydroxyflavone; a TrkB binding small molecule and LM11A-24 and LM11A-31, which are neurotrophic $p75^{NTR}$ binding non-peptide small molecules that structurally mimic loop1 of NGF. LM11A-24 and LM11A-31 displayed good oral bioavailability and penetration of BBB in vivo [279], inhibited pro-NGF induced apoptosis in oligodendrocytes and Aβ-induced toxicity in hippocampal neurons [280], improved recovery after spinal cord injury in animals

[279] and surprisingly alleviated behavioural deficits, reversed neurite dystrophy and reduced tau misfolding and phosphorylation in the $hAPP^{Lond/Swe}$ and Tg2576 mouse models of AD [281-283]. Currently phase II clinical trial of LM11A-31 in mild-moderate AD patients has been completed but results have not been released yet (ClinicalTrials.gov Identifier: NCT03069014).

p75ECD-Fc

Recent studies also focused on restoring the balance between the neuroprotective p75ECD and $p75^{NTR}$ full length receptor in the brain. Wang and Zhou group has made significant contribution to understand the roles of $p75^{NTR}$ and its extracellular domain in the pathogenesis of AD [242,243]. They showed that brain delivery of AAV-ECD reduced cognitive deficits and neuropathology in AD mice [238]. Furthermore, the intramuscular injection of AAV-p75ECD-Fc has reduced Aβ production and Tau phosphorylation and improved cognitive deficits [240]. In addition, p75ECD-Fc improved memory functions and suppressed Tau pathology in P301L, a mouse model of FTDP-17 [227]. Based on these findings, a human recombinant fusion protein of p75 extracellular domain and Fc fragment of human immunoglobulin IgG1 (p75ECD-Fc) was first synthesized in cooperation with Fujian Tiantai and Wuxi APPtec in China. It was successfully produced in Chinese Hamster Ovary (CHO) cells with stable expression and high purity as a homodimer with disulfide linkage between the two monomers (molecular weight 130 kDa). However, little is known about the mechanism of action of that recombinant protein and its pharmacokinetics and stability *in vivo* and *in vitro*.

In this dissertation, we aimed to investigate the efficacy of peripheral administration of the recombinant protein p75ECD-Fc in AD mice. In these ways, we overcome two drawbacks; first: the use of viral vector to deliver the gene as it is not desirable due to possible biohazard, second: brain delivery is not convenient in clinical settings due to the invasiveness of the

procedure. We also aimed to investigate the pharmacokinetics and tissue distribution of p75ECD-Fc following peripheral injection in rats and, primarily, to see if it can cross the BBB to better understand the possible mechanism of action. We propose that p75ECD-Fc may act through two possible mechanisms of action: first, centrally as a scavenger of Aβ and proneurotrophins and competitively antagonizes their neurotoxic effects by blocking the activation of the $p75^{NTR}$ full-length receptor. Second, we assume that p75ECD-Fc may act like anti-Aβ antibody which binds Aβ forming Aβ-p75ECD-Fc complex that is recognized and phagocytosed by the brain microglia and resident macrophages in the periphery through its Fc tail. We believe that such approach will have minimal side effects compared to those observed with Aβ antibodies due to its structural similarity with the endogenous molecule and will not result in central immune-related adverse events, possibly due to enhancing the peripheral Aβ clearance.

Clearance of Aβ through brain microglia is inefficient in AD due to defective phagocytic ability that is caused by persistent inflammatory responses, but this process can be enhanced by Aβ-binding molecules, such as anti-Aβ antibodies [284]. Beside enzymatic degradation of Aβ in the brain (via IDE, neprilysin and other enzymes) [285], Aβ is transported via the interstitial fluid (ISF) into the cerebrospinal fluid (CSF) via bulk flow; however, this has been proved to be a minor route for Aβ clearance, as it only accounts for nearly 10% of Aβ clearance [286]. The other main route of Aβ clearance from the brain is believed to occur through direct trafficking out of the brain via LDL receptor–related protein-1 (LRP-1) and P-glycoprotein [286] at the BBB into peripheral circulation, through which 40-60% of brain Aβ is cleared mainly through the liver and kidney [154]. Wang and colleagues have provided clear evidence of the significance and efficacy of peripheral Aβ clearance in AD, by constructing a parabiosis model in AD mice and found that peritoneal dialysis reduced brain Aβ burden and neuropathology in AD mice [287]. They also found that plasma Aβ levels significantly

decreased immediately after peritoneal dialysis in patients with chronic kidney disease [288]. In addition, levels of brain Aβ increased significantly in chronic kidney diseases or cirrhosis patients and that indicates the substantial impact of peripheral organs in clearing brain Aβ [289,290].

Based on the above-mentioned evidence, we assume that p75ECD-Fc may capture Aβ and enhance its peripheral clearance which will shift the balance towards Aβ efflux from the brain to the periphery and therefore, may promote plaque dissociation and clearance from the brain and this is referred to as "peripheral sink mechanism" for peripheral Aβ clearance.

4.2.3 Therapies based on reducing Tau phosphorylation and misfolding in AD and FTD-Tau

Work by Holzer et al. has developed small molecule inhibitors of three kinases: GSK-3β, Cdk5 and Cdk1, that are related to Tau pathology. These new agents were able to show selectivity and potency towards the corresponding kinases and significantly reduced tau phosphorylation [291]. Giacomini et al. developed a small molecule inhibitor to TAOKs (Thousand-and-One Amino Acid Kinases) which are recently identified to be involved in tau phosphorylation and are activated at the tangles of AD and FTD brain. This TAOK inhibitor reduced aberrant Tau phosphorylation in induced pluripotent stem cell-derived neurons (iPSCs) from FTLD patients, as well as cortical neurons from a transgenic mouse model of tauopathy [292]. Other potential drug candidates have been recently screened for their efficacy to reduce Tau phosphorylation in vitro such as Roscovitine (CDK5 inhibitor), Saracatinib (Src/Fyn kinase inhibitor), TBB (a casein kinase II inhibitor) and three GSK-3 small molecule kinase inhibitors (Lithium Chloride, AR, and A-107) [293]. However, the phase IIa randomized clinical trial of Saracatinib in mild AD patients showed no significant effects of the drug on either CSF total Tau or pTau [294]. Another strategy is to enhance Tau elimination using anti-tau immunotherapies. Clinical trials of several anti-tau monoclonal antibodies and vaccines are still ongoing to assess their safety

and immunogenicity in patients with AD and other tauopathies. Initial results from a clinical study of subcutaneous injections of AADvac-1 active immunization in mild to moderate AD patients are encouraging (ClinicalTrials.gov Identifier: NCT02579252) [295]. The use of small interfering RNAs (siRNAs) to reduce Tau expression proved to be effective in animal models of tauopathies. Another different strategy is to prevent Tau aggregation via reduction of tau proteins levels using antisense oligonucleotides (ASOs). Preliminary clinical studies with ASOs in patients with mild AD are currently underway (ClinicalTrials.gov Identifier NCT03186989) [296]. Nusinersen, an ASO drug that modulates pre-messenger RNA splicing has already been approved for clinical use in spinal muscular atrophy [297].

4.2.4 Oxidative stress-based therapies, anti-inflammatory and neuroprotective approaches

Therapeutic approaches including vitamins (Vitamin E, C and B_{12}), flavonoids (Curcumin and Resveratrol) and active antioxidants (Selenium, Selegiline and α-lipoic acid) represent a hopeful strategy to delay or prevent the disease progression. Several studies have reported promising results of antioxidants in AD animal models in terms of neuroprotection, antioxidant and anti-inflammatory effects [298-300], however, results from randomized clinical trials are not consistent and inconclusive [301-304]. Administration of cocktail antioxidants combined with traditional therapies may be more effective than when the antioxidant is given alone [250]. Besides, developing compounds that can cross the BBB and directly target the mitochondria such as Coenzyme Q may be promising. Curcumin has been reported to have potential benefits in cognition and is effective in reducing Aβ and Tau aggregation besides its many-sided actions as antioxidant, anti-inflammatory, anti-angiogenic, and neuroprotective. Studies showed that Curcumin stimulates Aβ uptake and phagocytosis by microglia/macrophages [305] and inhibits JNK signaling pathway [306]. Clinical studies are ongoing to assess the efficacy and tolerability of a number of novel curcumin formulations and analogues with enhanced oral

bioavailability [307]. Another compound; *scyllo*-Inositol (one of the stereoisomers of Inositol) is a naturally occurring compound that can cross the BBB and has been shown to inhibit Aβ aggregation and break up oligomers [308].

Other therapeutic strategies have been investigated and some have demonstrated beneficial effects in clinical trials through their anti-inflammatory and neuroprotective effects besides reducing the activity of BACE and γ-secretases such as non-steroidal anti-inflammatory drugs (NSAIDs), anti-TNF-α, Peroxisome proliferators activated receptor (PPARγ) agonists [309]. Non-pharmacological treatments and lifestyle interventions such as regular physical activity and caloric restriction have gained much attention due to their benefits on health and life span and improving cognitive function specifically with prediabetic individuals [310,311].

Edaravone

Edaravone (3-methyl-1-phenyl-2-pyrazolin-5-one, MCI-186) is a potent free radical scavenger and antioxidant, developed by Mitsubishi Tanabe Pharma Corporation (Osaka, Japan). It is a white to yellowish white crystalline powder that is freely soluble in acetic acid, methanol, or ethanol, while poorly soluble in water or diethyl ether [312]. The lipophilic moieties in Edaravone (phenyl and methyl groups) render it able to penetrate the BBB [313].

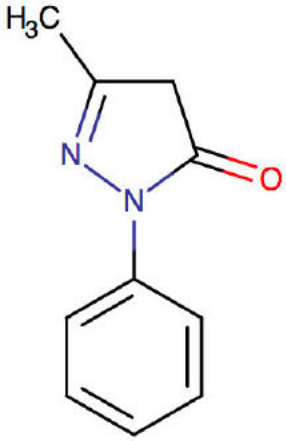


Figure 9 Chemical structure of Edaravone.

Edaravone may act by reducing the oxidative injury in neurons and eliminating free radicals and lipid peroxidation products [314]. Studies showed that Edaravone attenuates cell apoptosis and protects the stability and integrity of the BBB through activation of Nrf2/HO-1 pathway (the nuclear factor erythroid 2-related factor/ hemeoxygenase-1) [315,316]. Researchers also found that Edaravone may exert neuroprotective effect through suppressing gene expression of Fas signaling pathway following ischemia in rats [317,318]. Edaravone may exert

neuroprotection and antiapoptotic effects by blocking cytosolic release of cytochrome *c* and caspase-3 activation in hypoxic-ischemic (HI) brain injury in neonatal rats [319], besides, it reportedly upregulated Bcl-2 and downregulated Bax expression in a transient focal ischemia model in rats [320].

Currently, Edaravone is approved for treatment of acute ischemic stroke in Japan and other Asian countries and for the treatment of amyotrophic lateral sclerosis (ALS) by the FDA under the name of Radicava® provided as intravenous infusion. Clinical studies showed that EDR reduces neuronal damage and suppressed proinflammatory responses following brain ischemia [321,322] and inhibits motor functional deterioration in ALS patients [323]. However, the main drawback for Edaravone use is that it requires to be administered as IV infusion on regular basis which is inconvenient and challenging for patients with progressive degenerative disorders. Currently, a Phase III clinical trial is ongoing to assess the efficacy and Safety of two dosing regimens of oral Edaravone administration in subjects with ALS (ClinicalTrials.gov Identifier: NCT04569084).

Edaravone is considered the first disease modifying therapy to be approved and holds great promise to alleviate several other neurodegenerative diseases by targeting multiple key pathways of the disease pathogenesis. In this respect, animal studies showed that treatment of APP/PS1 AD mice with Edaravone intraperitoneal injection either before or after the onset of Aβ disposition reduced the plaque load in the brain, alleviated oxidative stress and reduced downstream pathologies including neuroinflammation, synaptic dysfunction and apoptosis and ameliorated cognitive deficits in AD mice [324]. Edaravone also reduced Tau phosphorylation through inhibiting GSK-3β activity in AD mice. Studies also reported that Edaravone suppressed the fibrillation of Aβ *in vitro* and induced dissociation of the preformed Aβ fibrils. Furthermore, Edaravone protected human neuroblastoma derived neurons (SH-SY5Y cells) against Aβ-induced neurotoxicity and neurite collapse [324].

In line with this study, Parikh and colleagues [325,326] have successfully designed a novel oral Edaravone formulation and demonstrated that it can dose-dependently reverse the cognitive deficits and mood disorders of very old APP/PS1 mice (17 months). The new formulation was designed by using self-nano micellizing solid dispersion strategy of Edaravone and Soluplus as a drug carrier in a ratio of 1:5 EDR/Soluplus and it proved to be safe and effective *in vitro* and in AD mice. This formulation displayed high aqueous solubility and enhanced oral bioavailability compared to Edaravone suspension in rats. Authors also reported that effective micellar encapsulation of Edaravone by Soluplus reduced the intestinal metabolic degradation of the drug and inhibited P-glycoprotein efflux, which could explain the improved oral bioavailability of this formulation.

Therefore, in this dissertation, we aimed to investigate the effect of Edaravone treatment on cognitive deficits and tau pathology of P301L mice, a model of frontotemporal dementia with parkinsonism linked to chromosome-17 (FTDP-17), that develops age-dependent hyperphosphorylated Tau in several brain regions and shows behavioural and motor deficits similar to that observed in certain tauopathies in humans [327,328]. Besides, this animal model shows signs of oxidative stress and mitochondrial dysfunction that becomes significant at advanced age [119]. We hypothesized that EDR will suppress oxidative stress and subsequent microglial activation and therefore might inhibit the disease progression and protect neurons against progressive damage in P301L mice. These experiments will reveal the potential benefits of Edaravone as a disease-modifying therapy for AD and FTD.

5. Animal models of Alzheimer's disease and Frontotemporal dementia with Tau pathology

Many transgenic animal models of AD and FTD have been developed in the past few years. So far, there are 10 transgenic AD mouse models including PDAPP, TG2576, APP23,

TgCRND8, J20, APP/PS1, TG2576+PS1(M146L), APP/PS1KI, 5×FAD, and 3×Tg-AD) [329]. These animal models have been useful to test mechanistic hypotheses of the disease and to assess and predict outcomes of potential therapeutic interventions. However, no single mouse model of AD or FTD has fully recapitulated all neuropathological aspects of the disease in human. This might explain why many therapeutics especially of disease-modifying approaches have failed in clinical settings [330].

There are many discrepancies in behaviour and neuropathology between transgenic AD models and the disease in humans [331]. For example, most AD models lack Tau tangles and extensive neuronal loss, and the severity and nature of inflammation in AD is not exactly modelled in mice. Also, the size and exact distribution of plaques seen in the brains of AD patients have not been observed in any available model [332]. Besides, the time course of cognitive decline and the progression of pathological changes differ among different mouse models and poorly correlate to the disease progression in humans [333,334]. Moreover, most of these models represent the genetic form of the disease (familial type) which accounts for 1-5% of AD cases. Hence, there is no desirable model which mimics all pathological features of AD and none of them could represent the prevailing sporadic AD [329].

The most common AD mouse model is APP/PS1 (a double transgenic bearing the APP Swedish mutation and PSEN1) was first described by Jankowsky et al. [335]. It only partially mimics some features of the disease, and these occur against the natural consequential events; i.e. amyloid plaques occur first, cognitive impairment occurs very late and there are no obvious tangles or neuronal death. More evidence indicates that inflammation in the brain is one of the earliest markers for sporadic AD. In the period between the appearance of initial symptoms and the full development of the disease, the sequence of events occurring in the brain starts with inflammation of the nervous tissue, followed by synaptic dysfunction and mild cognitive impairment. Subsequently, the accumulation of abnormal amyloid plaques and the

development of tangles and nerve cell death occur (66-68). Thus, the best model of AD should not only model the hallmarks of the disease but also model the sequential events of the disease's progression.

In this perspective, studies have shown that upon injecting rats and mice once or twice directly into the brain with streptozotocin (STZ), they develop Alzheimer's disease-like features in a sequence similar to that which occurs in human Alzheimer's disease (69) characterized by a progressive deterioration of memory, cerebral glucose and energy dysmetabolism as well as presence of oxidative stress (71-73). Thus, intracerebroventricular (ICV) STZ model in rodents has been described as a non-transgenic animal model of sporadic AD that models the risk factors of the disease such as type 2 Diabetes.

Thus, the aim of this experiment was to develop and characterise an animal model of AD that reproduces most features of the disease and is progressive in nature. We also aimed to combine genetic and etiologic risk factors, to better represent the most prevailing and multifactorial sporadic AD. To achieve our goal, APP/PS1 mice received one dose of STZ ICV injection and the effects of STZ on cognitive and pathologic hallmarks were assessed.

Animal models of Tauopathies Mouse lines expressing human tau with mutations P301L, G272V, V337M, R406W, P301S and the triple mutation G272V, P301L and V337M have been developed [20]. P301L mouse (pR5 construct), first characterized by Götz et al. in 2001, is widely used as a model of FTD with MAPT gene mutation with parkinsonism linked to chromosome 17. It expresses the longest human Tau40 isoform (4R/2N) under the control of murine Thy1.2 promoter [328]. This mouse exhibits progressive neuropathology with aging that is consistent with human tauopathies (FTDP-17). Hyperphosphorylated tau at distinct epitopes is expressed in the cortex, hippocampus, and amygdala as well as pretangle Tau filaments associated with apoptosis and astrocytosis that were detected in the cortical area and

amygdala but not in the hippocampus. This mouse also shows mitochondrial dysfunction associated with high levels of ROS with aging, consistent with carriers of P301L mutation who have reduction in mitochondrial complex V [119]. Besides memory impairment, this mouse develops minor motor deficits at late age, reflecting the expression of Tau transgene in the spinal cord [328,336,337].

P301L mouse model was utilized in this dissertation to study the effect of Edaravone treatment on Tau pathology and oxidative stress as a potential disease modifying therapy for AD and FTD.

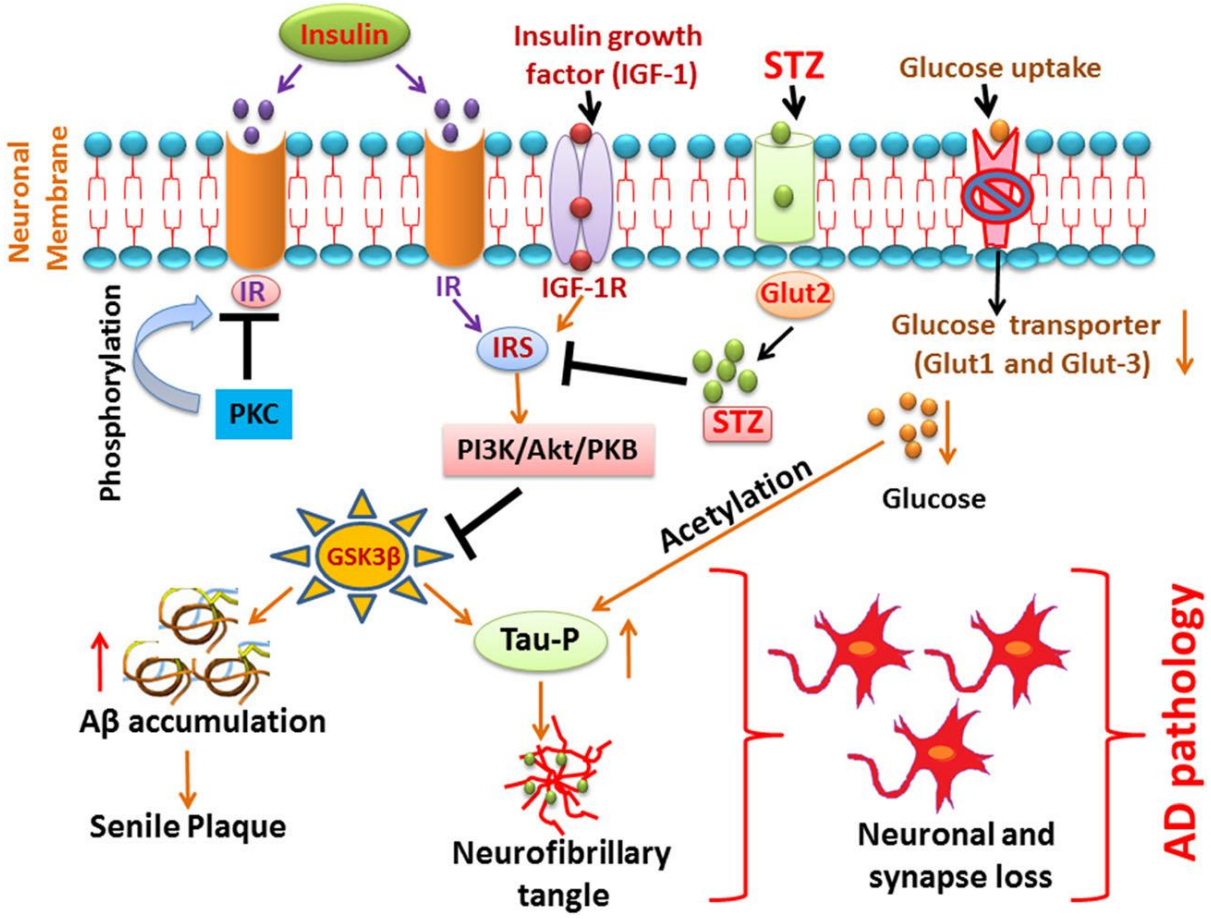


Figure 10 Mechanism of STZ-induced neurotoxicity and AD pathology. Schematic diagram represents how insulin and STZ are taken up by the receptor through membrane channels. There is a glucose receptor in the membrane which facilitates the intake of STZ GLUT2 receptor and other GLUT1 and GLUT3 that are also involved in the uptake of glucose. Insulin is mainly taken up by the insulin receptor. Insulin growth factor is usually taken up by its receptor IGF-1R. After intake of STZ in the cells, STZ inhibits the insulin receptor signaling (IRS) and thus PI3K and AKT. Inhibition of PI3K and AKT also inhibits the GSK-3β which facilitates the Aβ accumulation and tau hyperphosphorylation. Aβ accumulation promotes the senile plaque formation, and tau hyperphosphorylation promotes the neurofibrillary tangle formation. These abnormal processes cause degeneration of synapse and thus abolish the neurons. On the other hand, the protein kinases B/C also inhibit the insulin receptor (IR) by their hyperphosphorylation and hinder the normal function of insulin in neurons. Reproduced with permission from Kamat et al. 2016 [338].

6. Hypotheses and Aims.

Hypotheses:

1. Restorations of the abnormally low levels of p75ECD in AD brain through IV injection of p75ECD-Fc in AD animal model (APP/PS1 mouse) could retain the neurotrophin balance and rescue neurons against degeneration.

2. The antioxidant Edaravone can provide a promising therapeutic approach to target oxidative stress, the key factor in the pathophysiology of neurodegenerative disorders, in an animal model of FTD (P301L mouse).

3. Streptozotocin ICV injection in APP/PS1 could recapitulate most neuropathological features of AD and is a promising approach to test future therapies for AD.

Aims:

1. To describe the pharmacokinetics of recombinant p75ECD-Fc by IV and SC injection in Sprague Dawley rats.

2. To investigate whether the drug candidate p75ECD-Fc has the therapeutic effect and improves cognitive decline in APP/PS1 AD mice.

3. To investigate the efficacy of Edaravone in alleviating Tau pathology in P301L mouse model of FTDP-17.

4. To establish a new model of Alzheimer's disease by intracerebroventricular injection of streptozotocin into the brain of APP/PS1.

References:

1. Braak H, Braak E, Bohl J (1993) Staging of Alzheimer-related cortical destruction. Eur Neurol 33 (6):403-408. doi:10.1159/000116984
2. Alzheimer's Disease International: World Alzheimer Report 2018; The state of the art of dementia research: New frontiers (2018).
3. DA 2020. Dementia statistics. Australia: DA.
4. Reitz C, Mayeux R (2014) Alzheimer disease: epidemiology, diagnostic criteria, risk factors and biomarkers. Biochem Pharmacol 88 (4):640-651. doi:10.1016/j.bcp.2013.12.024
5. Campion D, Dumanchin C, Hannequin D, Dubois B, Belliard S, Puel M, Thomas-Anterion C, Michon A, Martin C, Charbonnier F, Raux G, Camuzat A, Penet C, Mesnage V, Martinez M, Clerget-Darpoux F, Brice A, Frebourg T (1999) Early-Onset Autosomal Dominant Alzheimer Disease: Prevalence, Genetic Heterogeneity, and Mutation Spectrum. The American Journal of Human Genetics 65 (3):664-670. doi:https://doi.org/10.1086/302553
6. Farrer LA, Cupples LA, Haines JL, Hyman B, Kukull WA, Mayeux R, Myers RH, Pericak-Vance MA, Risch N, van Duijn CM (1997) Effects of age, sex, and ethnicity on the association between apolipoprotein E genotype and Alzheimer disease. A meta-analysis. APOE and Alzheimer Disease Meta Analysis Consortium. Jama 278 (16):1349-1356
7. Roses AD (2006) On the discovery of the genetic association of Apolipoprotein E genotypes and common late-onset Alzheimer disease. J Alzheimers Dis 9 (3 Suppl):361-366. doi:10.3233/jad-2006-9s340
8. Aleshkov S, Abraham CR, Zannis VI (1997) Interaction of nascent ApoE2, ApoE3, and ApoE4 isoforms expressed in mammalian cells with amyloid peptide beta (1-40). Relevance to Alzheimer's disease. Biochemistry 36 (34):10571-10580. doi:10.1021/bi9626362
9. Holtzman DM, Morris JC, Goate AM (2011) Alzheimer's disease: the challenge of the second century. Sci Transl Med 3 (77):77sr71. doi:10.1126/scitranslmed.3002369
10. Sieben A, Van Langenhove T, Engelborghs S, Martin JJ, Boon P, Cras P, De Deyn PP, Santens P, Van Broeckhoven C, Cruts M (2012) The genetics and neuropathology of frontotemporal lobar degeneration. Acta Neuropathol 124 (3):353-372. doi:10.1007/s00401-012-1029-x
11. Bott NT, Radke A, Stephens ML, Kramer JH (2014) Frontotemporal dementia: diagnosis, deficits and management. Neurodegener Dis Manag 4 (6):439-454. doi:10.2217/nmt.14.34
12. Onyike CU, Diehl-Schmid J (2013) The epidemiology of frontotemporal dementia. Int Rev Psychiatry 25 (2):130-137. doi:10.3109/09540261.2013.776523
13. Rademakers R, Neumann M, Mackenzie IR (2012) Advances in understanding the molecular basis of frontotemporal dementia. Nature reviews Neurology 8 (8):423-434. doi:10.1038/nrneurol.2012.117
14. Panza F, Lozupone M, Seripa D, Daniele A, Watling M, Giannelli G, Imbimbo BP (2020) Development of disease-modifying drugs for frontotemporal dementia spectrum disorders. Nature Reviews Neurology 16 (4):213-228. doi:10.1038/s41582-020-0330-x
15. Hutton M, Lendon CL, Rizzu P, Baker M, Froelich S, Houlden H, Pickering-Brown S, Chakraverty S, Isaacs A, Grover A, Hackett J, Adamson J, Lincoln S, Dickson D, Davies P, Petersen RC, Stevens M, de Graaff E, Wauters E, van Baren J, Hillebrand M, Joosse M, Kwon JM, Nowotny P, Che LK, Norton J, Morris JC, Reed LA, Trojanowski J, Basun H, Lannfelt L, Neystat M, Fahn S, Dark F, Tannenberg T, Dodd PR, Hayward N, Kwok JB, Schofield PR, Andreadis A, Snowden J, Craufurd D, Neary D, Owen F, Oostra BA, Hardy J, Goate A, van Swieten J, Mann D, Lynch T, Heutink P (1998) Association of missense and 5'-splice-site mutations in tau with the inherited dementia FTDP-17. Nature 393 (6686):702-705. doi:10.1038/31508

16. Snowden JS, Rollinson S, Thompson JC, Harris JM, Stopford CL, Richardson AM, Jones M, Gerhard A, Davidson YS, Robinson A, Gibbons L, Hu Q, DuPlessis D, Neary D, Mann DM, Pickering-Brown SM (2012) Distinct clinical and pathological characteristics of frontotemporal dementia associated with C9ORF72 mutations. Brain 135 (Pt 3):693-708. doi:10.1093/brain/awr355
17. Pickering-Brown SM, Baker M, Gass J, Boeve BF, Loy CT, Brooks WS, Mackenzie IR, Martins RN, Kwok JB, Halliday GM, Kril J, Schofield PR, Mann DM, Hutton M (2006) Mutations in progranulin explain atypical phenotypes with variants in MAPT. Brain 129 (Pt 11):3124-3126. doi:10.1093/brain/awl289
18. Watts GD, Wymer J, Kovach MJ, Mehta SG, Mumm S, Darvish D, Pestronk A, Whyte MP, Kimonis VE (2004) Inclusion body myopathy associated with Paget disease of bone and frontotemporal dementia is caused by mutant valosin-containing protein. Nat Genet 36 (4):377-381. doi:10.1038/ng1332
19. Skibinski G, Parkinson NJ, Brown JM, Chakrabarti L, Lloyd SL, Hummerich H, Nielsen JE, Hodges JR, Spillantini MG, Thusgaard T, Brandner S, Brun A, Rossor MN, Gade A, Johannsen P, Sørensen SA, Gydesen S, Fisher EM, Collinge J (2005) Mutations in the endosomal ESCRTIII-complex subunit CHMP2B in frontotemporal dementia. Nat Genet 37 (8):806-808. doi:10.1038/ng1609
20. Goedert M, Jakes R (2005) Mutations causing neurodegenerative tauopathies. Biochim Biophys Acta 1739 (2-3):240-250. doi:10.1016/j.bbadis.2004.08.007
21. De Strooper B, Karran E (2016) The Cellular Phase of Alzheimer's Disease. Cell 164 (4):603-615. doi:10.1016/j.cell.2015.12.056
22. Serrano-Pozo A, Frosch MP, Masliah E, Hyman BT (2011) Neuropathological alterations in Alzheimer disease. Cold Spring Harb Perspect Med 1 (1):a006189. doi:10.1101/cshperspect.a006189
23. Querfurth HW, LaFerla FM (2010) Alzheimer's Disease. New England Journal of Medicine 362 (4):329-344. doi:10.1056/NEJMra0909142
24. Bartus RT, Dean RL, 3rd, Beer B, Lippa AS (1982) The cholinergic hypothesis of geriatric memory dysfunction. Science 217 (4558):408-414. doi:10.1126/science.7046051
25. Haass C, Selkoe DJ (2007) Soluble protein oligomers in neurodegeneration: lessons from the Alzheimer's amyloid beta-peptide. Nat Rev Mol Cell Biol 8 (2):101-112. doi:10.1038/nrm2101
26. Zhang T, Chen D, Lee TH (2019) Phosphorylation Signaling in APP Processing in Alzheimer's Disease. Int J Mol Sci 21 (1). doi:10.3390/ijms21010209
27. Morley JE, Farr SA, Nguyen AD, Xu F (2019) What is the Physiological Function of Amyloid-Beta Protein? The journal of nutrition, health & aging 23 (3):225-226. doi:10.1007/s12603-019-1162-5
28. Bishop GM, Robinson SR (2004) Physiological roles of amyloid-beta and implications for its removal in Alzheimer's disease. Drugs Aging 21 (10):621-630. doi:10.2165/00002512-200421100-00001
29. Selkoe DJ (2001) Alzheimer's disease: genes, proteins, and therapy. Physiol Rev 81 (2):741-766. doi:10.1152/physrev.2001.81.2.741
30. Busciglio J, Pelsman A, Wong C, Pigino G, Yuan M, Mori H, Yankner BA (2002) Altered metabolism of the amyloid beta precursor protein is associated with mitochondrial dysfunction in Down's syndrome. Neuron 33 (5):677-688. doi:10.1016/s0896-6273(02)00604-9
31. Lue LF, Kuo YM, Roher AE, Brachova L, Shen Y, Sue L, Beach T, Kurth JH, Rydel RE, Rogers J (1999) Soluble amyloid beta peptide concentration as a predictor of synaptic change in Alzheimer's disease. Am J Pathol 155 (3):853-862. doi:10.1016/s0002-9440(10)65184-x
32. Selkoe DJ (2008) Soluble oligomers of the amyloid beta-protein impair synaptic plasticity and behavior. Behav Brain Res 192 (1):106-113. doi:10.1016/j.bbr.2008.02.016

33. Klein WL (2002) Abeta toxicity in Alzheimer's disease: globular oligomers (ADDLs) as new vaccine and drug targets. Neurochem Int 41 (5):345-352. doi:10.1016/s0197-0186(02)00050-5
34. Lacor PN, Buniel MC, Furlow PW, Sanz Clemente A, Velasco PT, Wood M, Viola KL, Klein WL (2007) Aβ Oligomer-Induced Aberrations in Synapse Composition, Shape, and Density Provide a Molecular Basis for Loss of Connectivity in Alzheimer's Disease. The Journal of Neuroscience 27 (4):796-807. doi:10.1523/jneurosci.3501-06.2007
35. Glabe CC (2005) Amyloid accumulation and pathogensis of Alzheimer's disease: significance of monomeric, oligomeric and fibrillar Abeta. Subcell Biochem 38:167-177. doi:10.1007/0-387-23226-5_8
36. Townsend M, Shankar GM, Mehta T, Walsh DM, Selkoe DJ (2006) Effects of secreted oligomers of amyloid beta-protein on hippocampal synaptic plasticity: a potent role for trimers. J Physiol 572 (Pt 2):477-492. doi:10.1113/jphysiol.2005.103754
37. Kamenetz F, Tomita T, Hsieh H, Seabrook G, Borchelt D, Iwatsubo T, Sisodia S, Malinow R (2003) APP processing and synaptic function. Neuron 37 (6):925-937. doi:10.1016/s0896-6273(03)00124-7
38. Kanemitsu H, Tomiyama T, Mori H (2003) Human neprilysin is capable of degrading amyloid beta peptide not only in the monomeric form but also the pathological oligomeric form. Neurosci Lett 350 (2):113-116. doi:10.1016/s0304-3940(03)00898-x
39. Qiu WQ, Walsh DM, Ye Z, Vekrellis K, Zhang J, Podlisny MB, Rosner MR, Safavi A, Hersh LB, Selkoe DJ (1998) Insulin-degrading enzyme regulates extracellular levels of amyloid beta-protein by degradation. J Biol Chem 273 (49):32730-32738. doi:10.1074/jbc.273.49.32730
40. Leissring MA, Farris W, Chang AY, Walsh DM, Wu X, Sun X, Frosch MP, Selkoe DJ (2003) Enhanced proteolysis of beta-amyloid in APP transgenic mice prevents plaque formation, secondary pathology, and premature death. Neuron 40 (6):1087-1093. doi:10.1016/s0896-6273(03)00787-6
41. Iwata N, Tsubuki S, Takaki Y, Shirotani K, Lu B, Gerard NP, Gerard C, Hama E, Lee HJ, Saido TC (2001) Metabolic regulation of brain Abeta by neprilysin. Science 292 (5521):1550-1552. doi:10.1126/science.1059946
42. Farris W, Mansourian S, Chang Y, Lindsley L, Eckman EA, Frosch MP, Eckman CB, Tanzi RE, Selkoe DJ, Guenette S (2003) Insulin-degrading enzyme regulates the levels of insulin, amyloid beta-protein, and the beta-amyloid precursor protein intracellular domain in vivo. Proc Natl Acad Sci U S A 100 (7):4162-4167. doi:10.1073/pnas.0230450100
43. Miners JS, Baig S, Tayler H, Kehoe PG, Love S (2009) Neprilysin and insulin-degrading enzyme levels are increased in Alzheimer disease in relation to disease severity. J Neuropathol Exp Neurol 68 (8):902-914. doi:10.1097/NEN.0b013e3181afe475
44. Götz J, Halliday G, Nisbet R (2019) Molecular Pathogenesis of the Tauopathies. Annual Review of Pathology: Mechanisms of Disease 14. doi:10.1146/annurev-pathmechdis-012418-012936
45. Arriagada PV, Growdon JH, Hedley-Whyte ET, Hyman BT (1992) Neurofibrillary tangles but not senile plaques parallel duration and severity of Alzheimer's disease. Neurology 42 (3 Pt 1):631-639. doi:10.1212/wnl.42.3.631
46. Ingelsson M, Fukumoto H, Newell KL, Growdon JH, Hedley-Whyte ET, Frosch MP, Albert MS, Hyman BT, Irizarry MC (2004) Early Abeta accumulation and progressive synaptic loss, gliosis, and tangle formation in AD brain. Neurology 62 (6):925-931. doi:10.1212/01.wnl.0000115115.98960.37
47. Giannakopoulos P, Herrmann FR, Bussière T, Bouras C, Kövari E, Perl DP, Morrison JH, Gold G, Hof PR (2003) Tangle and neuron numbers, but not amyloid load, predict cognitive

status in Alzheimer's disease. Neurology 60 (9):1495-1500. doi:10.1212/01.wnl.0000063311.58879.01
48. Braak H, Braak E (1991) Neuropathological stageing of Alzheimer-related changes. Acta Neuropathologica 82 (4):239-259. doi:10.1007/BF00308809
49. Sharma VM, Litersky JM, Bhaskar K, Lee G (2007) Tau impacts on growth-factor-stimulated actin remodeling. Journal of Cell Science 120 (5):748-757. doi:10.1242/jcs.03378
50. Mietelska-Porowska A, Wasik U, Goras M, Filipek A, Niewiadomska G (2014) Tau protein modifications and interactions: their role in function and dysfunction. International journal of molecular sciences 15 (3):4671-4713. doi:10.3390/ijms15034671
51. Ittner LM, Ke YD, Delerue F, Bi M, Gladbach A, van Eersel J, Wölfing H, Chieng BC, Christie MJ, Napier IA, Eckert A, Staufenbiel M, Hardeman E, Götz J (2010) Dendritic function of tau mediates amyloid-beta toxicity in Alzheimer's disease mouse models. Cell 142 (3):387-397. doi:10.1016/j.cell.2010.06.036
52. DuBoff B, Götz J, Feany MB (2012) Tau promotes neurodegeneration via DRP1 mislocalization in vivo. Neuron 75 (4):618-632. doi:10.1016/j.neuron.2012.06.026
53. Stamer K, Vogel R, Thies E, Mandelkow E, Mandelkow EM (2002) Tau blocks traffic of organelles, neurofilaments, and APP vesicles in neurons and enhances oxidative stress. J Cell Biol 156 (6):1051-1063. doi:10.1083/jcb.200108057
54. Oddo S, Vasilevko V, Caccamo A, Kitazawa M, Cribbs DH, LaFerla FM (2006) Reduction of soluble Abeta and tau, but not soluble Abeta alone, ameliorates cognitive decline in transgenic mice with plaques and tangles. J Biol Chem 281 (51):39413-39423. doi:10.1074/jbc.M608485200
55. Iqbal K, Alonso Adel C, Chen S, Chohan MO, El-Akkad E, Gong CX, Khatoon S, Li B, Liu F, Rahman A, Tanimukai H, Grundke-Iqbal I (2005) Tau pathology in Alzheimer disease and other tauopathies. Biochim Biophys Acta 1739 (2-3):198-210. doi:10.1016/j.bbadis.2004.09.008
56. Lee HG, Perry G, Moreira PI, Garrett MR, Liu Q, Zhu X, Takeda A, Nunomura A, Smith MA (2005) Tau phosphorylation in Alzheimer's disease: pathogen or protector? Trends Mol Med 11 (4):164-169. doi:10.1016/j.molmed.2005.02.008
57. Gamblin TC, Chen F, Zambrano A, Abraha A, Lagalwar S, Guillozet AL, Lu M, Fu Y, Garcia-Sierra F, LaPointe N, Miller R, Berry RW, Binder LI, Cryns VL (2003) Caspase cleavage of tau: linking amyloid and neurofibrillary tangles in Alzheimer's disease. Proc Natl Acad Sci U S A 100 (17):10032-10037. doi:10.1073/pnas.1630428100
58. Guillozet-Bongaarts AL, Garcia-Sierra F, Reynolds MR, Horowitz PM, Fu Y, Wang T, Cahill ME, Bigio EH, Berry RW, Binder LI (2005) Tau truncation during neurofibrillary tangle evolution in Alzheimer's disease. Neurobiol Aging 26 (7):1015-1022. doi:10.1016/j.neurobiolaging.2004.09.019
59. Rissman RA, Poon WW, Blurton-Jones M, Oddo S, Torp R, Vitek MP, LaFerla FM, Rohn TT, Cotman CW (2004) Caspase-cleavage of tau is an early event in Alzheimer disease tangle pathology. The Journal of clinical investigation 114 (1):121-130. doi:10.1172/JCI20640
60. Cotman CW, Poon WW, Rissman RA, Blurton-Jones M (2005) The Role of Caspase Cleavage of Tau in Alzheimer Disease Neuropathology. Journal of Neuropathology & Experimental Neurology 64 (2):104-112. doi:10.1093/jnen/64.2.104
61. Terwel D, Muyllaert D, Dewachter I, Borghgraef P, Croes S, Devijver H, Van Leuven F (2008) Amyloid activates GSK-3beta to aggravate neuronal tauopathy in bigenic mice. The American journal of pathology 172 (3):786-798. doi:10.2353/ajpath.2008.070904
62. Zheng WH, Bastianetto S, Mennicken F, Ma W, Kar S (2002) Amyloid beta peptide induces tau phosphorylation and loss of cholinergic neurons in rat primary septal cultures. Neuroscience 115 (1):201-211. doi:10.1016/s0306-4522(02)00404-9

63. Kim HS, Kim EM, Lee JP, Park CH, Kim S, Seo JH, Chang KA, Yu E, Jeong SJ, Chong YH, Suh YH (2003) C-terminal fragments of amyloid precursor protein exert neurotoxicity by inducing glycogen synthase kinase-3beta expression. Faseb j 17 (13):1951-1953. doi:10.1096/fj.03-0106fje
64. Hoshi M, Sato M, Matsumoto S, Noguchi A, Yasutake K, Yoshida N, Sato K (2003) Spherical aggregates of beta-amyloid (amylospheroid) show high neurotoxicity and activate tau protein kinase I/glycogen synthase kinase-3beta. Proc Natl Acad Sci U S A 100 (11):6370-6375. doi:10.1073/pnas.1237107100
65. Liu T, Perry G, Chan HW, Verdile G, Martins RN, Smith MA, Atwood CS (2004) Amyloid-beta-induced toxicity of primary neurons is dependent upon differentiation-associated increases in tau and cyclin-dependent kinase 5 expression. J Neurochem 88 (3):554-563. doi:10.1046/j.1471-4159.2003.02196.x
66. Oddo S, Caccamo A, Shepherd JD, Murphy MP, Golde TE, Kayed R, Metherate R, Mattson MP, Akbari Y, LaFerla FM (2003) Triple-transgenic model of Alzheimer's disease with plaques and tangles: intracellular Abeta and synaptic dysfunction. Neuron 39 (3):409-421. doi:10.1016/s0896-6273(03)00434-3
67. Götz J, Chen F, van Dorpe J, Nitsch RM (2001) Formation of neurofibrillary tangles in P301l tau transgenic mice induced by Abeta 42 fibrils. Science 293 (5534):1491-1495. doi:10.1126/science.1062097
68. Lewis J, Dickson DW, Lin WL, Chisholm L, Corral A, Jones G, Yen SH, Sahara N, Skipper L, Yager D, Eckman C, Hardy J, Hutton M, McGowan E (2001) Enhanced neurofibrillary degeneration in transgenic mice expressing mutant tau and APP. Science 293 (5534):1487-1491. doi:10.1126/science.1058189
69. Roberson ED, Scearce-Levie K, Palop JJ, Yan F, Cheng IH, Wu T, Gerstein H, Yu GQ, Mucke L (2007) Reducing endogenous tau ameliorates amyloid beta-induced deficits in an Alzheimer's disease mouse model. Science 316 (5825):750-754. doi:10.1126/science.1141736
70. Rapoport M, Dawson HN, Binder LI, Vitek MP, Ferreira A (2002) Tau is essential to beta -amyloid-induced neurotoxicity. Proc Natl Acad Sci U S A 99 (9):6364-6369. doi:10.1073/pnas.092136199
71. Hoozemans JJ, Veerhuis R, Van Haastert ES, Rozemuller JM, Baas F, Eikelenboom P, Scheper W (2005) The unfolded protein response is activated in Alzheimer's disease. Acta Neuropathol 110 (2):165-172. doi:10.1007/s00401-005-1038-0
72. López Salon M, Morelli L, Castaño EM, Soto EF, Pasquini JM (2000) Defective ubiquitination of cerebral proteins in Alzheimer's disease. J Neurosci Res 62 (2):302-310. doi:10.1002/1097-4547(20001015)62:2<302::Aid-jnr15>3.0.Co;2-l
73. Lue LF, Brachova L, Civin WH, Rogers J (1996) Inflammation, A beta deposition, and neurofibrillary tangle formation as correlates of Alzheimer's disease neurodegeneration. J Neuropathol Exp Neurol 55 (10):1083-1088
74. Duan Y, Dong S, Gu F, Hu Y, Zhao Z (2012) Advances in the Pathogenesis of Alzheimer's Disease: Focusing on Tau-Mediated Neurodegeneration. Translational Neurodegeneration 1 (1):24. doi:10.1186/2047-9158-1-24
75. Selkoe DJ (2002) Alzheimer's disease is a synaptic failure. Science 298 (5594):789-791. doi:10.1126/science.1074069
76. DeKosky ST, Scheff SW (1990) Synapse loss in frontal cortex biopsies in Alzheimer's disease: correlation with cognitive severity. Ann Neurol 27 (5):457-464. doi:10.1002/ana.410270502
77. Scheff SW, Price DA, Schmitt FA, DeKosky ST, Mufson EJ (2007) Synaptic alterations in CA1 in mild Alzheimer disease and mild cognitive impairment. Neurology 68 (18):1501-1508. doi:10.1212/01.wnl.0000260698.46517.8f

78. Masliah E, Mallory M, Alford M, DeTeresa R, Hansen LA, McKeel DW, Jr., Morris JC (2001) Altered expression of synaptic proteins occurs early during progression of Alzheimer's disease. Neurology 56 (1):127-129. doi:10.1212/wnl.56.1.127
79. Masliah E, Crews L, Hansen L (2006) Synaptic remodeling during aging and in Alzheimer's disease. J Alzheimers Dis 9 (3 Suppl):91-99. doi:10.3233/jad-2006-9s311
80. Chen Q-S, Wei W-Z, Shimahara T, Xie C-W (2002) Alzheimer Amyloid β-Peptide Inhibits the Late Phase of Long-Term Potentiation through Calcineurin-Dependent Mechanisms in the Hippocampal Dentate Gyrus. Neurobiology of Learning and Memory 77 (3):354-371. doi:https://doi.org/10.1006/nlme.2001.4034
81. Shankar GM, Bloodgood BL, Townsend M, Walsh DM, Selkoe DJ, Sabatini BL (2007) Natural Oligomers of the Alzheimer Amyloid-β Protein Induce Reversible Synapse Loss by Modulating an NMDA-Type Glutamate Receptor-Dependent Signaling Pathway. The Journal of Neuroscience 27 (11):2866-2875. doi:10.1523/jneurosci.4970-06.2007
82. Zhou Q, Homma KJ, Poo MM (2004) Shrinkage of dendritic spines associated with long-term depression of hippocampal synapses. Neuron 44 (5):749-757. doi:10.1016/j.neuron.2004.11.011
83. Snyder EM, Nong Y, Almeida CG, Paul S, Moran T, Choi EY, Nairn AC, Salter MW, Lombroso PJ, Gouras GK, Greengard P (2005) Regulation of NMDA receptor trafficking by amyloid-β. Nature Neuroscience 8 (8):1051-1058. doi:10.1038/nn1503
84. Hsieh H, Boehm J, Sato C, Iwatsubo T, Tomita T, Sisodia S, Malinow R (2006) AMPAR removal underlies Abeta-induced synaptic depression and dendritic spine loss. Neuron 52 (5):831-843. doi:10.1016/j.neuron.2006.10.035
85. Foster TC, Norris CM (1997) Age-associated changes in Ca(2+)-dependent processes: relation to hippocampal synaptic plasticity. Hippocampus 7 (6):602-612. doi:10.1002/(sici)1098-1063(1997)7:6<602::Aid-hipo3>3.0.Co;2-g
86. Lin H, Bhatia R, Lal R (2001) Amyloid beta protein forms ion channels: implications for Alzheimer's disease pathophysiology. Faseb j 15 (13):2433-2444. doi:10.1096/fj.01-0377com
87. Hoover BR, Reed MN, Su J, Penrod RD, Kotilinek LA, Grant MK, Pitstick R, Carlson GA, Lanier LM, Yuan L-L, Ashe KH, Liao D (2010) Tau mislocalization to dendritic spines mediates synaptic dysfunction independently of neurodegeneration. Neuron 68 (6):1067-1081. doi:10.1016/j.neuron.2010.11.030
88. Tai HC, Serrano-Pozo A, Hashimoto T, Frosch MP, Spires-Jones TL, Hyman BT (2012) The synaptic accumulation of hyperphosphorylated tau oligomers in Alzheimer disease is associated with dysfunction of the ubiquitin-proteasome system. Am J Pathol 181 (4):1426-1435. doi:10.1016/j.ajpath.2012.06.033
89. Liu L, Drouet V, Wu JW, Witter MP, Small SA, Clelland C, Duff K (2012) Trans-synaptic spread of tau pathology in vivo. PLoS One 7 (2):e31302. doi:10.1371/journal.pone.0031302
90. Dujardin S, Lécolle K, Caillierez R, Bégard S, Zommer N, Lachaud C, Carrier S, Dufour N, Aurégan G, Winderickx J, Hantraye P, Déglon N, Colin M, Buée L (2014) Neuron-to-neuron wild-type Tau protein transfer through a trans-synaptic mechanism: relevance to sporadic tauopathies. Acta neuropathologica communications 2:14-14. doi:10.1186/2051-5960-2-14
91. de Calignon A, Polydoro M, Suárez-Calvet M, William C, Adamowicz DH, Kopeikina KJ, Pitstick R, Sahara N, Ashe KH, Carlson GA, Spires-Jones TL, Hyman BT (2012) Propagation of tau pathology in a model of early Alzheimer's disease. Neuron 73 (4):685-697. doi:10.1016/j.neuron.2011.11.033
92. Ahmed Z, Cooper J, Murray TK, Garn K, McNaughton E, Clarke H, Parhizkar S, Ward MA, Cavallini A, Jackson S, Bose S, Clavaguera F, Tolnay M, Lavenir I, Goedert M, Hutton ML, O'Neill MJ (2014) A novel in vivo model of tau propagation with rapid and progressive

neurofibrillary tangle pathology: the pattern of spread is determined by connectivity, not proximity. Acta Neuropathol 127 (5):667-683. doi:10.1007/s00401-014-1254-6
93. Walker LC, Diamond MI, Duff KE, Hyman BT (2013) Mechanisms of Protein Seeding in Neurodegenerative Diseases. JAMA Neurology 70 (3):304-310. doi:10.1001/jamaneurol.2013.1453
94. Pooler AM, Polydoro M, Maury EA, Nicholls SB, Reddy SM, Wegmann S, William C, Saqran L, Cagsal-Getkin O, Pitstick R, Beier DR, Carlson GA, Spires-Jones TL, Hyman BT (2015) Amyloid accelerates tau propagation and toxicity in a model of early Alzheimer's disease. Acta Neuropathologica Communications 3 (1):14. doi:10.1186/s40478-015-0199-x
95. Wyss-Coray T, Mucke L (2002) Inflammation in neurodegenerative disease--a double-edged sword. Neuron 35 (3):419-432. doi:10.1016/s0896-6273(02)00794-8
96. Nichols NR, Day JR, Laping NJ, Johnson SA, Finch CE (1993) GFAP mRNA increases with age in rat and human brain. Neurobiol Aging 14 (5):421-429. doi:10.1016/0197-4580(93)90100-p
97. Geula C, Wu CK, Saroff D, Lorenzo A, Yuan M, Yankner BA (1998) Aging renders the brain vulnerable to amyloid beta-protein neurotoxicity. Nat Med 4 (7):827-831. doi:10.1038/nm0798-827
98. Streit WJ, Sammons NW, Kuhns AJ, Sparks DL (2004) Dystrophic microglia in the aging human brain. Glia 45 (2):208-212. doi:10.1002/glia.10319
99. Moore AH, O'Banion MK (2002) Neuroinflammation and anti-inflammatory therapy for Alzheimer's disease. Adv Drug Deliv Rev 54 (12):1627-1656. doi:10.1016/s0169-409x(02)00162-x
100. Barger SW, Harmon AD (1997) Microglial activation by Alzheimer amyloid precursor protein and modulation by apolipoprotein E. Nature 388 (6645):878-881. doi:10.1038/42257
101. Hu J, Van Eldik LJ (1999) Glial-derived proteins activate cultured astrocytes and enhance beta amyloid-induced glial activation. Brain Res 842 (1):46-54. doi:10.1016/s0006-8993(99)01804-1
102. Webster S, Yang A, Margol L, Garzon-Rodriguez W, Glabe C, Tenner A (2000) Complement Component C1q Modulates the Phagocytosis of Aβ by Microglia. Experimental neurology 161:127-138. doi:10.1006/exnr.1999.7260
103. Akama KT, Albanese C, Pestell RG, Van Eldik LJ (1998) Amyloid beta-peptide stimulates nitric oxide production in astrocytes through an NFkappaB-dependent mechanism. Proceedings of the National Academy of Sciences of the United States of America 95 (10):5795-5800. doi:10.1073/pnas.95.10.5795
104. Lue LF, Walker DG, Brachova L, Beach TG, Rogers J, Schmidt AM, Stern DM, Yan SD (2001) Involvement of microglial receptor for advanced glycation endproducts (RAGE) in Alzheimer's disease: identification of a cellular activation mechanism. Exp Neurol 171 (1):29-45. doi:10.1006/exnr.2001.7732
105. Lorton D, Schaller J, Lala A, De Nardin E (2000) Chemotactic-like receptors and Abeta peptide induced responses in Alzheimer's disease. Neurobiol Aging 21 (3):463-473. doi:10.1016/s0197-4580(00)00092-0
106. Manczak M, Anekonda TS, Henson E, Park BS, Quinn J, Reddy PH (2006) Mitochondria are a direct site of A beta accumulation in Alzheimer's disease neurons: implications for free radical generation and oxidative damage in disease progression. Hum Mol Genet 15 (9):1437-1449. doi:10.1093/hmg/ddl066
107. Maurer I, Zierz S, Möller HJ (2000) A selective defect of cytochrome c oxidase is present in brain of Alzheimer disease patients. Neurobiol Aging 21 (3):455-462. doi:10.1016/s0197-4580(00)00112-3

108. Subbarao KV, Richardson JS, Ang LC (1990) Autopsy Samples of Alzheimer's Cortex Show Increased Peroxidation In Vitro. Journal of Neurochemistry 55 (1):342-345. doi:https://doi.org/10.1111/j.1471-4159.1990.tb08858.x
109. Mungarro-Menchaca X, Ferrera P, Morán J, Arias C (2002) beta-Amyloid peptide induces ultrastructural changes in synaptosomes and potentiates mitochondrial dysfunction in the presence of ryanodine. J Neurosci Res 68 (1):89-96. doi:10.1002/jnr.10193
110. Devi L, Prabhu BM, Galati DF, Avadhani NG, Anandatheerthavarada HK (2006) Accumulation of amyloid precursor protein in the mitochondrial import channels of human Alzheimer's disease brain is associated with mitochondrial dysfunction. J Neurosci 26 (35):9057-9068. doi:10.1523/JNEUROSCI.1469-06.2006
111. Caspersen C, Wang N, Yao J, Sosunov A, Chen X, Lustbader JW, Xu HW, Stern D, McKhann G, Yan SD (2005) Mitochondrial Abeta: a potential focal point for neuronal metabolic dysfunction in Alzheimer's disease. Faseb j 19 (14):2040-2041. doi:10.1096/fj.05-3735fje
112. Pallo SP, Johnson GV (2015) Tau facilitates Aβ-induced loss of mitochondrial membrane potential independent of cytosolic calcium fluxes in mouse cortical neurons. Neurosci Lett 597:32-37. doi:10.1016/j.neulet.2015.04.021
113. Barsoum MJ, Yuan H, Gerencser AA, Liot G, Kushnareva Y, Gräber S, Kovacs I, Lee WD, Waggoner J, Cui J, White AD, Bossy B, Martinou JC, Youle RJ, Lipton SA, Ellisman MH, Perkins GA, Bossy-Wetzel E (2006) Nitric oxide-induced mitochondrial fission is regulated by dynamin-related GTPases in neurons. Embo j 25 (16):3900-3911. doi:10.1038/sj.emboj.7601253
114. Mattson MP, Partin J, Begley JG (1998) Amyloid beta-peptide induces apoptosis-related events in synapses and dendrites. Brain Res 807 (1-2):167-176. doi:10.1016/s0006-8993(98)00763-x
115. Coskun PE, Beal MF, Wallace DC (2004) Alzheimer's brains harbor somatic mtDNA control-region mutations that suppress mitochondrial transcription and replication. Proc Natl Acad Sci U S A 101 (29):10726-10731. doi:10.1073/pnas.0403649101
116. Mondragón-Rodríguez S, Perry G, Zhu X, Moreira PI, Acevedo-Aquino MC, Williams S (2013) Phosphorylation of tau protein as the link between oxidative stress, mitochondrial dysfunction, and connectivity failure: implications for Alzheimer's disease. Oxid Med Cell Longev 2013:940603. doi:10.1155/2013/940603
117. Tramutola A, Lanzillotta C, Perluigi M, Butterfield DA (2017) Oxidative stress, protein modification and Alzheimer disease. Brain Res Bull 133:88-96. doi:10.1016/j.brainresbull.2016.06.005
118. Tönnies E, Trushina E (2017) Oxidative Stress, Synaptic Dysfunction, and Alzheimer's Disease. Journal of Alzheimer's disease : JAD 57 (4):1105-1121. doi:10.3233/JAD-161088
119. David DC, Hauptmann S, Scherping I, Schuessel K, Keil U, Rizzu P, Ravid R, Dröse S, Brandt U, Müller WE, Eckert A, Götz J (2005) Proteomic and functional analyses reveal a mitochondrial dysfunction in P301L tau transgenic mice. J Biol Chem 280 (25):23802-23814. doi:10.1074/jbc.M500356200
120. Srikanth V, Maczurek A, Phan T, Steele M, Westcott B, Juskiw D, Münch G (2011) Advanced glycation endproducts and their receptor RAGE in Alzheimer's disease. Neurobiol Aging 32 (5):763-777. doi:10.1016/j.neurobiolaging.2009.04.016
121. Münch G, Schinzel R, Loske C, Wong A, Durany N, Li JJ, Vlassara H, Smith MA, Perry G, Riederer P (1998) Alzheimer's disease--synergistic effects of glucose deficit, oxidative stress and advanced glycation endproducts. J Neural Transm (Vienna) 105 (4-5):439-461. doi:10.1007/s007020050069

122. Su B, Wang X, Nunomura A, Moreira PI, Lee Hg, Perry G, Smith MA, Zhu X (2008) Oxidative stress signaling in Alzheimer's disease. Current Alzheimer research 5 (6):525-532. doi:10.2174/156720508786898451
123. Zhu X, Castellani RJ, Takeda A, Nunomura A, Atwood CS, Perry G, Smith MA (2001) Differential activation of neuronal ERK, JNK/SAPK and p38 in Alzheimer disease: the 'two hit' hypothesis. Mech Ageing Dev 123 (1):39-46. doi:10.1016/s0047-6374(01)00342-6
124. Zhu X, Raina AK, Rottkamp CA, Aliev G, Perry G, Boux H, Smith MA (2001) Activation and redistribution of c-jun N-terminal kinase/stress activated protein kinase in degenerating neurons in Alzheimer's disease. J Neurochem 76 (2):435-441. doi:10.1046/j.1471-4159.2001.00046.x
125. Pérez M, Cuadros R, Smith MA, Perry G, Avila J (2000) Phosphorylated, but not native, tau protein assembles following reaction with the lipid peroxidation product, 4-hydroxy-2-nonenal. FEBS Letters 486 (3):270-274. doi:https://doi.org/10.1016/S0014-5793(00)02323-1
126. Colombo A, Bastone A, Ploia C, Sclip A, Salmona M, Forloni G, Borsello T (2009) JNK regulates APP cleavage and degradation in a model of Alzheimer's disease. Neurobiol Dis 33 (3):518-525. doi:10.1016/j.nbd.2008.12.014
127. Savage MJ, Lin Y-G, Ciallella JR, Flood DG, Scott RW (2002) Activation of c-Jun N-Terminal Kinase and p38 in an Alzheimer's Disease Model Is Associated with Amyloid Deposition. The Journal of Neuroscience 22 (9):3376-3385. doi:10.1523/jneurosci.22-09-03376.2002
128. Tong Y, Zhou W, Fung V, Christensen MA, Qing H, Sun X, Song W (2005) Oxidative stress potentiates BACE1 gene expression and Abeta generation. J Neural Transm (Vienna) 112 (3):455-469. doi:10.1007/s00702-004-0255-3
129. Shoji M, Iwakami N, Takeuchi S, Waragai M, Suzuki M, Kanazawa I, Lippa CF, Ono S, Okazawa H (2000) JNK activation is associated with intracellular beta-amyloid accumulation. Brain Res Mol Brain Res 85 (1-2):221-233. doi:10.1016/s0169-328x(00)00245-x
130. Hsu M-J, Hsu CY, Chen B-C, Chen M-C, Ou G, Lin C-H (2007) Apoptosis Signal-Regulating Kinase 1 in Amyloid β Peptide-Induced Cerebral Endothelial Cell Apoptosis. The Journal of Neuroscience 27 (21):5719-5729. doi:10.1523/jneurosci.1874-06.2007
131. Akhter R, Sanphui P, Das H, Saha P, Biswas SC (2015) The regulation of p53 up-regulated modulator of apoptosis by JNK/c-Jun pathway in β-amyloid-induced neuron death. Journal of Neurochemistry 134 (6):1091-1103. doi:https://doi.org/10.1111/jnc.13128
132. Paradis E, Douillard H, Koutroumanis M, Goodyer C, LeBlanc A (1996) Amyloid beta peptide of Alzheimer's disease downregulates Bcl-2 and upregulates bax expression in human neurons. J Neurosci 16 (23):7533-7539. doi:10.1523/jneurosci.16-23-07533.1996
133. Tamagno E, Parola M, Guglielmotto M, Santoro G, Bardini P, Marra L, Tabaton M, Danni O (2003) Multiple signaling events in amyloid beta-induced, oxidative stress-dependent neuronal apoptosis. Free Radic Biol Med 35 (1):45-58. doi:10.1016/s0891-5849(03)00244-2
134. Hoyer S (2000) Brain glucose and energy metabolism abnormalities in sporadic Alzheimer disease. Causes and consequences: an update. Exp Gerontol 35 (9-10):1363-1372. doi:10.1016/s0531-5565(00)00156-x
135. Biessels GJ, Kappelle LJ (2005) Increased risk of Alzheimer's disease in Type II diabetes: insulin resistance of the brain or insulin-induced amyloid pathology? Biochem Soc Trans 33 (Pt 5):1041-1044. doi:10.1042/bst0331041
136. Craft S, Peskind E, Schwartz MW, Schellenberg GD, Raskind M, Porte D, Jr. (1998) Cerebrospinal fluid and plasma insulin levels in Alzheimer's disease: relationship to severity of dementia and apolipoprotein E genotype. Neurology 50 (1):164-168. doi:10.1212/wnl.50.1.164

137. Frölich L, Blum-Degen D, Riederer P, Hoyer S (1999) A disturbance in the neuronal insulin receptor signal transduction in sporadic Alzheimer's disease. Annals of the New York Academy of Sciences 893:290-293. doi:10.1111/j.1749-6632.1999.tb07839.x
138. Steen E, Terry BM, Rivera EJ, Cannon JL, Neely TR, Tavares R, Xu XJ, Wands JR, de la Monte SM (2005) Impaired insulin and insulin-like growth factor expression and signaling mechanisms in Alzheimer's disease--is this type 3 diabetes? J Alzheimers Dis 7 (1):63-80. doi:10.3233/jad-2005-7107
139. Hoyer S (2004) Glucose metabolism and insulin receptor signal transduction in Alzheimer disease. European Journal of Pharmacology 490 (1):115-125. doi:https://doi.org/10.1016/j.ejphar.2004.02.049
140. Zhao W-Q, De Felice FG, Fernandez S, Chen H, Lambert MP, Quon MJ, Krafft GA, Klein WL (2008) Amyloid beta oligomers induce impairment of neuronal insulin receptors. The FASEB Journal 22 (1):246-260. doi:https://doi.org/10.1096/fj.06-7703com
141. Pessin JE, Saltiel AR (2000) Signaling pathways in insulin action: molecular targets of insulin resistance. J Clin Invest 106 (2):165-169. doi:10.1172/jci10582
142. Morris HR, Khan MN, Janssen JC, Brown JM, Perez-Tur J, Baker M, Ozansoy M, Hardy J, Hutton M, Wood NW, Lees AJ, Revesz T, Lantos P, Rossor MN (2001) The genetic and pathological classification of familial frontotemporal dementia. Arch Neurol 58 (11):1813-1816. doi:10.1001/archneur.58.11.1813
143. Mackenzie IR, Neumann M, Bigio EH, Cairns NJ, Alafuzoff I, Kril J, Kovacs GG, Ghetti B, Halliday G, Holm IE, Ince PG, Kamphorst W, Revesz T, Rozemuller AJ, Kumar-Singh S, Akiyama H, Baborie A, Spina S, Dickson DW, Trojanowski JQ, Mann DM (2010) Nomenclature and nosology for neuropathologic subtypes of frontotemporal lobar degeneration: an update. Acta Neuropathol 119 (1):1-4. doi:10.1007/s00401-009-0612-2
144. Mackenzie IR, Rademakers R, Neumann M (2010) TDP-43 and FUS in amyotrophic lateral sclerosis and frontotemporal dementia. Lancet Neurol 9 (10):995-1007. doi:10.1016/s1474-4422(10)70195-2
145. Neumann M, Sampathu DM, Kwong LK, Truax AC, Micsenyi MC, Chou TT, Bruce J, Schuck T, Grossman M, Clark CM, McCluskey LF, Miller BL, Masliah E, Mackenzie IR, Feldman H, Feiden W, Kretzschmar HA, Trojanowski JQ, Lee VM (2006) Ubiquitinated TDP-43 in frontotemporal lobar degeneration and amyotrophic lateral sclerosis. Science 314 (5796):130-133. doi:10.1126/science.1134108
146. Lipton AM, White CL, 3rd, Bigio EH (2004) Frontotemporal lobar degeneration with motor neuron disease-type inclusions predominates in 76 cases of frontotemporal degeneration. Acta Neuropathol 108 (5):379-385. doi:10.1007/s00401-004-0900-9
147. Dickson D, R W (2011) Neurodegeneration: the molecular pathology of dementia and movement disorders. WileyBlackwell, West Sussex
148. Jiang Z, Tang H, Havlioglu N, Zhang X, Stamm S, Yan R, Wu JY (2003) Mutations in tau gene exon 10 associated with FTDP-17 alter the activity of an exonic splicing enhancer to interact with Tra2 beta. J Biol Chem 278 (21):18997-19007. doi:10.1074/jbc.M301800200
149. Mirra SS, Murrell JR, Gearing M, Spillantini MG, Goedert M, Crowther RA, Levey AI, Jones R, Green J, Shoffner JM, Wainer BH, Schmidt ML, Trojanowski JQ, Ghetti B (1999) Tau pathology in a family with dementia and a P301L mutation in tau. J Neuropathol Exp Neurol 58 (4):335-345. doi:10.1097/00005072-199904000-00004
150. Goedert M, Spillantini MG (2011) Pathogenesis of the Tauopathies. Journal of Molecular Neuroscience 45 (3):425. doi:10.1007/s12031-011-9593-4
151. Hardy J, Allsop D (1991) Amyloid deposition as the central event in the aetiology of Alzheimer's disease. Trends Pharmacol Sci 12 (10):383-388. doi:10.1016/0165-6147(91)90609-v

152. Hardy JA, Higgins GA (1992) Alzheimer's disease: the amyloid cascade hypothesis. Science 256 (5054):184-185. doi:10.1126/science.1566067
153. Selkoe DJ, Hardy J (2016) The amyloid hypothesis of Alzheimer's disease at 25 years. EMBO Mol Med 8 (6):595-608. doi:10.15252/emmm.201606210
154. Karran E, Mercken M, De Strooper B (2011) The amyloid cascade hypothesis for Alzheimer's disease: an appraisal for the development of therapeutics. Nat Rev Drug Discov 10 (9):698-712. doi:10.1038/nrd3505
155. Sherrington R, Rogaev EI, Liang Y, Rogaeva EA, Levesque G, Ikeda M, Chi H, Lin C, Li G, Holman K, Tsuda T, Mar L, Foncin JF, Bruni AC, Montesi MP, Sorbi S, Rainero I, Pinessi L, Nee L, Chumakov I, Pollen D, Brookes A, Sanseau P, Polinsky RJ, Wasco W, Da Silva HAR, Haines JL, Pericak-Vance MA, Tanzi RE, Roses AD, Fraser PE, Rommens JM, St George-Hyslop PH (1995) Cloning of a gene bearing missense mutations in early-onset familial Alzheimer's disease. Nature 375 (6534):754-760. doi:10.1038/375754a0
156. Levy-Lahad E, Wasco W, Poorkaj P, Romano DM, Oshima J, Pettingell WH, Yu CE, Jondro PD, Schmidt SD, Wang K, et al. (1995) Candidate gene for the chromosome 1 familial Alzheimer's disease locus. Science 269 (5226):973-977. doi:10.1126/science.7638622
157. Tomiyama T, Nagata T, Shimada H, Teraoka R, Fukushima A, Kanemitsu H, Takuma H, Kuwano R, Imagawa M, Ataka S, Wada Y, Yoshioka E, Nishizaki T, Watanabe Y, Mori H (2008) A new amyloid beta variant favoring oligomerization in Alzheimer's-type dementia. Ann Neurol 63 (3):377-387. doi:10.1002/ana.21321
158. Holtzman DM, Bales KR, Tenkova T, Fagan AM, Parsadanian M, Sartorius LJ, Mackey B, Olney J, McKeel D, Wozniak D, Paul SM (2000) Apolipoprotein E isoform-dependent amyloid deposition and neuritic degeneration in a mouse model of Alzheimer's disease. Proc Natl Acad Sci U S A 97 (6):2892-2897. doi:10.1073/pnas.050004797
159. Kim J, Basak JM, Holtzman DM (2009) The role of apolipoprotein E in Alzheimer's disease. Neuron 63 (3):287-303. doi:10.1016/j.neuron.2009.06.026
160. Jones L, Holmans PA, Hamshere ML, Harold D, Moskvina V, Ivanov D, Pocklington A, Abraham R, Hollingworth P, Sims R, Gerrish A, Pahwa JS, Jones N, Stretton A, Morgan AR, Lovestone S, Powell J, Proitsi P, Lupton MK, Brayne C, Rubinsztein DC, Gill M, Lawlor B, Lynch A, Morgan K, Brown KS, Passmore PA, Craig D, McGuinness B, Todd S, Holmes C, Mann D, Smith AD, Love S, Kehoe PG, Mead S, Fox N, Rossor M, Collinge J, Maier W, Jessen F, Schürmann B, van den Bussche H, Heuser I, Peters O, Kornhuber J, Wiltfang J, Dichgans M, Frölich L, Hampel H, Hüll M, Rujescu D, Goate AM, Kauwe JSK, Cruchaga C, Nowotny P, Morris JC, Mayo K, Livingston G, Bass NJ, Gurling H, McQuillin A, Gwilliam R, Deloukas P, Al-Chalabi A, Shaw CE, Singleton AB, Guerreiro R, Mühleisen TW, Nöthen MM, Moebus S, Jöckel K-H, Klopp N, Wichmann HE, Rüther E, Carrasquillo MM, Pankratz VS, Younkin SG, Hardy J, O'Donovan MC, Owen MJ, Williams J (2010) Genetic Evidence Implicates the Immune System and Cholesterol Metabolism in the Aetiology of Alzheimer's Disease. PLOS ONE 5 (11):e13950. doi:10.1371/journal.pone.0013950
161. Sala Frigerio C, Wolfs L, Fattorelli N, Thrupp N, Voytyuk I, Schmidt I, Mancuso R, Chen WT, Woodbury ME, Srivastava G, Möller T, Hudry E, Das S, Saido T, Karran E, Hyman B, Perry VH, Fiers M, De Strooper B (2019) The Major Risk Factors for Alzheimer's Disease: Age, Sex, and Genes Modulate the Microglia Response to Aβ Plaques. Cell Rep 27 (4):1293-1306.e1296. doi:10.1016/j.celrep.2019.03.099
162. Price JL, McKeel DW, Jr., Buckles VD, Roe CM, Xiong C, Grundman M, Hansen LA, Petersen RC, Parisi JE, Dickson DW, Smith CD, Davis DG, Schmitt FA, Markesbery WR, Kaye J, Kurlan R, Hulette C, Kurland BF, Higdon R, Kukull W, Morris JC (2009) Neuropathology of nondemented aging: presumptive evidence for preclinical Alzheimer disease. Neurobiol Aging 30 (7):1026-1036. doi:10.1016/j.neurobiolaging.2009.04.002

163. Braak H, Zetterberg H, Del Tredici K, Blennow K (2013) Intraneuronal tau aggregation precedes diffuse plaque deposition, but amyloid-β changes occur before increases of tau in cerebrospinal fluid. Acta Neuropathol 126 (5):631-641. doi:10.1007/s00401-013-1139-0
164. Arnsten AFT, Datta D, Tredici KD, Braak H (2021) Hypothesis: Tau pathology is an initiating factor in sporadic Alzheimer's disease. Alzheimer's & Dementia 17 (1):115-124. doi:https://doi.org/10.1002/alz.12192
165. Park SY, Ferreira A (2005) The generation of a 17 kDa neurotoxic fragment: an alternative mechanism by which tau mediates beta-amyloid-induced neurodegeneration. J Neurosci 25 (22):5365-5375. doi:10.1523/jneurosci.1125-05.2005
166. Mark R, Hana ND, Lester IB, Michael PV, Adriana F (2002) Tau Is Essential to β-Amyloid-Induced Neurotoxicity. Proc Natl Acad Sci U S A 99 (9):6364-6369. doi:10.1073/pnas.092136199
167. Amadoro G, Corsetti V, Ciotti MT, Florenzano F, Capsoni S, Amato G, Calissano P (2011) Endogenous Aβ causes cell death via early tau hyperphosphorylation. Neurobiol Aging 32 (6):969-990. doi:10.1016/j.neurobiolaging.2009.06.005
168. Wu H-Y, Kuo P-C, Wang Y-T, Lin H-T, Roe AD, Wang BY, Han C-L, Hyman BT, Chen Y-J, Tai H-C (2018) β-Amyloid Induces Pathology-Related Patterns of Tau Hyperphosphorylation at Synaptic Terminals. Journal of Neuropathology & Experimental Neurology 77 (9):814-826. doi:10.1093/jnen/nly059
169. Roberson ED, Scearce-Levie K, Palop JJ, Yan F, Cheng IH, Wu T, Gerstein H, Yu GQ, Mucke L (2007) Reducing Endogenous Tau Ameliorates Amyloid -Induced Deficits in an Alzheimer's Disease Mouse Model. Science (American Association for the Advancement of Science) 316 (5825):750-754. doi:10.1126/science.1141736
170. Oddo S, Vasilevko V, Caccamo A, Kitazawa M, Cribbs DH, LaFerla FM (2006) Reduction of Soluble Ab and Tau, but Not Soluble Ab Alone, Ameliorates Cognitive Decline in Transgenic Mice with Plaques and Tangles. Journal of Biological Chemistry 281 (51):39413-39423. doi:10.1074/jbc.M608485200
171. Oddo S, Billings L, Kesslak JP, Cribbs DH, LaFerla FM (2004) Abeta immunotherapy leads to clearance of early, but not late, hyperphosphorylated tau aggregates via the proteasome. Neuron 43 (3):321-332. doi:10.1016/j.neuron.2004.07.003
172. Benilova I, Karran E, De Strooper B (2012) The toxic Aβ oligomer and Alzheimer's disease: an emperor in need of clothes. Nat Neurosci 15 (3):349-357. doi:10.1038/nn.3028
173. Small SA, Duff K (2008) Linking Abeta and tau in late-onset Alzheimer's disease: a dual pathway hypothesis. Neuron 60 (4):534-542. doi:10.1016/j.neuron.2008.11.007
174. Musiek ES, Holtzman DM (2015) Three dimensions of the amyloid hypothesis: time, space and 'wingmen'. Nature neuroscience 18 (6):800-806. doi:10.1038/nn.4018
175. Braak H, Thal DR, Ghebremedhin E, Del Tredici K (2011) Stages of the pathologic process in Alzheimer disease: age categories from 1 to 100 years. J Neuropathol Exp Neurol 70 (11):960-969. doi:10.1097/NEN.0b013e318232a379
176. Zhou X-F (2016) The imbalance of neurotrophic signalling: an alternate hypothesis for the pathogenesis and drug development of Alzheimer's disease. Proc Neurosci 1 (1):13-18
177. Costantini C, Scrable H, Puglielli L (2006) An aging pathway controls the TrkA to p75NTR receptor switch and amyloid beta-peptide generation. The EMBO journal 25 (9):1997-2006. doi:10.1038/sj.emboj.7601062
178. Cattaneo A, Calissano P (2012) Nerve Growth Factor and Alzheimer's Disease: New Facts for an Old Hypothesis. Mol Neurobiol 46 (3):588-604. doi:10.1007/s12035-012-8310-9
179. Capsoni S, Ugolini G, Comparini A, Ruberti F, Berardi N, Cattaneo A (2000) Alzheimer-like neurodegeneration in aged antinerve growth factor transgenic mice. Proceedings of the National Academy of Sciences 97 (12):6826-6831. doi:10.1073/pnas.97.12.6826

180. Capsoni S, Giannotta S, Cattaneo A (2002) Nerve growth factor and galantamine ameliorate early signs of neurodegeneration in anti-nerve growth factor mice. Proceedings of the National Academy of Sciences 99 (19):12432-12437. doi:10.1073/pnas.192442999
181. Costantini C, Rossi F, Formaggio E, Bernardoni R, Cecconi D, Della-Bianca V (2005) Characterization of the signaling pathway downstream p75 neurotrophin receptor involved in β-amyloid peptide-dependent cell death. Journal of Molecular Neuroscience 25 (2):141-156. doi:10.1385/JMN:25:2:141
182. Knowles JK, Rajadas J, Nguyen T-VV, Yang T, LeMieux MC, Vander Griend L, Ishikawa C, Massa SM, Wyss-Coray T, Longo FM (2009) The p75 Neurotrophin Receptor Promotes Amyloid-β(1-42)-Induced Neuritic Dystrophy *In Vitro* and *In Vivo*. The Journal of Neuroscience 29 (34):10627-10637. doi:10.1523/jneurosci.0620-09.2009
183. Sotthibundhu A, Sykes AM, Fox B, Underwood CK, Thangnipon W, Coulson EJ (2008) Beta-amyloid(1-42) induces neuronal death through the p75 neurotrophin receptor. J Neurosci 28 (15):3941-3946. doi:10.1523/JNEUROSCI.0350-08.2008
184. Yaar M, Zhai S, Pilch PF, Doyle SM, Eisenhauer PB, Fine RE, Gilchrest BA (1997) Binding of beta-amyloid to the p75 neurotrophin receptor induces apoptosis. A possible mechanism for Alzheimer's disease. The Journal of clinical investigation 100 (9):2333-2340. doi:10.1172/JCI119772
185. Yaar M, Zhai S, Fine RE, Eisenhauer PB, Arble BL, Stewart KB, Gilchrest BA (2002) Amyloid β Binds Trimers as Well as Monomers of the 75-kDa Neurotrophin Receptor and Activates Receptor Signaling. Journal of Biological Chemistry 277 (10):7720-7725. doi:10.1074/jbc.M110929200
186. Chao MV (2003) Neurotrophins and their receptors: A convergence point for many signalling pathways. Nature Reviews Neuroscience 4 (4):299-309. doi:10.1038/nrn1078
187. Huang EJ, Reichardt LF (2001) Neurotrophins: roles in neuronal development and function. Annu Rev Neurosci 24:677-736. doi:10.1146/annurev.neuro.24.1.677
188. Roux PP, Barker PA (2002) Neurotrophin signaling through the p75 neurotrophin receptor. Prog Neurobiol 67 (3):203-233. doi:10.1016/s0301-0082(02)00016-3
189. Arancio O, Chao MV (2007) Neurotrophins, synaptic plasticity and dementia. Current Opinion in Neurobiology 17 (3):325-330. doi:https://doi.org/10.1016/j.conb.2007.03.013
190. Pang PT, Teng HK, Zaitsev E, Woo NT, Sakata K, Zhen S, Teng KK, Yung W-H, Hempstead BL, Lu B (2004) Cleavage of proBDNF by tPA/plasmin is essential for long-term hippocampal plasticity. Science (New York, NY) 306 (5695):487-491. doi:10.1126/science.1100135
191. Woo NH, Teng HK, Siao CJ, Chiaruttini C, Pang PT, Milner TA, Hempstead BL, Lu B (2005) Activation of p75NTR by proBDNF facilitates hippocampal long-term depression. Nat Neurosci 8 (8):1069-1077. doi:10.1038/nn1510
192. Rösch H, Schweigreiter R, Bonhoeffer T, Barde Y-A, Korte M (2005) The neurotrophin receptor p75^{NTR} modulates long-term depression and regulates the expression of AMPA receptor subunits in the hippocampus. Proceedings of the National Academy of Sciences of the United States of America 102 (20):7362-7367. doi:10.1073/pnas.0502460102
193. Nykjaer A, Lee R, Teng KK, Jansen P, Madsen P, Nielsen MS, Jacobsen C, Kliemannel M, Schwarz E, Willnow TE, Hempstead BL, Petersen CM (2004) Sortilin is essential for proNGF-induced neuronal cell death. Nature 427 (6977):843-848. doi:10.1038/nature02319
194. Harrington AW, Kim JY, Yoon SO (2002) Activation of Rac GTPase by p75 Is Necessary for c-jun N-Terminal Kinase-Mediated Apoptosis. The Journal of Neuroscience 22 (1):156-166. doi:10.1523/jneurosci.22-01-00156.2002
195. Wang Y-J, Valadares D, Sun Y, Wang X, Zhong J-H, Liu X-H, Majd S, Chen L, Gao C-Y, Chen S, Lim Y, Pollard A, Aguilar E, Gai W-P, Yang M, Zhou X-F (2010) Effects of

proNGF on Neuronal Viability, Neurite Growth and Amyloid-beta Metabolism. Neurotoxicity Research 17 (3):257-267. doi:10.1007/s12640-009-9098-x
196. Susen K, Heumann R, Blöchl A (1999) Nerve growth factor stimulates MAPK via the low affinity receptor p75(LNTR). FEBS Lett 463 (3):231-234. doi:10.1016/s0014-5793(99)01628-2
197. Carter BD, Kaltschmidt C, Kaltschmidt B, Offenhäuser N, Böhm-Matthaei R, Baeuerle PA, Barde YA (1996) Selective activation of NF-kappa B by nerve growth factor through the neurotrophin receptor p75. Science 272 (5261):542-545. doi:10.1126/science.272.5261.542
198. Mamidipudi V, Li X, Wooten MW (2002) Identification of interleukin 1 receptor-associated kinase as a conserved component in the p75-neurotrophin receptor activation of nuclear factor-kappa B. J Biol Chem 277 (31):28010-28018. doi:10.1074/jbc.M109730200
199. Khursigara G, Bertin J, Yano H, Moffett H, DiStefano PS, Chao MV (2001) A prosurvival function for the p75 receptor death domain mediated via the caspase recruitment domain receptor-interacting protein 2. J Neurosci 21 (16):5854-5863. doi:10.1523/jneurosci.21-16-05854.2001
200. Khursigara G, Orlinick JR, Chao MV (1999) Association of the p75 Neurotrophin Receptor with TRAF6 *. Journal of Biological Chemistry 274 (5):2597-2600. doi:10.1074/jbc.274.5.2597
201. Yamashita T, Tucker KL, Barde YA (1999) Neurotrophin binding to the p75 receptor modulates Rho activity and axonal outgrowth. Neuron 24 (3):585-593. doi:10.1016/s0896-6273(00)81114-9
202. Charalampopoulos I, Vicario A, Pediaditakis I, Gravanis A, Simi A, Ibáñez Carlos F (2012) Genetic Dissection of Neurotrophin Signaling through the p75 Neurotrophin Receptor. Cell Reports 2 (6):1563-1570. doi:10.1016/j.celrep.2012.11.009
203. Siegel GJ, Chauhan NB (2000) Neurotrophic factors in Alzheimer's and Parkinson's disease brain. Brain Res Brain Res Rev 33 (2-3):199-227. doi:10.1016/s0165-0173(00)00030-8
204. Verdi JM, Birren SJ, Ibáñez CF, Persson H, Kaplan DR, Benedetti M, Chao MV, Anderson DJ (1994) p75LNGFR regulates Trk signal transduction and NGF-induced neuronal differentiation in MAH cells. Neuron 12 (4):733-745. doi:10.1016/0896-6273(94)90327-1
205. Culmsee C, Gerling N, Lehmann M, Nikolova-Karakashian M, Prehn JH, Mattson MP, Krieglstein J (2002) Nerve growth factor survival signaling in cultured hippocampal neurons is mediated through TrkA and requires the common neurotrophin receptor P75. Neuroscience 115 (4):1089-1108. doi:10.1016/s0306-4522(02)00539-0
206. Vesa J, Kruttgen A, Shooter EM (2000) p75 reduces TrkB tyrosine autophosphorylation in response to brain-derived neurotrophic factor and neurotrophin 4/5. J Biol Chem 275 (32):24414-24420. doi:10.1074/jbc.M001641200
207. Bibel M, Hoppe E, Barde YA (1999) Biochemical and functional interactions between the neurotrophin receptors trk and p75NTR. The EMBO journal 18 (3):616-622. doi:10.1093/emboj/18.3.616
208. Curtis R, Adryan KM, Stark JL, Park JS, Compton DL, Weskamp G, Huber LJ, Chao MV, Jaenisch R, Lee KF, et al. (1995) Differential role of the low affinity neurotrophin receptor (p75) in retrograde axonal transport of the neurotrophins. Neuron 14 (6):1201-1211. doi:10.1016/0896-6273(95)90267-8
209. Casaccia-Bonnefil P, Gu C, Khursigara G, Chao MV (1999) p75 neurotrophin receptor as a modulator of survival and death decisions. Microsc Res Tech 45 (4-5):217-224. doi:10.1002/(sici)1097-0029(19990515/01)45:4/5<217::Aid-jemt5>3.0.Co;2-5
210. Zampieri N, Xu CF, Neubert TA, Chao MV (2005) Cleavage of p75 neurotrophin receptor by alpha-secretase and gamma-secretase requires specific receptor domains. J Biol Chem 280 (15):14563-14571. doi:10.1074/jbc.M412957200

211. Kanning KC, Hudson M, Amieux PS, Wiley JC, Bothwell M, Schecterson LC (2003) Proteolytic Processing of the p75 Neurotrophin Receptor and Two Homologs Generates C-Terminal Fragments with Signaling Capability. The Journal of Neuroscience 23 (13):5425-5436. doi:10.1523/jneurosci.23-13-05425.2003
212. Urra S, Escudero CA, Ramos P, Lisbona F, Allende E, Covarrubias P, Parraguez JI, Zampieri N, Chao MV, Annaert W, Bronfman FC (2007) TrkA receptor activation by nerve growth factor induces shedding of the p75 neurotrophin receptor followed by endosomal gamma-secretase-mediated release of the p75 intracellular domain. J Biol Chem 282 (10):7606-7615. doi:10.1074/jbc.M610458200
213. Majdan M, Lachance C, Gloster A, Aloyz R, Zeindler C, Bamji S, Bhakar A, Belliveau D, Fawcett J, Miller FD, Barker PA (1997) Transgenic mice expressing the intracellular domain of the p75 neurotrophin receptor undergo neuronal apoptosis. J Neurosci 17 (18):6988-6998. doi:10.1523/jneurosci.17-18-06988.1997
214. Coulson EJ, Reid K, Baca M, Shipham KA, Hulett SM, Kilpatrick TJ, Bartlett PF (2000) Chopper, a new death domain of the p75 neurotrophin receptor that mediates rapid neuronal cell death. J Biol Chem 275 (39):30537-30545. doi:10.1074/jbc.M005214200
215. Phillips HS, Hains JM, Armanini M, Laramee GR, Johnson SA, Winslow JW (1991) BDNF mRNA is decreased in the hippocampus of individuals with Alzheimer's disease. Neuron 7 (5):695-702. doi:10.1016/0896-6273(91)90273-3
216. Fahnestock M, Michalski B, Xu B, Coughlin MD (2001) The Precursor Pro-Nerve Growth Factor Is the Predominant Form of Nerve Growth Factor in Brain and Is Increased in Alzheimer's Disease. Molecular and Cellular Neuroscience 18 (2):210-220. doi:https://doi.org/10.1006/mcne.2001.1016
217. Mufson EJ, Conner JM, Kordower JH (1995) Nerve growth factor in Alzheimer's disease: defective retrograde transport to nucleus basalis. Neuroreport 6 (7):1063-1066. doi:10.1097/00001756-199505090-00028
218. Matrone C, Ciotti MT, Mercanti D, Marolda R, Calissano P (2008) NGF and BDNF signaling control amyloidogenic route and Aβ production in hippocampal neurons. Proceedings of the National Academy of Sciences 105 (35):13139-13144. doi:10.1073/pnas.0806133105
219. Pedraza CE, Podlesniy P, Vidal N, Arévalo JC, Lee R, Hempstead B, Ferrer I, Iglesias M, Espinet C (2005) Pro-NGF Isolated from the Human Brain Affected by Alzheimer's Disease Induces Neuronal Apoptosis Mediated by p75NTR. The American Journal of Pathology 166 (2):533-543. doi:https://doi.org/10.1016/S0002-9440(10)62275-4
220. Triaca V, Sposato V, Bolasco G, Ciotti MT, Pelicci P, Bruni AC, Cupidi C, Maletta R, Feligioni M, Nisticò R, Canu N, Calissano P (2016) NGF controls APP cleavage by downregulating APP phosphorylation at Thr668: relevance for Alzheimer's disease. Aging Cell 15 (4):661-672. doi:10.1111/acel.12473
221. Zheng C, Geetha T, Gearing M, Ramesh Babu J (2015) Amyloid β-abrogated TrkA ubiquitination in PC12 cells analogous to Alzheimer's disease. Journal of Neurochemistry 133 (6):919-925. doi:https://doi.org/10.1111/jnc.13076
222. Tiernan CT, Ginsberg SD, He B, Ward SM, Guillozet-Bongaarts AL, Kanaan NM, Mufson EJ, Counts SE (2018) Pretangle pathology within cholinergic nucleus basalis neurons coincides with neurotrophic and neurotransmitter receptor gene dysregulation during the progression of Alzheimer's disease. Neurobiol Dis 117:125-136. doi:10.1016/j.nbd.2018.05.021
223. Tiernan CT, Combs B, Cox K, Morfini G, Brady ST, Counts SE, Kanaan NM (2016) Pseudophosphorylation of tau at S422 enhances SDS-stable dimer formation and impairs both anterograde and retrograde fast axonal transport. Exp Neurol 283 (Pt A):318-329. doi:10.1016/j.expneurol.2016.06.030

224. Ibáñez CF, Simi A (2012) p75 neurotrophin receptor signaling in nervous system injury and degeneration: paradox and opportunity. Trends in Neurosciences 35 (7):431-440. doi:10.1016/j.tins.2012.03.007
225. Zeng F, Lu J-J, Zhou X-F, Wang Y-J (2011) Roles of p75NTR in the pathogenesis of Alzheimer's disease: A novel therapeutic target. Biochemical Pharmacology 82 (10):1500-1509. doi:https://doi.org/10.1016/j.bcp.2011.06.040
226. Frade JM, López-Sánchez N (2010) A novel hypothesis for Alzheimer disease based on neuronal tetraploidy induced by p75 (NTR). Cell Cycle 9 (10):1934-1941. doi:10.4161/cc.9.10.11582
227. Shen L-L, Mañucat-Tan NB, Gao S-H, Li W-W, Zeng F, Zhu C, Wang J, Bu X-L, Liu Y-H, Gao C-Y, Xu Z-Q, Bobrovskaya L, Lei P, Yu J-T, Song W, Zhou H-D, Yao X-Q, Zhou X-F, Wang Y-J (2018) The ProNGF/p75NTR pathway induces tau pathology and is a therapeutic target for FTLD-tau. Molecular Psychiatry 23 (8):1813-1824. doi:10.1038/s41380-018-0071-z
228. Wang Y-J, Wang X, Lu J-J, Li Q-X, Gao C-Y, Liu X-H, Sun Y, Yang M, Lim Y, Evin G, Zhong J-H, Masters C, Zhou X-F (2011) p75NTR regulates Abeta deposition by increasing Abeta production but inhibiting Abeta aggregation with its extracellular domain. J Neurosci 31 (6):2292-2304. doi:10.1523/JNEUROSCI.2733-10.2011
229. Patnaik A, Zagrebelsky M, Korte M, Holz A (2020) Signaling via the p75 neurotrophin receptor facilitates amyloid-β-induced dendritic spine pathology. Scientific Reports 10 (1):13322. doi:10.1038/s41598-020-70153-4
230. Susen K, Blöchl A (2005) Low concentrations of aggregated β-amyloid induce neurite formation via the neurotrophin receptor p75. Journal of Molecular Medicine 83 (9):720-735. doi:10.1007/s00109-005-0671-3
231. Chakravarthy B, Gaudet C, Ménard M, Atkinson T, Brown L, Laferla FM, Armato U, Whitfield J (2010) Amyloid-beta peptides stimulate the expression of the p75(NTR) neurotrophin receptor in SHSY5Y human neuroblastoma cells and AD transgenic mice. J Alzheimers Dis 19 (3):915-925. doi:10.3233/jad-2010-1288
232. Saadipour K, Yang M, Lim Y, Georgiou K, Sun Y, Keating D, Liu J, Wang YR, Gai WP, Zhong JH, Wang YJ, Zhou XF (2013) Amyloid beta$_{1–42}$ (Aβ$_{42}$) up-regulates the expression of sortilin via the p75(NTR)/RhoA signaling pathway. J Neurochem 127 (2):152-162. doi:10.1111/jnc.12383
233. Finan GM, Okada H, Kim TW (2011) BACE1 retrograde trafficking is uniquely regulated by the cytoplasmic domain of sortilin. J Biol Chem 286 (14):12602-12616. doi:10.1074/jbc.M110.170217
234. Saadipour K, Mañucat-Tan NB, Lim Y, Keating DJ, Smith KS, Zhong J-h, Liao H, Bobrovskaya L, Wang Y-J, Chao MV, Zhou X-F (2018) p75 neurotrophin receptor interacts with and promotes BACE1 localization in endosomes aggravating amyloidogenesis. Journal of Neurochemistry 144 (3):302-317. doi:https://doi.org/10.1111/jnc.14206
235. Saadipour K, Tiberi A, Lombardo S, Grajales E, Montroull L, Mañucat-Tan NB, LaFrancois J, Cammer M, Mathews PM, Scharfman HE, Liao F-F, Friedman WJ, Zhou X-F, Tesco G, Chao MV (2019) Regulation of BACE1 expression after injury is linked to the p75 neurotrophin receptor. Molecular and Cellular Neuroscience 99:103395. doi:https://doi.org/10.1016/j.mcn.2019.103395
236. Matrone C, Marolda R, Ciafrè S, Ciotti MT, Mercanti D, Calissano P (2009) Tyrosine kinase nerve growth factor receptor switches from prosurvival to proapoptotic activity via Abeta-mediated phosphorylation. Proceedings of the National Academy of Sciences 106 (27):11358-11363. doi:10.1073/pnas.0904998106
237. Ovsepian SV, Antyborzec I, O'Leary VB, Zaborszky L, Herms J, Oliver Dolly J (2014) Neurotrophin receptor p75 mediates the uptake of the amyloid beta (Aβ) peptide, guiding it to

lysosomes for degradation in basal forebrain cholinergic neurons. Brain Struct Funct 219 (5):1527-1541. doi:10.1007/s00429-013-0583-x
238. Yao XQ, Jiao SS, Saadipour K, Zeng F, Wang QH, Zhu C, Shen LL, Zeng GH, Liang CR, Wang J, Liu YH, Hou HY, Xu X, Su YP, Fan XT, Xiao HL, Lue LF, Zeng YQ, Giunta B, Zhong JH, Walker DG, Zhou HD, Tan J, Zhou XF, Wang YJ (2015) p75NTR ectodomain is a physiological neuroprotective molecule against amyloid-beta toxicity in the brain of Alzheimer's disease. Molecular psychiatry 20 (11):1301-1310. doi:10.1038/mp.2015.49
239. Pietri M, Dakowski C, Hannaoui S, Alleaume-Butaux A, Hernandez-Rapp J, Ragagnin A, Mouillet-Richard S, Haik S, Bailly Y, Peyrin J-M, Launay J-M, Kellermann O, Schneider B (2013) PDK1 decreases TACE-mediated α-secretase activity and promotes disease progression in prion and Alzheimer's diseases. Nature Medicine 19:1124. doi:10.1038/nm.3302

https://www.nature.com/articles/nm.3302#supplementary-information
240. Wang Q-H, Wang Y-R, Zhang T, Jiao S-S, Liu Y-H, Zeng F, Li J, Yao X-Q, Zhou H-D, Zhou X-F, Wang Y-J (2016) Intramuscular delivery of p75NTR ectodomain by an AAV vector attenuates cognitive deficits and Alzheimer's disease-like pathologies in APP/PS1 transgenic mice. Journal of Neurochemistry 138 (1):163-173. doi:10.1111/jnc.13616
241. Shen LL, Li WW, Xu YL, Gao SH, Xu MY, Bu XL, Liu YH, Wang J, Zhu J, Zeng F, Yao XQ, Gao CY, Xu ZQ, Zhou XF, Wang YJ (2019) Neurotrophin receptor p75 mediates amyloid β-induced tau pathology. Neurobiol Dis 132:104567. doi:10.1016/j.nbd.2019.104567
242. Zhou X-F, Wang Y-J (2011) The p75NTR extracellular domain. Prion 5:161-163. doi:10.4161/pri.5.3.16896
243. Jiao SS, Bu XL, Liu YH, Wang QH, Liu CH, Yao XQ, Zhou XF, Wang YJ (2015) Differential levels of p75NTR ectodomain in CSF and blood in patients with Alzheimer's disease: a novel diagnostic marker. Translational Psychiatry 5 (10):e650-e650. doi:10.1038/tp.2015.146
244. Xu Y, Li WW, Wang J, Zhu C, Shen YY, Shi AY, Zeng GH, Xu ZQ, Zhou XF, Wang YJ (2019) Neurotrophin Receptor p75 mRNA Level in Peripheral Blood Cells of Patients with Alzheimer's Disease. Neurotox Res 36 (1):101-107. doi:10.1007/s12640-019-00035-9
245. Becker K, Cana A, Baumgärtner W, Spitzbarth I (2018) p75 Neurotrophin Receptor: A Double-Edged Sword in Pathology and Regeneration of the Central Nervous System. Veterinary Pathology 55 (6):786-801. doi:10.1177/0300985818781930
246. Martínez A, Carmona M, Portero-Otin M, Naudí A, Pamplona R, Ferrer I (2008) Type-Dependent Oxidative Damage in Frontotemporal Lobar Degeneration: Cortical Astrocytes Are Targets of Oxidative Damage. Journal of Neuropathology & Experimental Neurology 67 (12):1122-1136. doi:10.1097/NEN.0b013e31818e06f3
247. Gerst JL, Siedlak SL, Nunomura A, Castellani R, Perry G, Smith MA (1999) Role of Oxidative Stress in Frontotemporal Dementia. Dementia and Geriatric Cognitive Disorders 10(suppl 1) (Suppl. 1):85-87. doi:10.1159/000051220
248. Ilieva EV, Ayala V, Jové M, Dalfó E, Cacabelos D, Povedano M, Bellmunt MJ, Ferrer I, Pamplona R, Portero-Otín M (2007) Oxidative and endoplasmic reticulum stress interplay in sporadic amyotrophic lateral sclerosis. Brain 130 (Pt 12):3111-3123. doi:10.1093/brain/awm190
249. Birnbaum JH, Wanner D, Gietl AF, Saake A, Kündig TM, Hock C, Nitsch RM, Tackenberg C (2018) Oxidative stress and altered mitochondrial protein expression in the absence of amyloid-β and tau pathology in iPSC-derived neurons from sporadic Alzheimer's disease patients. Stem Cell Research 27:121-130. doi:https://doi.org/10.1016/j.scr.2018.01.019
250. Kamat PK, Kalani A, Rai S, Swarnkar S, Tota S, Nath C, Tyagi N (2016) Mechanism of Oxidative Stress and Synapse Dysfunction in the Pathogenesis of Alzheimer's Disease:

Understanding the Therapeutics Strategies. Molecular Neurobiology 53 (1):648-661. doi:10.1007/s12035-014-9053-6
251. Holmström KM, Finkel T (2014) Cellular mechanisms and physiological consequences of redox-dependent signalling. Nat Rev Mol Cell Biol 15 (6):411-421. doi:10.1038/nrm3801
252. Swerdlow RH, Burns JM, Khan SM (2014) The Alzheimer's disease mitochondrial cascade hypothesis: Progress and perspectives. Biochimica et Biophysica Acta (BBA) - Molecular Basis of Disease 1842 (8):1219-1231. doi:https://doi.org/10.1016/j.bbadis.2013.09.010
253. Swerdlow RH, Khan SM (2009) The Alzheimer's disease mitochondrial cascade hypothesis: an update. Exp Neurol 218 (2):308-315. doi:10.1016/j.expneurol.2009.01.011
254. Feng Y, Xia Y, Yu G, Shu X, Ge H, Zeng K, Wang J, Wang X (2013) Cleavage of GSK-3β by calpain counteracts the inhibitory effect of Ser9 phosphorylation on GSK-3β activity induced by H_2O_2. J Neurochem 126 (2):234-242. doi:10.1111/jnc.12285
255. Mattson MP, Magnus T (2006) Ageing and neuronal vulnerability. Nat Rev Neurosci 7 (4):278-294. doi:10.1038/nrn1886
256. Yao J, Irwin RW, Zhao L, Nilsen J, Hamilton RT, Brinton RD (2009) Mitochondrial bioenergetic deficit precedes Alzheimer's pathology in female mouse model of Alzheimer's disease. Proc Natl Acad Sci U S A 106 (34):14670-14675. doi:10.1073/pnas.0903563106
257. Wang Y, Martinez-Vicente M, Krüger U, Kaushik S, Wong E, Mandelkow EM, Cuervo AM, Mandelkow E (2009) Tau fragmentation, aggregation and clearance: the dual role of lysosomal processing. Hum Mol Genet 18 (21):4153-4170. doi:10.1093/hmg/ddp367
258. Lim F, Hernández F, Lucas JJ, Gómez-Ramos P, Morán MA, Avila J (2001) FTDP-17 mutations in tau transgenic mice provoke lysosomal abnormalities and Tau filaments in forebrain. Mol Cell Neurosci 18 (6):702-714. doi:10.1006/mcne.2001.1051
259. Silva DF, Esteves AR, Arduino DM, Oliveira CR, Cardoso SM (2011) Amyloid-β-induced mitochondrial dysfunction impairs the autophagic lysosomal pathway in a tubulin dependent pathway. J Alzheimers Dis 26 (3):565-581. doi:10.3233/jad-2011-110423
260. Iourov IY, Vorsanova SG, Liehr T, Yurov YB (2009) Aneuploidy in the normal, Alzheimer's disease and ataxia-telangiectasia brain: differential expression and pathological meaning. Neurobiol Dis 34 (2):212-220. doi:10.1016/j.nbd.2009.01.003
261. Mosch B, Morawski M, Mittag A, Lenz D, Tarnok A, Arendt T (2007) Aneuploidy and DNA replication in the normal human brain and Alzheimer's disease. J Neurosci 27 (26):6859-6867. doi:10.1523/jneurosci.0379-07.2007
262. Cassidy L, Fernandez F, Johnson JB, Naiker M, Owoola AG, Broszczak DA (2020) Oxidative stress in alzheimer's disease: A review on emergent natural polyphenolic therapeutics. Complementary Therapies in Medicine 49:102294. doi:https://doi.org/10.1016/j.ctim.2019.102294
263. Krstic D, Knuesel I (2013) Deciphering the mechanism underlying late-onset Alzheimer disease. Nat Rev Neurol 9 (1):25-34. doi:10.1038/nrneurol.2012.236
264. Deardorff WJ, Feen E, Grossberg GT (2015) The Use of Cholinesterase Inhibitors Across All Stages of Alzheimer's Disease. Drugs & Aging 32 (7):537-547. doi:10.1007/s40266-015-0273-x
265. Rogawski MA, Wenk GL (2003) The neuropharmacological basis for the use of memantine in the treatment of Alzheimer's disease. CNS Drug Rev 9 (3):275-308. doi:10.1111/j.1527-3458.2003.tb00254.x
266. Madav Y, Wairkar S, Prabhakar B (2019) Recent therapeutic strategies targeting beta amyloid and tauopathies in Alzheimer's disease. Brain Res Bull 146:171-184. doi:10.1016/j.brainresbull.2019.01.004
267. Doody RS, Raman R, Farlow M, Iwatsubo T, Vellas B, Joffe S, Kieburtz K, He F, Sun X, Thomas RG, Aisen PS, Siemers E, Sethuraman G, Mohs R (2013) A Phase 3 Trial of

Semagacestat for Treatment of Alzheimer's Disease. New England Journal of Medicine 369 (4):341-350. doi:10.1056/NEJMoa1210951
268. Coric V, van Dyck CH, Salloway S, Andreasen N, Brody M, Richter RW, Soininen H, Thein S, Shiovitz T, Pilcher G, Colby S, Rollin L, Dockens R, Pachai C, Portelius E, Andreasson U, Blennow K, Soares H, Albright C, Feldman HH, Berman RM (2012) Safety and tolerability of the γ-secretase inhibitor avagacestat in a phase 2 study of mild to moderate Alzheimer disease. Arch Neurol 69 (11):1430-1440. doi:10.1001/archneurol.2012.2194
269. DeMattos RB, Bales KR, Cummins DJ, Paul SM, Holtzman DM (2002) Brain to Plasma Amyloid-β Efflux: a Measure of Brain Amyloid Burden in a Mouse Model of Alzheimer's Disease. Science 295 (5563):2264-2267. doi:10.1126/science.1067568
270. DeMattos RB, Bales KR, Cummins DJ, Dodart JC, Paul SM, Holtzman DM (2001) Peripheral anti-A beta antibody alters CNS and plasma A beta clearance and decreases brain A beta burden in a mouse model of Alzheimer's disease. Proceedings of the National Academy of Sciences of the United States of America 98 (15):8850-8855. doi:10.1073/pnas.151261398
271. Schenk D, Barbour R, Dunn W, Gordon G, Grajeda H, Guido T, Hu K, Huang J, Johnson-Wood K, Khan K, Kholodenko D, Lee M, Liao Z, Lieberburg I, Motter R, Mutter L, Soriano F, Shopp G, Vasquez N, Vandevert C, Walker S, Wogulis M, Yednock T, Games D, Seubert P (1999) Immunization with amyloid-beta attenuates Alzheimer-disease-like pathology in the PDAPP mouse. Nature 400 (6740):173-177. doi:10.1038/22124
272. Bard F, Cannon C, Barbour R, Burke RL, Games D, Grajeda H, Guido T, Hu K, Huang J, Johnson-Wood K, Khan K, Kholodenko D, Lee M, Lieberburg I, Motter R, Nguyen M, Soriano F, Vasquez N, Weiss K, Welch B, Seubert P, Schenk D, Yednock T (2000) Peripherally administered antibodies against amyloid beta-peptide enter the central nervous system and reduce pathology in a mouse model of Alzheimer disease. Nat Med 6 (8):916-919. doi:10.1038/78682
273. Yamada K, Yabuki C, Seubert P, Schenk D, Hori Y, Ohtsuki S, Terasaki T, Hashimoto T, Iwatsubo T (2009) Aβ Immunotherapy: Intracerebral Sequestration of Aβ by an Anti-Aβ Monoclonal Antibody 266 with High Affinity to Soluble Aβ. The Journal of Neuroscience 29 (36):11393-11398. doi:10.1523/jneurosci.2021-09.2009
274. Liu Y-H, Wang Y-R, Xiang Y, Zhou H-D, Giunta B, Manucat N, Tan J, Zhou X-F, Wang Y-J (2014) Clearance of Amyloid-Beta in Alzheimer’s Disease: Shifting the Action Site from Center to Periphery. Molecular neurobiology 51. doi:10.1007/s12035-014-8694-9
275. Longo FM, Massa SM (2013) Small-molecule modulation of neurotrophin receptors: a strategy for the treatment of neurological disease. Nature Reviews Drug Discovery 12 (7):507-525. doi:10.1038/nrd4024
276. Rafii MS, Baumann TL, Bakay RA, Ostrove JM, Siffert J, Fleisher AS, Herzog CD, Barba D, Pay M, Salmon DP, Chu Y, Kordower JH, Bishop K, Keator D, Potkin S, Bartus RT (2014) A phase1 study of stereotactic gene delivery of AAV2-NGF for Alzheimer's disease. Alzheimers Dement 10 (5):571-581. doi:10.1016/j.jalz.2013.09.004
277. Eriksdotter Jönhagen M, Nordberg A, Amberla K, Bäckman L, Ebendal T, Meyerson B, Olson L, Seiger, Shigeta M, Theodorsson E, Viitanen M, Winblad B, Wahlund LO (1998) Intracerebroventricular infusion of nerve growth factor in three patients with Alzheimer's disease. Dement Geriatr Cogn Disord 9 (5):246-257. doi:10.1159/000017069
278. Tuszynski MH, Thal L, Pay M, Salmon DP, U HS, Bakay R, Patel P, Blesch A, Vahlsing HL, Ho G, Tong G, Potkin SG, Fallon J, Hansen L, Mufson EJ, Kordower JH, Gall C, Conner J (2005) A phase 1 clinical trial of nerve growth factor gene therapy for Alzheimer disease. Nature Medicine 11 (5):551-555. doi:10.1038/nm1239
279. Tep C, Lim TH, Ko PO, Getahun S, Ryu JC, Goettl VM, Massa SM, Basso M, Longo FM, Yoon SO (2013) Oral administration of a small molecule targeted to block proNGF binding to

p75 promotes myelin sparing and functional recovery after spinal cord injury. J Neurosci 33 (2):397-410. doi:10.1523/jneurosci.0399-12.2013
280. Massa SM, Xie Y, Yang T, Harrington AW, Kim ML, Yoon SO, Kraemer R, Moore LA, Hempstead BL, Longo FM (2006) Small, Nonpeptide $p75^{NTR}$ Ligands Induce Survival Signaling and Inhibit proNGF-Induced Death. The Journal of Neuroscience 26 (20):5288-5300. doi:10.1523/jneurosci.3547-05.2006
281. Knowles JK, Simmons DA, Nguyen TV, Vander Griend L, Xie Y, Zhang H, Yang T, Pollak J, Chang T, Arancio O, Buckwalter MS, Wyss-Coray T, Massa SM, Longo FM (2013) Small molecule p75NTR ligand prevents cognitive deficits and neurite degeneration in an Alzheimer's mouse model. Neurobiol Aging 34 (8):2052-2063. doi:10.1016/j.neurobiolaging.2013.02.015
282. Simmons DA, Knowles JK, Belichenko NP, Banerjee G, Finkle C, Massa SM, Longo FM (2014) A small molecule p75NTR ligand, LM11A-31, reverses cholinergic neurite dystrophy in Alzheimer's disease mouse models with mid- to late-stage disease progression. PloS one 9 (8):e102136-e102136. doi:10.1371/journal.pone.0102136
283. Nguyen TV, Shen L, Vander Griend L, Quach LN, Belichenko NP, Saw N, Yang T, Shamloo M, Wyss-Coray T, Massa SM, Longo FM (2014) Small molecule p75NTR ligands reduce pathological phosphorylation and misfolding of tau, inflammatory changes, cholinergic degeneration, and cognitive deficits in AβPP(L/S) transgenic mice. J Alzheimers Dis 42 (2):459-483. doi:10.3233/jad-140036
284. Lai AY, McLaurin J (2012) Clearance of amyloid-β peptides by microglia and macrophages: the issue of what, when and where. Future Neurol 7 (2):165-176. doi:10.2217/fnl.12.6
285. Wang D-S, Dickson DW, Malter JS (2006) beta-Amyloid degradation and Alzheimer's disease. Journal of biomedicine & biotechnology 2006 (3):58406-58406. doi:10.1155/JBB/2006/58406
286. Shibata M, Yamada S, Kumar SR, Calero M, Bading J, Frangione B, Holtzman DM, Miller CA, Strickland DK, Ghiso J, Zlokovic BV (2000) Clearance of Alzheimer's amyloid-ss(1-40) peptide from brain by LDL receptor-related protein-1 at the blood-brain barrier. J Clin Invest 106 (12):1489-1499. doi:10.1172/jci10498
287. Xiang Y, Bu XL, Liu YH, Zhu C, Shen LL, Jiao SS, Zhu XY, Giunta B, Tan J, Song WH, Zhou HD, Zhou XF, Wang YJ (2015) Physiological amyloid-beta clearance in the periphery and its therapeutic potential for Alzheimer's disease. Acta Neuropathol 130 (4):487-499. doi:10.1007/s00401-015-1477-1
288. Jin W-S, Shen L-L, Bu X-L, Zhang W-W, Chen S-H, Huang Z-L, Xiong J-X, Gao C-Y, Dong Z, He Y-N, Hu Z-A, Zhou H-D, Song W, Zhou X-F, Wang Y-Z, Wang Y-J (2017) Peritoneal dialysis reduces amyloid-beta plasma levels in humans and attenuates Alzheimer-associated phenotypes in an APP/PS1 mouse model. Acta Neuropathologica 134 (2):207-220. doi:10.1007/s00401-017-1721-y
289. Wang Y-R, Wang Q-H, Zhang T, Liu Y-H, Yao X-Q, Zeng F, Li J, Zhou F-Y, Wang L, Yan J-C, Zhou H-D, Wang Y-J (2017) Associations Between Hepatic Functions and Plasma Amyloid-Beta Levels—Implications for the Capacity of Liver in Peripheral Amyloid-Beta Clearance. Molecular Neurobiology 54 (3):2338-2344. doi:10.1007/s12035-016-9826-1
290. Liu YH, Xiang Y, Wang YR, Jiao SS, Wang QH, Bu XL, Zhu C, Yao XQ, Giunta B, Tan J, Zhou HD, Wang YJ (2015) Association Between Serum Amyloid-Beta and Renal Functions: Implications for Roles of Kidney in Amyloid-Beta Clearance. Mol Neurobiol 52 (1):115-119. doi:10.1007/s12035-014-8854-y
291. Holzer M, Schade N, Opitz A, Hilbrich I, Stieler J, Vogel T, Neukel V, Oberstadt M, Totzke F, Schächtele C, Sippl W, Hilgeroth A (2018) Novel Protein Kinase Inhibitors Related

to Tau Pathology Modulate Tau Protein-Self Interaction Using a Luciferase Complementation Assay. Molecules 23 (9):2335
292. Giacomini C, Koo CY, Yankova N, Tavares IA, Wray S, Noble W, Hanger DP, Morris JDH (2018) A new TAO kinase inhibitor reduces tau phosphorylation at sites associated with neurodegeneration in human tauopathies. Acta Neuropathol Commun 6 (1):37. doi:10.1186/s40478-018-0539-8
293. Yadikar H, Torres I, Aiello G, Kurup M, Yang Z, Lin F, Kobeissy F, Yost R, Wang KK (2020) Screening of tau protein kinase inhibitors in a tauopathy-relevant cell-based model of tau hyperphosphorylation and oligomerization. PLOS ONE 15 (7):e0224952. doi:10.1371/journal.pone.0224952
294. van Dyck CH, Nygaard HB, Chen K, Donohue MC, Raman R, Rissman RA, Brewer JB, Koeppe RA, Chow TW, Rafii MS, Gessert D, Choi J, Turner RS, Kaye JA, Gale SA, Reiman EM, Aisen PS, Strittmatter SM (2019) Effect of AZD0530 on Cerebral Metabolic Decline in Alzheimer Disease: A Randomized Clinical Trial. JAMA Neurology 76 (10):1219-1229. doi:10.1001/jamaneurol.2019.2050
295. Pluta R, Ułamek-Kozioł M (2020) Tau Protein-Targeted Therapies in Alzheimer's Disease: Current State and Future Perspectives. In: X H (ed) Alzheimer's Disease: Drug Discovery. Exon Publications, Brisbane, Australia.,
296. Rösler TW, Tayaranian Marvian A, Brendel M, Nykänen N-P, Höllerhage M, Schwarz SC, Hopfner F, Koeglsperger T, Respondek G, Schweyer K, Levin J, Villemagne VL, Barthel H, Sabri O, Müller U, Meissner WG, Kovacs GG, Höglinger GU (2019) Four-repeat tauopathies. Progress in Neurobiology 180:101644. doi:https://doi.org/10.1016/j.pneurobio.2019.101644
297. Mercuri E, Darras BT, Chiriboga CA, Day JW, Campbell C, Connolly AM, Iannaccone ST, Kirschner J, Kuntz NL, Saito K, Shieh PB, Tulinius M, Mazzone ES, Montes J, Bishop KM, Yang Q, Foster R, Gheuens S, Bennett CF, Farwell W, Schneider E, De Vivo DC, Finkel RS (2018) Nusinersen versus Sham Control in Later-Onset Spinal Muscular Atrophy. New England Journal of Medicine 378 (7):625-635. doi:10.1056/NEJMoa1710504
298. Nadeau A, Roberge AG (1988) Effects of vitamin B12 supplementation on choline acetyltransferase activity in cat brain. Int J Vitam Nutr Res 58 (4):402-406
299. Rajasekar N, Dwivedi S, Tota SK, Kamat PK, Hanif K, Nath C, Shukla R (2013) Neuroprotective effect of curcumin on okadaic acid induced memory impairment in mice. Eur J Pharmacol 715 (1-3):381-394. doi:10.1016/j.ejphar.2013.04.033
300. Sung S, Yao Y, Uryu K, Yang H, Lee VM, Trojanowski JQ, Praticò D (2004) Early vitamin E supplementation in young but not aged mice reduces Abeta levels and amyloid deposition in a transgenic model of Alzheimer's disease. Faseb j 18 (2):323-325. doi:10.1096/fj.03-0961fje
301. Ringman JM, Frautschy SA, Teng E, Begum AN, Bardens J, Beigi M, Gylys KH, Badmaev V, Heath DD, Apostolova LG, Porter V, Vanek Z, Marshall GA, Hellemann G, Sugar C, Masterman DL, Montine TJ, Cummings JL, Cole GM (2012) Oral curcumin for Alzheimer's disease: tolerability and efficacy in a 24-week randomized, double blind, placebo-controlled study. Alzheimer's research & therapy 4 (5):43-43. doi:10.1186/alzrt146
302. Galasko DR, Peskind E, Clark CM, Quinn JF, Ringman JM, Jicha GA, Cotman C, Cottrell B, Montine TJ, Thomas RG, Aisen P (2012) Antioxidants for Alzheimer disease: a randomized clinical trial with cerebrospinal fluid biomarker measures. Arch Neurol 69 (7):836-841. doi:10.1001/archneurol.2012.85
303. Sano M, Ernesto C, Thomas RG, Klauber MR, Schafer K, Grundman M, Woodbury P, Growdon J, Cotman CW, Pfeiffer E, Schneider LS, Thal LJ (1997) A controlled trial of selegiline, alpha-tocopherol, or both as treatment for Alzheimer's disease. The Alzheimer's

Disease Cooperative Study. N Engl J Med 336 (17):1216-1222. doi:10.1056/nejm199704243361704
304. Pavlik VN, Doody RS, Rountree SD, Darby EJ (2009) Vitamin E Use Is Associated with Improved Survival in an Alzheimer's Disease Cohort. Dementia and Geriatric Cognitive Disorders 28 (6):536-540. doi:10.1159/000255105
305. Zhang L, Fiala M, Cashman J, Sayre J, Espinosa A, Mahanian M, Zaghi J, Badmaev V, Graves MC, Bernard G, Rosenthal M (2006) Curcuminoids enhance amyloid-beta uptake by macrophages of Alzheimer's disease patients. J Alzheimers Dis 10 (1):1-7. doi:10.3233/jad-2006-10101
306. Chen YR, Tan TH (1998) Inhibition of the c-Jun N-terminal kinase (JNK) signaling pathway by curcumin. Oncogene 17 (2):173-178. doi:10.1038/sj.onc.1201941
307. Soeda Y, Takashima A (2020) New Insights Into Drug Discovery Targeting Tau Protein. Frontiers in Molecular Neuroscience 13 (231). doi:10.3389/fnmol.2020.590896
308. Lee D, Lee W-S, Lim S, Kim YK, Jung H-Y, Das S, Lee J, Luo W, Kim K-T, Chung S-K (2017) A guanidine-appended scyllo-inositol derivative AAD-66 enhances brain delivery and ameliorates Alzheimer's phenotypes. Scientific Reports 7 (1):14125. doi:10.1038/s41598-017-14559-7
309. Jiang T, Yu JT, Tan L (2012) Novel disease-modifying therapies for Alzheimer's disease. J Alzheimers Dis 31 (3):475-492. doi:10.3233/jad-2012-120640
310. Ntsapi C, Loos B (2016) Caloric restriction and the precision-control of autophagy: A strategy for delaying neurodegenerative disease progression. Exp Gerontol 83:97-111. doi:10.1016/j.exger.2016.07.014
311. Baker LD, Frank LL, Foster-Schubert K, Green PS, Wilkinson CW, McTiernan A, Cholerton BA, Plymate SR, Fishel MA, Watson GS, Duncan GE, Mehta PD, Craft S (2010) Aerobic exercise improves cognition for older adults with glucose intolerance, a risk factor for Alzheimer's disease. J Alzheimers Dis 22 (2):569-579. doi:10.3233/jad-2010-100768
312. Cruz MP (2018) Edaravone (Radicava): A Novel Neuroprotective Agent for the Treatment of Amyotrophic Lateral Sclerosis. P T 43 (1):25-28
313. Watanabe T, Tahara M, Todo S (2008) The Novel Antioxidant Edaravone: From Bench to Bedside. Cardiovascular Therapeutics 26 (2):101-114. doi:10.1111/j.1527-3466.2008.00041.x
314. Watanabe K, Tanaka M, Yuki S, Hirai M, Yamamoto Y (2018) How is edaravone effective against acute ischemic stroke and amyotrophic lateral sclerosis? J Clin Biochem Nutr 62 (1):20-38. doi:10.3164/jcbn.17-62
315. Pan Y, Li W, Feng Y, Xu J, Cao H (2020) Edaravone attenuates experimental asthma in mice through induction of HO-1 and the Keap1/Nrf2 pathway. Exp Ther Med 19 (2):1407-1416. doi:10.3892/etm.2019.8351
316. Liu J, Jiang Y, Zhang G, Lin Z, Du S (2019) Protective effect of edaravone on blood-brain barrier by affecting NRF-2/HO-1 signaling pathway. Exp Ther Med 18 (4):2437-2442. doi:10.3892/etm.2019.7859
317. Xiao B, Bi FF, Hu YQ, Tian FF, Wu ZG, Mujlli HM, Ding L, Zhou XF (2007) Edaravone neuroprotection effected by suppressing the gene expression of the Fas signal pathway following transient focal ischemia in rats. Neurotoxicity Research 12 (3):155-162. doi:10.1007/BF03033912
318. Li C, Mo Z, Lei J, Li H, Fu R, Huang Y, Luo S, Zhang L (2018) Edaravone Attenuates Neuronal Apoptosis in Hypoxic-Ischemic Brain Damage Rat Model via Suppression of TRAIL Signaling Pathway. The International Journal of Biochemistry & Cell Biology 99. doi:10.1016/j.biocel.2018.03.020

319. Yasuoka N, Nakajima W, Ishida A, Takada G (2004) Neuroprotection of edaravone on hypoxic-ischemic brain injury in neonatal rats. Brain Res Dev Brain Res 151 (1-2):129-139. doi:10.1016/j.devbrainres.2004.04.006
320. Amemiya S, Kamiya T, Nito C, Inaba T, Kato K, Ueda M, Shimazaki K, Katayama Y (2005) Anti-apoptotic and neuroprotective effects of edaravone following transient focal ischemia in rats. Eur J Pharmacol 516 (2):125-130. doi:10.1016/j.ejphar.2005.04.036
321. Feng S, Yang Q, Liu M, Li W, Yuan W, Zhang S, Wu B, Li J (2011) Edaravone for acute ischaemic stroke. Cochrane Database Syst Rev (12):Cd007230. doi:10.1002/14651858.CD007230.pub2
322. Yoshida H, Yanai H, Namiki Y, Fukatsu-Sasaki K, Furutani N, Tada N (2006) Neuroprotective effects of edaravone: a novel free radical scavenger in cerebrovascular injury. CNS Drug Rev 12 (1):9-20. doi:10.1111/j.1527-3458.2006.00009.x
323. Yoshino H (2019) Edaravone for the treatment of amyotrophic lateral sclerosis. Expert Rev Neurother 19 (3):185-193. doi:10.1080/14737175.2019.1581610
324. Jiao S-S, Yao X-Q, Liu Y-H, Wang Q-H, Zeng F, Lu J-J, Liu J, Zhu C, Shen L-L, Liu C-H, Wang Y-R, Zeng G-H, Parikh A, Chen J, Liang C-R, Xiang Y, Bu X-L, Deng J, Li J, Xu J, Zeng Y-Q, Xu X, Xu H-W, Zhong J-H, Zhou H-D, Zhou X-F, Wang Y-J (2015) Edaravone alleviates Alzheimer's disease-type pathologies and cognitive deficits. Proceedings of the National Academy of Sciences of the United States of America 112 (16):5225-5230. doi:10.1073/pnas.1422998112
325. Parikh A, Kathawala K, Tan CC, Garg S, Zhou X-F (2018) Self-nanomicellizing solid dispersion of edaravone: part I - oral bioavailability improvement. Drug Des Devel Ther 12:2051-2069. doi:10.2147/DDDT.S161940
326. Parikh A, Kathawala K, Li J, Chen C, Shan Z, Cao X, Wang YJ, Garg S, Zhou XF (2018) Self-nanomicellizing solid dispersion of edaravone: part II: in vivo assessment of efficacy against behavior deficits and safety in Alzheimer's disease model. Drug Des Devel Ther 12:2111-2128. doi:10.2147/dddt.S161944
327. Pennanen L, Wolfer DP, Nitsch RM, Götz J (2006) Impaired spatial reference memory and increased exploratory behavior in P301L tau transgenic mice. Genes, Brain and Behavior 5 (5):369-379. doi:10.1111/j.1601-183X.2005.00165.x
328. Götz J, Chen F, Barmettler R, Nitsch RM (2001) Tau filament formation in transgenic mice expressing P301L tau. J Biol Chem 276 (1):529-534. doi:10.1074/jbc.M006531200
329. Webster SJ, Bachstetter AD, Nelson PT, Schmitt FA, Van Eldik LJ (2014) Using mice to model Alzheimer's dementia: an overview of the clinical disease and the preclinical behavioral changes in 10 mouse models. Frontiers in Genetics 5 (88). doi:10.3389/fgene.2014.00088
330. Ribeiro FM, Camargos ER, de Souza LC, Teixeira AL (2013) Animal models of neurodegenerative diseases. Braz J Psychiatry 35 Suppl 2:S82-91. doi:10.1590/1516-4446-2013-1157
331. Newman M, Kretzschmar D, Khan I, Chen M, Verdile G, Lardelli M (2017) Chapter 40 - Animal Models of Alzheimer's Disease. In: Conn PM (ed) Animal Models for the Study of Human Disease (Second Edition). Academic Press, pp 1031-1085. doi:https://doi.org/10.1016/B978-0-12-809468-6.00040-1
332. LaFerla FM, Green KN (2012) Animal models of Alzheimer disease. Cold Spring Harbor perspectives in medicine 2 (11):a006320. doi:10.1101/cshperspect.a006320
333. Götz J, Streffer JR, David D, Schild A, Hoerndli F, Pennanen L, Kurosinski P, Chen F (2004) Transgenic animal models of Alzheimer's disease and related disorders: histopathology, behavior and therapy. Mol Psychiatry 9 (7):664-683. doi:10.1038/sj.mp.4001508
334. Calhoun ME, Wiederhold KH, Abramowski D, Phinney AL, Probst A, Sturchler-Pierrat C, Staufenbiel M, Sommer B, Jucker M (1998) Neuron loss in APP transgenic mice. Nature 395 (6704):755-756. doi:10.1038/27351

335. Jankowsky JL, Slunt HH, Ratovitski T, Jenkins NA, Copeland NG, Borchelt DR (2001) Co-expression of multiple transgenes in mouse CNS: a comparison of strategies. Biomol Eng 17 (6):157-165. doi:10.1016/s1389-0344(01)00067-3
336. Götz J, Deters N, Doldissen A, Bokhari L, Ke Y, Wiesner A, Schonrock N, Ittner LM (2007) A decade of tau transgenic animal models and beyond. Brain Pathol 17 (1):91-103. doi:10.1111/j.1750-3639.2007.00051.x
337. Götz JJ, Götz J (2019) Experimental Models of Tauopathy - From Mechanisms to Therapies. Adv Exp Med Biol 1184:381-391. doi:10.1007/978-981-32-9358-8_28
338. Kamat PK, Kalani A, Rai S, Tota SK, Kumar A, Ahmad AS (2016) Streptozotocin Intracerebroventricular-Induced Neurotoxicity and Brain Insulin Resistance: a Therapeutic Intervention for Treatment of Sporadic Alzheimer's Disease (sAD)-Like Pathology. Mol Neurobiol 53 (7):4548-4562. doi:10.1007/s12035-015-9384-y

CHAPTER 2: Pharmacokinetics of p75ECD-Fc

Sally Kelliny, Ho Yin Lam, Ankit Parikh, Yan-Jiang Wang, Larisa Bobrovskaya, Richard Upton and Xin-Fu Zhou

Preclinical Study of the Pharmacokinetics of p75ECD-Fc, a Novel Human Recombinant Protein for Treatment of Alzheimer's Disease, in Sprague Dawley Rats. Current Drug Metabolism; 2020.

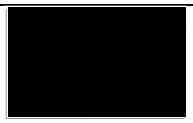
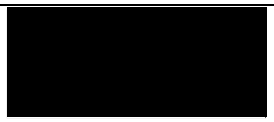
Publication status: Published

The published version is available at: https://www.eurekaselect.com/181568/article

Author Contributions

Author	Wrote Manuscript	Revised Manuscript	Designed Research	Performed Research	Analysis of Data	Data Interpretation
Kelliny, S	✔	✔	✔	✔	✔	✔
Lam, HY		✔		✔	✔	✔
Parikh, A		✔			✔	
Wang, YJ		✔				
Bobrovskaya, L		✔	✔			✔
Upton, R		✔			✔	✔
Zhou, X. F		✔	✔	✔	✔	✔

Full name of co-author	Signature	Date
Sally Kelliny	[redacted]	15-03-2021
Ho Yin Lam	[redacted] on behalf of Lam HY	20/04/2021
Ankit Parikh	A.y.parikh	26/03/2021

Yan-Jiang Wang		20/04/2021
Larisa Bobrovskaya		20/04/2021
Richard Upton		20/04/2021
Xin-Fu Zhou		20/04/2021

Send Orders for Reprints to reprints@benthamscience.net

Current Drug Metabolism, 2020, *21*, 000-000

RESEARCH ARTICLE

Preclinical Study of the Pharmacokinetics of p75ECD-Fc, a Novel Human Recombinant Protein for Treatment of Alzheimer's Disease, in Sprague Dawley Rats

Sally Kelliny[a,d], Ho Yin Lam[a], Ankit Parikh[a], Yan-Jiang Wang[b], Larisa Bobrovskaya[a], Richard Upton[c] and Xin-Fu Zhou[a,*]

[a]*School of Pharmacy and Medical Sciences, Division of Health Sciences, University of South Australia, Adelaide, Australia;* [b]*Department of Neurology, Daping Hospital, Third Military Medical University, Chongqing, China;* [c]*Australian Centre for Pharmacometrics, University of South Australia, School of Pharmacy and Medical Sciences, Division of Health Sciences, University of South Australia, Adelaide, Australia;* [d]*Faculty of Pharmacy, Assiut University, Assiut, Egypt*

Abstract: ***Background*** p75ECD-Fc is a recombinant human protein that has recently been developed as a novel therapy for Alzheimer's disease. Current studies showed that it is able to alleviate Alzheimer's disease pathologies in animal models of dementia. Thus, knowledge about the pharmacokinetic behavior and tissue distribution of this novel protein is crucial in order to better understand its pharmacodynamics and more importantly for its clinical development.

Methods: The aim of this study is to characterize the pharmacokinetics of p75ECD-Fc after single intravenous and subcutaneous injection of 3mg/kg in Sprague Dawley rats. We calculated the bioavailability of the SC route and studied the distribution of that protein in different tissues, cerebrospinal fluid and urine using ELISA and immunofluorescence techniques. In-vitro stability of the drug was also assessed. Data obtained were analyzed with Non-compartmental pharmacokinetic method using R.

Results Results showed that the bioavailability of SC route was 66.15%. Half-life time was 7.5 ± 1.7 and 6.2 ± 2.4 days for IV and SC injection, respectively. Tissue distribution of p75ECD-Fc was modest with the ability to penetrate the blood brain barrier. It showed high in-vitro stability in human plasma.

Conclusion: These acceptable pharmacokinetic properties of p75ECD-Fc present it as a potential candidate for clinical development for the treatment of Alzheimer's disease.

ARTICLE HISTORY

Received: January 17, 2020
Revised: February 11, 2020
Accepted: March 26, 2020

DOI:
10.2174/1389200221666200502015203

Keywords: Alzheimer's disease, pharmacokinetics, p75ECD-Fc, amyloid-β, p75 neurotrophin receptor, non-compartmental analysis.

1. INTRODUCTION

Alzheimer's disease (AD) is one of the most common causes of dementia among elderly people affecting more than 50 million people worldwide. It is characterized by a progressive decline in memory, along with behavioral and mood disturbances that finally lead to death [1]. Amyloid beta (Aβ) plaques and phosphorylated tau protein accumulation within the brain are considered the main disease manifestations. However, the underlying molecular mechanism of the disease is still illusive. Several therapeutic strategies have been developed based on the concept that Aβ is a central component of the disease progression. This concept was derived from the amyloid cascade hypothesis, which postulates that accumulation of Aβ plaques is a result of overproduction, aggregation and deposition of Aβ peptide specifically Aβ42 and that other hallmarks of the disease are downstream events in that cascade [2]. In addition, failure of the central innate immune system of demented patients to clear this misfolded protein aggregates from the brain rather than its overproduction was found to be the main driving force for plaque formation [3-4]. Unfortunately, all antibodies and other immune-based therapies targeting Aβ have failed to date [5-7].

Recently, p75 neurotrophin (p75NTR) receptor was identified to be involved in the pathogenesis of AD [8]. p75NTR is the pan receptor for both proneurotrophins and mature neurotrophins playing a diverse role in neurite growth and development, cell survival and neurodegeneration. Current studies showed that it has a dual role in mediating cell growth when activated with mature neurotrophins while promoting cell death and neurodegeneration in elderly people as a co-receptor of proneurotrophins with sortilin [9-10]. Mounting evidence indicates that the upregulation of p75NTR and proneurotrophins is considered the underlying mechanism of AD, so-called as neurotrophin theory [11]. Wang and Zhou *et al*. proved that p75NTR can mediate Aβ production through enhancing the amyloidogenic processing of the amyloid precursor protein (APP) resulting in Aβ plaque formation and deposition. They also proved that the extracellular domain (ECD) of p75NTR can produce opposite effect by sequestering soluble Aβ monomers enhancing its clearance from the brain [12-14]. Interestingly, Aβ was found to have a high affinity to bind to p75NTR [15], thus promoting the overproduction of more toxic Aβ peptides and neurodegeneration [16-17]. Furthermore, it can inhibit the cleavage of p75NTR, releasing its extracellular domain, which has a neuroprotective effect, thus inhibiting its clearance from the brain and maintaining a vicious cycle leading to cell death [18]. This hypothesis was supported by data from clinical studies showing that the level of ECD is dramatically reduced in AD patients while the full-length receptor p75NTR and proneurotrophins are upregulated [8, 19].

In this context, p75ECD-Fc was recently developed as a novel therapeutic approach of AD. It is a recombinant fusion protein of the extracellular domain of the human nerve growth factor receptor p75 and Fc fragment of the human immunoglobulin IgG1. It resembles the structure of Etanercept, the FDA approved drug for in-

*Address correspondence to this author at the School of Pharmacy and Medical Sciences, Division of Health Sciences, University of South Australia, Adelaide, Australia; E-mail: Xin-Fu.Zhou@unisa.edu.au

1389-2002/20 $65.00+.00 © 2020 Bentham Science Publishers

flammatory arthritis, which is a fusion protein of the extracellular domain of Tumour Necrosis Factor alpha (TNF-α) receptor and Fc fragment of IgG1 [20]. Injection of p75ECD-Fc in brains of AD transgenic mice reduced Aβ plaque load and improved their cognitive function [19]. The mechanism of action of that molecule could be attributed to its ability to sequester toxic Aβ and proneurotrophins, thus preventing its binding to full-length p75NTR and in turn inhibiting the production of more toxic Aβ [13]. Moreover, p75ECD-Fc binding to Aβ can promote its clearance through immune system through its Fc part, thus inhibiting its aggregation and promoting plaque defibrillation [19]. Administering p75ECD-Fc peripherally is postulated to be superior to anti-Aβ antibodies. It is worth mentioning that anti-Aβ antibodies bind to Aβ centrally provoking neuroinflammation, edema and microhemorrhage as central clearance of these complex structures was found to have drastic effects [21]. In contrast, p75ECD-Fc could bind toxic ligands in the periphery as Aβ and proneurotrophins, thus favoring the balance towards Aβ efflux out of the brain to the periphery; a theory previously known as "peripheral sink" hypothesis [22]. Taking into consideration that Aβ levels in the periphery and brain can be equilibrated and almost 50% of Aβ in the body is cleared through the liver and kidney [23], we believe that p75ECD-Fc, as a novel and unique approach, would be safer and more effective.

Based on the aforementioned and in order to best understand the pharmacokinetics and pharmacodynamics of p75ECD-Fc, Sprague Dawley rats were given a single dose of 3 mg/kg p75ECD-Fc IV and SC, then blood and tissue samples were separated at different time points as represented in Scheme **1**. The level of the drug was measured using an ELISA assay. Non-compartmental pharmacokinetic analysis was used to calculate the clearance, half-life and the bioavailability after SC injection. Tissues were subjected to double immunofluorescence to detect the drug localization and the cells that could internalize it. We also studied the in-vitro stability of the protein in human plasma. The data obtained from the current study enabled us to understand the mechanism of action, the pharmacokinetics of p75ECD-Fc and will provide good support for future development of that drug in clinical studies.

2. MATERIALS AND METHODS

2.1. Materials

P75ECD-Fc (25 mg/ml) was obtained from Tiantai Medical Technology, Fuzhou, China and diluted to 3 mg/ml with phosphate-buffered saline (PBS) then stored at -80◦C till further use. Human NGFR/TNFRSF16 DuoSet ELISA was purchased from R&D Systems, Minneapolis, USA, to be used for the sandwich ELISA procedure. The detection antibody (biotinylated mouse anti-human IgG Fc secondary antibody) was obtained from Thermo Scientific, USA, (05-4240) and diluted with glycerol and stored at -80◦C for future use. Biotinylated goat anti-human Fc was purchased from ThermoFisher scientific. Mouse anti-rat CD11b, Iba-1 and S100 primary antibodies, to detect macrophages and lymphocytes were obtained from Abcam and Sigma Aldrich. Cy2 and Cy3-conjugated secondary antibodies were purchased from Jackson ImmunoResearch Laboratories (USA). ELISA plates were purchased from Thermo Scientific, Denmark. Horseradish peroxidase (HRP) conjugated Streptavidin, Tetramethylbenzidine (TMB) liquid substrate (T0440), Bovine serum albumin (BSA), Tween-20 and Triton-X 100 were purchased from Sigma Aldrich, USA. Protease cocktail inhibitor tablets easy pack was purchased from Roche Diagnostics GmbH, Mannheim, Germany.

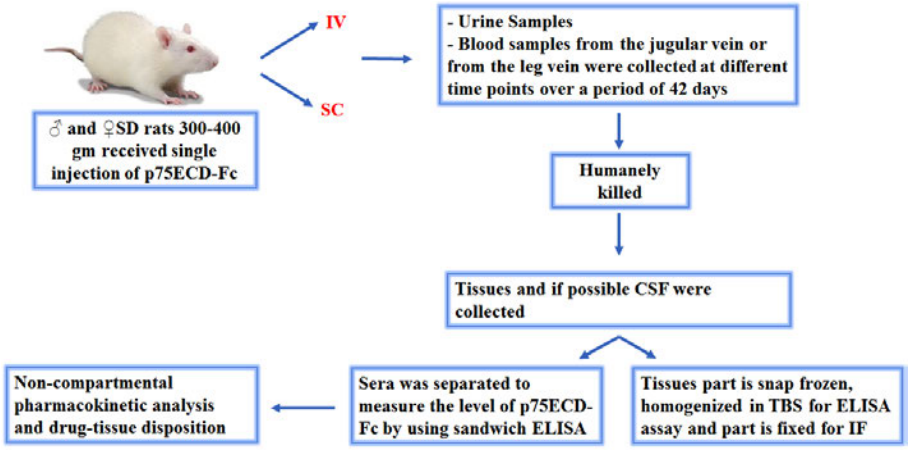
2.2. Animal Procedures and Tissue Sampling

All animal experiments were done in accordance with the South Australian Animal Welfare Regulations 2012 and guidelines and approved by the Animal Ethics Committee (AEC) of the University of South Australia (approval number: U14/16).

Fifteen 3-month old male and female Sprague Dawley rats weighing between 300-400g were obtained from the animal facility at the School of Pharmacy and Medical Sciences, University of South Australia. Before starting experiments, animals were maintained under standard conditions at 22°C and a 12-hr light/dark cycle with food and water ad libitum. Then, they were divided randomly into two groups. Group A consisted of 8 animals (5 males and 3 females) which received a single dose of p75ECD-Fc 3mg/kg intravenously (IV) by jugular vein cannulation or tail vein injection while group B consisted of 7 animals (5 males and 2 females) and they received the same dose of p75ECD-Fc subcutaneously (SC). Each animal has undergone a surgical procedure under isoflurane anesthesia to place the jugular vein cannula and maintained using heparinized saline flushes.

2.3. Serum, Tissues, CSF and Urine Samples Collection

Blood samples were collected from the jugular vein cannula (for the first two days) and from the saphenous (leg) vein (after the cannula is blocked) at the following time points (0, 15, 30 minutes, post dose followed by 1, 3, 5, 8, 24 hours and then 2 days, 3, 7, 14, 21, 28, 35 and 42 days). Urine samples were collected at different time points whenever possible. 3 days post dose, one male from each group was humanely killed (HK) and, their blood and tissues samples were collected. At 14 days post dose, another 4 rats were separated randomly from each group and were HK and their sera, CSF and tissue samples were collected. After 42 days post dose, all remaining rats were HK and blood, urine and CSF samples were separated for analysis. Blood and urine samples obtained were centrifuged at 3000xg for 10 minutes and supernatant was separated.



Scheme 1. Schematic illustration of different steps of the study starting with IV and SC injection of p75ECD-Fc into Sprague Dawley rats followed by samples collection, histochemical and pharmacokinetics analysis.

Serum, urine and CSF samples were stored in -80°C until further analysis with enzyme-linked immunosorbent assay (ELISA).

2.4. Frozen and Fixed Tissue Preparation

After perfusing the animal carcasses with cold PBS intracardially, brain, spinal cord, liver, heart, kidney, lungs, spleen, skin, lymph nodes and muscle were dissected. These tissues were divided into two parts. One part was snap frozen in liquid nitrogen and stored at -80°C. The other part was washed in ice-cold PBS and then fixed in 4% paraformaldehyde for 24 hours at 4°C and then tissues were washed with PBS for 10 min at room temperature and stored in PBS containing 0.02% sodium azide. Prior to cryosectioning, tissues were placed in 30% sucrose/PBS overnight at 4°C. Subsequently, tissues were embedded in optimal cutting temperature compound (OCT) and were cut at a thickness of 8µm using cryo-sectioning microtome (Leica CM 3050 S), then sections were directly placed on SuperFrost charged glass slides (Menzel-Gläser, Germany). Tissue sections were fixed to slides by placing the slides on 60°C hot plate for 1 hour and then stored in -20 °C for subsequent histological analysis. Frozen tissues were homogenized with liquid nitrogen and sonicated in tris-buffered saline (TBS, pH 7.4) containing protease cocktail inhibitors. Then, the homogenates were centrifuged at 15,000 rpm for 30 minutes at 4°C and the supernatant was collected and stored at -80°C.

2.5. *In-vitro* Stability of p75ECD-Fc in Human Plasma

Fresh human plasma was obtained from a hospital and stored at -20°C until use for experiments. p75ECD-Fc was mixed with human plasma to a final concentration of 10µg/ml. The mixture was divided into triplicates and stored at 37°C incubator for 35 days. 2µl were separated at various time points (1, 3, 7, 14, 21, 28 and 35 days). Samples were stored at -80 °C until further analysis with sandwich ELISA.

2.6. Development of Standard curves for p75ECD-Fc in Sandwich ELISA

The concentration of p75ECD-Fc in sera and tissue homogenates was measured by sandwich ELISA using Human NGF R/TNFRSF16 kit (R&D Systems, Minneapolis, USA).

Standard curve of p75ECD-Fc was generated according to the kit procedure. Mouse anti-human NGF R capture antibody (CA) was reconstituted with 1ml of PBS to a concentration of 360 µg/ml and aliquoted and stored at -80°C. Before coating the plate, CA was diluted to the working concentration of 1µg/ml with the coating buffer (0.05M sodium carbonate buffer, pH 9.6). Standard of human recombinant p75ECD-Fc was diluted with 0.5 ml 1%BSA/PBS and aliquoted and stored at -80°C at 100 ng/ml. Biotinylated mouse anti-human IgG Fc (diluted 1:1000) in sample diluent (1% BSA in 1xPBS/0.05% Tween-20) was used as the detection antibody which detects the Fc portion of p75ECD-Fc. A seven-point standard curve using 2-fold serial dilutions of the standard in the sample diluent (1%BSA/PBST) with concentrations ranging from 62.5 pg/ml to 4000 pg/ml were obtained. The lower limit of quantification of the assay was 0.0625 ng/ml (Fig. **1**).

2.7. Sera, Urine, CSF and Tissue Samples Analysis

Prior to samples analysis, 96-well ELISA plates were coated with 100 µl /well R&D capture antibody (mouse anti-human NGF R) at 1µg/ml in coating buffer at 25◦C overnight. Plates were washed three times with 300 µl/well PBS and blocked with 170 µl/well 3% BSA/PBS for 1 h at 37◦C. Serial dilutions of the standard of p75ECD-Fc (110 ng/ml) were made in a range from 62.5 to 4000 pg/mL in 1%BSA/PBS/0.05%Tween-20. Sera samples and tissue samples were diluted with a specific ratio of dilution factor according to their specific blood sampling time. After 1hr blocking, the blocking solution was discarded, and 100 µl/well standards and samples were then added in duplicate to the plate and incubated at 37°C for 1hr. After that, 100 µl/well of the detection antibody biotinylated mouse anti-human IgG Fc diluted in a sample diluent (1:1000) were added to the plate and incubated at 37°C for 1 hr. Then, the plates were washed with 300µl/well PBST (0.05%Tween-20/PBS). Afterwards, 100 µl/well Streptavidin-HRP diluted in sample diluent (1:5000) were then added into plates and incubated again at 37◦C for 1 hr. The plates were washed thoroughly with 300 µl/well PBST, 100 µl/well TMB liquid substrate were then added to each well and incubated for 10 min at room temperature in the dark. The reaction was stopped by adding 100 µl/well 0.1N HCl, and the optical density of each well was determined immediately using a PerkinElmer Victor-x4 Plate Reader (Waltham, MA) set to 450 nm (0.1s).

The concentration of p75ECD-Fc in blood, CSF and different tissues was determined by p75ECD-Fc sandwich ELISA, according to equation 1 obtained from the standard curve of p75ECD-Fc (Fig. **1**) as follows:

The concentration of p75ECD−Fc (pg/ml) = (The obtained absorbance value – 0.177)/0.0003× Dilution factor **Equation 1**

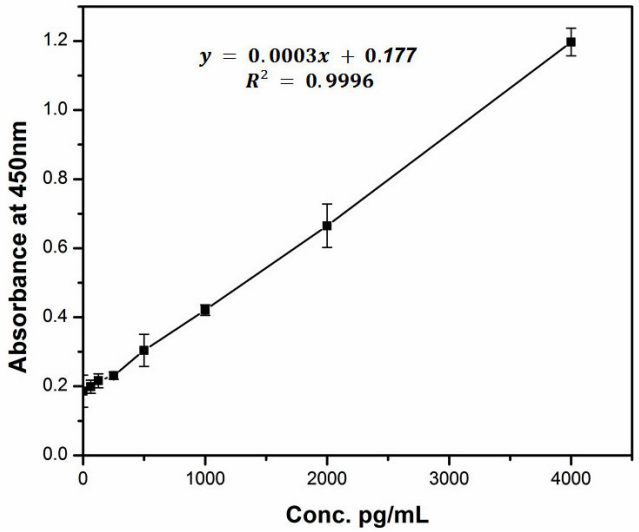


Fig. (1). Standard curve of p75ECD-Fc is generated using sandwich ELISA technique. Each point represents mean absorbance plotted for each concentration ±S.D. The concentration of p75ECD-Fc in sera and tissues is calculated using the equation obtained from the standard curve and multiplied by the dilution factor for each sample. (*A higher resolution / colour version of this figure is available in the electronic copy of the article*).

2.8. Immunofluorescent Analysis of p75ECD-Fc in Tissues

Sections of different tissues were double stained to detect both p75ECD-Fc and possible cells that internalized the molecule with its Fc part. Sections were washed several times with PBS and then antigen retrieval was done using 1% SDS for 5 minutes. After that, tissue sections were blocked with 20% normal horse serum (NHS) in PBS for 2 hours at room temperature, then incubated with biotinylated goat anti-human Fc antibody and mouse anti-rat CD11b at room temperature for two hours (diluted 1:200 in 1%NHS/PBS/0.3%triton-X 100). Sections were washed with 0.3%tritonX-100/PBS 3 times and then incubated with Cys-3 streptavidin and donkey anti-mouse Cy2 (1:1000) for 30 min at room temperature. Nuclei were stained with DAPI. Finally, sections were washed thoroughly 3 times with PBST, and coverslip with aqueous media. Images were taken using an Olympus Microscope (CX40) using 40x magnification.

The presence of p75ECD-Fc in different tissues was detected specifically by focusing on leukocytes, macrophages, microglia, T-cells and all related phagocytes in different tissues such as Kupffer cells in the liver, and dendritic cells in the skin and alveolar macrophages in the lung since these cells express Fc gamma receptors which may internalize the drug.

2.9. Non-Compartmental Pharmacokinetic Analysis (NCA)

Non-compartmental pharmacokinetic analysis was performed using the R data analysis (R version 3.6.0) [24] with the package PKNCA [25]. The area under the plasma concentration time curve from time zero till the last measurable concentration (AUC0-tlast) was calculated by trapezoidal integration and then extrapolated to infinity to get AUC_{inf} where the AUC_{exp} is calculated by dividing the last measurable concentration by the elimination rate constant ($C_{last}/ \lambda z$). The NCA settings used linear up, log down integration and allowed C_{max} to be included in the log-linear extrapolation of the terminal concentrations. The number of extrapolated points was determined by optimizing the R2 value of the log-linear fit. Peak plasma concentration (C_{max}) and time to reach C_{max} (T_{max}) were extracted from the data. The elimination rate constant K_{el} (λz) was calculated from the slope of the log concentration versus time for the terminal concentrations. The elimination half-life ($t_{1/2}$) was calculated as $0.693/K_{el}$. MRT (mean residence time) was obtained by dividing $AUMC_{inf}$ (area under the first moment curve) by AUC_{inf}. Total body clearance (CLt) for IV and SC was calculated as the dose administered divided by the AUC_{inf}. The volume of distribution at steady-state (V_{ss}) was calculated as CL multiplied by MRT. The bioavailability (F) after SC administration was calculated by dividing the AUC_{inf} obtained from SC data by the AUC_{inf} of the IV data.

2.10. Statistical Analysis

Statistical analyses were performed using R and OriginPro 8.5. All data obtained are expressed as mean ± SD (standard deviation).

3. RESULTS

3.1. Non-Compartmental Pharmacokinetic Analysis

A single dose of p75ECD-Fc (3mg/kg) was administered IV and SC into two animal groups. Serum and tissue samples were collected at different time points for analysis using sandwich ELISA. The observed serum and tissue concentrations are shown in Fig. (**2**).

After IV administration of 3mg/kg of p75ECD-Fc, C_{max} was 85.205 ± 6.625 µg/ml and the t1/2 was 7.492 ± 1.7 days. After SC administration, serum concentration increased reaching maximum level (C_{max}) of 11.493 ± 1.045 µ g/ml at 3.13 ± 0.11 days (T_{max}) after which it started to decrease gradually with an elimination half-

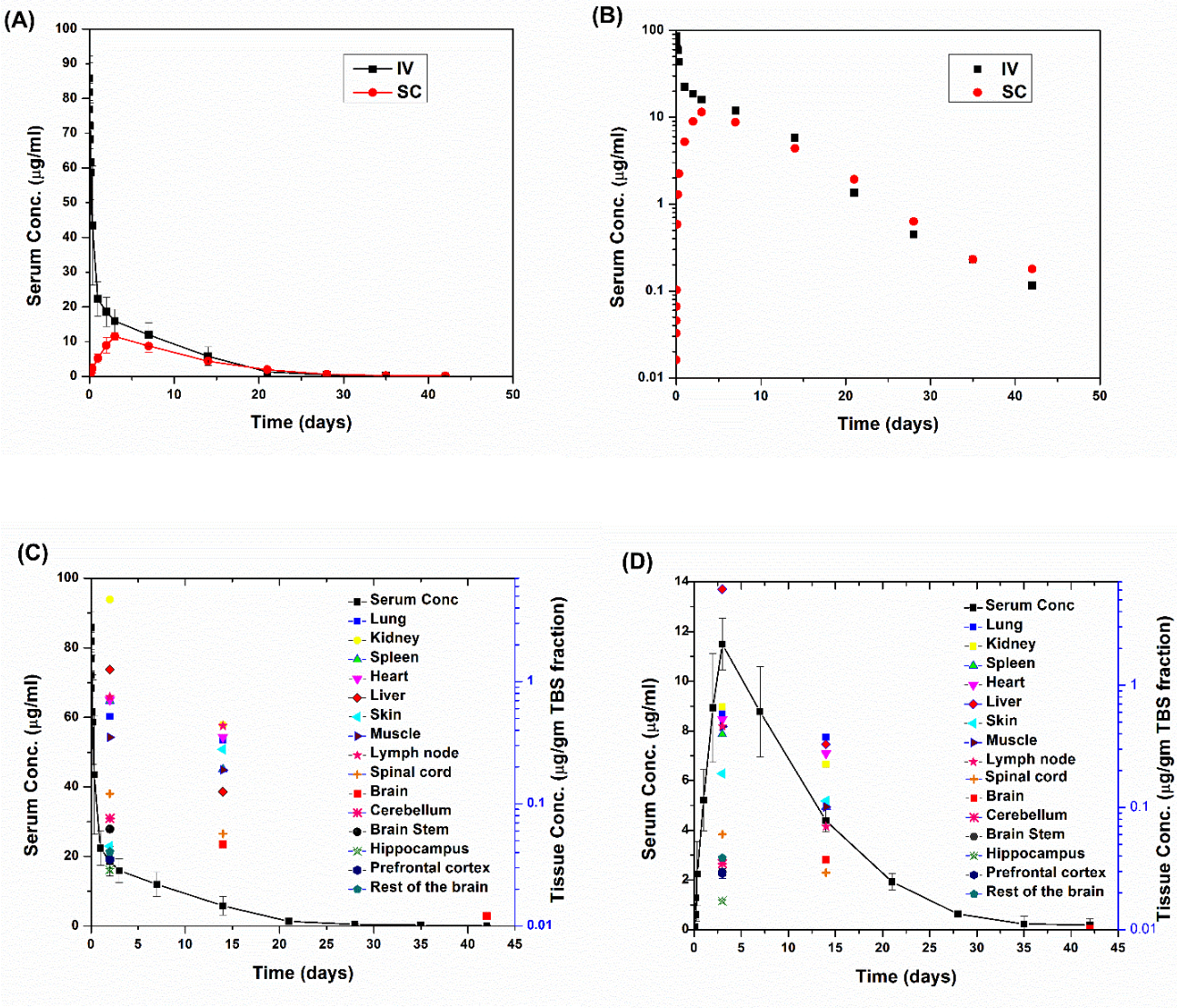


Fig. (2). (**A**) and (**B**) Concentration-time curves of p75ECD-Fc after single IV (black squares) and SC (red circles) injection of 3mg/kg in SD rats. Each point represents the mean ± S D. (**C**) and (**D**) Concentration-time curve of p75ECD-Fc in tissues in relation to serum at different time points after single IV (**2C**) and SC injection (**2D**). (*A higher resolution / colour version of this figure is available in the electronic copy of the article*).

life ($t_{1/2}$) of 6.2 ± 2.4 days. Serum levels of the drug decreased gradually but were still detectable after 42 days of single dose administration. The values of AUC_{inf} were 257.867 ± 97.5 and 146.156 ± 21.0 µg.day/ml for IV and SC administration, respectively. The bioavailability (F) of SC route of administration was found to be 66.15%. The elimination rate constant for IV and SC was 0.11 and 0.088 day^{-1} respectively which means that p75ECD-Fc is slowly eliminated from the body, a finding that is further supported by the long $t_{1/2}$ and mean residence time (MRT); that was found to be 9.68 ± 2.6 and 11.38 ± 1.1 days for IV and SC respectively. V_{ss} was 42.58 ± 7.8 for IV and 81.87 ± 12.3 ml in case of SC. CLt was estimated to be 7.275 ± 1.5 ml/day for SC administration, which was higher than that of IV (4.81 ± 1.9 ml/day). In conclusion, PK profile of p75ECD-Fc shows a rapid distribution phase and a slow rate of elimination with moderate volume of distribution, which is consistent with the pk behavior of monoclonal antibodies (mAb) [26]. The primary PK parameters for p75ECD-Fc are shown in Table **1**.

3.2. Distribution of p75ECD-Fc in Different Tissues

After animals were humanely killed, different tissues were collected for analysis. The level of p75ECD-Fc in tissues, CSF and urine after different time points is shown in Table **2**. p75ECD-Fc was highly detected in most tissues after 2 and 3 days of single IV and SC injection and remained detectable for up to 2 weeks after a single dose. Tissue levels of the drug followed a similar trend to that seen in the serum. p75ECD-Fc tissue concentrations after single IV injection were higher than that observed after SC injection. However, the liver showed a higher drug level after SC injection than that observed after IV. This unpredicted result may be attributable to contamination caused by residual blood in the tissue.

After a single dose of IV (at 2nd day) and SC (at 3rd day) injection of p75ECD-Fc, the level of the drug in urine was about 0.2 µg/ml, which is 1.6 – 1.8 % of the amount detected in serum at the same time point. This indicates that elimination is primarily mediated through either proteolytic catabolism or FCγ receptors, but not through renal clearance due to its large molecular size [27-28]. In CSF, the drug level detected after 14 days of single IV dose was 6.7 ±1.23 ng/ml. The level of the drug in CSF after 3 days of SC injection was found to be 3.6 ng/ml. The distribution of the drug in different tissues varied according to the tissue perfusion with the highly perfused tissues (e.g. the lung, liver and kidney) showing the highest drug levels at 2-, 3- and 14-days post dose. Also, we found that the drug levels observed in lymph nodes were high after 2- and 3-days and stayed high after 14 days of injection. This finding agrees with the assumption that the tissue uptake, distribution and clearance of mAb is predominantly controlled by the lymphatic drainage and convection pathways [29].

Although the brain is highly perfused, the distribution of the drug is primarily affected by the ability to penetrate the blood brain barrier (BBB) according to its molecular size, the extent to protein binding, hydrophilicity and the ionization state of the molecule. After 2 days of single IV injection, p75ECD-Fc was detected in the spinal cord and various regions in the brain at a concentration ranging from 28 to 163.6 ng/gm which is 3-folds the levels detected after 3 days of single SC injection. After 14 days, the level of the protein in the brain was reduced significantly but still detected after 42 days of single IV injection at a very low concentration of around 11 ± 1.7 ng/gm. Overall, these results showed that p75ECD-Fc exhibits modest tissue distribution and the ability to penetrate the central nervous system (CNS) in detectable amounts.

3.3. Immunofluorescence Staining of p75ECD-Fc in Tissues

Tissues separated at day 2 and 3 post dose were double immune-stained with a pan macrophage marker; anti-CD11b, anti-Iba-1, anti- S100 and with anti-human Fc to detect the localization of p75ECD-Fc inside cells. Results showed the internalization of p75ECD-Fc by Kupffer cells in the liver, macrophages in the lung and Langerhans cells in the skin. We found S100+ astrocytes are colocalized with anti-human Fc antibodies (Fig. **3**). This indicates that p75ECD-Fc is mainly metabolized through phagocytosis by its Fc part through binding to Fcγ receptor located on the surface of resident macrophages.

3.4. In-vitro Stability of p75ECD-Fc in Human Plasma

It is important for drugs administered either IV or SC to be stable in plasma till they reach their site of action. To assess the stability of p75ECD-Fc in plasma, we incubated the protein with human plasma at physiological temperature (i.e. 37 ˚C) for 35 days. According to the results of ELISA and the standard curve (Fig. **1**), the concentrations of native p75ECD-Fc at different incubation times were calculated (Table **3**) and a drug concentration-time

Table 1. Noncompartmental pharmacokinetics of p75ECD-Fc after single IV and SC injection of 3mg/kg to SD rats (IV: n= 7, SC: n=5). Results are presented as means ± standard deviation (S.D.).

Parameters (Units)	Intravenous (n = 7)			Subcutaneous (n = 5)		
	Mean	SD	CV%	Mean	SD	CV%
AUC_{inf} (µg.day/ml)	257.867	97.495	37.81	146.156	21.052	14.40
T_{max} (day)	0.003472	0	0	3.13	0.11	3.514
C_{max} (µg/ml)	85.205	6.635	7.79	11.493	1.045	9.09
Bioavailability (F)	1	NA	NA	0.6615	NA	NA
K_{el} (λ_z) elimination rate constant (day^{-1})	0.111	0.033	30.19	0.0885	0.009	9.72
$t_{1/2}$ (day)	7.492	1.665	22.23	6.2	2.412	38.91
$AUMC_{inf}$ (µg.day^2/ml)	2700.427	1678.102	62.1421	1678.247	374.678	22.33
Clearance (ml/day)	4.812	1.897	39.42	7.275	1.548	21.28
MRT (day)	9.686	2.581	26.65	11.381	1.118	9.82
V_{ss} (ml)	42.586	7.828	18.38	81.875	12.334	15.06

Table 2. Tissue, urine and CSF concentration of p75ECD-Fc after single IV and SC injection of 3mg/kg in SD rats. This table shows the concentration of p75ECD-Fc in different tissues (ng/gm tissue), CSF and urine (ng/ml) obtained at different time points. Tissues were homogenized with TBS to extract p75ECD-Fc and then were analyzed with sandwich ELISA to measure the levels of p75ECD-Fc. Data are represented as mean ± standard deviation (S.D.).

	Tissue Concentration[a] (ng/g) of p75ECD-Fc at a dose of 3mg/Kg				
	Day of Tissue Collection				
Tissue	IV (ng/g)		SC (ng/g)		
	Day 2 (n = 1)	Day 14 (n = 4)	Day 3 (n = 1)	Day 14 (n = 4)	Day 42 (n=3)
Lung	517.94	333.23 ± 132.44	577.06	376 13 ±191.07	
Kidney	4691.14	443.09 ± 73 16	665.42	225.64 ± 90.12	
Spleen	692.75	191.9 ± 80.49	397.20	100.87 ± 31.84	
Heart	710.24	350.39 ± 81.45	524.01	276 54 ± 133.8	
Liver	1256.63	125.16 ± 51.88	6095.62	328 39 ± 182.5	
Skin	1573.32	278.9 ± 80.29	27.8	112.978 ± 106.86	
Muscle	349.99	189.23 ± 134.16	459.42	101 15 ± 41.84	
Lymph node	747.36	434.12 ± 130.21	463.52	69.96 ± 12.81	
Spinal Cord	120.56	56.87 ± 45.04	60.22	29.26 ± 10.75	
Brain		46.49 ± 20.59		37 3 ± 21.05	12.06 ± 1.74 (IV) 10.12 ± 1.4 (SC)
Cerebellum	75.91		34.68		
Brain Stem	62.10		29.58		
Hippocampus	28.87		17.14		
Prefrontal Cortex	34.99		28.92		
Rest of Brain tissue	40.46		38.56		
CSF (ng/ml)	N/A[b]	6.77 ±1.62	3.64	N/A	N/A
Urine (ng/ml)	222.29	N/A	214.19	NA	N/A

Data[a] represent mean ± standard deviation (SD) N/A[b]: data for this time point is not available

Table 3. Concentrations of p75ECD-Fc in human plasma at different incubation times. This table shows the changes in p75ECD-Fc concentration when incubated in human plasma at 37 °C at an initial concentration of 10 µg/ml. Samples were analyzed by sandwich ELISA. Data represent mean ± standard deviation (S.D.).

Time (days)	0	1	3	7	14	21	28	35
Average Concentration (µg/ml) ± SD	-	8.427 ± 0.47	7.718 ± 0.66	7.266 ± 0.48	6.874 ± 0.96	6.584 ± 0.68	6.335 ± 0.27	6.115 ± 0 30

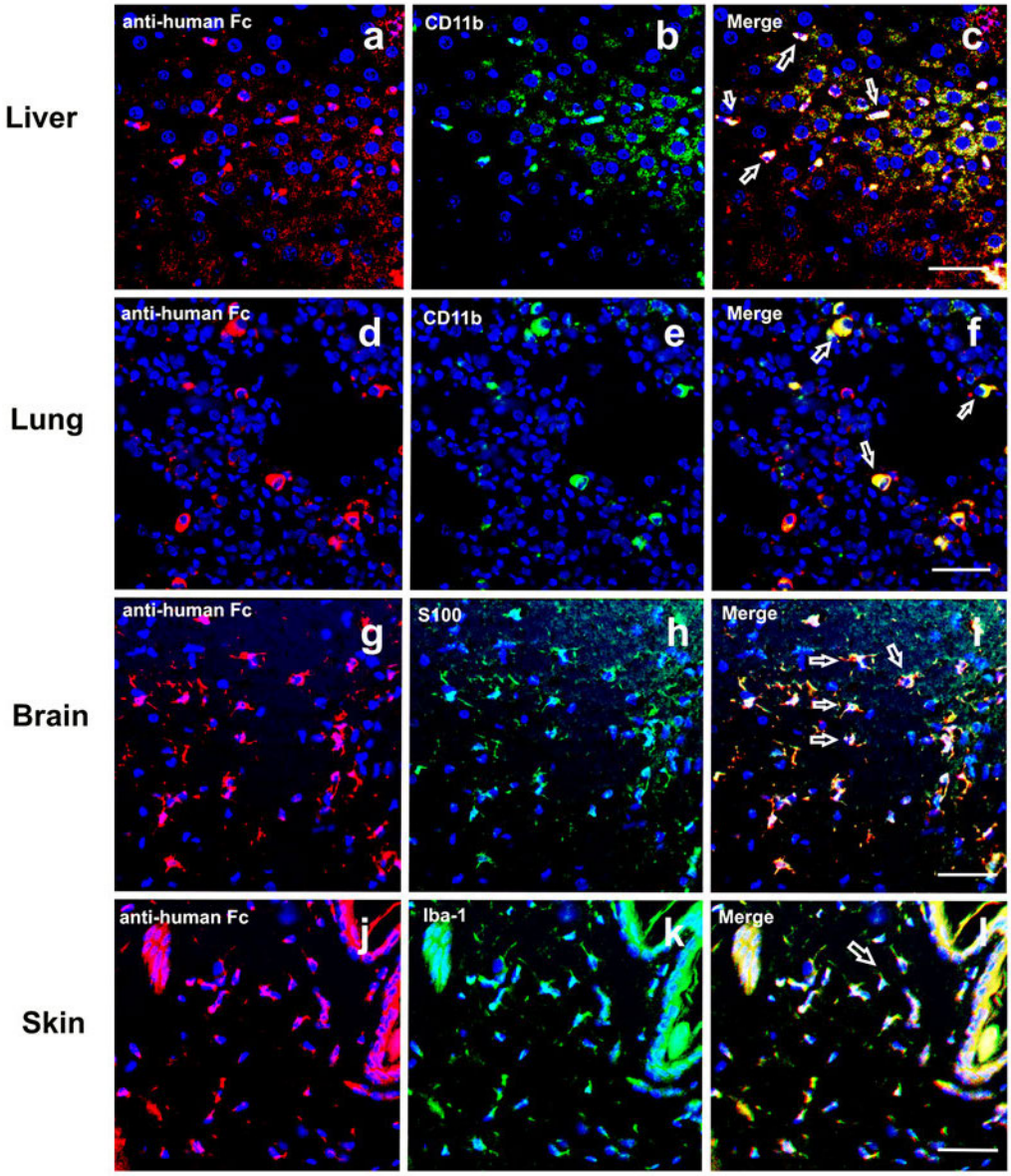


Fig. (3). Double-label immunofluorescence showing the in-vivo colocalization of p75ECD-Fc (red) in CD11b-positive cells of the liver, lung, Iba-1 positive cells in the skin and S100-positive cells in the brain (green). Nuclei were stained with DAPI (blue). p75ECD-Fc was detected in different tissues using biotinylated anti-human IgG Fc and developed with secondary cy3-conjugated streptavidin antibody (red) (a, d, g, j). Resident macrophages were detected with different macrophage markers; CD11b, Iba-1 and S100 (b, e, h, k) and secondary cy2-conjugated secondary antibody (green) (scale bar = 200 μm). (*A higher resolution / colour version of this figure is available in the electronic copy of the article*).

curve is represented (Fig. **4**). Results showed that p75ECD-Fc was stable in plasma with 64% of its initial concentration retained after 35 days.

4. DISCUSSION

In this study, we investigated the pharmacokinetics of p75ECD-Fc after single IV and SC injection of 3mg/kg in SD rats. Data indicate that p75ECD-Fc has long half-life time *in vivo*, indicating prolonged exposure with a slow rate of elimination. First, we tested the stability of the protein at 37°C, we incubated the drug in human plasma, and measured the drug concentration over a period of 35 days. Data showed that p75ECD-Fc was slowly degraded with a very long half-life time approaching 80 days, indicating this drug is peptidase/proteinase resistant.

Tissue distribution of the drug is modest. This is due to its large size 130KDa (as a dimer) and high hydrophilicity. Ability to penetrate the BBB was also confirmed. In addition, we showed that the drug is mainly metabolized through phagocytosis by resident macrophages in different tissues, in particular, liver, lung and skin. As a high level of p75ECD-Fc was detected in kidney and urine, this drug is also likely eliminated from urine. Our data is consistent with the reports that high levels of p75ECD can be detected in normal human and in amyotrophic lateral sclerosis [30]. These data clearly demonstrate that p75ECD-Fc mainly exerts its effect peripherally rather than centrally. Thus, it is assumed that p75ECD-Fc can bind soluble Aβ, forming immune complexes that will promote binding to Fcγ receptors and subsequent catabolism and clearance by the peripheral macrophages [26].

Scavenging Aβ by p75ECD-Fc in the periphery will promote the disaggregation and defibrillation of plaques centrally, followed by the transport of soluble monomers and oligomers through the BBB and the lymphatic system [31] to be cleared by peripheral organs. This effect will reduce the Aβ load in the brain and consequently antagonize the toxic effects mediated by the Aβ and

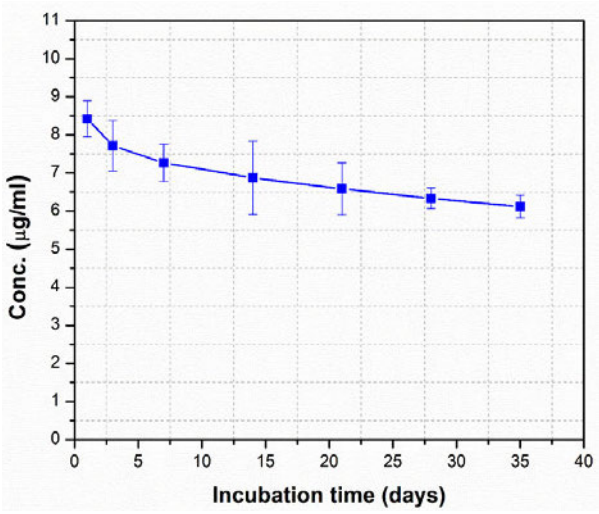


Fig. (4). Drug concentration-time curve of plasma incubation of p75ECD-Fc. Each point represents mean ± S D. (*A higher resolution / colour version of this figure is available in the electronic copy of the article*).

proneurotrophins through binding to p75NTR. Besides, this will restore the level of the neuroprotective extracellular domain in the brain. This approach has benefits that outweigh that of central clearance of Aβ by antibodies for two reasons. The first reason is that active and passive immunization with Aβ antibodies was accompanied by autoimmune meningoencephalitis, cerebral hemorrhage and edema. These adverse events were observed in both animal and clinical studies, possibly caused by the abnormal T lymphocytes infiltration into the brain triggered by the T cell-activating domain of Aβ vaccine [5, 32]. The second one is the failure of the central immune system to clear Aβ deposits in AD patients due to impairment of the phagocytic activity of resident microglia by the neurotoxic Aβ oligomers, which create a state of severe inflammation and oxidation resulting in disruption of the phagocytic system [33-35]. In contrast, healthy peripheral macrophages seem to be more effective to degrade fibrillar Aβ than resident microglia [4]. Therefore, p75ECD-Fc acts like anti-Aβ antibody that can promote its clearance from the brain through the peripheral immune system and by antagonizing its toxic effects on the p7NTR. The proposed mechanism of action of p75ECD-Fc is shown in Fig. (**5**).

CONCLUSION AND FUTURE DIRECTIONS

In summary, the preclinical pharmacokinetic data of p75ECD-Fc obtained from both *in vivo* and *in vitro* studies support its further development as a new drug candidate for AD. The obtained parameters showed moderate slow clearance rate with a long half-life time *in vivo* after IV and SC administration in SD rats and good *in vitro* stability in human plasma. In addition, these results help us to reveal the possible mechanism of action of p75ECD-Fc and showed that it possesses better pharmacodynamic properties than anti-Aβ antibodies.

This excellent preclinical PK profile paves the way for further animal studies to evaluate the pharmacological effects of p75ECD-Fc as well as the best regimen to be applied in the treatment of AD, which is currently tested in our lab and will be available for publishing soon.

As a result, this will provide comprehensive knowledge about p75ECD-Fc as a valuable drug for the treatment of Alzheimer's disease.

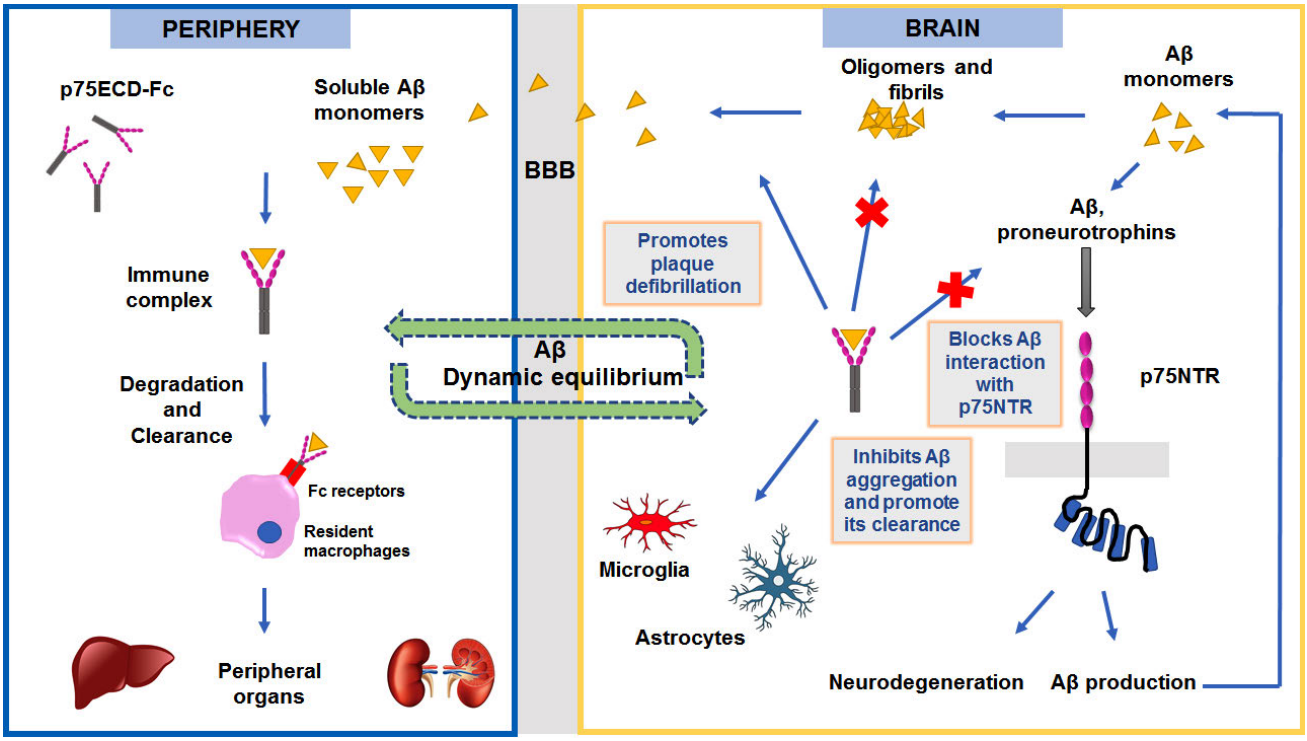


Fig. (5). Representative diagram illustrating the proposed mechanism of action of p75ECD-Fc in AD. In the periphery, p75ECD-Fc binds to soluble Aβ monomers forming immune complexes that are cleared through peripheral organs, mainly; liver and kidney. This effect will shift the balance towards moving Aβ from the brain to the periphery, which, in turn, may result in plaque solubilization and defibrillation and consequently may reduce the plaque load in the brain [21, 22, 36]. Centrally, it acts as a competitive antagonist through binding to Aβ and proneurotrophins and, therefore, blocking the neurotoxic signaling pathways mediated by the interaction between these toxic legends and p75NTR. This will prevent the production of more toxic Aβ and inhibit Aβ aggregation and deposition [12, 14]. (*A higher resolution / colour version of this figure is available in the electronic copy of the article*).

LIST OF ABBREVIATIONS

AD	=	Alzheimer's disease
Aβ	=	Amyloid beta
APP	=	Amyloid precursor protein
AUC	=	Area under the curve
$AUMC_{inf}$	=	Area under the first moment curve
Bioavailability	=	F
BBB	=	Blood brain barrier
CA	=	Capture antibody
CD11b and S-100	=	name of proteins expressed on surface of macrophages
CLt	=	Total body clearance
C_{max}	=	Peak plasma concentration
CNS	=	Central nervous system
CSF	=	Cerebrospinal fluid
cy2 and cy3	=	Cyanine dyes
DAPI	=	4′,6-diamidino-2-phenylindole
Elimination half-life ($t_{1/2}$)		
Elimination rate constant K_{el} (λz)		
ELISA	=	Enzyme-linked immunosorbent assay
ECD	=	Extracellular domain
HRP	=	Horseradish peroxidase
HK	=	Humanely killed
HCl	=	Hydrochloric acid
IgG	=	Immunoglobulin G
IV	=	Intravenous
Iba-1	=	Ionized calcium binding adaptor molecule 1
mAb	=	Monoclonal antibody
MRT	=	mean residence time
NCA	=	Non-compartmental pharmacokinetic analysis
NHS	=	Normal horse serum
OCT	=	Optimal cutting temperature compound
p75NTR	=	p75 neurotrophin receptor
PK	=	Pharmacokinetics
PBS	=	Phosphate-buffered saline
SDS	=	Sodium dodecyl sulfate
S.D.	=	Standard deviation
SC	=	Subcutaneous
TMB	=	Tetramethylbenzidine
Tris	=	(2-amino-2-hydroxymethylpropane-1,3-diol (systematic), tris(hydroxymethyl) aminomethane (manufacturer)
TBS	=	Tris-buffered saline
TNF-α	=	Tumour Necrosis Factor alpha
Vss	=	Volume of distribution at steady-state

CONSENT FOR PUBLICATION

Not applicable.

FUNDING

None.

CONFLICT OF INTEREST

JW and XFZ are inventors of a Chinese patent on p75ECD-Fc. The other authors declare no conflict of interest, financial or otherwise.

ACKNOWLEDGEMENTS

This work was supported by NHMRC grants (APP1020567, APP1021409) and supporting grant from the University of South Australia. The authors also acknowledge the support provided to S. Kelliny by Commonwealth Research and Training scholarship and Egyptian Ministry of Higher Education. The recombinant p75ECD-Fc was provided by Fujian Tiantai Medical Technology Ltd.

REFERENCES

[1] Alzheimer's Disease International: World Alzheimer Report *The state of the art of dementia research New frontiers.,* **2018**.

[2] Hardy, J A.; Higgins, G.A. Alzheimer's disease: the amyloid cascade hypothesis. *Science,* **1992**, *256*(5054), 184-185. http://dx.doi.org/10.1126/science.1566067 PMID: 1566067

[3] Mawuenyega, K.G.; Sigurdson, W.; Ovod, V.; Munsell, L.; Kasten, T.; Morris, J.C.; Yarasheski, K E.; Bateman, R.J. Decreased clearance of CNS beta-amyloid in Alzheimer's disease. *Science,* **2010**, *330*(6012), 1774-1774. http://dx.doi.org/10.1126/science.1197623 PMID: 21148344

[4] Zuroff, L.; Daley, D.; Black, K.L.; Koronyo-Hamaoui, M. Clearance of cerebral Aβ in Alzheimer's disease: reassessing the role of microglia and monocytes. *Cell. Mol. Life Sci.,* **2017**, *74*(12), 2167-2201. http://dx.doi.org/10.1007/s00018-017-2463-7 PMID: 28197669

[5] Carlson, C.; Estergard, W.; Oh, J.; Suhy, J.; Jack, C.R., Jr; Siemers, E.; Barakos, J. Prevalence of asymptomatic vasogenic edema in pretreatment Alzheimer's disease study cohorts from phase 3 trials of semagacestat and solanezumab. *Alzheimers Dement.,* **2011**, *7*(4), 396-401. http://dx.doi.org/10.1016/j.jalz.2011.05.2353 PMID: 21784350

[6] Sperling, R.; Salloway, S.; Brooks, D.J.; Tampieri, D.; Barakos, J.; Fox, N.C.; Raskind, M.; Sabbagh, M.; Honig, L.S.; Porsteinsson, A.P.; Lieberburg, I.; Arrighi, H.M.; Morris, K.A.; Lu, Y.; Liu, E.; Gregg, K.M.; Brashear, H.R.; Kinney, G.G.; Black, R.; Grundman, M. Amyloid-related imaging abnormalities in patients with Alzheimer's disease treated with bapineuzumab: a retrospective analysis. *Lancet Neurol.,* **2012**, *11*(3), 241-249. http://dx.doi.org/10.1016/S1474-4422(12)70015-7 PMID: 22305802

[7] Morgan, D. Immunotherapy for Alzheimer's disease. *J. Intern. Med.,* **2011**, *269*(1), 54-63. http://dx.doi.org/10.1111/j.1365-2796.2010.02315.x PMID: 21158978

[8] Hu, X-Y.; Zhang, H-Y.; Qin, S.; Xu, H.; Swaab, D.F.; Zhou, J-N. Increased p75(NTR) expression in hippocampal neurons containing hyperphosphorylated τ in Alzheimer patients. *Exp. Neurol.,* **2002**, *178*(1), 104-111. http://dx.doi.org/10.1006/exnr.2002.8018 PMID: 12460612

[9] Friedman, W.J. Neurotrophins induce death of hippocampal neurons via the p75 receptor. *J. Neurosci.,* **2000**, *20*(17), 6340-6346. http://dx.doi.org/10.1523/JNEUROSCI.20-17-06340.2000 PMID: 10964939

[10] Reichardt, L.F. Neurotrophin-regulated signalling pathways. *Philos. Trans. R. Soc. Lond. B Biol. Sci.,* **2006**, *361*(1473), 1545-1564. http://dx.doi.org/10.1098/rstb.2006.1894 PMID: 16939974

[11] Yaar, M.; Zhai, S.; Pilch, P.F ; Doyle, S.M.; Eisenhauer, P.B.; Fine, R.E.; Gilchrest, B.A. Binding of beta-amyloid to the p75 neurotrophin receptor induces apoptosis. A possible mechanism for Alzheimer's disease. *J. Clin. Invest.,* **1997**, *100*(9), 2333-2340. http://dx.doi.org/10.1172/JCI119772 PMID: 9410912

[12] Wang, Y.J.; Wang, X.; Lu, J.J.; Li, Q.X.; Gao, C.Y.; Liu, X.H.; Sun, Y.; Yang, M ; Lim, Y.; Evin, G.; Zhong, J H.; Masters, C.; Zhou, X.F. p75NTR regulates Abeta deposition by increasing Abeta production but inhibiting Abeta aggregation with its extracellular domain. *J. Neurosci.,* **2011**, *31*(6), 2292-2304. http://dx.doi.org/10.1523/JNEUROSCI.2733-10.2011 PMID: 21307265

[13] Zeng, F.; Lu, J.J.; Zhou, X.F.; Wang, Y.J. Roles of p75NTR in the pathogenesis of Alzheimer's disease: a novel therapeutic target. *Biochem. Pharmacol.,* **2011**, *82*(10), 1500-1509. http://dx.doi.org/10.1016/j.bcp.2011.06.040 PMID: 21762680

[14] Zhou, X.F.; Wang, Y.J. The p75NTR extracellular domain: a potential molecule regulating the solubility and removal of amyloid-β. *Prion,* **2011**, *5*(3), 161-163. http://dx.doi.org/10.4161/pri.5.3.16896 PMID: 21814043

[15] Yaar, M.; Zhai, S.; Fine, R.E.; Eisenhauer, P.B.; Arble, B.L.; Stewart, K.B.; Gilchrest, B.A. Amyloid β binds trimers as well as monomers of

the 75-kDa neurotrophin receptor and activates receptor signaling. *J. Biol. Chem.*, **2002**, *277*(10), 7720-7725.
http://dx.doi.org/10.1074/jbc.M110929200 PMID: 11756426

[16] Knowles, J.K.; Rajadas, J.; Nguyen, T-V.V.; Yang, T ; LeMieux, M.C.; Vander Griend, L.; Ishikawa, C.; Massa, S M.; Wyss-Coray, T.; Longo, F.M. The p75 neurotrophin receptor promotes amyloid-beta(1-42)-induced neuritic dystrophy *in vitro* and *in vivo*. *J. Neurosci.,* **2009**, *29*(34), 10627-10637.
http://dx.doi.org/10.1523/JNEUROSCI.0620-09.2009 PMID: 19710315

[17] Costantini, C ; Rossi, F.; Formaggio, E ; Bernardoni, R.; Cecconi, D ; Della-Bianca, V. Characterization of the signaling pathway downstream p75 neurotrophin receptor involved in β -amyloid peptide-dependent cell death. *J. Mol. Neurosci.,* **2005**, *25*(2), 141-156.
http://dx.doi.org/10.1385/JMN:25:2:141 PMID: 15784962

[18] Pietri, M.; Dakowski, C.; Hannaoui, S. Alleaume- Butaux, A ; Hernandez-Rapp, J.; Ragagnin, A.; Mouillet-Richard, S.; Haik, S.; Bailly, Y.; Peyrin, J.- M.; Launay, J.-M.; Kellermann, O.; Schneider, B., PDK1 decreases TACE-mediated α-secretase activity and promotes disease progression in prion and Alzheimer's diseases. *Nat. Med.,* **2013**, *19*, 1124.
http://dx.doi.org/10.1038/nm.3302 PMID: 23955714

[19] Yao, X.Q.; Jiao, S.S.; Saadipour, K.; Zeng, F.; Wang, Q H.; Zhu, C.; Shen, L.L.; Zeng, G.H.; Liang, C.R ; Wang, J.; Liu, Y.H.; Hou, H.Y.; Xu, X.; Su, Y.P.; Fan, X.T.; Xiao, H.L.; Lue, L.F.; Zeng, Y.Q.; Giunta, B.; Zhong, J.H.; Walker, D.G ; Zhou, H.D.; Tan, J.; Zhou, X.F.; Wang, Y J. p75NTR ectodomain is a physiological neuroprotective molecule against amyloid-beta toxicity in the brain of Alzheimer's disease. *Mol. Psychiatry,* **2015**, *20*(11), 1301-1310.
http://dx.doi.org/10.1038/mp.2015.49 PMID: 25917367

[20] Enbrel, Pharmaceuticals. *Amgen Inc. and Wyeth- Ayerst, Thousand Oaks* ; , **2004**.

[21] Liu, Y-H.; Wang, Y-R ; Xiang, Y.; Zhou, H-D.; Giunta, B.; Manucat, N.; Tan, J.; Zhou, X-F.; Wang, Y-J. Clearance of Amyloid-Beta in Alzheimer's Disease: Shifting the Action Site from Center to Periphery. *Mol. Neurobiol.,* **2014**, 51.
PMID: 24733588

[22] Nalivaeva, N.N.; Turner, A.J. Targeting amyloid clearance in Alzheimer's disease as a therapeutic strategy. *Br. J. Pharmacol.,* **2019**, *176*(18), 3447-3463.
http://dx.doi.org/10.1111/bph.14593 PMID: 30710367

[23] Wang, J.; Gu, B.J.; Masters, C.L.; Wang, Y.J. A systemic view of Alzheimer disease - insights from amyloid-β metabolism beyond the brain. *Nat. Rev. Neurol.,* **2017**, *13*(10), 612-623.
http://dx.doi.org/10.1038/nrneurol.2017.111 PMID: 28960209

[24] R Core Team. R: A language and environment for statistical computing. R Foundation for Statistical Computing, Vienna, Austria. URL project.org/

[25] Denney, W.; Duvvuri, S.; Buckeridge, C. Simple, Automatic Noncompartmental Analysis: The PKNCA R Package. *J. Pharmacokinet. Pharmacodyn.,* **2015**, *42*, S65-S65.

[26] Kamath, A.V. Translational pharmacokinetics and pharmacodynamics of monoclonal antibodies. *Drug Discov. Today. Technol.,* **2016**, *21-22*, 75-83.
http://dx.doi.org/10.1016/j.ddtec.2016.09.004 PMID: 27978991

[27] Wang, W.; Wang, E.Q.; Balthasar, J.P. Monoclonal antibody pharmacokinetics and pharmacodynamics. *Clin. Pharmacol. Ther.,* **2008**, *84*(5), 548-558.
http://dx.doi.org/10.1038/clpt.2008.170 PMID: 18784655

[28] Deng, R.; Jin, F.; Prabhu, S.; Iyer, S. Monoclonal antibodies: what are the pharmacokinetic and pharmacodynamic considerations for drug development? *Expert Opin. Drug Metab. Toxicol.,* **2012**, *8*(2), 141-160.
http://dx.doi.org/10.1517/17425255.2012.643868 PMID: 22248267

[29] Cao, Y.; Balthasar, J.P.; Jusko, W.J. Second-generation minimal physiologically-based pharmacokinetic model for monoclonal antibodies. *J. Pharmacokinet. Pharmacodyn.,* **2013**, *40*(5), 597-607.
http://dx.doi.org/10.1007/s10928-013-9332-2 PMID: 23996115

[30] Shepheard, S.R.; Wuu, J.; Cardoso, M.; Wiklendt, L.; Dinning, P.G.; Chataway, T.; Schultz, D.; Benatar, M.; Rogers, M.L. Urinary $p75^{ECD}$: A prognostic, disease progression, and pharmacodynamic biomarker in ALS. *Neurology,* **2017**, *88*(12), 1137-1143.
http://dx.doi.org/10.1212/WNL.0000000000003741 PMID: 28228570

[31] Iliff, J.J.; Nedergaard, M. Is there a cerebral lymphatic system? *Stroke,* **2013**, *44*(6)(Suppl. 1), S93-S95.
http://dx.doi.org/10.1161/STROKEAHA.112.678698 PMID: 23709744

[32] Gilman, S.; Koller, M.; Black, R.S.; Jenkins, L.; Griffith, S.G.; Fox, N.C.; Eisner, L.; Kirby, L.; Rovira, M.B.; Forette, F.; Orgogozo, J-M. AN1792(QS-21)-201 Study Team. Clinical effects of Abeta immunization (AN1792) in patients with AD in an interrupted trial. *Neurology,* **2005**, *64*(9), 1553-1562.
http://dx.doi.org/10.1212/01.WNL.0000159740 16984.3C PMID: 15883316

[33] Pan, X-D.; Zhu, Y-G.; Lin, N.; Zhang, J.; Ye, Q-Y.; Huang, H-P.; Chen, X-C. Microglial phagocytosis induced by fibrillar β-amyloid is attenuated by oligomeric β-amyloid: implications for Alzheimer's disease. *Mol. Neurodegener.,* **2011**, *6*, 45-45.
http://dx.doi.org/10.1186/1750-1326-6-45 PMID: 21718498

[34] Hellwig, S.; Masuch, A.; Nestel, S.; Katzmarski, N.; Meyer-Luehmann, M.; Biber, K. Forebrain microglia from wild-type but not adult 5xFAD mice prevent amyloid-β plaque formation in organotypic hippocampal slice cultures. *Sci. Rep.,* **2015**, *5*, 14624-14624.
http://dx.doi.org/10.1038/srep14624 PMID: 26416689

[35] Krabbe, G.; Halle, A.; Matyash, V.; Rinnenthal, J.L.; Eom, G.D.; Bernhardt, U.; Miller, K R.; Prokop, S.; Kettenmann, H.; Heppner, F.L. Functional impairment of microglia coincides with Beta-amyloid deposition in mice with Alzheimer-like pathology. *PLoS One,* **2013**, *8*(4), e60921-e60921.
http://dx.doi.org/10.1371/journal.pone.0060921 PMID: 23577177

[36] Xiang, Y.; Bu, X.L ; Liu, Y.H.; Zhu, C.; Shen, L.L.; Jiao, S.S.; Zhu, X.Y.; Giunta, B.; Tan, J.; Song, W.H.; Zhou, H.D.; Zhou, X.F.; Wang, Y.J. Physiological amyloid-beta clearance in the periphery and its therapeutic potential for Alzheimer's disease. *Acta Neuropathol.,* **2015**, *130*(4), 487-499.
http://dx.doi.org/10.1007/s00401-015-1477-1 PMID: 26363791

Sally Kelliny, Larisa Bobrovskaya, Xin-Fu Zhou and Richard Upton

Pharmacokinetic Modelling of Human Recombinant Protein, p75ECD-Fc: A Novel Therapeutic Approach for Treatment of Alzheimer's Disease, in Serum and Tissue of Sprague Dawley Rats. European Journal of Drug Metabolism and Pharmacokinetics; 2021.

Publication status: Published

The published version is available at: https://link.springer.com/article/10.1007/s13318-020-00662-0

Author Contributions

Author	Wrote Manuscript	Revised Manuscript	Designed Research	Performed Research	Analysis of Data	Data Interpretation
Kelliny, S	✔	✔	✔	✔	✔	✔
Bobrovskaya, L		✔	✔			
Upton, R	✔	✔	✔		✔	✔
Zhou, X. F		✔	✔	✔		✔

Full name of co-author	Signature	Date
Sally Kelliny	[redacted]	15-03-2021
Larisa Bobrovskaya	[redacted]	20/04/2021
Richard Upton	[redacted]	20/04/2021
Xin-Fu Zhou	[redacted]	20/04/2021

European Journal of Drug Metabolism and Pharmacokinetics
https://doi.org/10.1007/s13318-020-00662-0

ORIGINAL RESEARCH ARTICLE

Pharmacokinetic Modelling of Human Recombinant Protein, p75ECD-Fc: A Novel Therapeutic Approach for Treatment of Alzheimer's Disease, in Serum and Tissue of Sprague Dawley Rats

Sally Kelliny[1,3] · Larisa Bobrovskaya[1] · Xin-Fu Zhou[1] · Richard Upton[2]

Accepted: 13 November 2020
© Springer Nature Switzerland AG 2021

Abstract

Background and Objective p75ECD-Fc is a novel antagonist of toxic amyloid beta protein and other neurodegenerative factors with potential for the treatment of Alzheimer's disease (AD). Preclinical studies showed that it can alleviate the AD pathologies in animal models of dementia. In a previous paper, we used non-compartmental pharmacokinetic analysis to obtain preliminary pharmacokinetic data for p75ECD-Fc in Sprague Dawley (SD) rats. We also studied the tissue distribution in terms of drug metabolism that helped us to understand possible mechanisms of action. Here, we aim to develop population pharmacokinetic models that can describe the pharmacokinetics of p75ECD-Fc in serum and tissues.

Methods p75ECD-Fc was delivered to SD rats via two routes (intravenous and subcutaneous) at a single dose of 3 mg/kg (n = 15). Blood (n = 12) and tissue samples (n = 10–15) were then separated at different time points for a total duration of 42 days post dosage. The concentration of p75ECD-Fc in serum and tissues was measured using an enzyme-linked immunosorbent assay.

Results Data were best fitted to a 2-compartment model with linear elimination kinetics. The population parameter estimates for clearance, and volume of central and peripheral compartments were 0.000176 L/h, 0.0145 L and 0.0263 L, respectively. The presence of anti-drug antibodies was added to the final model as a covariate on clearance. The subcutaneous bioavailability was estimated to be 53.5% with a first-order absorption rate constant of 0.00745 1/h. By modeling of individual tissue concentrations, p75ECD-Fc was found to exhibit modest tissue distribution with estimated tissue/plasma partition coefficients (R) ranging from 0.004 to 0.2.

Conclusion This is the first report of a pharmacokinetic model for p75ECD-Fc and these results may facilitate the ongoing development of p75ECD-Fc and translation to clinical studies.

Key Points

p75ECD-Fc is a novel human recombinant protein developed for the treatment of Alzheimer's disease (AD)

Pharmacokinetic modelling suggested a systemic two-compartment model of p75ECD-Fc with linear elimination kinetics following single intravenous and subcutaneous injection in Sprague Dawley rats and modest tissue distribution with estimated tissue/plasma partition coefficients (R) ranging from 0.004 to 0.2

Highly perfused tissues including liver and kidney showed the highest partition coefficient, while brain was the lowest, indicating that the periphery is the main site of action following systemic administration

This study is significant as currently there is no disease modifying therapy for AD and therefore, these results can pave the way for future clinical studies of p75ECD-Fc

Electronic supplementary material The online version of this article (https://doi.org/10.1007/s13318-020-00662-0) contains supplementary material, which is available to authorized users.

✉ Xin-Fu Zhou
xin-fu.zhou@unisa.edu.au

✉ Richard Upton
richard.upton@unisa.com.au

[1] University of South Australia, Clinical and Health Sciences, Adelaide, SA 5000, Australia

[2] University of South Australia, Clinical and Health Sciences, Australian Centre for Pharmacometrics, Adelaide, SA 5000, Australia

[3] Faculty of Pharmacy, Assiut University, Assiut, Egypt

Published online: 28 January 2021

1 Introduction

Alzheimer's disease (AD) is a progressive neurodegenerative disorder characterized by memory loss, abnormal behavior, decline in thinking ability and failure to perform daily activities. It is considered the main cause of dementia among elderly people, and this group accounts for about 70% of dementia cases. According to the World Alzheimer Report 2018, around 50 million people suffer from dementia and this number is expected to rise sharply to reach 152 million by 2050 [1]. This rapid rise in cases is due to increasing life expectancy as well as the absence of effective therapy to treat AD or stop the disease progression. Unfortunately, the only four approved medications i.e., memantine and cholinesterase inhibitors, galantamine, rivastigmine, and donepezil, can only alleviate the symptoms [2] and proved to be ineffective in the long term and were associated with adverse effects [3]. Thus, a disease-modifying therapy that could alter the underlying pathophysiology of the disease is urgently required.

AD is characterized by the accumulation of extracellular senile plaques (composed of amyloid beta [Aβ] proteins) and intracellular neurofibrillary tangles of hyperphosphorylated tau protein. These changes are eventually accompanied by neurodegeneration [4, 5]. The exact mechanism of the disease is yet unclear. However, recent studies have revealed the role of neurotrophin imbalance in the pathogenesis of AD [6].

It has been found that lack of neurotrophin support in elderly individuals could be the key event that initiates the neurodegeneration in AD [7]. Several studies proved that the levels of mature neurotrophins and their tropomyosin receptor kinase that mediate neuron growth and survival are down-regulated [8]. Conversely, the levels of proneurotrophins and their pan receptor p75NTR, together with sortilin are upregulated, mediating neurodegeneration in AD patients [9, 10]. This aging-induced imbalance in neurotrophin levels and their receptors shifts the equilibrium towards neurodegeneration.

In this respect, p75NTR has been found to be involved in Aβ protein homeostasis in the brain. The full-length receptor can stimulate the production of $A\beta_{1\text{-}42}$ through stabilizing the rate-limiting enzyme of the amyloidogenic process, resulting in overproduction of protein oligomers that accumulate to form Aβ plaques. Sequentially, the formed Aβ peptides can bind to p75NTR resulting in cell death and stimulate the production of more toxic Aβ, maintaining a vicious cycle of Aβ production [11, 12]. However, the full-length receptor undergoes cleavage by an α-secretase enzyme to release its extracellular domain (ECD) which is a soluble moiety that, in contrast to the full-length (fl) domain, displays neuroprotective ability. Studies showed that the shedding process of ECD is significantly suppressed in AD, resulting in increased p75NTRfl and a reduction of ECD levels in the brain and cerebrospinal fluid (CSF) of AD patients [13, 14]. In order to understand how ECD exerts its neuroprotective effects, Wang et al. showed that ECD can act as a scavenger of toxic Aβ and other proneurotrophins, preventing its binding to p75NTRfl and thus acting as a competitive antagonist, inhibiting the overproduction of Aβ and promoting its clearance. [15] Therefore, restoration of the abnormal level of ECD in the brain and CSF can be an effective therapeutic strategy to alleviate AD pathologies. Recent studies showed that brain and intramuscular delivery of gene encoding p75ECD (AAV-p75ECD) can alleviate AD pathologies in animal models of dementia [14, 16].

In this context, p75ECD-Fc, a recombinant fusion protein of p75 extracellular domain and Fc fragment of the human immunoglobulin IgG1 was first synthesized in cooperation with Fujian Tiantai and Wuxi APPtec in China. It was successfully produced in Chinese Hamster Ovary (CHO) cells with stable expression and high purity. The product is a homodimer (molecular weight 130 kDa) with disulfide linkage between the two monomers (Fig. 1). It is a novel drug with the potential to treat AD. p75ECD-Fc is structurally analogous to the FDA-approved drug etanercept for inflammatory arthritis [17], which is an extracellular ligand-binding protein of the human p75 tumor necrosis factor-α receptor that belongs to the same receptor family and Fc fragment of human IgG1.

Previously, we reported pharmacokinetic data for intravenous (i.v.) and subcutaneous (s.c.) administration of p75ECD-Fc in rats with non-compartmental analsysis (NCA) of the data [18]. We also measured the concentration of p75ECD-Fc in different tissues including the brain and CSF and the cellular localization of the protein has been studied in tissues using a double immunofluorescence method. In addition, we studied the in vitro drug stability in plasma, and found that it is highly stable with minimal degradation [18]. Here, we aim to develop a compartmental pharmacokinetic model of these data that can describe p75ECD-Fc pharmacokinetics in blood. Semi-physiological models of p75ECD-Fc kinetics in a number of tissues are also described. In addition, we aim to investigate the quantitative importance of catabolic degradation and if these findings could explain the good stability observed in human plasma in vitro [18]. Furthermore, we examined if administration of human p75ECD-Fc in rats could have resulted in production of endogenous antibodies against the protein and whether these antibodies affect disposition and stability as previously reported with other protein drugs [19]. The results obtained from this study are expected to give us insight into the mechanism of drug action and to determine the most favorable route of administration. To the best of our

knowledge, this is the first model-based description of the pharmacokinetics of p75ECD-Fc in serum and tissues that will hopefully facilitate its development for further preclinical and clinical studies, which could be further translated to potential treatment of AD.

2 Methods

2.1 Data Set and General Modeling Methods

Model development, as described below, was based on data collected in a preclinical study described previously [18]. In this study, male and female Sprague Dawley (SD) rats (n = 15) were divided into 2 groups and were given a single dose of p75ECD-Fc (Fujian Tiantai Medical Technology Ltd., China) 3 mg/kg by i.v. (n = 8) or s.c. (n = 7) injection. Serum samples were collected over the whole study period from time zero until the 14-day time point (n = 7 rats), while data up to the 42-day time point were collected from the remaining animals in the study (n = 5). Tissues including liver, lung, heart, spleen, kidney, muscle, skin, lymph nodes, spinal cord and brain were collected at the 2-day post i.v. dose (n = 1), 3-day post s.c. dose (n = 1) and at the 14-day time point (n = 4/group). Samples were analyzed using validated enzyme-linked immunosorbent assay (ELISA) for p75ECD-Fc at a wavelength of 450 nm with a lower limit of quantification of 0.0625 ng/mL (Human NGF R/TNFRSF16 kit, R&D Systems, MN, USA), as previously described [18]. The absence or presence of anti-drug antibodies (ADAs) was detected in serum collected at the 42-day time point (n = 5) as follows. Several dilutions of serum samples that may contain rat antibodies against the drug including blank serum samples were captured with pure p75ECD-Fc as an antigen using ELISA and then detected with anti-rat antibodies. Color development further confirmed the reaction and indicated the presence of anti-drug antibodies. For detailed information about animal procedures and sample collection, please refer to the Supplementary material.

Modeling analysis was performed using the R software (version 3.6.1) with the dplyr and nonlinear mixed-effects modeling (nlmixr) 1.1.0 packages [20]. Models were defined using differential equations and fitted to data using the SAEM algorithm. First-order conditional estimation method with interaction (FOCE I) was used to fit models to test time-dependent covariates. Diagnostic plots were constructed using R package ggplot. Calculations for visual predictive checks were generated using the 'nlmixr vpc' tool and graphical representation was performed with the ggplot2 package in R and OriginPro v8.5. Statistical analyses were performed using R.

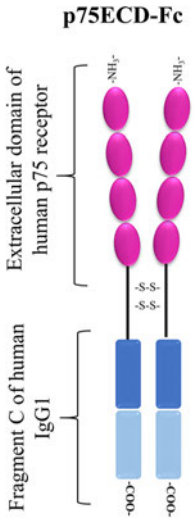


Fig. 1 Representative structure of p75ECD-Fc

Between-subject variability was modeled as a log-normal distribution. Combined additive and proportional errors were used to describe random residual variability. The need for omega block structures allowing covariance in between-subject variability was investigated as indicated.

The modeling approach involved 3 steps—(i) development of a compartmental population pharmacokinetic model that described only the i.v. serum data to estimate clearance with high certainty; (ii) development of a compartmental population pharmacokinetic model that combined both i.v. and s.c. serum data to estimate subcutaneous absorption characteristics with certainty; and (iii) development of semi-physiologically based pharmacokinetic model(s) to describe distribution of the p75ECD-Fc in individual tissues.

2.2 Compartmental Model Development

2.2.1 Intravenous Model

The following structural models were evaluated based on visual inspection of the data—1-compartment, 2-compartment with linear or mixed elimination pathways (Michaelis–Menten) and 3-compartment models. Body weight was not included as a covariate as the rats were approximately all the same size. Models were defined as differential equations and fitted to the data using SAEM parameter estimation. The model was parameterized as the volume of central and peripheral compartments (V1 and V2, respectively), intercompartmental transit rates (Q) and clearance from the central compartment (CL) where appropriate. [18]. The differential equations can be found in Supplementary material 1.

2.2.2 Intravenous and Subcutaneous Model

The final estimated values for the key parameters obtained after fitting the i.v. data were carried forward as initial

estimates to the differential equations (Supplementary material 2) to describe the kinetics of s.c. administration. Absorption from the s.c. site (depot) was described as first-order kinetics. This model estimated the absorption rate constant (ka) from the s.c. injection site, the bioavailability of the s.c. route (F), clearance rate (CL) and volume of central and peripheral compartments (V1 and V2). Initially, we tested 1-, 2- and 3-compartment models with clearance fixed at the value determined for the i.v. data alone. After selecting the best model that described the data adequately, we studied the effect of unfixing the initial clearance estimate.

2.2.3 Model Refinements

Several refinements of the best i.v. and s.c. model were examined. First, we examined if modeling could quantitate any metabolic losses that occur from either the central or the peripheral compartments, other than that mediated through central clearance. This would be consistent with the in vitro degradation of the drug in plasma observed previously [18]. The first- and zero-order losses from the central and peripheral compartments were tested via consideration of changes in model objective function (fit) and the precision of parameter estimates.

Second, we studied the effect of the development of ADAs on the pharmacokinetic profile and whether the inclusion of ADAs as a binary covariate could improve the model fitting. The development of ADAs in serum was considered to be a time-dependent covariate and analyzed using nlmixr-FOCEi fitting and analysis, where the value of ADA was set to be 1 if ADAs are present or 0 if ADAs are absent according to the Eq. (1):

$$CL = \exp(tCL + etaCL) \times (1 + ADA * adaCL)$$

2.3 Semi-Physiological Tissue Models

The compartment models defined above provide a description of the serum time course of p75ECD-Fc in the rat. To describe the time course of p75ECD-Fc in selected tissues, we developed semi-physiologically based pharmacokinetic (PBPK) models to characterize the individual distribution kinetics of p75ECD-Fc in tissues. In order to describe the model structure, all systemic pharmacokinetic parameter estimates previously obtained by fitting serum data were fixed and the resultant serum concentrations used as a forcing function were applied to the differential equations of a semi-PBPK model of each tissue. Tissues were assumed to equilibrate with the p75ECD-Fc plasma concentration as described by flow-limited kinetics. More complex models of tissue kinetics were not considered identifiable given the sparse tissue data. The tissues included in the model were the liver, lung, heart, kidney, spleen, lymph nodes, muscle, spinal cord and brain, each of which was assessed separately. Two key parameters were measured to describe the distribution kinetics of the drug for each tissue—QV (1/h) which is the apparent ratio of tissue-plasma flow to volume (describing the rate of equilibration of the tissue with the plasma), and R (ratio) which is the partition coefficient between tissue and plasma (describing the steady-state ratio of the concentrations). The differential equations used to describe the distribution kinetics of p75ECD-Fc in tissues can be found in Supplementary material 3.

2.4 Model Selection

Models were selected based on the goodness-of-fit as directed by changes in the objective function using the likelihood ratio test or the Akaike Information Criteria [21]; the parameter estimates precision as well as considering the least inter-individual variability. Additionally, diagnostic plots including predicted [PRED] and individual predicted [IPRED] versus observed data, conditional weighted residuals [CWRES] versus time and CWRES versus PRED and IPRED were used to judge the model adequacy. Models that resulted in high standard error of the estimated parameters (> 35% of the parameter estimate), models showing a high degree of correlation between parameters (> 90%) and models that involved a covariate(s) that poorly improved the prediction of the estimated parameters were re-evaluated and the parameters were re-adjusted, or rejected if a negligible effect was observed.

2.5 Model Evaluation

Visual predictive checks were conducted on selected and final models to assess the simulation performance of the models. One thousand versions of the original data were simulated using the selected model based on the final parameter values. The observed data, median and 90% confidence interval (CI) of the simulated data were plotted. The model performance was evaluated as satisfactory if most of the observed data points lay within the 90% CI of the predicted data with no significant aberration between the observed and the model-predicted data.

3 Results

3.1 Description of the Observed Data

Preclinical serum data were obtained from 12 SD rats that received a single dose of p75ECD-Fc (3 mg/kg) either i.v. ($n = 7$) or s.c. ($n = 5$). A total of 160 serum pharmacokinetic observations were obtained over a period of 42 days.

Thirty observations were below the limit of quantification and these were located near the zero time point and in the terminal phase of the washout tail. These were treated as missing data. Serum samples from one rat in the s.c. group were not collected at the time of the experiment and were not included in serum data analysis. Figure 2 shows a graphical plot of observed serum concentrations versus time. Tissue data were obtained at two time points—the first specimen was obtained after 2 days (for i.v. group) and 3 days (for s.c. group) from one individual/group early after dose administration and the second was obtained at the 14-day time point ($n = 4$/group). Brain samples were obtained at the last time point (42 days) to test the presence of any drug at the end of the total study period.

3.2 Compartment Models

3.2.1 Intravenous Model

The best model that fitted the i.v. serum data was the 2-compartment model with linear elimination kinetics which included central volume (V1), peripheral volume (V2), inter-compartmental clearance (Q) and clearance (CL) from the central compartment. The population parameter estimates for clearance, volume of central and peripheral compartments and inter-compartmental clearance were 0.000183 L/h, 0.013726 L, 0.029483 L and 0.001172 L/h, respectively. Inclusion of non-linear elimination kinetics, described by a Michaelis–Menten model, did not improve the goodness-of-fit plots and increased the objective function value (OFV). Furthermore, fitting the i.v. serum data to 1- and 3-compartment models did not improve the parameter estimates and resulted in high standard errors and between-subject variability, which further indicated the incompatibility of these models. The OFV values for the 1-, 2-, and 3-compartment models and non-linear 2-compartment model were 1911.4, 1749.4, 1767.6 and 1756.8, respectively. The final estimates for the model parameters obtained by fitting the i.v. serum data to the 2-compartment model are shown in Table 1.

3.2.2 Intravenous and subcutaneous Model

The i.v. and s.c. pharmacokinetic data were best described by a 2-compartment model (central V1, peripheral V2) and inter-compartmental clearance (Q), with first-order absorption rate (ka) from the s.c. route and linear elimination kinetics from the central compartment (CL). Subcutaneous p75ECD-Fc administration was characterized by a bioavailability of 57.4% and a slow absorption rate (ka) of 0.00726 1/h (absorption half-life = 3.9 days). The estimated clearance rate (CL) and the volume of central (V1) and peripheral compartments (V2) were found to be 0.00018 L/h, 0.0137 L and 0.0262 L, respectively. The 1- and 3-compartment models showed higher OFV (2754.9 and 2793.0, respectively) compared to the 2-compartment model (OFV = 2603.9) and provided poor goodness-of-fit plots.

Unfixing the initial estimate of the CL value increased the between-subject variability of the inter-compartmental clearance (Q) by 12% and did not improve the OFV or the goodness-of-fit plots (OFV = 2603.3) as shown in Table 2.

3.2.3 Model Refinements

Including any metabolic loss value from either the central or peripheral compartment resulted in a slight increase in OFV (2608.7, 2609.4, respectively) but reduced the between-subject variability of the inter-compartmental clearance (Q) by up to 40% (Table 2) and further improved the goodness-of-fit plots. Loss from the central compartment was best described by zero-order kinetics at an estimated amount of 0.000836 µg/h; this further indicates that catabolic degradation by proteases in plasma is quite minimal and saturable. Therefore, the drug concentration in the central compartment was mainly affected by both the central clearance (possible renal and hepatic clearance) and inter-compartmental clearance (Q). These findings are consistent with the high in vitro stability of p75ECD-Fc noticed when the drug was incubated with human plasma for 35 days at 37 °C [18]. The drug was found to be quite stable and with a minimal degradation rate that was not altered by the initial concentration. On the other hand, loss from the peripheral compartment was best described by first-order kinetics and the estimated loss rate was found to be 0.00002 L/h, which may be explained by the ability of this compartment to clear the drug by either receptor-mediated degradation or through lymphatic drainage. The estimates of the population parameters of the 2-compartment model including drug loss parameters are listed in Table 2. Key diagnostic plots of the 2-compartment model with the inclusion of a loss parameter can be found in Supplementary figures 1 and 2. As the inclusion of a loss term did not improve the OFV, it was not carried forward to the final model.

Based on visual examination of the data, a sudden drop in serum concentration seen in some rats was speculated to be due to the presence of ADAs. This model included ADAs as a time-dependent covariate in the dataset that allowed increased drug clearance with the presence of ADAs. The covariate was assigned a value of 0 or 1 based on either the absence or the presence of ADAs on the last day, with ADA-positive values carried backwards to the point of inflection in the concentration-time curve. The fitting of the 2-compartment model was repeated either with or

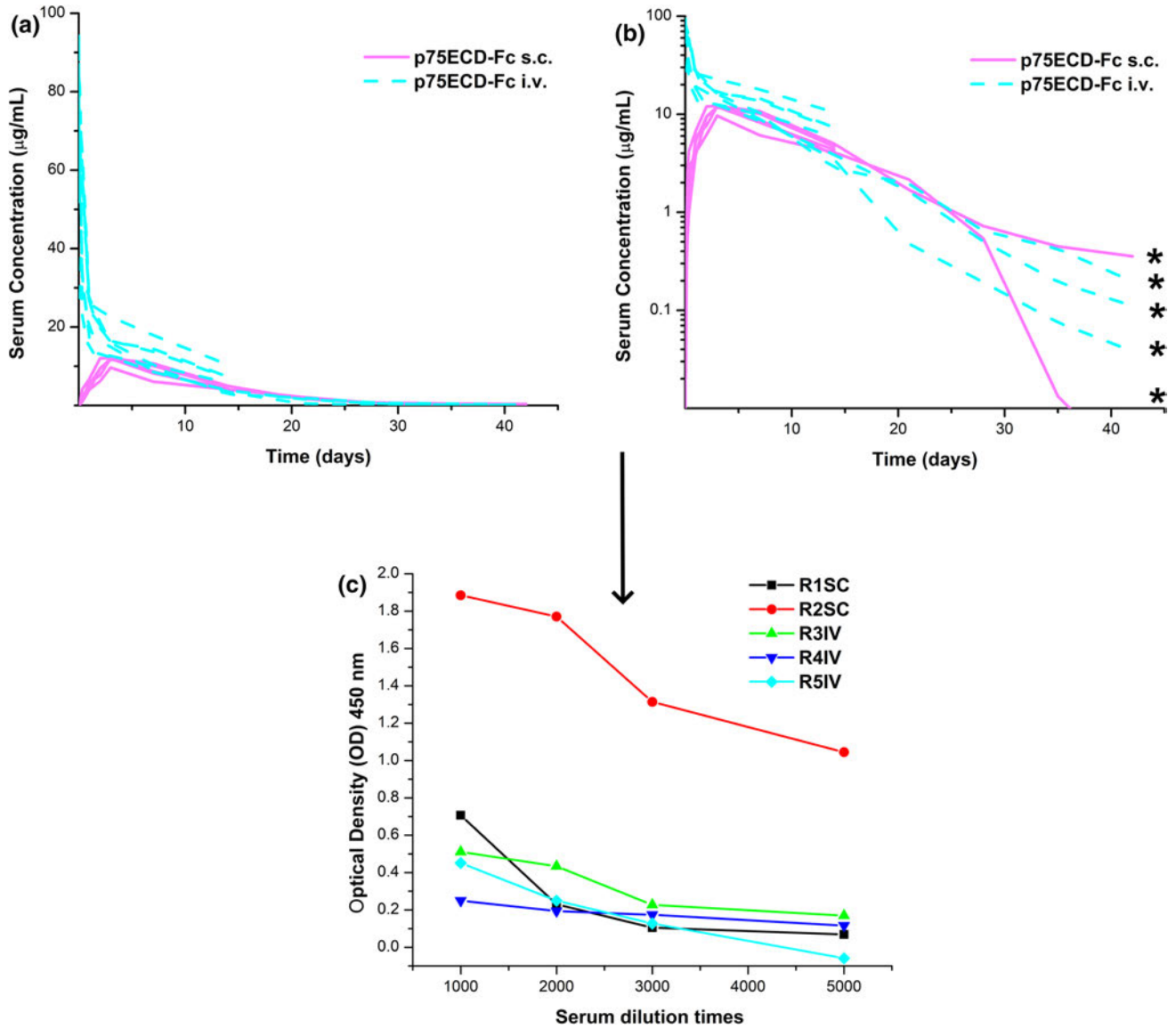


Fig. 2 **a** Observed serum concentration-time curve of p75ECD-Fc in 12 male and female Sprague Dawley rats after i.v. (dashed line) and s.c. (solid line) administration of 3 mg/kg p75ECD-Fc. **b** The logarithmic scale, showing serum concentration of 5 rats until day 42 (marked as star sign). **c** Graphical plot showing the detection of ADAs in the 42-day time point serum of the marked rats. Serum samples were diluted 1:1000–1:5000 and probed with the pure antigen p75ECD-Fc and ADAs using the ELISA technique. Color development at absorbance wavelength 450 nm indicated the presence of rat antibodies against the drug. *R* rat, *SC* subcutaneous, *IV* intravenous

without the proposed covariate relationship. The inclusion of ADAs resulted in improvement in the OFV (2601.1 vs 2805.5, using FOCE-I estimation method) and diagnostic plots over its exclusion and caused a 90% drop in between-subject variability of the Q estimated value. The clearance was approximately 31% higher in the presence of ADAs. This indicates that this model was capable of describing the changes in clearance rate more precisely (Table 2). Inclusion of ADAs as a time-dependent covariate parameter improved the parameter estimates and provided better goodness-of-fit plots. This covariate was carried forward to the final model.

3.2.4 Model Evaluation

The final compartmental model of serum pharmacokinetic data was, therefore, a 2-compartment model with linear elimination kinetics and with ADAs as a time-dependent covariate of clearance. This was considered sufficient to describe the systemic kinetics of p75ECD-Fc in rats. The final structure of the 2-compartment model is shown in Fig. 3 and the final parameter values in Table 2. Model parameters were precisely estimated with a narrow 95% CI. Goodness-of-fit plots showed that observed data are well represented by

Table 1 Final estimates of population pharmacokinetic parameters obtained by fitting the i.v. data to a 2-compartment model with linear elimination kinetics in the terminal phase

Parameter	Estimate	SE	%RSE	Back transformed	BSV (CV%)	Shrink (SD)%
CL (L/h)	− 8.6094	0.17	1.94	0.000183	44.756	− 4.369
V1 (L)	− 4.2884	0.03	0.66	0.013726	1.034	80.477
Q (L/h)	− 6.7494	0.24	3.51	0.001172	62.796	− 0.601
V2 (L)	− 3.5239	0.09	2.63	0.029483	19.711	12.838

CL apparent clearance, *V1* central volume of distribution, *V2* peripheral volume of distribution, *Q* intercompartmental clearance

the predicted concentrations, although showing some misspecifications seen at low concentrations (Figs. 4 and 5). This may be due to treating ADAs as a categorical rather than a continuous covariate. The latter may be possible when the quantitative consequences of the development of ADAs are better understood. The conditional standardized residual for the final model showed that observations were scattered around the null ordinate and quite symmetrical. Visual predictive checks further confirmed the appropriateness of the selected model and showed that simulated and observed data were similar (Fig. 6). Therefore, these results indicate that this model could adequately replicate p75ECD-Fc serum concentration-time profiles after i.v. or s.c. administration.

3.3 Semi-Physiological Tissue Models

A schematic illustration of the model structure for a single tissue model is shown in Fig. 7. Exchange between plasma

Table 2 Population parameters for the 2-compartment base model and final model

Parameter	Base model [%RSE] (BSV)	Unfixed clearance model [%RSE] (BSV)	Loss from central compartment (zero-order) [%RSE] (BSV)	Loss from peripheral compartment (first-order) [%RSE] (BSV)	ADA model (final model) [%RSE] (BSV)
OFV	2603.9	2603.3	2608.7	2609.4	NC
ka (1/h)	0.00726 [3.12] (7.79)	0.00712 [3.75] (8.43)	0.00694 [2.86] (5.91)	0.00703 [2.88] (10.09)	0.00745 [1.70] (16.70)
F	0.574 [27.18] (–)	0.571 [33.23] (–)	0.678 [36.20] (–)	0.670 [33.66] (–)	0.535 [14.86] (–)
CL (L/h)	0.000183 [–] (35.29)	0.000179 [1.54] (35.87)	0.000183 [–] (35.59)	0.000183 [–] (37.59)	0.000176 [1.41] (32.14)
V1 (L)	0.0137 [0.90] (6.78)	0.0137 [0.99] (8.49)	0.0142 [0.83] (5.41)	0.0144 [0.77] (3.18)	0.0145 [1.01] (9.16)
Q (L/h)	0.00056 [11.31] (3,064.16)	0.00056 [11.57] (3,450.67)	0.00062 [10.56] (2,166.08)	0.00062 [10.08] (1,645.43)	0.00065 [6.18] (186.59)
V2 (L)	0.0262 [3.05] (27.08)	0.0265 [2.96] (25.79)	0.0260 [2.91] (25.17)	0.0272 [3.07] (24.77)	0.0263 [3.94] (35.95)
Loss	–	–	0.000836 µg/h [12.11] (26.653)	0.000016 L/h [8.25] (18.728)	–
adaCL (ratio)	–	–	–	–	0.3109 [33.86] (–)

ADA anti-drug antibodies, *CL* apparent clearance, *ka* absorption rate constant, *F* bioavailability, *V1* central volume of distribution, *V2* peripheral volume of distribution, *Q* intercompartmental clearance, *SE* standard error, *%RSE* relative standard error as a percentage, *BSV* between subject variability, *CV%* coefficient of variation as a percentage, *OFV* objective function value, *NC* OFV not comparable due to different estimation method

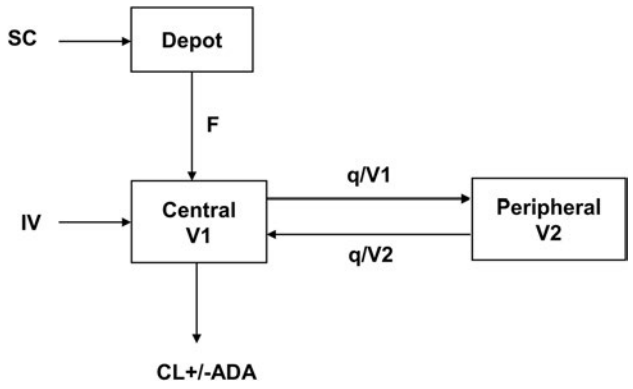


Fig. 3 Structural illustration of a population pharmacokinetic model of serum p75ECD-Fc concentration profile. The final model is a 2-compartment model with linear elimination kinetics and ADAs as a time covariate on clearance. *F* bioavailability of subcutaneous administration route, *CL* clearance, *ADA* anti-drug antibody-enhanced drug clearance, *q/V* rate constant of the inter-compartment drug transport, *V1* central volume, *V2* peripheral volume, *q* rate of change of the drug amount in the compartment

and tissues was characterized by two key parameters that could describe the kinetics for each tissue—QV which was the apparent ratio of tissue-plasma flow to volume (describing the rate of equilibration of the tissue with the plasma), and R which was the partition coefficient between tissue and plasma (describing the steady-state difference in concentration).

The estimated partition coefficient values for p75ECD-Fc (Table 3) suggest that the tissue concentrations were approximately 1–5% of the concurrent plasma concentration at steady state. p75ECD-Fc distribution was generally higher in the liver, spleen, heart and lungs. The liver showed the highest tissue distribution with a tissue/serum partition coefficient of 20.8% followed by the kidney with an estimated *R* value of 9.9%. The partition coefficient of lymph, skin and muscle ranged between 2 and 3%. On the other hand, the brain and spinal cord showed lower values for partition coefficients, possibly due to the limited ability to penetrate the blood–brain barrier (BBB). As evident from parameter estimates, these models were able to characterize the data

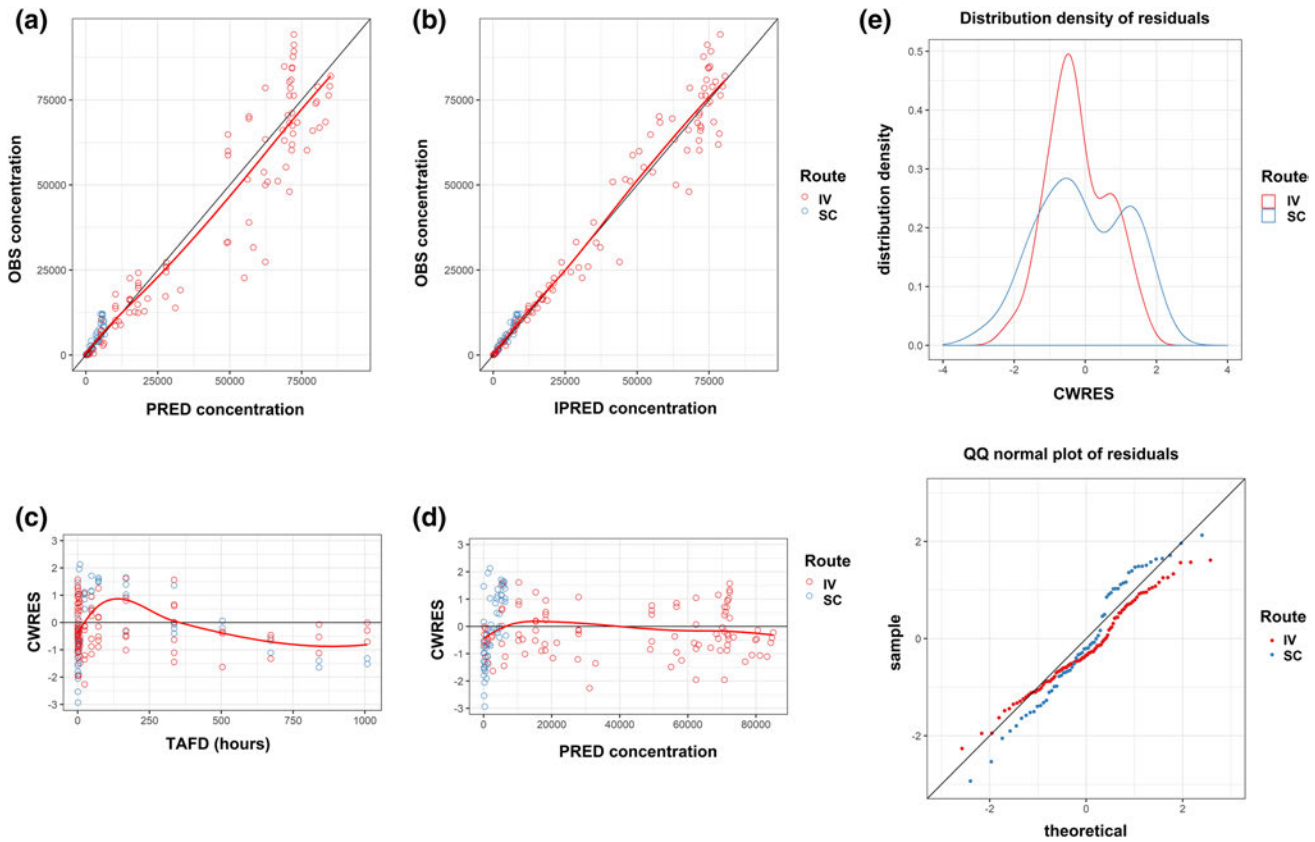


Fig. 4 Key diagnostic plots for p75ECD-Fc given by two routes (i.v., s.c.) comparing observed concentrations with individual- and population-predicted concentrations. In each plot, red circles represent i.v. data, blue represent s.c. data, the solid black line is a line with slope 1 or 0 and the solid red line is a Loess smoothed line. **a** Observed concentration (OBS) vs population-predicted concentration (PRED). **b** OBS vs individual-predicted concentration. **c** Conditional weighted residuals (CWRES) vs time after dose (TAFD). **d** CWRES vs population-predicted concentration. **e** The quantile–quantile (q–q) plot of that distribution. *CWRES* conditional weighted residuals, *IPRED* individual-predicted concentration, *OBS* observed, *PRED* predicted, *TAFD* time after first dose

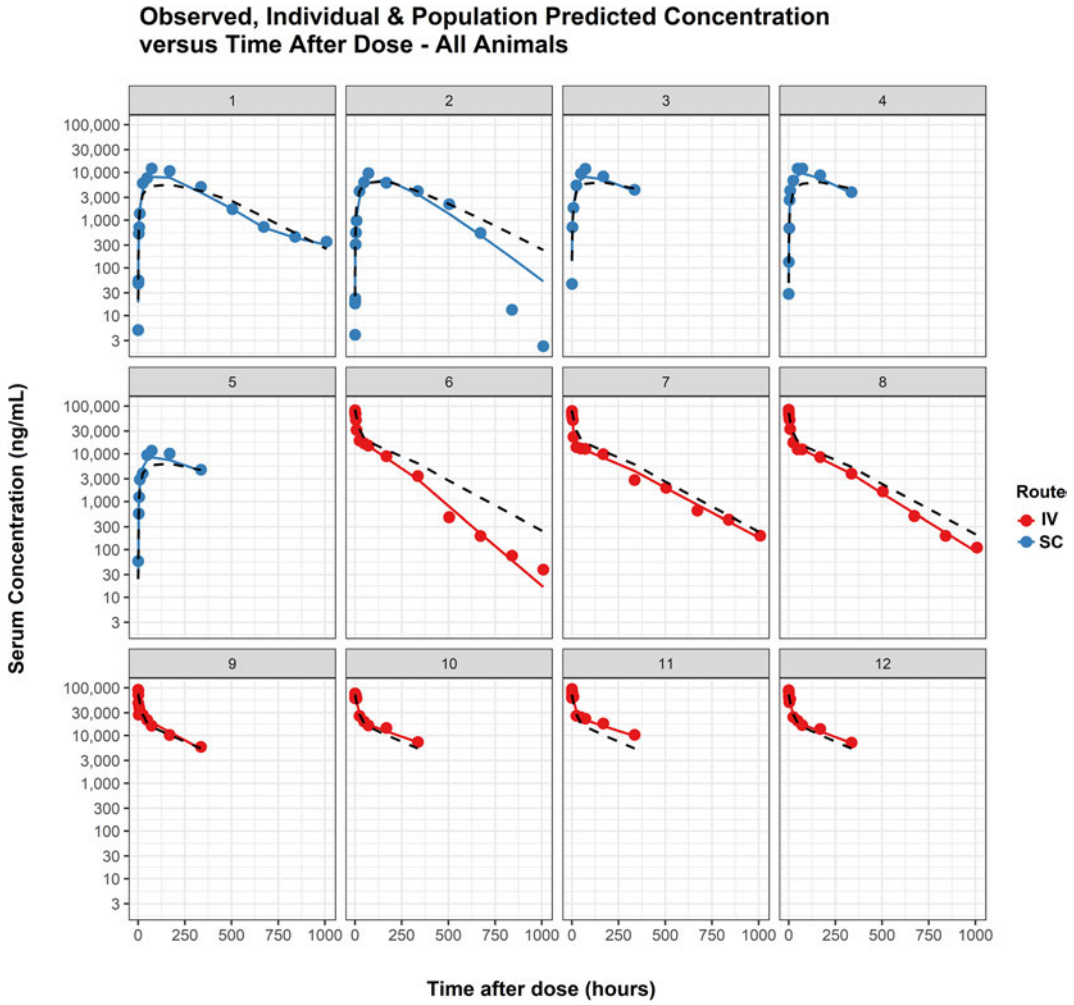


Fig. 5 Goodness-of-fit plots for p75ECD-Fc given by two routes (i.v. and s.c.) at a single dose of 3 mg/kg in 12 SD rats. Each panel shows data for one animal. Symbols represent observed drug concentrations; solid lines are the individual-predicted drug concentrations and dashed lines are the population-predicted drug concentrations

reasonably well, except for the concentration values in the heart which were under-predicted at the 14-day time point, while the lung and kidney were the best predicted. Generally, this simplified model predicted early p75ECD-Fc concentrations quite well, while becoming less precise at later time points. This may reflect some model mis-specification, but the available data were not considered sufficient to estimate more than two parameters per tissue. A graphical plot of estimated tissue partition coefficient values is shown in Fig. 8. Diagnostic plots displaying the observed and model-generated tissue pharmacokinetics of p75ECD-Fc in SD rats after administration of 3 mg/kg i.v. or s.c. are shown in Fig. 9.

4 Discussion

Here, pharmacokinetic models have been developed to describe the serum and tissue pharmacokinetics of p75ECD-Fc after single i.v and s.c. dose administration in SD rats. These models in combination are sufficient to provide descriptions of the plasma time-course of p75ECD-Fc in rats as well as the time-course in selected tissues.

The best compartment model of serum concentrations was the 2-compartment model with linear kinetics defined by a central volume that was approximately similar to plasma volume [22]. First-order kinetics were used to describe the absorption profile following s.c. administration. The bioavailability of the s.c. route was moderate with an estimated value of 53.5% and slow absorption rate constant of 0.00745 1/h, with maximal serum concentration observed after 3

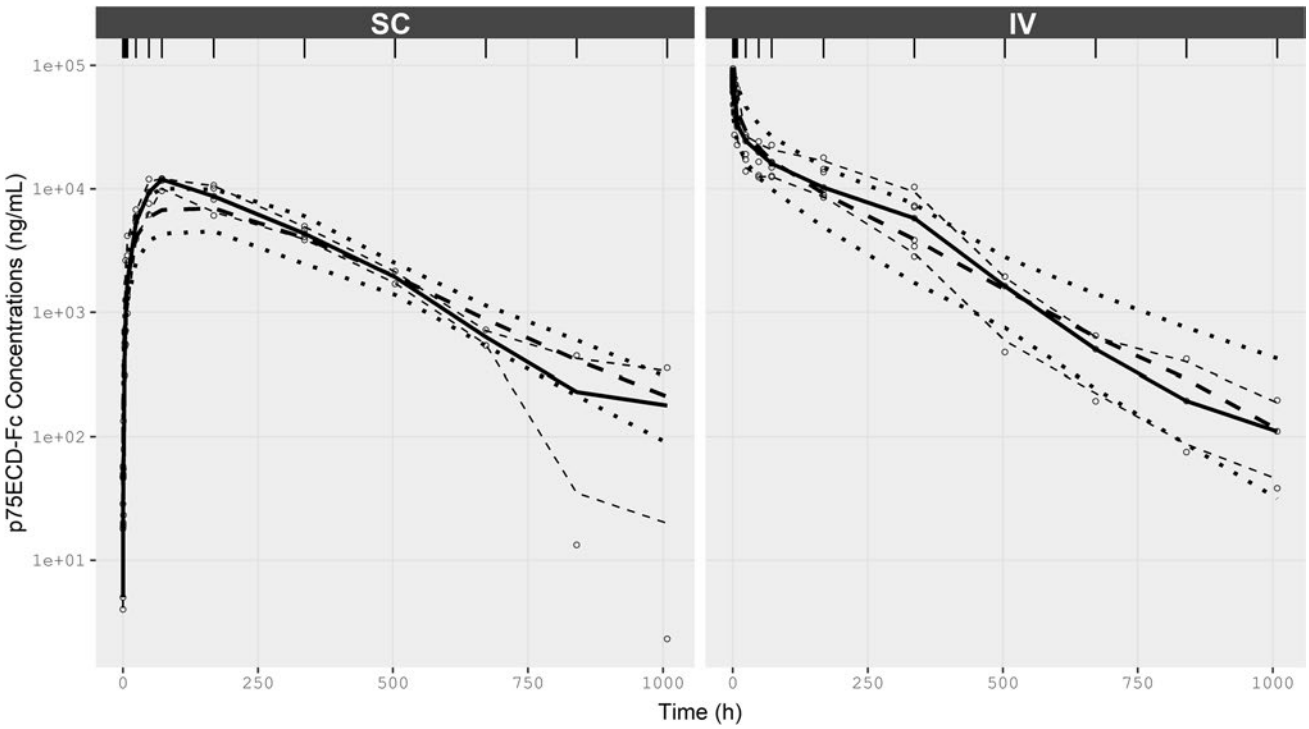


Fig. 6 Visual predictive check (VPC). A visual predictive check for the final 2-compartment model. VPC compares the simulated predictions with the original data. Circles represent the real observed data points. The solid line represents the median of the observed serum concentration data. The small dashed lines represent 5% and 95% percentiles of the observed data. The large dashed line represents the median of the simulated data, while the dotted line represents the 5th and 95th percentiles of the simulated data. The left panel is for the s.c. doses, the right panel for the i.v. doses

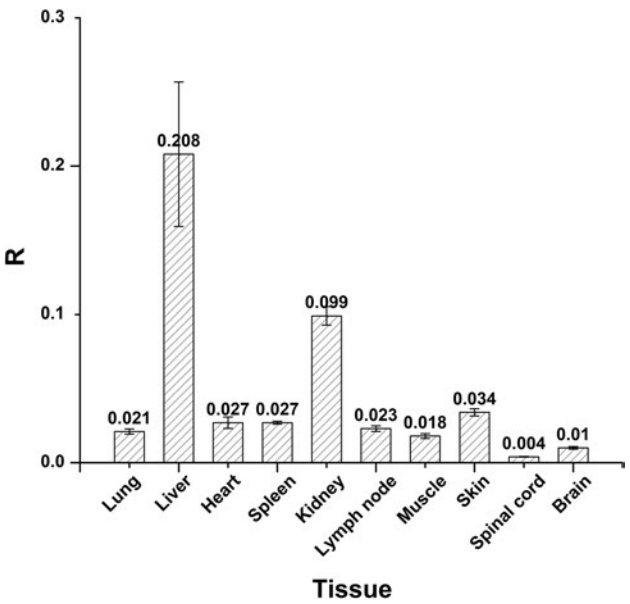


Fig. 7 Tissue plasma partition coefficient (R) of p75ECD-Fc after single i.v. and s.c. injection of 3 mg/kg in SD rats (n = 10–15). Data represent the estimated R value ± SE

days following s.c. injection. It is well established that the absorption of large proteins (> 16 kDa) from the skin is primarily mediated by the lymphatic system which then carries the drug to the venous system. This may explain the slow rate of absorption and may account for the reduced bioavailability due to possible degradation that can occur at the site of injection [23–26].These results are in accordance with a previously reported pharmacokinetic modeling analysis of etanercept and other therapeutic monoclonal antibodies that share similar structures [27, 28].

Based on these modeling results, the values of CL and Vss were 0.000587 L/h.kg and 0.136 L/kg and the alpha (distribution) and beta (elimination) half-lives were 0.37 and 7.49 days, respectively, while the s.c. bioavailability was 53.5%. Based on the previous NCA results [18], the values of CL and Vss were 0.0006 L/h.kg and 0.128 L/kg for i.v. and 0.0009 L/h.kg and 0.245 L/kg for s.c. Elimination half-life was found to be 7.49 and 6.2 days for i.v. and s.c., respectively, and the s.c. bioavailability was calculated around 66%. Therefore, it seems that the estimated values for i.v. pharmacokinetic parameters by NCA and compartmental analysis are similar and the NCA method was not compromised by censoring of concentrations due to the assay quantification limits.

Table 3 Estimated values for p75ECD-Fc tissue-plasma partition coefficient (R) and the apparent ratio of tissue-plasma flow to tissue volume (QV)

Tissue	QV (1/h)				*R* (ratio)			
	Estimate	Back transformed	SE	%RSE	Estimate	Back transformed	SE	%RSE
Lung	− 0.2127	0.808	0.2202	27.25	− 3.8756	0.021	0.0018	8.51
Liver	− 0.3032	0.738	0.0708	9.59	− 1.5719	0.208	0.0487	23.43
Heart	− 0.5858	0.557	0.1429	25.66	− 3.6151	0.027	0.0038	14.24
Spleen	− 0.3651	0.694	0.1016	14.64	− 3.5924	0.027	0.0010	3.63
Kidney	0.1551	1.168	0.3440	29.45	− 2.3099	0.099	0.0061	6.21
Lymph node	− 0.3196	0.726	0.5226	71.98	− 3.7554	0.023	0.0019	8.14
Muscle	− 0.1864	0.830	0.2701	32.54	− 4.0216	0.018	0.0016	9.05
Skin	− 0.2459	0.782	0.1744	22.30	− 3.3867	0.034	0.0024	7.16
Spinal cord	− 0.2371	0.789	5.9956	759.90	− 5.6027	0.004	0.0002	4.59
Brain	− 0.3642	0.695	0.1006	14.47	− 4.5499	0.010	0.0009	8.72

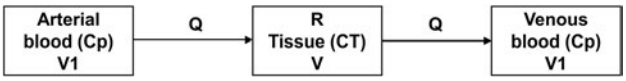


Fig. 8 Scheme for a single tissue model to characterize the biodistribution of p75ECD-Fc in various tissues. Tissue concentration is affected by the tissue-plasma flow rate (Q) and partition coefficient between plasma and tissue (*R*). The tissues were fitted individually using the serum concentration as a forcing function. *Cp* plasma concentration, *CT* tissue concentration, *V1* volume of central compartment (plasma) and *V* is the tissue volume

Similar to other biotherapeutics, p75ECD-Fc could undergo degradation through either intracellular lysosomal catabolism or extracellular proteolytic hydrolysis [29]. Catabolic degradation is also influenced by the route of administration. Following s.c. administration, degradation may occur during transport through the lymphatic system [24]. In our previous study, we found that the drug was co-localized in macrophages of different organs in vivo, which may indicate possible intracellular protein degradation through phagocytosis by the Fcγ receptors. However, the presence of Fc moiety may prolong its half-life through neonatal Fc receptor recycling which could slightly protect the molecule against lysosomal degradation [30, 31]. Therefore, a loss parameter from the central and peripheral compartments was included to describe the effect of catabolic degradation on drug clearance. We found that the effect of including a loss parameter was minimal on central clearance. This may explain either the absence of any non-specific elimination or that this loss cannot be distinguished from central clearance (a model identification problem). First-order kinetics best described the loss from the peripheral compartment, while loss from the central compartment (plasma) was zero-order kinetics. These results may suggest the good stability of the protein against non-specific proteases in human plasma and, as such, this catabolic pathway could be saturable. While peripheral elimination could be receptor mediated. However, further studies are required to explore the exact mechanism of p75ECD-Fc degradation.

ADAs included as a time-dependent covariate on clearance were able to improve the description of the relationship between the increase in drug clearance and the development of ADAs in the serum of some animals. These results indicate that the formation of an ADA–protein complex could represent an additional pathway for drug elimination. Generally, immunogenicity of monoclonal antibodies is very common depending on the type of protein and varies across species. It is also related to the route of administration with the s.c. route being highly immunogenic compared to the i.v. route [32]. Therefore, the generation of ADAs might have a significant impact on the pharmacokinetic profile and might account for the reduced bioavailability and inconsistent tissue distribution [33]. Inclusion of ADAs as a time covariate improved the data fitting and OFV significantly over its exclusion. Moreover, it had a positive effect by reducing the between-subject variability of the inter-compartment clearance term.

In addition, we developed single tissue semi-PBPK models to describe the tissue distribution kinetics of p75ECD-Fc. p75ECD-Fc tissue concentration data were obtained from two time points following a single i.v. and s.c. injection (data for the brain were available for the 2-day time point [detailed concentration for each part of the brain; data not shown] and for the 14- and 42-day time points). The results showed that highly perfused tissues including liver, lung, heart, and kidney showed the highest biodistribution and partition coefficient. p75ECD-Fc was also well distributed in lymph nodes, which is in agreement with previous reports showing that the lymphatic system plays a main role in the transport of large proteins throughout conviction and clearance [34]. p75ECD-Fc distribution in the kidneys and liver agrees with previously reported data of similar monoclonal antibodies and

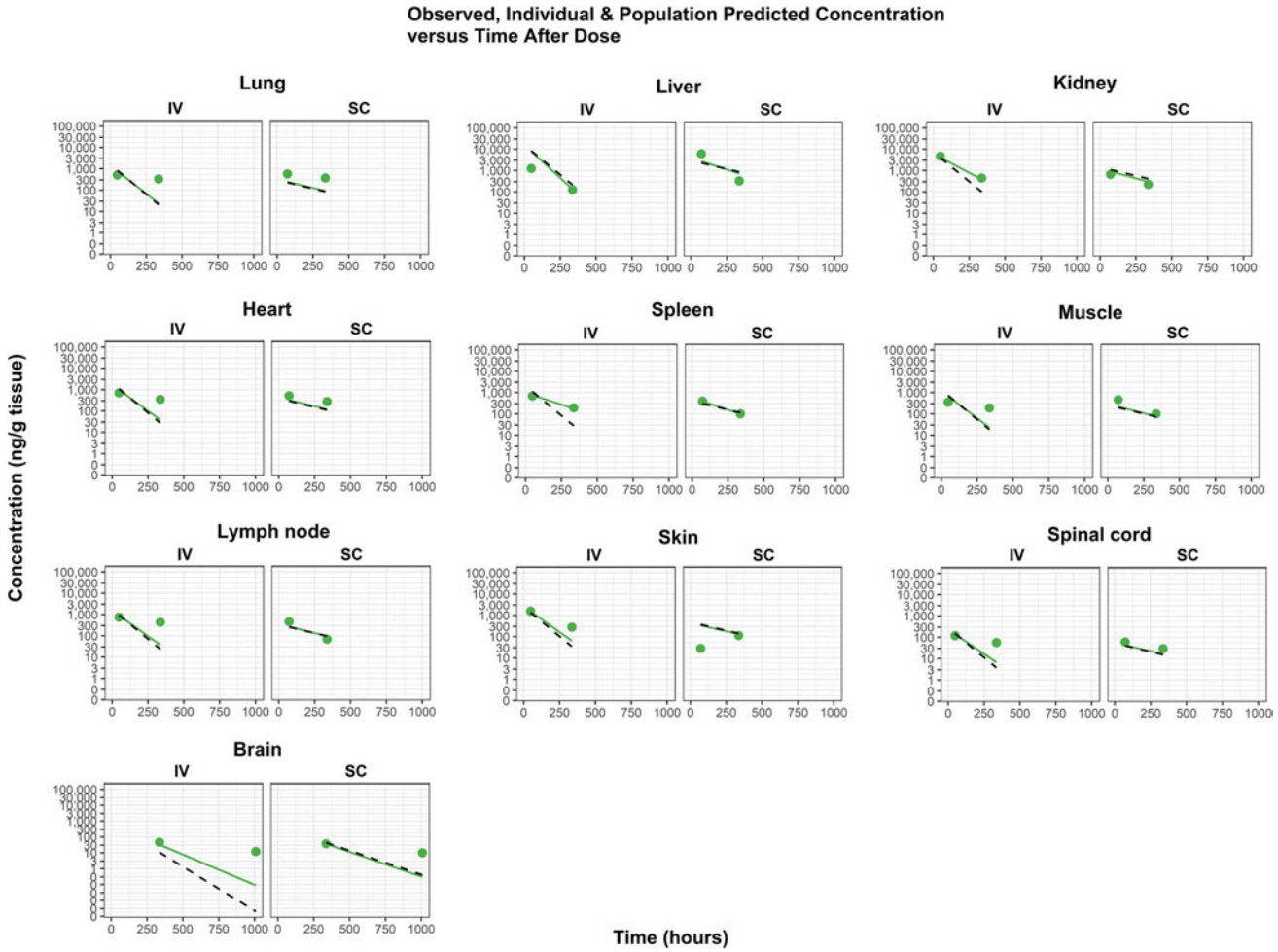


Fig. 9 p75ECDFc concentration–time profiles in multiple tissues. The dots represent observed data from the preclinical data set, solid lines are the individual-predicted drug concentrations and dashed lines are the population-predicted drug concentrations.

suggests that renal elimination as well as enhanced hepatic uptake could be a possible pathway of plasma elimination of the drug [35, 36]. Based on its molecular size and physicochemical properties, p75ECD-Fc showed limited ability to penetrate the BBB. Therefore, the partition coefficient of brain and spinal cord was the lowest. The observed pattern of tissue distribution suggests that p75ECD-Fc may exert its pharmacological effects primarily through antagonizing toxic Aβ peptides and proneurotrophins in the periphery besides its central role, as evident by its ability to cross the BBB as detected in the brain and CSF [18]. Based on partition coefficient data, the tissue distribution kinetics and our previous findings that indicated the co-localization of p75ECD-Fc in tissue-resident macrophages, we assume that p75ECD-Fc could act through binding to Aβ in the periphery and to some extent centrally to form immune complexes which are then cleared through phagocytosis by macrophages mainly in the liver and kidney. This effect would consequently drive the efflux of Aβ from the central nervous system to the periphery according to the 'peripheral sink mechanism' hypothesis [37]. In summary, these simplified semi-PBPK models described the tissue concentrations and yielded quite reasonable parameter estimates.

There are some limitations to the present study. Tissue concentrations were only obtained at two time points (day 2/3: $n = 1$, and day 14: $n = 4$) and the PBPK model was based on total tissue concentration disregarding interstitial and vascular fractions or permeability limitations in tissues. A more extensive study of kinetics in tissues may be indicated as the key sites of the action and elimination of p75ECD-Fc become apparent.

5 Conclusion

In this study, we developed pharmacokinetic models to describe serum and tissue distribution of p75ECD-Fc after single dose i.v. and s.c. administration of 3 mg/kg in SD

rats. The 2-compartment model with linear elimination kinetics sufficiently described the pharmacokinetic profile of p75ECD-Fc when considering the inclusion of ADAs as a covariate on clearance. p75ECD-Fc was slowly and moderately absorbed from the s.c. route (absorption rate constant = 0.00745 1/h, $F = 53.5\%$) and slowly eliminated from the central compartment at a rate of 0.000176 L/h. This study also provided a simplified semi-PBPK model to describe the distribution kinetics in tissues and investigated the partition coefficient and tissue-plasma flow rate for p75ECD-Fc. The favorable pharmacokinetic data for p75ECD-Fc taken together with its good reported efficacy in alleviating AD pathologies in animal studies [14] make it a potentially valuable candidate for further study and development for the treatment of dementia. Future extension involves the use of mass spectrometry techniques to study the metabolites of the drug and their possible intrinsic activity. Further studies are also required to understand the mechanism of drug biotransformation.

Declarations

Funding This work was supported by NHMRC grants (APP1020567, APP1021409) and a supporting grant from the University of South Australia. The authors also acknowledge the support provided to S. Kelliny by a Commonwealth Research and Training scholarship and the Egyptian Ministry of Higher Education. p75ECD-Fc was provided by Fujian Tiantai Medical Technology Ltd.

Conflict of interest Xin-Fu Zhou is one of the inventors of p75ECD-Fc for the treatment of AD. The other authors declare no conflict of interest.

Ethical approval All animal procedures performed in this study were approved by the Animal Ethics Committee (AEC) of the University of South Australia (approval number U14/16) and in compliance with the South Australian Animal Welfare Act 1985 and Regulations 2012.

Consent to participate Not applicable.

Consent for publication Not applicable.

Availability of data and material Data are available on negotiation with the authors.

Code availability Code are available on negotiation with the authors.

Author Contributions All authors participated in the study design and/or data interpretation. S.K. conducted the animal study and samples analysis. Statistical analysis, model development and evaluation were performed by R.U. and S.K. The first draft of the manuscript was written by S.K. and R.U. and all authors commented on previous versions of the manuscript. All authors read and approved the final manuscript.

References

1. Alzheimer's Disease International: World Alzheimer Report 2018; The state of the art of dementia research: new frontiers. 2018.
2. Alzheimer's association: FDA-approved treatments for Alzheimer's. 2019.
3. Khoury R, Rajamanickam J, Grossberg GT. An update on the safety of current therapies for Alzheimer's disease: focus on rivastigmine. Ther Adv Drug Saf. 2018;9(3):171–8. https://doi.org/10.1177/2042098617750555.
4. Hardy J, Selkoe DJ. The amyloid hypothesis of Alzheimer's disease: progress and problems on the road to therapeutics. Science. 2002;297(5580):353–6. https://doi.org/10.1126/science.1072994.
5. Braak H, Braak E. Neuropathological stageing of Alzheimer-related changes. Acta Neuropathol. 1991;82(4):239–59.
6. Zhou X-F. The imbalance of neurotrophic signalling: an alternate hypothesis for the pathogenesis and drug development of Alzheimer's disease. Proc Neurosci. 2016;1(1):13–8.
7. Cattaneo A, Calissano P. Nerve growth factor and Alzheimer's disease: new facts for an old hypothesis. Mol Neurobiol. 2012;46(3):588–604. https://doi.org/10.1007/s12035-012-8310-9.
8. Ginsberg SD, Che S, Wuu J, Counts SE, Mufson EJ. Down regulation of trk but not p75NTR gene expression in single cholinergic basal forebrain neurons mark the progression of Alzheimer's disease. J Neurochem. 2006;97(2):475–87. https://doi.org/10.1111/j.1471-4159.2006.03764.x.
9. Wang YJ, Valadares D, Sun Y, Wang X, Zhong JH, Liu XH, et al. Effects of proNGF on neuronal viability, neurite growth and amyloid-beta metabolism. Neurotox Res. 2010;17(3):257–67. https://doi.org/10.1007/s12640-009-9098-x.
10. Ibáñez CF, Simi A. p75 neurotrophin receptor signaling in nervous system injury and degeneration: paradox and opportunity. Trends Neurosci. 2012;35(7):431–40. https://doi.org/10.1016/j.tins.2012.03.007.
11. Yaar M, Zhai S, Pilch PF, Doyle SM, Eisenhauer PB, Fine RE, et al. Binding of beta-amyloid to the p75 neurotrophin receptor induces apoptosis. A possible mechanism for Alzheimer's disease. J Clin Invest. 1997;100(9):2333–40. https://doi.org/10.1172/JCI119772.
12. Mamada N, Tanokashira D, Hosaka A, Kametani F, Tamaoka A, Araki W. Amyloid β-protein oligomers upregulate the β-secretase, BACE1, through a post-translational mechanism involving its altered subcellular distribution in neurons. Mol Brain. 2015;8(1):73. https://doi.org/10.1186/s13041-015-0163-5.
13. Zhou XF, Wang YJ. The p75NTR extracellular domain. Prion. 2011;5:161–3. https://doi.org/10.4161/pri.5.3.16896.
14. Yao XQ, Jiao SS, Saadipour K, Zeng F, Wang QH, Zhu C, et al. p75NTR ectodomain is a physiological neuroprotective molecule against amyloid-beta toxicity in the brain of Alzheimer's disease. Mol Psychiatry. 2015;20(11):1301–10. https://doi.org/10.1038/mp.2015.49.
15. Wang YJ, Wang X, Lu JJ, Li QX, Gao CY, Liu XH, et al. p75NTR regulates Abeta deposition by increasing Abeta production but inhibiting Abeta aggregation with its extracellular domain. J Neurosci. 2011;31(6):2292–304. https://doi.org/10.1523/JNEUROSCI.2733-10.2011.
16. Wang Q-H, Wang Y-R, Zhang T, Jiao S-S, Liu Y-H, Zeng F, et al. Intramuscular delivery of p75NTR ectodomain by an AAV vector attenuates cognitive deficits and Alzheimer's disease-like pathologies in APP/PS1 transgenic mice. J Neurochem. 2016;138(1):163–73. https://doi.org/10.1111/jnc.13616.

17. Enbrel. Pharmaceuticals. Amgen Inc. and Wyeth-Ayerst, Thousand Oaks. 2004.
18. Kelliny S, Lam HY, Parikh A, Wang Y, Bobrovskaya L, Upton R, et al. Preclinical study of the pharmacokinetics of p75ECD-Fc, a novel human recombinant protein for treatment of Alzheimer's disease, in Sprague Dawley rats. Curr Drug Metab. 2020;21:1–10. https://doi.org/10.2174/1389200221666200502015203.
19. Lin JH. Pharmacokinetics of biotech drugs: peptides, proteins and monoclonal antibodies. Curr Drug Metab. 2009;10(7):661–91. https://doi.org/10.2174/138920009789895499.
20. R Core Team. R: a language and environment for statistical computing. R Foundation for Statistical Computing, Vienna, Austria. URL https://www.R-project.org/. 2017.
21. Akaike H. A new look at the statistical model identification. IEEE Trans Autom Control. 1974;19(6):716–23. https://doi.org/10.1109/TAC.1974.1100705.
22. Probst RJ, Lim JM, Bird DN, Pole GL, Sato AK, Claybaugh JR. Gender differences in the blood volume of conscious Sprague-Dawley rats. J Am Assoc Lab Anim Sci. 2006;45(2):49–52.
23. Factors affecting the lymphatic absorption of macromolecules following extravascular administration. Pharmaceutical Research (New York). 1996;13((New York):S396-S.
24. McLennan DN, Porter CJH, Charman SA. Subcutaneous drug delivery and the role of the lymphatics. Drug Discov Today Technol. 2005;2(1):89–96. https://doi.org/10.1016/j.ddtec.2005.05.006.
25. Kagan L, Gershkovich P, Mendelman A, Amsili S, Ezov N, Hoffman A. The role of the lymphatic system in subcutaneous absorption of macromolecules in the rat model. Eur J Pharm Biopharm. 2007;67(3):759–65. https://doi.org/10.1016/j.ejpb.2007.04.002.
26. Wang W, Chen N, Shen X, Cunningham P, Fauty S, Michel K, et al. Lymphatic transport and catabolism of therapeutic proteins after subcutaneous administration to rats and dogs. Drug Metab Dispos. 2012;40(5):952–62. https://doi.org/10.1124/dmd.111.043604.
27. Chen X, DuBois DC, Almon RR, Jusko WJ. Biodistribution of etanercept to tissues and sites of inflammation in arthritic rats. Drug Metab Dispos. 2015a;43(6):898–907. https://doi.org/10.1124/dmd.114.062901.
28. Lee B-y, Kwon K-i, Kim M-S, Baek I-h. Michaelis–Menten elimination kinetics of etanercept, rheumatoid arthritis biologics, after intravenous and subcutaneous administration in rats. Eur J Drug Metab Pharmacokinet. 2016;41(4):433-9. https://doi.org/10.1007/s13318-015-0270-9.
29. Hall MP. Biotransformation and in vivo stability of protein biotherapeutics: impact on candidate selection and pharmacokinetic profiling. Drug Metab Dispos. 2014;42(11):1873–80. https://doi.org/10.1124/dmd.114.058347.
30. Suzuki T, Ishii-Watabe A, Tada M, Kobayashi T, Kanayasu-Toyoda T, Kawanishi T, et al. Importance of neonatal FcR in regulating the serum half-life of therapeutic proteins containing the Fc domain of human IgG1: a comparative study of the affinity of monoclonal antibodies and Fc-fusion proteins to human neonatal FcR. J Immunol. 2010;184(4):1968–76. https://doi.org/10.4049/jimmunol.0903296.
31. Roopenian DC, Akilesh S. FcRn: the neonatal Fc receptor comes of age. Nat Rev Immunol. 2007;7(9):715–25. https://doi.org/10.1038/nri2155.
32. Gómez-Mantilla JD, Trocóniz IF, Parra-Guillén Z, Garrido MJ. Review on modeling anti-antibody responses to monoclonal antibodies. J Pharmacokinet Pharmacodyn. 2014;41(5):523–36. https://doi.org/10.1007/s10928-014-9367-z.
33. Kamath AV. Translational pharmacokinetics and pharmacodynamics of monoclonal antibodies. Drug Discov Today Technol. 2016;21–22:75–83. https://doi.org/10.1016/j.ddtec.2016.09.004.
34. Chen X, DuBois DC, Almon RR, Jusko WJ. Biodistribution of etanercept to tissues and sites of inflammation in arthritic rats. Drug Metab Dispos. 2015b;43(6):898–907. https://doi.org/10.1124/dmd.114.062901.
35. Conner KP, Rock BM, Kwon GK, Balthasar JP, Abuqayyas L, Wienkers LC, et al. Evaluation of near infrared fluorescent labeling of monoclonal antibodies as a tool for tissue distribution. Drug Metab Dispos. 2014;42(11):1906–13. https://doi.org/10.1124/dmd.114.060319.
36. Cohen R, Stammes MA, de Roos IH, Stigter-van Walsum M, Visser GW, van Dongen GA. Inert coupling of IRDye800CW to monoclonal antibodies for clinical optical imaging of tumor targets. EJNMMI Res. 2011;1(1):31. https://doi.org/10.1186/2191-219X-1-31.
37. Liu Y-H, Wang Y-R, Xiang Y, Zhou H-D, Giunta B, Manucat N, et al. Clearance of amyloid-beta in Alzheimer's disease: shifting the action site from center to periphery. Mol Neurobiol. 2014. https://doi.org/10.1007/s12035-014-8694-9.

Supplementary Material

Journal name: *European Journal of Drug Metabolism and Pharmacokinetics*

Article title: Pharmacokinetic modelling of p75ECD-Fc, a novel therapeutic approach for treatment of Alzheimer's disease, in Sprague Dawley rats

Authors: Sally Kelliny[1,3], Larisa Bobrovskaya[1], Xin-Fu Zhou[1*], Richard Upton[2*]

*Corresponding authors

XF Zhou: xin-fu.zhou@unisa.edu.au

R Upton: richard.upton@unisa.com.au

Affiliations: [1]University of South Australia, Clinical and Health Sciences, SA, 5000, Australia; [2]University of South Australia, Clinical and Health Sciences, Australian Centre for Pharmacometrics, SA, 5000, Australia; [3]Faculty of Pharmacy, Assiut University, Assiut, Egypt.

Animal procedures and samples collection

All animal procedures were approved by the Animal Ethics Committee (AEC) of University of South Australia (UNISA) (approval no. U14/16) and done in compliance with the South Australian animal welfare Act 1985 and Regulations 2012.

Male and female Sprague Dawley rats (n = 15, age = 4 – 6 months old) weighing between 300-400g were obtained from the Core animal facility at the School of Pharmacy and Medical Sciences, University of South Australia (UNISA). Prior to starting, animals were maintained under standard conditions of 22°C and a 12-h light/dark cycle with food and water provided ad libitum. They were divided randomly into two groups each received a single dose of p75ECD-Fc. Group A (n = 8, 5 males and 3 females) received p75ECD-Fc 3mg/kg intravenously (i.v.) by jugular vein cannulation or tail vein injection while group B (n = 7, 5 males and 2 females) received the same dose of p75ECD-Fc subcutaneously (s.c.). Blood samples (50-100 µl) were collected from the jugular vein cannula (the first few samples) and then from the saphenous (leg) vein at different time points as follows : pre-dosing then 5,10,15, 30 minutes, post dose followed by 1, 3, 5, 8, 24 hours and then 2 days, 3, 7, 14, 21, 28, 35, 42 days. Tissue samples including brain, spinal cord, liver, spleen, kidney, lung, heart, lymph nodes, muscle and skin were collected at 2-, 3- and 14-post dose time points as follows. One rat from the i.v. group was humanely killed after 2 days and then another rat from the s.c. group was HK at 3-day post dose (peak plasma level). At 14-day time point, 4 rats from each group were HK. After proper perfusion of carcasses with PBS, tissue samples were harvested and snap frozen in liquid nitrogen. All remaining animals were kept to the end of 42 days. At the end of 42 days, all remaining animals were HK and blood as well as brain samples were collected to test if there is any remaining drug in the brain after 42 days of single dose injection.

Blood samples were centrifuged at 3000xg for 10 minutes at 4°C to separate serum and then stored at -80°C until further analysis with ELISA. Tissue samples were pulverized with liquid nitrogen, and then sonicated with tris-buffer saline (TBS, pH 7.4) in the ratio of 10 mg:100 µL parts of buffer, containing protease cocktail inhibitor at 4°C. This mixture was finally centrifuged at 15,000 rpm for 30 minutes to separate the supernatant. All samples were then kept at -80°C to be analyzed with ELISA.

Analysis of p75ECD-Fc

Serum and tissue p75ECD-Fc concentration was measured by validated ELISA assay (Human NGF R/TNFRSF16 kit, R & D systems, Minneapolis, USA), with minor modifications, using anti-human nerve growth factor receptor as capture antibody and biotinylated mouse anti-human IgG Fc as detection antibody. A seven-point standard curve was obtained by 2-fold serial dilutions of the standard with concentrations ranging from 62.5 pg/ml to 4000 pg/ml. The lower limit of quantification of the assay was 0.0625 ng/ml. The standard curve was linear over the concentration range of 62.5 to 4000 pg/mL ($r \geq 0.999$). Samples were diluted with 1% bovine serum albumin (BSA) in phosphate buffer saline and Tween-20 (PBST) to the desired linear concentration range prior to analysis. The final concentrations were reported as ng/mL or µg/L serum and ng/gm tissue.

Supplementary Material 1: Differential equations used in i.v. pharmacokinetic model.

1-compartment model:

$\frac{\mathrm{d}}{\mathrm{dt}}(\mathrm{centr}) = -\left(\frac{\mathrm{cl}}{\mathrm{v1}}\right) \times \mathrm{centr}$

1-compartment blk:

$eta.cl + eta.v1 \sim c(0.3,$

0.01,0.3)

2-compartment model with linear elimination kinetics:

$\frac{d}{dt}(centr) = \left(\frac{q}{v2}\right) \times periph - \left(\frac{q}{v1}\right) \times centr - \left(\frac{cl}{v1}\right) \times centr$

$\frac{d}{dt}(periph) = \left(\frac{q}{v1}\right) \times centr - \left(\frac{q}{v2}\right) \times periph$

2-compartment model with non-linear elimination kinetics (Michaelis -Menten):

$\frac{d}{dt}(centr) = \left(\frac{q}{v2}\right) \times periph - \left(\frac{q}{v1}\right) \times centr - \left(\frac{vmax \times \frac{centr}{v1}}{km + \frac{centr}{v1}}\right)$

$\frac{d}{dt}(periph) = \left(\frac{q}{v1}\right) \times centre - \left(\frac{q}{v2}\right) \times periph$

2-compartment blk:

$eta.cl + eta.v1 + eta.q + eta.v2 \sim c(0.3,$

0.01,0.3,

0.01,0.01,0.3,

0.01,0.01,0.01,0.3)

3-compartment model:

$\frac{d}{dt}(centr) = +\left(\frac{q2}{v2}\right) \times periph1 - \left(\frac{q2}{v1}\right) \times centr + \left(\frac{q3}{v3}\right) \times periph2 - \left(\frac{q3}{v1}\right) \times centr - \left(\frac{c1}{v1}\right) \times centr$
(9)

$\frac{d}{dt}(periph1) = \left(\frac{q2}{v1}\right) \times centr - \left(\frac{q2}{v2}\right) \times periph1$

$\frac{d}{dt}(periph2) = \left(\frac{q3}{v1}\right) \times centr - \left(\frac{q3}{v3}\right) \times periph2$

Supplementary Material 2: Differential equations used in i.v. and s.c. pharmacokinetic- model.

$$\frac{d}{dt}(depot) = -ka \times depot$$

$$f(depot) = BA$$

$$\frac{d}{dt}(centr) = ka \times depot + \left(\frac{q}{v2}\right) \times periph - \left(\frac{q}{v1}\right) \times centr - \left(\frac{c1}{v1}\right) \times centr$$

$$\frac{d}{dt}(periph) = \left(\frac{q}{v1}\right) \times centr - \left(\frac{q}{v2}\right) \times periph$$

$$f(centr) = 1$$

Supplementary Material 3: Differential equations used in tissue modelling.

$$\frac{d}{dt}(depot) = -ka \times depot$$

$$f(depot) = BA$$

$$\frac{d}{dt}(centr) = ka \times depot + \left(\frac{q}{v2}\right) \times periph - \left(\frac{q}{v1}\right) \times centr - \left(\frac{c1}{v1}\right) \times centr$$

$$\frac{d}{dt}(periph) = \left(\frac{q}{v1}\right) \times centr - \left(\frac{q}{v2}\right) \times periph$$

$$f(centr) = 1$$

$$\frac{d}{dt}(tissue) = QV \times (\frac{centr}{v1} - \frac{tissue}{R})$$

$$f(tissue) = 1$$

Parameters

CL: clearance rate

V1: volume of central compartment,

V2: volume of peripheral compartment

q; rate of change of drug amount,

ka: absorption rate constant

F, BA: bioavailability

QV is apparent ratio of tissue plasma flow to volume

R is the tissue-plasma partition

Supplementary Figure 1: Key Diagnostic plots for weighted residual of Base model over the range of predicted concentrations with the inclusion of zero order loss parameter from the central compartment.

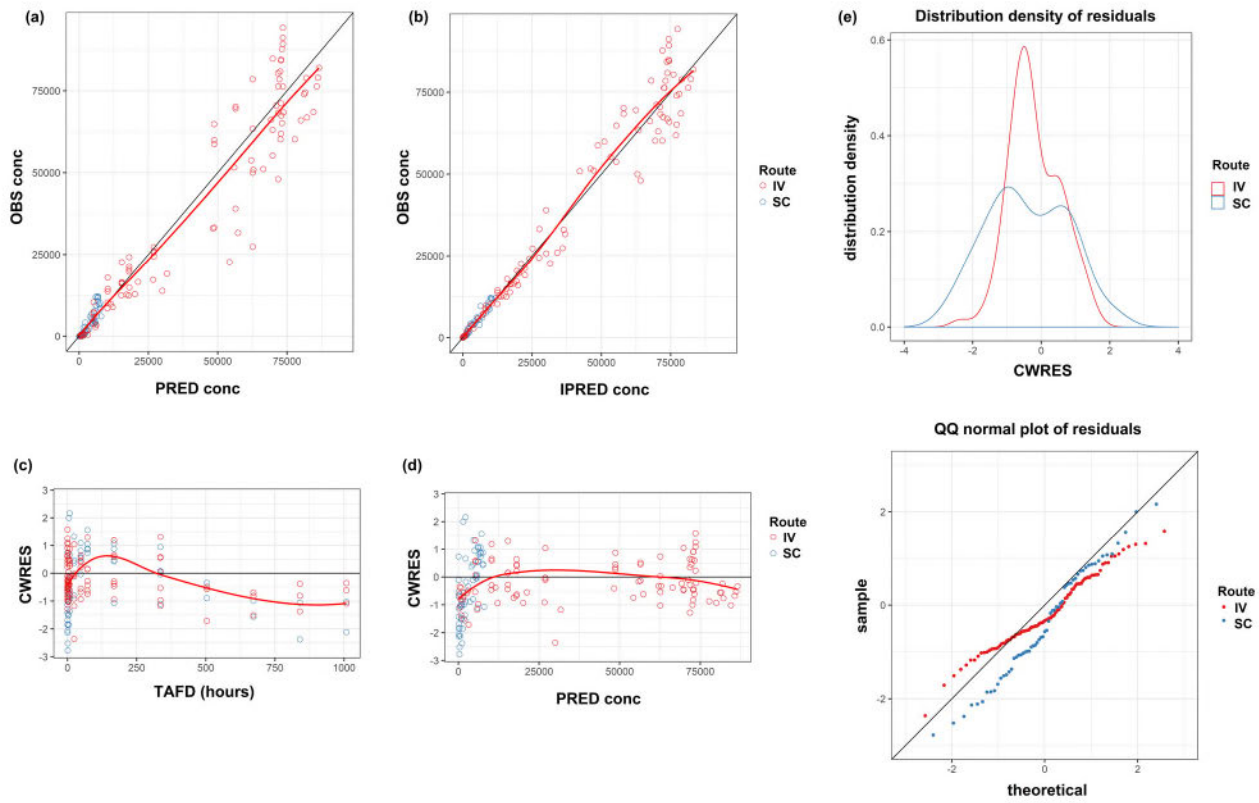


Fig. 1 Key diagnostic plots for p75ECD-Fc given by two routes (i.v., s.c.) comparing observed concentrations with individual and population predicted concentrations. In each plot, red circles represent i.v. data, blue represent s.c. data, the solid black line is a line with slope 1 or 0 and the solid red line is a Loess smoothed line. (a) Observed concentration (OBS) vs. population-predicted concentration (PRED). (b) OBS vs. individual-predicted concentration. (c) Conditional weighted residuals (CWRES) vs. time after dose (TAFD). (d) CWRES vs. population-predicted concentration. (E) The quantile–quantile (q–q) plot of that distribution. CWERS, conditional weighted residuals; IPRED, individual-predicted concentration; OBS, observed; PRED, predicted; TAFD, time after first dose.

Supplementary Figure 2: Key Diagnostic plots for weighted residual of Base model over the range of predicted concentrations with the inclusion of first order loss parameter from the peripheral compartment.

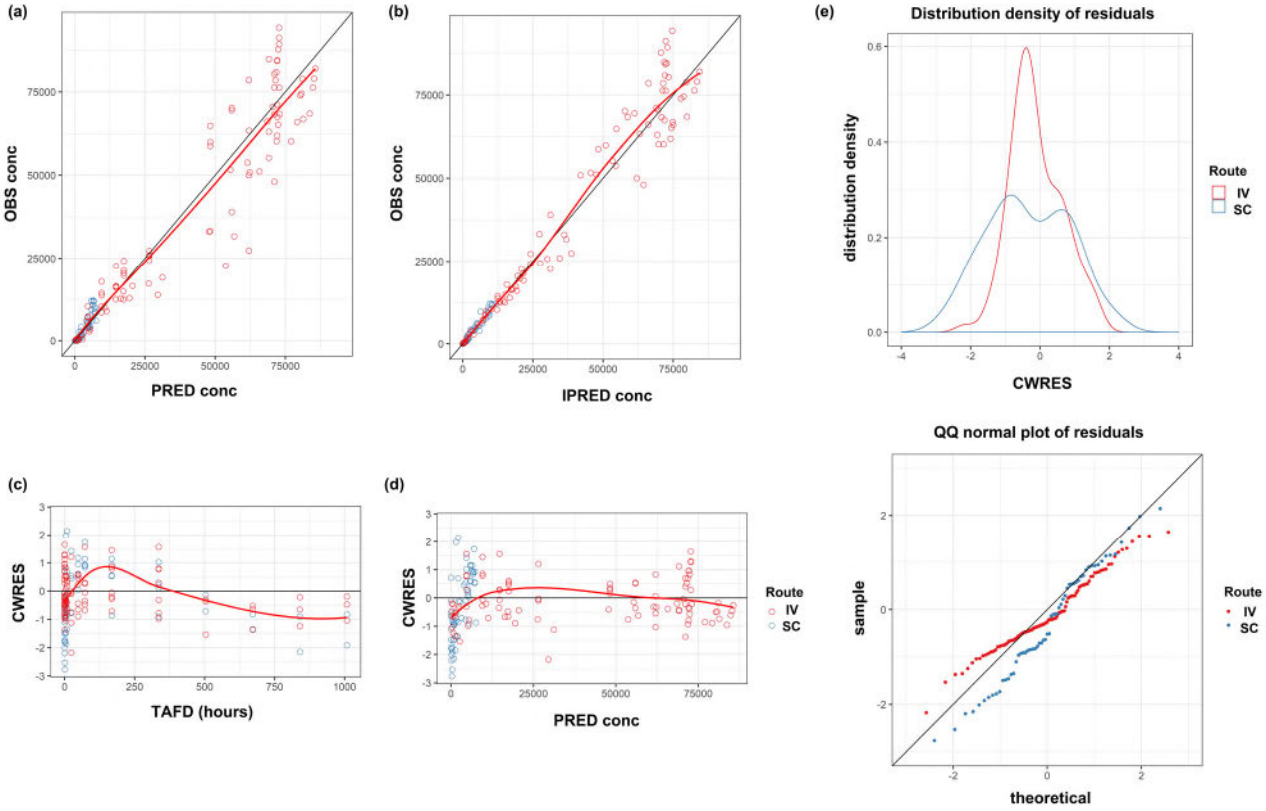


Fig. 2 Key diagnostic plots for p75ECD-Fc given by two routes (i.v., s.c.) comparing observed concentrations with individual and population predicted concentrations. In each plot, red circles represent i.v. data, blue represent s.c. data, the solid black line is a line with slope 1 or 0 and the solid red line is a Loess smoothed line. (a) Observed concentration (OBS) vs. population-predicted concentration (PRED). (b) OBS vs. individual-predicted concentration. (c) Conditional weighted residuals (CWRES) vs. time after dose (TAFD). (d) CWRES vs. population-predicted concentration. (E) The quantile–quantile (q–q) plot of that distribution. CWERS, conditional weighted residuals; IPRED, individual-predicted concentration; OBS, observed; PRED, predicted; TAFD, time after first dose.

CHAPTER 3: The Effect of Intravenous Injection of The Extracellular Domain of $p75^{NTR}$ On the Cognitive Deficits and Amyloid Plaque Load In APP/PS1 Alzheimer's Disease Transgenic Mice

Sally Kelliny: Designed and performed experiments, analyzed data, interpreted the results of the experiments, prepared figures, and drafted the manuscript.

Prof. Larisa Bobrovskaya: Co-supervised Sally and contributed to the study conception, design and reviewed and approved the final version of the manuscript.

Prof. Xin Fu Zhou: Conceived and designed experiments, contributed to the critical manuscript revision and acted as corresponding author.

1. Introduction

Alzheimer's disease (AD) is the most common cause of dementia among elderly people (more than 40 million worldwide and 400,833 in Australia). The main pathological hallmarks of the disease are the extracellular accumulation of senile amyloid plaques (consists of amyloid beta proteins) and intracellular neurofibrillary tangles (NFT) (consists of hyperphosphorylated tau protein) within certain brain regions. Along with reduced synaptic density, loss of dendritic spines and neurons, these plaques and tangles lead to widespread neurodegeneration particularly of the basal forebrain cholinergic neurons with subsequent cognitive impairment. Only 1-5% of all cases are familial due to certain gene mutations. However, majority of cases are sporadic that usually develop in old age (above 60 years) and causes remain unidentified. So far, this disease is not yet curable, thereby new and effective therapeutic strategies to treat the condition are urgently required [1,2] .

According to the amyloid cascade theory, the amyloid beta peptides are the primary cause that leads to neurodegeneration. However, all drugs that have targeted the amyloid beta peptides have failed to date. Thus, it is assumed that other pathophysiological pathways, still not sufficiently recognized, can trigger the accumulation of plaques and tangles and thus initiate the cascade of synaptic failure and cell death [3].

Evidence from recent studies has proven that lack of neurotrophin balance in the brains of aged population could play an important role in the pathogenesis of neurodegenerative diseases [4]. Zhou *et al*. has highlighted the role of neurotrophins and their pan-receptor p75 neurotrophin receptor ($p75^{NTR}$) in the pathogenesis of AD [5-7]. They illustrated that full length p75FL, a death receptor, could bind to proneurotrophins and promote the production of amyloid beta peptides (Aβ), thus initiate neurodegeneration and amyloidogenesis [8,9]. On the other hand, the extracellular domain p75ECD which is generated from p75FL cleavage by tumour

necrosis factor-α converting enzyme (TACE), can bind to and increase the clearance of amyloid beta Aβ from the AD brain and can also block the neurite collapse induced by pro-brain-derived neurotrophic factor (proBDNF) [10-12].

In this context, several studies have demonstrated that the levels of proneurotrophins and their receptor p75FL is upregulated in the brains of AD transgenic mice [7]. In contrast, the expression of mature neurotrophins is down regulated [13]. Moreover, the shedding of the extracellular domain from the full length p75 is switched off resulting in a significant decrease in the levels of p75ECD in cerebrospinal fluid (CSF) and post-mortem brains [14]. Surprisingly, studies have revealed that the injection of p75ECD-Fc (a fusion molecule of p75ECD and Fc fragment of human IgG) into the brains of AD mice improved the cognitive function of those mice [14]. Based on these findings, we propose that p75ECD is a neuroprotective molecule and thus restoration of its abnormally low levels in the brains of AD mice by injection of p75ECD-Fc could provide a novel and effective therapeutic strategy for the treatment of AD. However, brain injection of the drug is not clinically convenient. Therefore, the aim of this project is to investigate the effectiveness of peripheral injection of p75ECD-Fc in APP/PS1, a mouse model of AD. In the previous chapter, we studied the pharmacokinetics of p75ECD-Fc following peripheral administration in rats and examined its distribution in different tissues including the brain. It is expected that this work will provide results that might pave the way to clinical application of this new drug.

2. Review of Literature:

Aging is the major risk factor of sporadic Alzheimer disease (SAD). Several molecular and pathological features including oxidative stress, mitochondrial dysfunction, inflammation, insulin resistance and accumulation of plaques have been identified possible aetiology of AD in geriatric population [15]. Growing evidence indicates that neurotrophic imbalance predisposes cholinergic and synaptic deficits in aged population which in turn enhance the production of amyloid plaques and hence cognitive impairment [6]. Many studies have shown that mature neurotrophins, including brain-derived neurotrophic factor (BDNF), nerve growth factor (NGF), neurotrophin-3 (NT-3) and NT-4, mediate cell survival and proliferation and are important in synaptic plasticity together with learning and memory. Their functions are mediated by binding to p75 and tropomyosin kinase (Trk) receptors. Mature neurotrophins are synthesized as precursors from proneurotrophins which are cleaved to produce the mature form. On the other hand, proneurotrophins mediate opposite actions including apoptosis and neurodegeneration through binding to p75 and sortilin [16]. Evidence from previous studies indicates that the expression of mature neurotrophins and their cognate receptors Trk is down-regulated in the brains of SAD patients whereas proneurotrophins and their receptors p75 (at level of both protein [17] and mRNA [18]) and sortilin are upregulated [16].

p75, a transmembrane receptor for neurotrophic factors, is widely expressed in the nervous system specifically in the basal forebrain cholinergic neurons [19,20] . It was noticed that p75, increases in the brain with aging and participates in age-related conditions, thus, it has drawn vast concerns for its various roles depending on different ligands [21]. Basically, p75 is a co-receptor of sortilin for proneurotrophins (e.g. proNGF and proBDNF) mediating apoptosis [22], a co-receptor of Nogo receptor for myelin associated neurite growth inhibitors and a co-receptor of Trks for mature neurotrophins for cell survival. Dysregulation of the levels of neurotrophins or their receptor pathways contributes to age-associated vulnerability in neurons

[23,24]. Recently, Prof. Zhou's lab found that p75 plays an important role in the pathogenesis of AD [25,14,12]. Evidence has shown that p75, which is upregulated in the brain of AD patients [26], is also an important receptor of Aβ and mediates Aβ-induced neurotoxicity [27-29].

It is known that p75 transduces at least 3 different signals leading to different biological outcomes. The first signal is activated through binding with proBDNF, Aβ, and nogo receptor/ligands, p75 mediates the activation of RhoA-ROCK kinase pathway leading to neurite collapse. The second one occurs as a result of binding with proNGF and proBDNF, p75 activates c-June N-terminal Kinase (JNK) and caspases leading to apoptosis. Finally, the third one is produced through binding with mature neurotrophins p75 also mediates NF-kβ signal leading to cell survival, **Figure 1** [30,31].

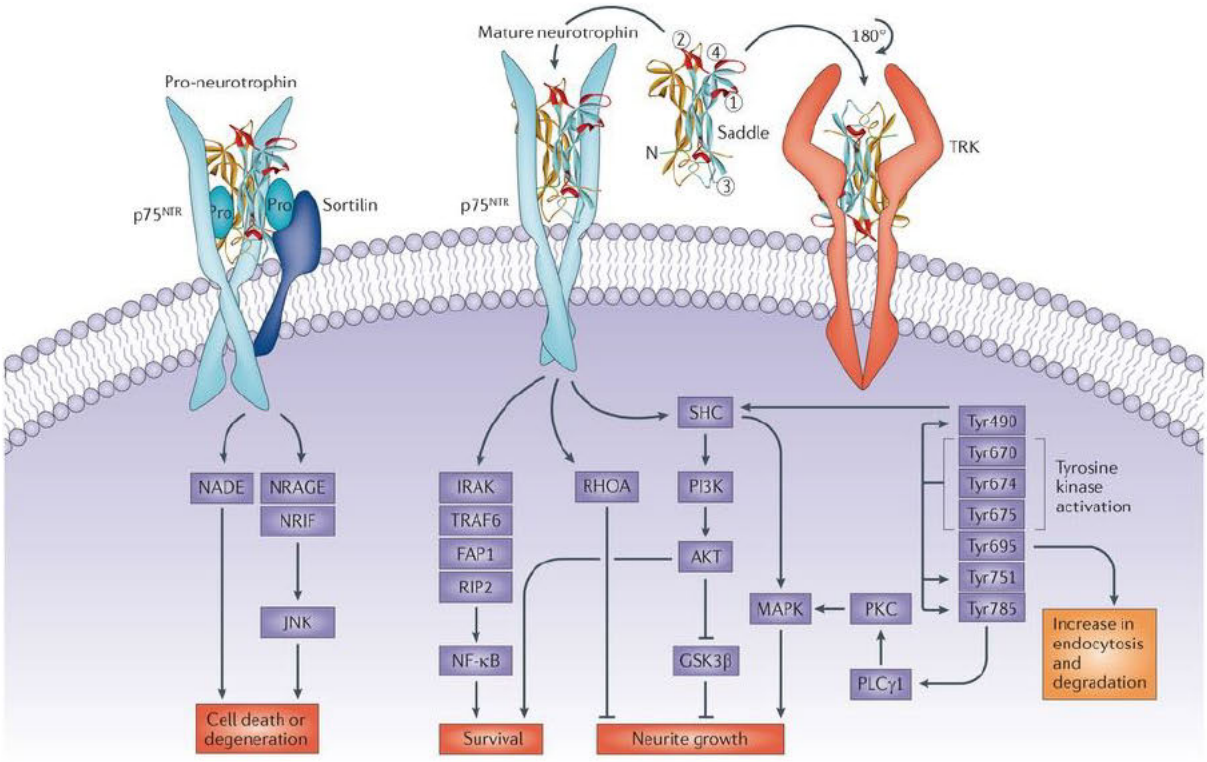


Figure 1 Neurotrophins, their receptors and signaling pathways (reproduced with permission from Longo et al. 2013.

Under physiological conditions, full length p75 receptor is cleaved first by the α-secretase tumour necrosis factor converting enzyme (TACE) to generate the diffusible extracellular domain (p75ECD) that can bind mature neurotrophins, and C-terminal fragment (CTF) transmembrane which is sequentially cleaved by ɣ-secretase to yield the intracellular domain (ICD) [32]. Previous studies showed that the extracellular domain (ECD) of p75 interacts with Aβ, and suppresses its disposition in the brain [33] . In contrast, its Full-length (p75FL) transduces neurotoxic signals, such as proNGF [7] , promotes the production of Aβ [33] and mediates Aβ-induced upregulation of the proNGF receptor sortilin [34]. Aβ induces neurotoxic signals through binding to p75 as well and mediates neurite collapse and apoptosis via activating the phosphorylation of JNK and RhoA pathways [9,35]. Thus, p75 could be considered a two-face molecule that could trigger either neuroregeneration or degeneration depending on the pathway activated, **Figure 2**.

It is speculated that the level of p75ECD decreases dramatically in AD due the neurotrophin imbalance. In this respect, studies have revealed that the activity and levels of TACE is reduced in AD by the action of Aβ. Thus, the shedding of the neuroprotective p75ECD is switched off

resulting in the increase in p75FL and reduction in p75ECD in CSF and post-mortem brains. As a result, the ratio of p75FL/p75ECD is several fold higher in AD than in healthy controls [14].

Recently, Pietri *et al.* revealed that Aβ reduces the activity and surface levels of TACE by promoting its phosphorylation and internalization via activation of 3-phosphoinositide-dependent kinase-1 (PDK-1). In addition, Aβ upregulates the expression of BACE1 which subsequently produces more toxic Aβ peptides through β-secretase cleavage of APP [36].

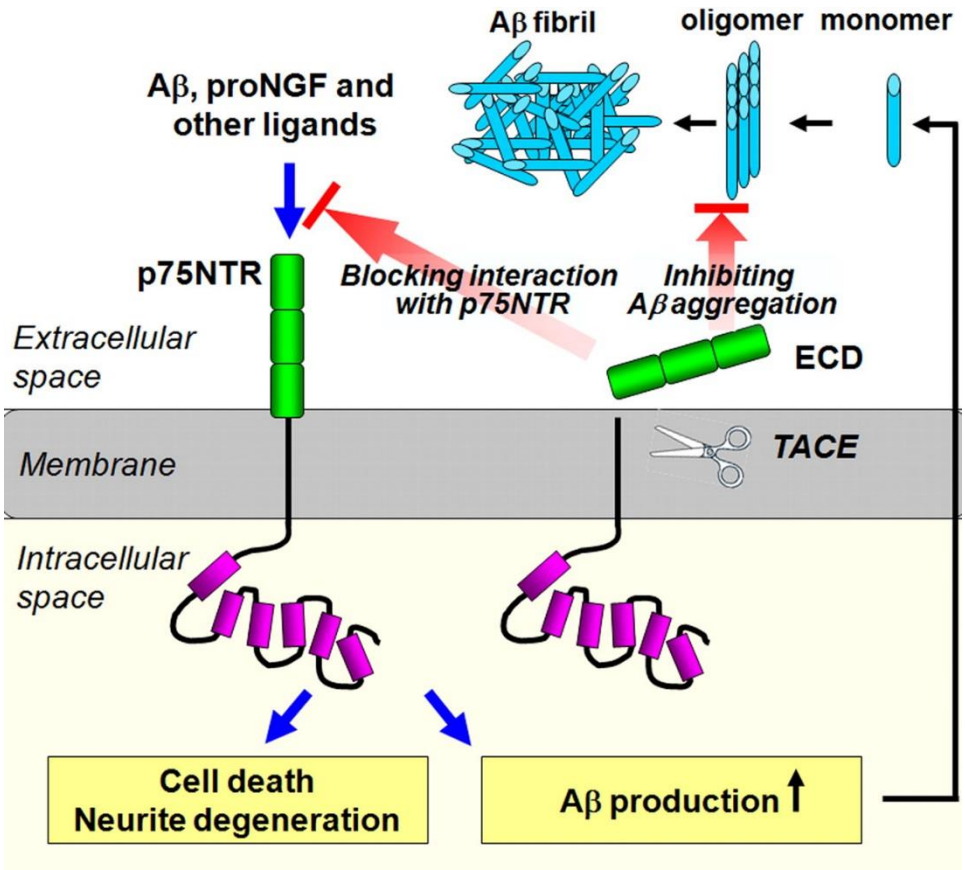


Figure 2 Illustration of functions of $p75^{NTR}$ in Aβ metabolism. $p75^{NTR}$ may have two-sided effects on Aβ metabolism. On one hand, $p75^{NTR}$ signalling may increase Aβ production and enhance steady-state levels of Aβ, which may increase AD pathology. In addition to Aβ production, $p75^{NTR}$ also mediates Aβ and proNGF-mediated neurotoxicity such as neuron death and neurite degeneration. On the other hand, the extracellular domain of $p75^{NTR}$ after shedding from the membrane may bind and sequester Aβ, and thus suppress Aβ aggregation and reduce Aβ deposition in the brain. Meanwhile, the extracellular domain of $p75^{NTR}$ may also block the interaction of $p75^{NTR}$ and its ligands (e.g., Aβ or proNGF) by competitive binding, and thus attenuate the $p75^{NTR}$ signaling that leads to the neurotoxicity. ECD denotes extracellular domain of $p75^{NTR}$ (reproduced with permission from Wang et al. 2011.

These data suggest that Aβ sustains its own production and toxicity by inhibiting TACE-mediated α-secretase cleavage of APP and promoting the opposing β-secretase cleavage that produces toxic $Aβ_{40,42}$ [37,38]. Furthermore, inhibiting TACE shedding activity of p75ECD from the p75FL will subsequently reduce the levels of p75ECD and accumulate p75FL in AD that in turn exacerbates neurotrophin imbalance [14]. Moreover, Urra *et al.* has shown that p75ECD shedding is regulated by activation of TrkA by NGF [32]. In this respect, studies have revealed that Aβ can induce the phosphorylation of TrkA and promote its interaction with p75, BACE1 and presenilin1 (PS1) thus switching the signals of TrkA from cell survival mediated by NGF to apoptotic signals of p75 [39,40].

Hence, according to the neurotrophin hypothesis for AD, therapies aimed at correcting the homeostatic imbalance between ligands and receptors of the neurotrophic pathway appear to have strong rationale, as truly disease-modifying approach [4]. The restoration of p75ECD levels in brains of AD can break that vicious cycle induced by Aβ and protect the brain from neurodegeneration, which may offer a new approach for AD.

Studies revealed that injection of p75ECD-Fc into the brain of AD transgenic mice alleviated AD pathologies as evident by reduced Aβ plaques, hyperphosphorylated tau, neuroinflammation, synaptic dysfunction and cell death in the brain and improved performance

of animals in Morris Water Maze [41]. Therefore, it is speculated that p75ECD can suppress amyloidogenesis by scavenging Aβ and inhibiting its aggregation and disposition. Besides, it can protect neurons from Aβ-induced neurotoxicity and suppress BACE1 expression and activity and tau phosphorylation [14]. Subsequently, p75ECD can inhibit the toxic signals of proneurotrophins and their receptors [33].

In the light of the previous findings and data, it is hypothesized that p75ECD is a neuroprotective molecule against the toxic signals of Aβ and proneurotrophins. Thus, restorations of the abnormally low levels of p75ECD in AD could retain the neurotrophin balance and rescue neurons against degeneration.

To test this hypothesis, the recombinant form p75ECD-Fc was injected intravenously (IV) in an animal model of AD and its pharmacological action was evaluated by assessing Aβ burden and tau pathology in the brain and by performing behavioral tests. This is explained in detail in the following sections.

3. Materials and methods

3.1. Materials

p75ECD-Fc was obtained from Tiantai Medical Technology, Fuzhou, China and stored at -80°C. Primary antibodies used in this study for western blotting and immunohistochemistry (IHC) are listed in **Table 1**. Biotinylated IgG conjugated secondary antibodies for IHC were purchased from Jackson ImmunoResearch Laboratories, USA and Thermo Fisher Scientific, Australia. Donkey anti-rabbit IRDye® 680RD, Donkey anti-goat IRDye® 800CW and Goat anti-mouse IRDye® 800CW conjugated secondary antibodies for western blotting were purchased from LI-COR Millennium Science, Victoria, Australia. VECTASTAIN ABC kit for IHC was purchased from Vector laboratories, USA. Fluorometric Tunnel staining kit was obtained from Promega, Australia. Enhanced Golgi-cox stain kit was obtained from Bioenno Tech, LLC (Westminster Ave, CA, USA). Pierce™ BCA Protein Assay Kit was obtained from Thermo Fisher Scientific, Australia. Protease and phosphatase cocktail inhibitors tablets were purchased from Roche Diagnostics GmbH, Mannheim, Germany. Congo red stain and other chemicals were obtained from Sigma Aldrich, Australia.

3.2. Animals

The double transgenic mice APP/PS1 expressing a chimeric mouse/human amyloid precursor protein (Swedish mutation; APP695swe) and a mutant human presenilin 1 (PS1-dE9) [42], and wild type (WT) mouse (C57BL/6 mice) were obtained from Jackson Laboratory (New Harbor, 124 ME, USA) and bred in the Core Animal Facility, University of South Australia. Mice were housed in groups of 4-5 animals per cage at controlled room temperature with a 12h light/dark cycle and food and water provided ad libitum. All procedures were approved by the Animal ethics committee of the University of South Australia (approval number: U13-18) and done in accordance with the South Australian Animal Welfare Act and Regulations 1985.

3.3. Treatment protocol

A total of 20 APP/PS1 mice (10 males and 10 females) aged 9 months old were divided into two groups; control group that received saline (n = 9, 5 males, 4 females) and treated group that received p75ECD-Fc (n = 11, 5 males, 6 females). The drug was administered intravenously through the tail vein at a single dose of 10 mg/kg once monthly for a duration of 6 months. Age matched WT littermates (n = 14, 10 females and 4 males) did not receive any treatment and were used as controls for behavioral tests. Behavioral tests were performed at the end of the treatment period followed by animal sacrifice through inhalation of CO_2 overdose. Animals were transcardially perfused with ice cold saline, then brains were immediately harvested. Left brain hemisphere was fixed with 4% paraformaldehyde in phosphate buffer saline (PBS, pH 7.4) at 4°C for 24h and then in 30% sucrose in PBS for 24h prior to cryosectioning. The other half was snap frozen in liquid nitrogen and stored at -80 °C for further biochemical analysis. Two hemibrains from each group; saline and p75ECD-Fc treated, were carefully separated for further analysis of dendritic spines using Golgi-Cox method of staining.

3.4. Behavioral Tests

3.4.1. Morris Water Maze

Morris water maze test (MWM) was used to assess the effect of p75ECD-Fc on spatial reference and long term memory [43]. The test was conducted in a circular black pool surrounded with visual cues attached to the walls and filled with water (22°C ±1) that is made opaque using white powder paint. The testing arena is divided into 4 quadrant zones using Any maze software (Stoelting Co., USA). A circular white platform is placed in the middle of one the quadrant zones. The test was conducted over 6 consecutive days. In the 1st day, each animal is initially habituated then exposed to 4

visible platform trials (30 min interval) in which the platform is placed above the water surface (1-1.5 cm) and the animal learns to escape from water and find the platform within 60 sec. In each trial, the animal is placed at different starting location facing the walls. If the animal failed to find the platform, it was guided gently and allowed to sit on it for 30 seconds, then dried well and returned to the home cage. After that, the platform was submerged underneath the water surface (1.5 cm), and each animal is exposed to 4 hidden trials per day for 4 consecutive days. Again, each animal was given 60 seconds to find the hidden platform. Time to find the hidden platform (escape latency) is calculated for each trial. At the last day (6^{th} day), the platform is removed, and each animal is exposed to a single probe trial for 60 seconds. Time spent in the platform quadrant zone and number of platform site crossing were recorded using ANY-maze video tracking system v4.5 (Stoelting Co., USA) as well as average speed and total distance travelled.

3.4.2. Open field test

This test was used to assess the effect of p75ECD-Fc on anxiety and exploratory behavior of APP/PS1 mice as described previously [14]. The test was performed in a PVC square arena (50x50x40 cm), that is divided theoretically into two zones: inner (central) and outer using the Any maze tracking software. The animal is placed in the outer zone facing the wall and the activity is recorded for 5 min. Time spent in the central (anxious) zone, percentage of time immobile and number of rearing episodes are calculated indicating anxiety and exploratory behavior. Average speed and total distance travelled are also calculated to assess locomotion behavior.

3.4.3. Novel Object Recognition test (NORT)

This test was performed to assess the effect of p75ECD-Fc on recognition memory of APP/PS1 mice as described previously [44]. The test was done in the open field box. Following habituation, each animal is allowed to explore two identical objects placed symmetrically from the centre for 5 minutes. 2-3 hours later, one of the familiar objects is removed and replaced by a different (novel) one. Then, each animal is allowed to explore the two different objects (familiar and novel) for 5 min (test phase), and time spent to explore each object is recorded. Recognition index is the novel object exploration time divided by to the total time spent to explore both objects and multiplied by 100%.

3.4.4. Y maze novel arm and Y maze spontaneous alternation tests

Y maze task was used to assess the short term working memory and tendency to explore new environment [44]. The test was conducted in a Y-shaped arena consisted of three opaque Plexiglas arms at 120° angle to each other. In the Y maze novel arm test, one arm is blocked, and the animal is allowed to explore the other open two arms freely for 5 min. Two hours later, the arm is opened, and the animal is allowed to explore the maze freely for 5min (test phase). Time spent and percentage of novel arm entries are recorded. Y maze spontaneous alternation task was performed few days later in the same maze, but the arms were rotated 45°. In this test, each animal explores the Y maze freely for 5 minutes. Readiness to enter less recently visited arms and to alternate between arms is assessed by measuring the percentage of spontaneous alternation and total number of arm visits. Animals displaying less than a total of 7 arm entries are excluded from analysis.

3.5. Immunohistochemical (IHC) and TUNEL staining

Fixed brain hemispheres of control and treated APP/PS1 mice were coronally cut at 35µm thickness using Leica cryostat (CM3050S, Germany) and kept in antifreeze solution (0.1M PBS containing 30% glycerol and 30% ethylene glycol) at -20°C until further use. Immunohistochemistry of free-floating sections was done as previously described [14]. Sections were treated with 1% SDS in PBS for 5 min for antigen retravel then incubated with 3% H_2O_2 for 15 min to inhibit endogenous peroxidases. For total Aβ detection, antigen retrieval was done using 70% Formic acid for 30 minutes at RT. Sections were then washed and blocked with 20% normal horse serum (NHS) in PBS for 2hr at RT. Sections were then incubated with 1ry antibodies overnight at 4°C. After washing, sections were incubated with biotinylated secondary antibodies at RT followed by avidin/biotinylated horseradish peroxidase (ABC kit) and then developed with diaminobenzidine (DAB). Finally, sections were mounted on gelatin-coated slides and dehydrated with serial ethanol concentrations then cleared with xylene and finally cover slipped with Depex mounting media (Sigma Aldrich). Slides were scanned using NanoZoomer S60 Automated Digital slide scanner (HAMAMATSU, Australia) and further image analysis was performed using Image J software (NIH, Bethesda, MD, USA). Primary antibodies used in this study are listed in **Table 1** Supplementary material.

TUNEL (terminal deoxynucleotidyl transferase mediated dUTP nick end labeling) staining for detection of neuronal apoptosis was done according to the kit protocol provided. Sections were incubated with Terminal Deoxynucleotidyl Transferase/Nucleotide mixture for 1 hour at 37°C in a humidified dark chamber. Localized green-fluorescent apoptotic tissue was visualized using Olympus (CX40) fluorescence microscope and quantified with Image J software.

3.6. Congo Red stain

Congo Red stain was done to detect compact Aβ plaques as described previously [14]. Briefly, sections were mounted and treated with working sodium chloride solution (3% NaCl, 80%

Ethanol and 0.01% NaOH) for 20 min at RT, followed directly by working Congo Red solution (0.2% in working sodium chloride solution) for 1 hour at RT. Sections were then rinsed with distilled water and rapidly dehydrated in absolute ethanol and xylene and then cover slipped with Depex mounting media. Slides were scanned with NanoZoomer and analyzed with Image J software.

3.7. Golgi-cox Stain

Following transcardial perfusion of animals with saline, hemibrains (n = 2/group) were freshly collected from control and treated mice and immediately incubated in the impregnation buffer A (potassium dichromate and mercuric chloride solution) at RT in the dark for 11 days. After several washes with distilled water, samples were placed in post impregnation buffer B at RT in the dark for 2 days. Samples were then stored in 30% sucrose overnight and sectioned at a thickness of 100-150 µm using a Leica cryostat. Sections were washed and mounted on gelatin-coated slides and allowed to dry. Sections were then stained with ammonium hydroxide solution, then dehydrated with absolute ethanol and xylene and cover slipped with Depex as stated in the kit protocol. Imaging was done using Olympus BX53 microscope (cellSens imaging software and Olympus XC50 camera). ImageJ software was used to analyze the length and spine density of the apical dendrites of the pyramidal neurons in the CA1 region of the hippocampus as described previously [45].

3.8. Western Blotting

For protein extraction, frozen hemibrains were homogenized in liquid nitrogen and sonicated with RIPA lysis buffer (50mM Tris-HCl, 2mM EDTA, 150mM NaCl, 0.1% SDS, 1% Sodium deoxycholate and 1% Nonidet-40, pH 7.4) containing protease and phosphatase cocktail inhibitors on ice in a ratio of 10 mg tissue: 100µL buffer. Samples were centrifuged at 15,000 rpm for 30 min. and the supernatant was collected and kept at -80°C. Total protein

concentration was measured using BCA (Bicinchoninic Acid) total protein assay kit. Samples were diluted in sample buffer (50mM Tris-HCl, 40% glycerol, 2% SDS, 0.15mM DTT, 0.02% bromophenol blue, pH 6.8) and denatured by boiling at 95°C for 5 min. Samples were then separated with SDS-PAGE (10-15% Acrylamide gels) and transferred onto 0.2 or 0.4μm nitrocellulose membrane (GE Healthcare, Life science, Germany). Membranes were blocked with 5% milk in Tris-HCl buffer with 0.5% Tween 20 for 1 hour at RT. Membranes were probed with primary antibodies overnight at 4°C and then developed with IRDye conjugated secondary antibodies. Membranes were scanned with Odyssey® CLx Infrared fluorescent scanner and analyzed using Image Studio Lite software (Li-COR Bioscience). Primary antibodies used in western blotting are listed in **Table 1**.

3.9. Analysis of antibodies against p75ECD using ELISA.

To determine whether mice injected with p75ECD-Fc generate antibodies against the human recombinant protein, we measured the levels of antibodies against the protein in serum. Briefly, Nunc 96-well ELISA plates were coated with pure p75ECD-Fc protein (2 μg/mL) in coating buffer (50 mM sodium bicarbonate/50 mM bicarbonate, pH 9.6) overnight at 4°C. The plates were blocked by 3% bovine serum albumin (BSA) in phosphate-buffered saline (PBS) at 37°C for 1 h. Serum samples were diluted in 1% BSA/PBS/Tween-20 (1:1000) and were incubated in duplicates for 1 h at 37°C. Biotinylated donkey anti-mouse IgG (1:1000, Thermo Scientific, USA) was used as the detection antibody. After incubation with Streptavidin HRP, samples were developed with tetramethyl benzidine (TMB, Sigma) for 10 min in the dark and the reaction was stopped by 0.1N Hydrochloric acid. The optical density was measured using a PerkinElmer Victor-x4 Plate Reader (Waltham, MA) set to 450 nm (0.1s).

3.10. Statistical analysis

Results are represented as mean ± SEM. One-way or two-way analysis of variance (ANOVA) followed by Tukey's Multiple Comparison Test or Fisher LSD post-hoc tests were used to analyze data of behavioral test between all groups. Unpaired two-tailed t test was used to compare means of two groups (control and treated APP/PS1 mice). Analysis was carried out using GraphPad Prism v8.4 (GraphPad Software). P value < 0.05 was considered statistically significant for all comparisons.

4. Results

4.1. Effect of p75ECD-Fc on the cognitive deficits in APP/PS1 AD mice

4.1.1. MWM Results indicated that p75ECD-Fc improved the learning acquisition of APP/PS1 mice as evident by reduced average escape latency compared to control untreated mice (Interaction: $F_{6, 36} = 0.5184$, $p = 0.7904$, Time factor: $F_{3, 36} = 2.340$, $p = 0.0897$, Treatment factor: $F_{2, 36} = 23.50$, $p < 0.0001$). In the probe trial, control mice spent the least time in the target quadrant zone (where the platform was placed during the hidden trials) compared to WT mice ($p = 0.022$) and p75ECD-Fc treated mice ($p = 0.049$), ($F_{2, 30} = 4.439$, $p = 0.0205$). Moreover, control APP/PS1 mice showed the least number of platform site crossing during the probe trial ($F_{2, 30} = 7.196$, $p = 0.002$ vs WT mice), while p75ECD-Fc significantly increased it compared to untreated group ($p = 0.0478$).

This indicates that p75ECD-Fc improved the learning and spatial reference memory in AD mice (**Figure 3**).

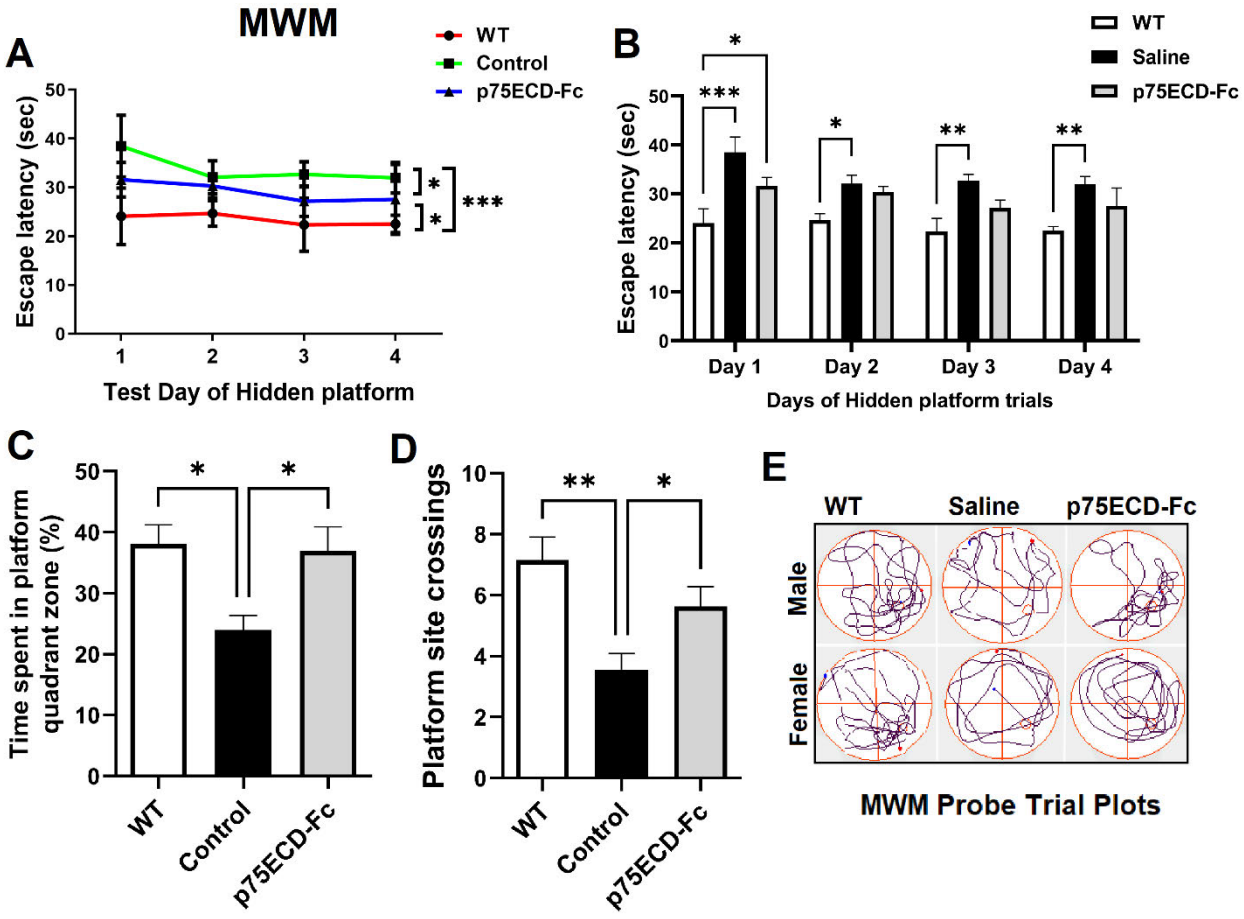


Figure 3 Acquisition and learning in the Morris water maze. The test was performed over 6 consecutive days, the 1st day is the visible platform training, 4 days of hidden platform testing, and a probe trial 24 h after the last hidden platform test. (**A, B**) Average escape latency over the hidden platform trials, two-way ANOVA, Tukey's test. (**C, D, E**) The probe trial showing (**C**) time that mice spent in the target quadrant zone, where the platform was previously hidden, (**D**) the number of platform site crossing and (**E**) the track plots. All data are presented as mean ± SEM. * $p < 0.05$, One-way ANOVA followed by Tukey's multiple comparison), n = 8-14/group.

4.1.2. Open field test. In the open field test, each animal was placed in the periphery of an open field arena and the activity was recorded for 5 min. WT mice showed the least immobility % (time spent immobile) compared to AD mice indicating less anxious behavior ($p = 0.0013$). p75ECD-Fc reduced immobility time % in treated mice compared to control AD mice ($p = 0.0463$). Data also showed that no difference was found between all groups in the time spent in central zone (anxious zone), although WT mice and p75ECD-Fc treated mice spent longer time in the central zone than untreated AD mice. For locomotion and exploration behavior, WT mice showed longer distance travelled ($p = 0.0251$) and higher average speed than AD mice ($p = 0.0003$). They also crossed the line between zones more frequently ($p = 0.0049$) and showed higher rearing activity ($p = 0.0133$). However, there was no difference between control and treated AD mice in exploration behavior. p7ECD-Fc treated AD mice showed high grooming activity similar to WT mice and higher than untreated AD mice, but overall difference was not significant (**Figure 4**).

4.1.3. Y maze and NORT. To investigate the effect of p75ECD-Fc on working memory and tendency of the animal to explore novel environment, Y maze and novel object recognition tasks were performed.

In novel object recognition test, WT and p75ECD-Fc treated APP/PS1 mice showed more tendency to explore the novel object over the familiar one in the test phase as described by the discrimination index (DI) which was found to be 15.39 ±7.178 for WT and 8.86 ±20.37 for p75ECD-Fc APP/PS1 treated. On the other hand, APP/PS1 control mice seemed to interact more with the familiar object over the novel one during the test

phase with DI of -1.548 ±19.03. However, the overall difference was not significant between all groups (**Figure 5A** and **B**).

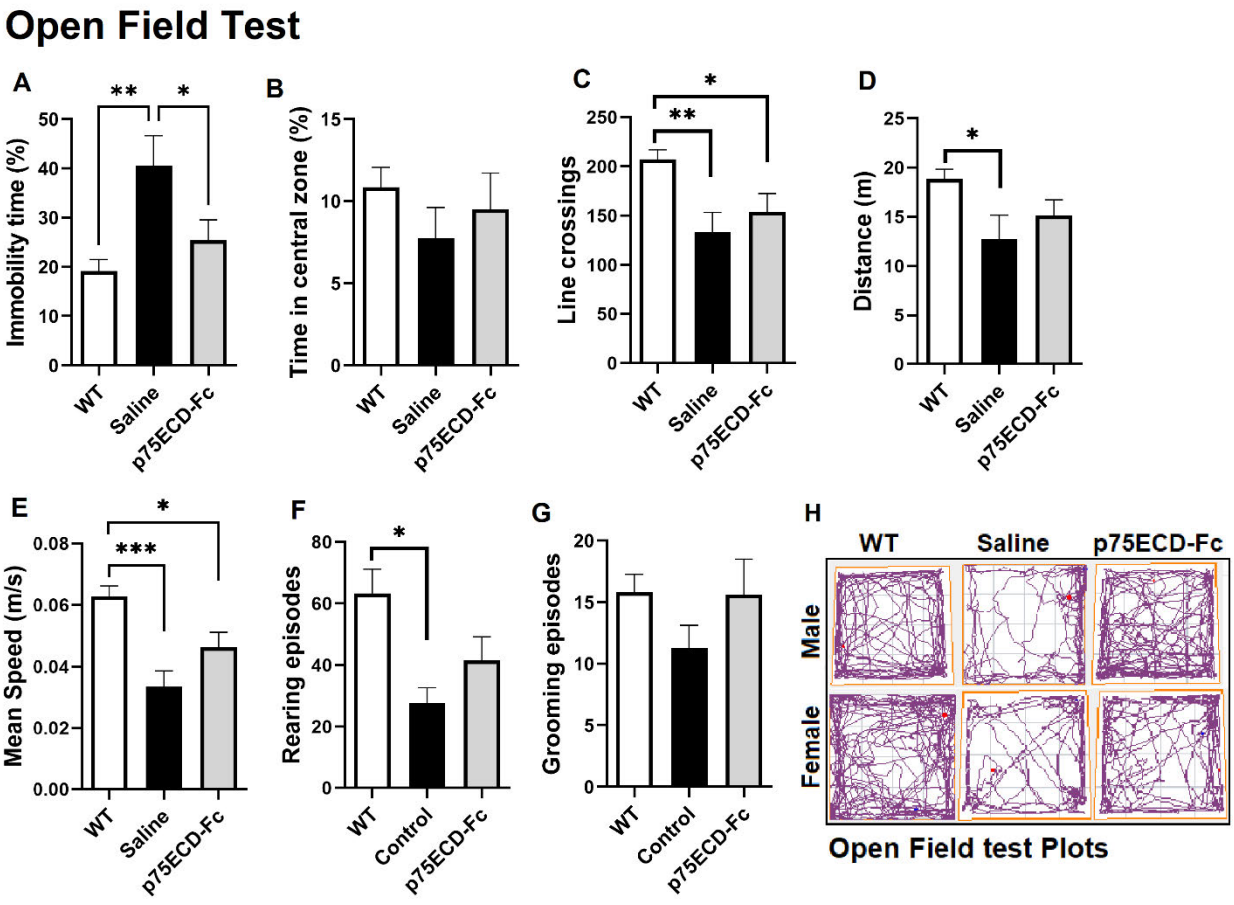


Figure 4 Open Field Test: (A) Time percentage spent immobile, (**B**) Time % spent in the central (anxious) zone, (**C**) Total number of lines crossing or transition between outer and inner zones, (**D**) Total distance travelled in meters (m) over 5 min testing period, (**E**) Average speed in m/s, (**F**) Number of rearing episodes, (**G**) Number of grooming episodes and (**H**) Track plots showing the mouse activity during the test. Data are presented as mean ± SEM. * $p < 0.05$, One-way ANOVA, Tukey's test, n = 8-14/group.

In the Y maze novel arm test, no difference was found between groups in number of visits or time spent in the novel arm (**Figure 5C** and **D**). In addition, all groups alternated with the same percentage in the spontaneous alternation test and showed comparable number of total arm entries (**Figure 5E** and **F**). This indicates no difference in working memory between WT mice and AD mice.

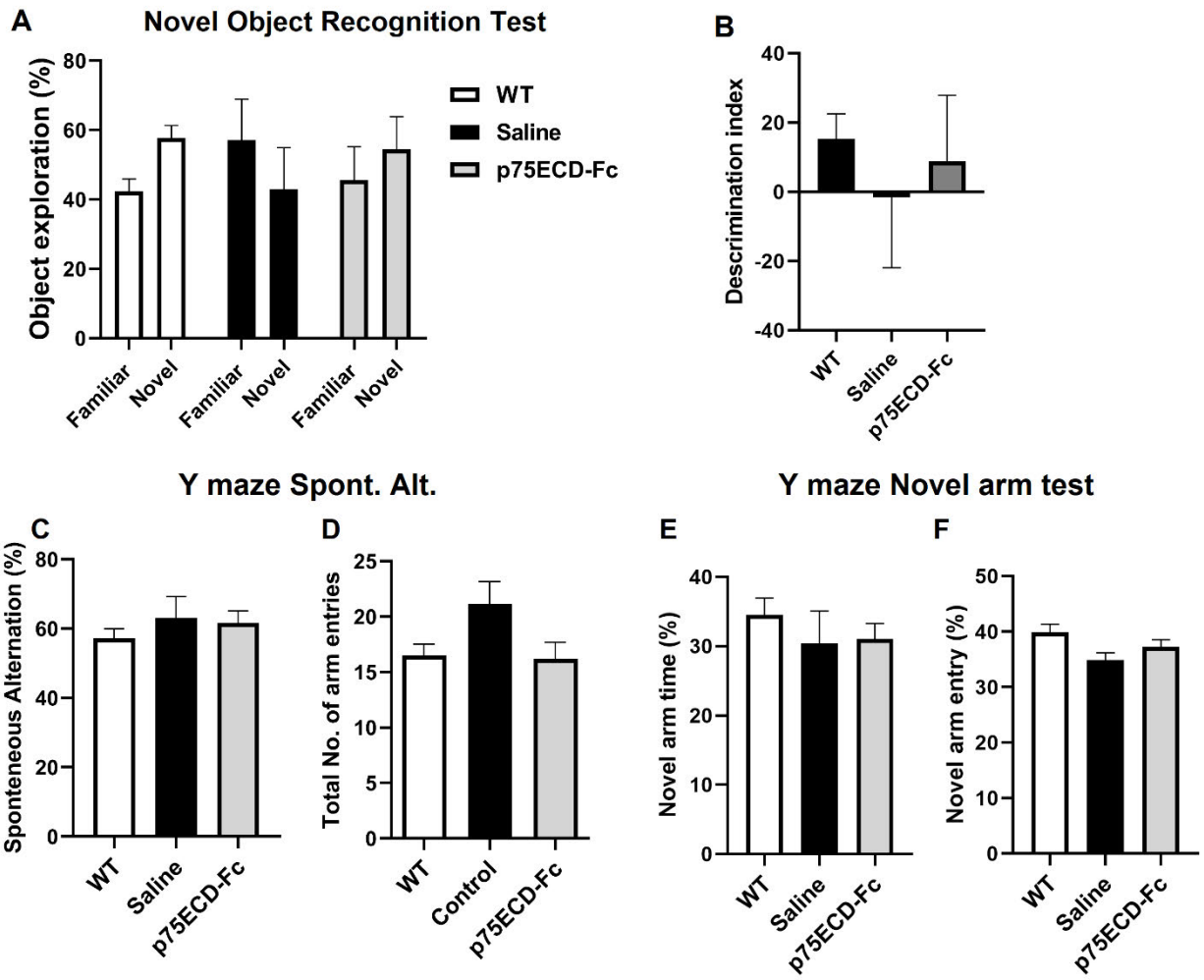


Figure 5 Novel Object Recognition and Y maze tasks: (**A**) Object exploration % showing the time spent to explore both familiar and novel objects during the test phase (two-way ANOVA, Tukey's test), (**B**) Overall discrimination index showing the animal preference to explore the novel object over the familiar one. (**C-D**) Y maze spontaneous alternation test showing the % of alternation and total arm entries. (**E-F**) Y maze novel arm test showing the number of entries (%) to the total number of arm entries and time spent in the novel arm during the test phase. Data are presented as mean ± SEM. * $p < 0.05$, One-way ANOVA,

4.2. Effect of p75ECD-Fc on Amyloid beta plaque load in APP/PS1 mice

To investigate the effect of p75ECD-Fc on the Aβ plaque load, and whether this effect could be correlated to the improved cognitive behavior observed in MWM, brain sections were stained with Congo Red stain for amyloid plaques and with MOAB-2 antibody to detects total plaque load. Results showed that p7ECD-Fc treatment significantly reduced plaque area fraction ($p < 0.0001$).

Immunohistochemistry using MOAB-2, a pan antibody that can detect several amyloid beta conformations including unaggregated, oligomeric and fibrillar, showed significant reduction in area fraction % of total Aβ in the hippocampus ($p = 0.0264$) and cortex ($p = 0.0355$) in p75ECD-Fc treated AD mice (**Figure 6A-D**).

In order to further investigate the effect of p75ECD-Fc treatment on the amyloidogenic processing of amyloid precursor protein (APP), western blot of full-length APP (APPfl), its phosphorylated form at Threonine 668 (T668) and its the cleavage fragments; APP C-terminal fragments (CTF-α and -β) and the N-terminus APP fragment (sAPPβ and sAPPα), was carried out. In addition, soluble Aβ peptides were detected using 4G8 antibody. Results showed that p75ECD-Fc significantly reduced the expression levels of CTFs ($p = 0.0353$) and Aβ levels ($p = 0.0448$), while the levels of sAPP and the phosphorylated forms did not change (**Figure 6E-F**).

To determine the mechanism by which p75ECD-Fc inhibited APP processing, we examined the expression of BACE1 and its phosphorylated form at Serine 498. BACE1 is a β-secretase enzyme that is found to be activated in AD and mediates the amyloidogenic cleavage of APP [46]. BACE1 can be activated through its phosphorylation in Threonine 252 through some kinases such as Cdk in the lumen of endosomes in which the β-secretase cleavage of APP usually occurs [47]. On the other hand, BACE1 phosphorylation at Serine 498 in its cytoplasmic domain regulates the retrieval of BACE from endocytosed vesicles and relocates the enzyme to juxtanuclear Golgi compartments. Sun et al. found that the levels of S498 pBACE1 is significantly reduced in AD patients. Absence of pS498 phosphorylation retains the enzyme in the endosomes and thus enhances the convergence of APP and BACE1 and thereby the β-secretase cleavage of APP [48,49]. Interestingly, we found that total protein levels of BACE1 did not differ between control and treated mice, while p75ECD-Fc

significantly increased the expression levels of pBACE1 S498 (**Figure 6G-H)**. These results suggest that p75ECD-Fc could reduce the amyloid beta plaque pathology in the brain of AD mouse.

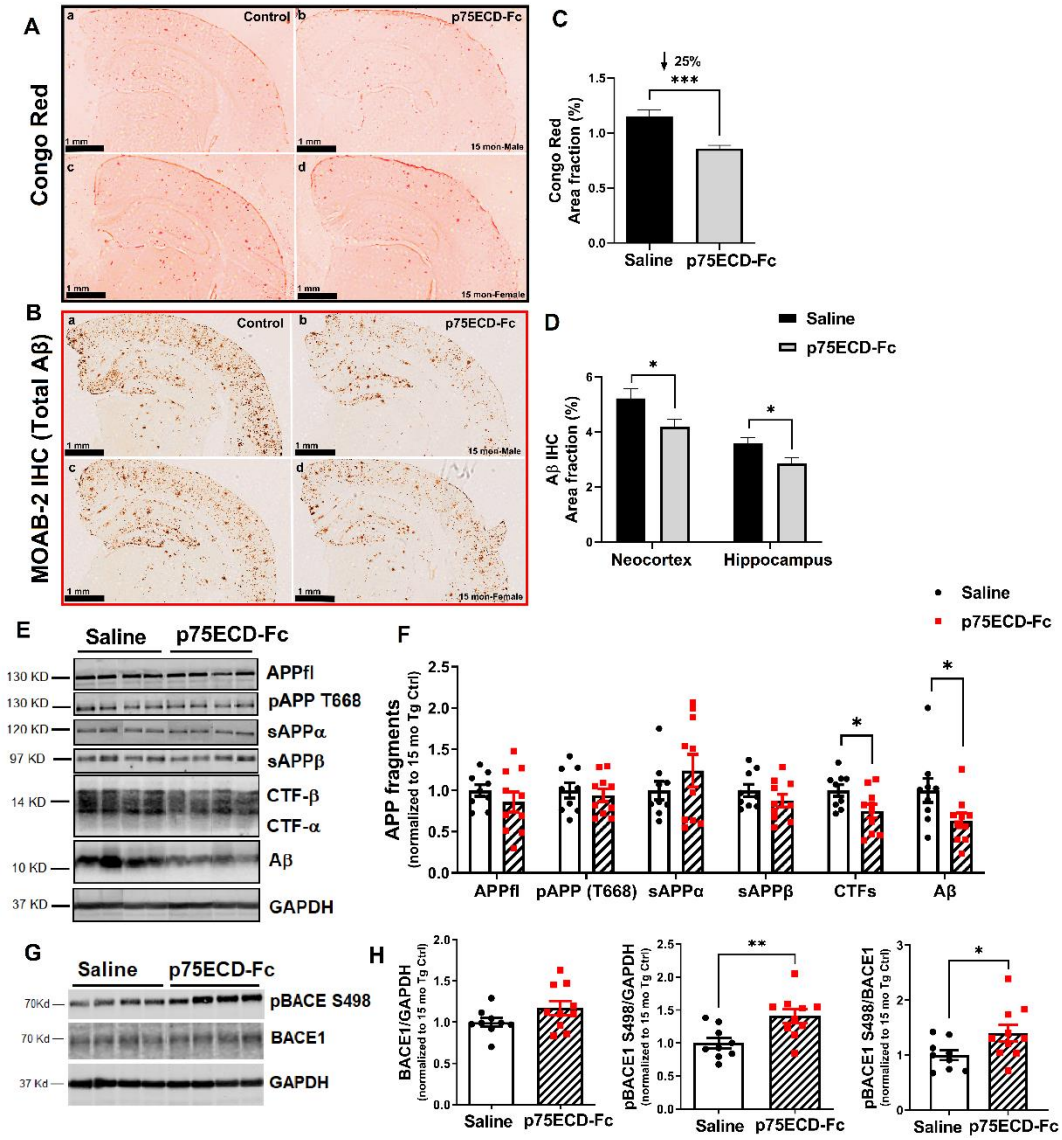


Figure 6 Effect of p75ECD-Fc treatment on the amyloid plaque pathology in APP/PS1 mice. **(A-B)** Representative images of brain sections of saline and p75ECD-Fc-treated AD mice showing Congo Red stain and MOAB-2 Aβ immunostaining. Scale bar = 1mm. (**C-D**) p75ECD-Fc significantly reduced the area fraction % of congophilic plaques and the total plaque load in the cortex and hippocampus of the transgenic mice brains (n = 7-8; 1-2 sections were analysed for each animal). (**E-F**) Representative blots and quantification show the expression levels of APP fragments including the levels of sAPPα, pAPP (T668), sAPPβ, CTFs and Aβ. Expression levels are normalized to total full-length protein (APPfl). (**G-H**) Representative blots and quantification showing the expression levels of BACE1 and its phosphorylated form at S498. GAPDH was used as a loading reference, n = 9-10/group. * $p < 0.05$ (Student t test, unpaired, two-tailed with Welch's correction). Results are presented as means ± SEM.

4.3. Effect of p75ECD-Fc on neuroinflammation in APP/PS1 mice

Neuroinflammation is a main hallmark of AD [50] and is considered a consequence to the amyloid plaque accumulation in the brain [51]. To investigate the effect of p75ECD-Fc treatment on neuroinflammation, levels of glial fibrillary acidic protein GFAP, a marker of astrocytosis, levels of CD45; a leukocyte common antigen and Iba-1; both detect activated microglia were studied using IHC and WB. Immunohistochemistry against GFAP did not show any difference between controls and treated APP/PS1 mice. However, CD45 expression was reduced significantly in the hippocampus ($p = 0.0206$) and neocortex ($p = 0.0492$) in treated mice compared to their control APP/PS1 mice (**Figure 7A-D**).

Further analysis using western blotting of the whole brain homogenate revealed that p75ECD-Fc did not reduce the expression levels of either GFAP, or Iba-1 compared to saline treated mice (**Figure 7E-G**).

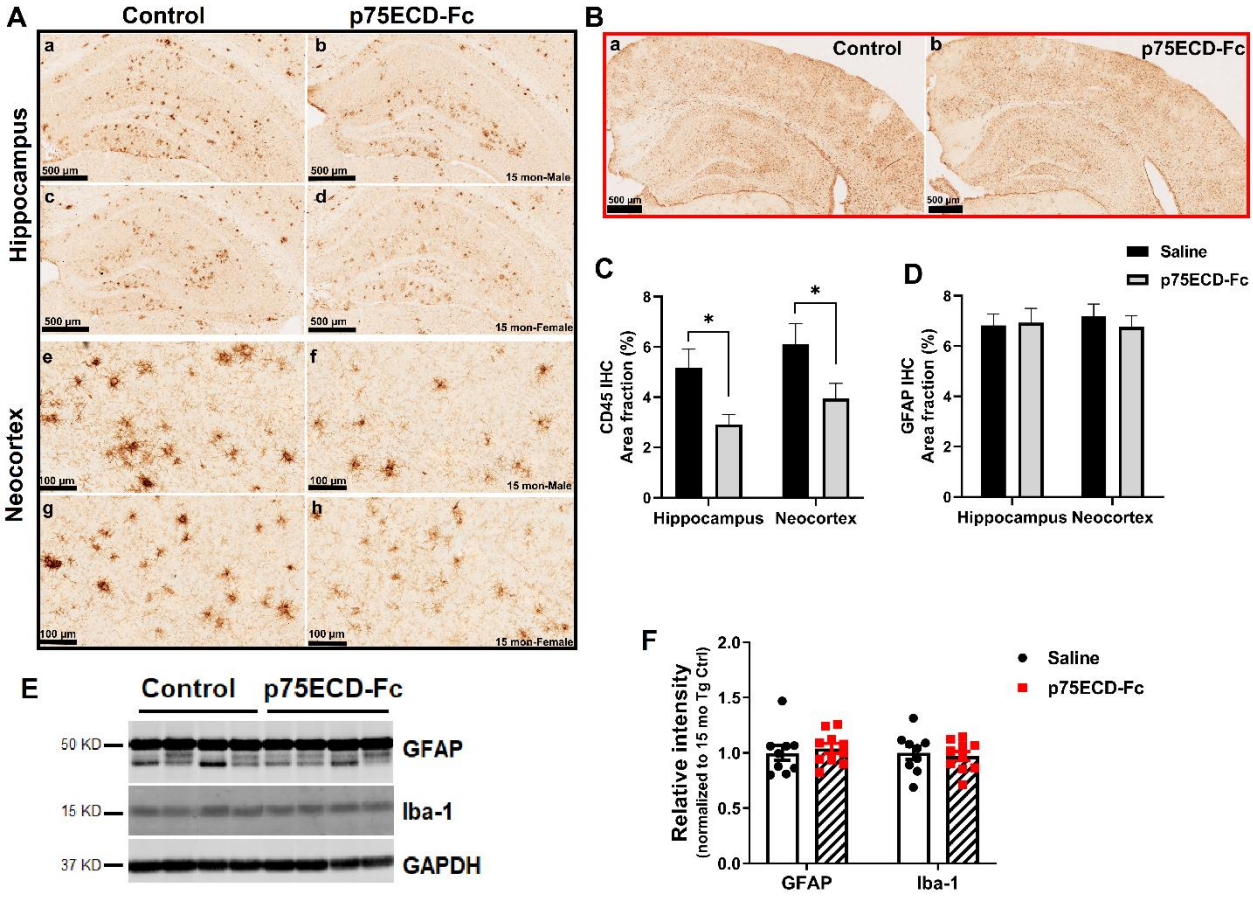


Figure 7 Effect of p75ECD-Fc treatment on neuroinflammation in APP/PS1 mice. **(A-D)** Immunostaining and quantification of inflammation markers in the hippocampus and neocortex of saline and p75ECD-Fc-treated mice: (**A**, **C**) CD45 for microgliosis (Scale bar = 500 µm for the upper panel, 100 µm for the lower panel) and (**B**, **D**) GFAP for astrocytosis (Scale bar = 500 µm), n = 8-10/group (1 section/animal), (**E**) Whole brain homogenates of AD mice were analyzed by western blots and probed with antibodies against GFAP and Iba-1. (**F**) Quantitative analysis of Iba-1 and GFAP protein expression normalized to GAPDH, n = 9-10/group. *p < 0.05 (Student t test, unpaired, two-tailed with Welch's correction). Results are presented as means ± SEM.

4.4. Effect of p75ECD-Fc treatment on the levels of synaptic proteins and synaptic plasticity in APP/PS1 mice

Synaptic loss is an early event and main feature in the pathogenesis of AD [52]. To investigate the effect of p75ECD-Fc on synaptic function, levels of postsynaptic density-95 (PSD-95) protein, a pre-synaptic protein synaptophysin as well as VAMP-2, a vesicle-associated membrane protein, were measured in the whole brain homogenate of AD mice using western blotting. In addition, we performed Golgi-cox stain to study the morphological changes of the dendrites of CA1 pyramidal neurons of the hippocampus of AD mice following p75ECD-Fc treatment. Results showed that p75ECD-Fc significantly increased synaptophysin levels (0.0033) while the levels of PSD-95 and VAMP-2 did not differ between control and treated mice (**Figure 8C-D)**. Second-order apical dendrites of the CA1 pyramidal neurons were analyzed using ImageJ software. Dendritic spine density represented as number of spines per μm of dendrite length as well as average spine length were assessed. Quantitative analysis showed a significant increase in the spine density ($p<0.0001$) and spine length ($p = 0.0369$) for p75ECD-Fc treated APP/PS1 compared to their controls. These data suggest that p75ECD-Fc could improve the synaptic function in AD mice (**Figure 8A-B)**.

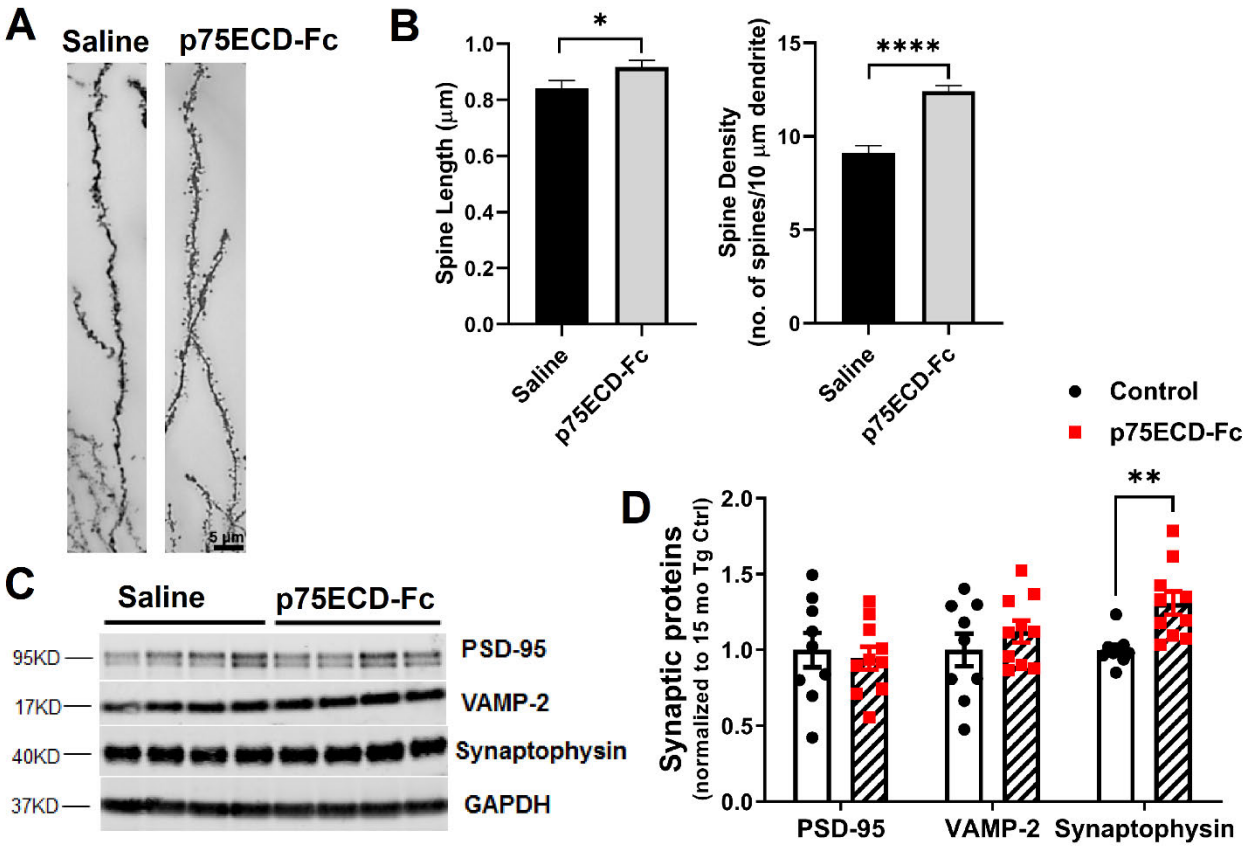


Figure 8 Effect of p75ECD-Fc on synaptic dysfunction in APP/PS1 mice. (**A-B**) Representative image and quantification of average spine length and density of the apical dendrites of CA1 pyramidal neurons of the hippocampus (n = 2/group, 6-7 neurons per mouse, Scale bar = 5 µm). (**C-D**) Immunoblot analysis and quantification for synapse-associated proteins including PSD-95, VAMP-2, and synaptophysin in whole brain homogenates (n = 9-10/group) *p < 0.05, Student t test, unpaired, two-tailed with Welch's correction. Results are presented as means ± SEM.

4.5. Effect of p75ECD-Fc treatment on apoptosis and neuron viability in APP/PS1 mice

Massive neuron cell death is a main pathological feature of late-stage AD [53]. To evaluate the effect of p7ECD-Fc on neuron cell viability in APP/PS1 mice, immunostaining of mature neuron nuclei using NeuN antibody as well as TUNEL staining, a marker of apoptosis, that can detect DNA fragmentation were performed. In addition, western blotting of whole brain homogenate was probed with antibodies against mature neuron nuclei (NeuN), caspase-3 a member of cysteine proteases family and JNK (c-Jun N-terminal kinase), which plays a central role in proapoptotic signaling pathways.

Results of immunohistochemistry showed no significant difference between control and treated APP/PS1 mice in NeuN expression in the hippocampus and cortex. TUNEL positive cells were detected in CA3 region of the hippocampus in both control and treated mice, while p75ECD-Fc treated mice showed less TUNEL positive cells, but no significant difference was found between the two groups ($p = 0.0944$, **Figure 9**).

Western blotting analysis of the whole brain homogenate of control and p75ECD-Fc treated APP/PS1 mice showed no significant difference in NeuN protein expression between the two groups. Also, the levels of cleaved caspase-3 normalized to the procaspase-3 were not different. Similarly, the ratio of the active phosphorylated JNK (pSAPK/JNK) to the total protein was not different between control and treated mice (**Figure 10**). Taken together, these results suggest that p75ECD-Fc did not improve the neuron cell viability or reduce apoptosis in APP/PS1 mice.

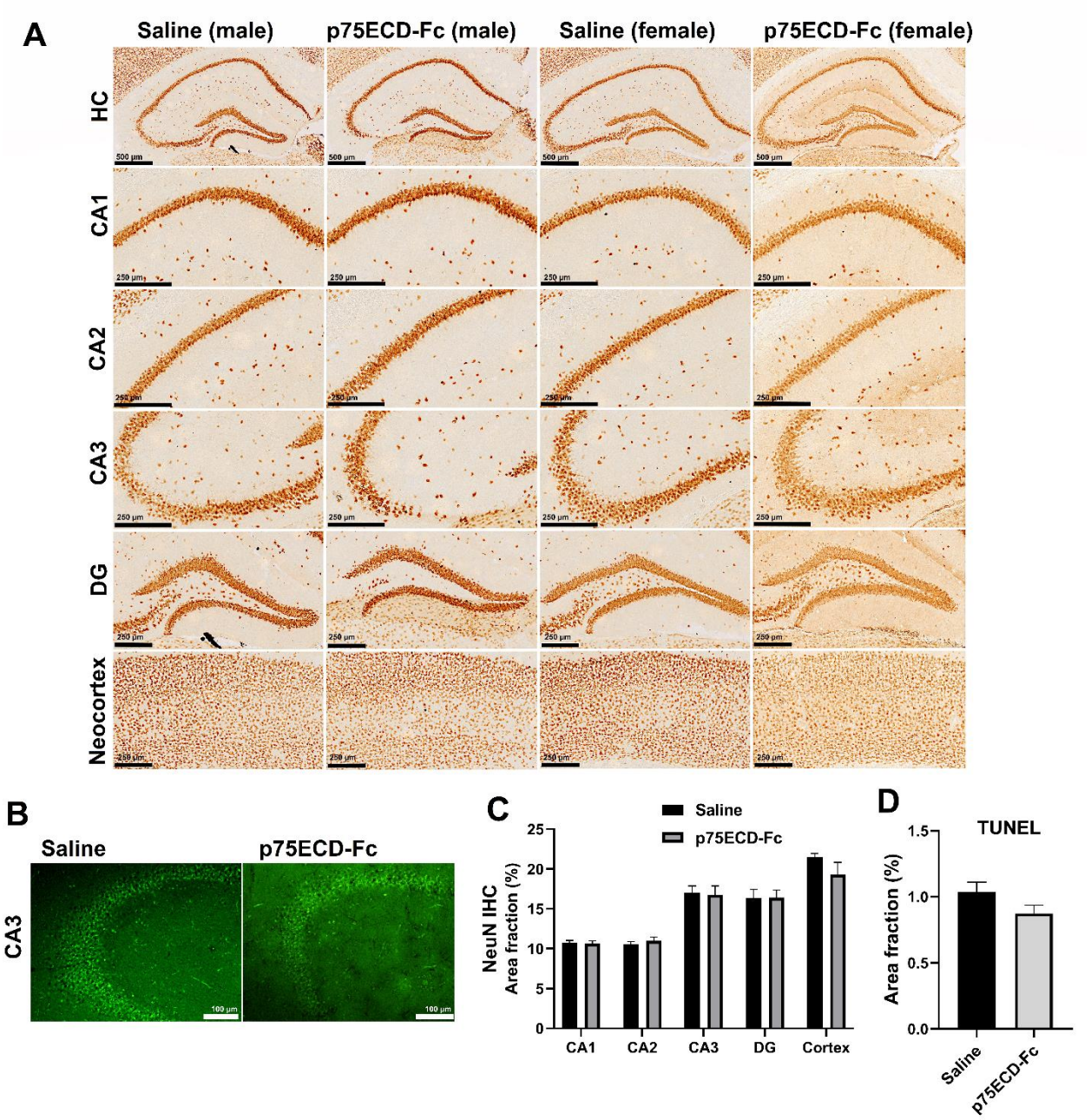


Figure 9 Effect of p75ECD-Fc on neuronal apoptosis in APP/PS1 mice. (**A**) Representative images of the hippocampus and neocortex immunostained with NeuN; a marker for mature neurons nuclei (Scale bar = 500 µm, 250 µm for focused regions). (**B**) A representative coronal section of the CA3 part of the mice hippocampus stained using a TUNEL assay to detect apoptotic cells in control and p75ECD-Fc treated groups (Scale bar = 100 µm). (**C-D**) Quantification of area fraction% of NeuN and TUNEL-positive staining in the cortex, whole hippocampus, and its subregions. n = 8-10, for NeuN, n = 4-6/group for TUNEL staining. * $p < 0.05$, Student t test, unpaired, two-tailed with Welch's correction. Results are presented as means ± SEM.

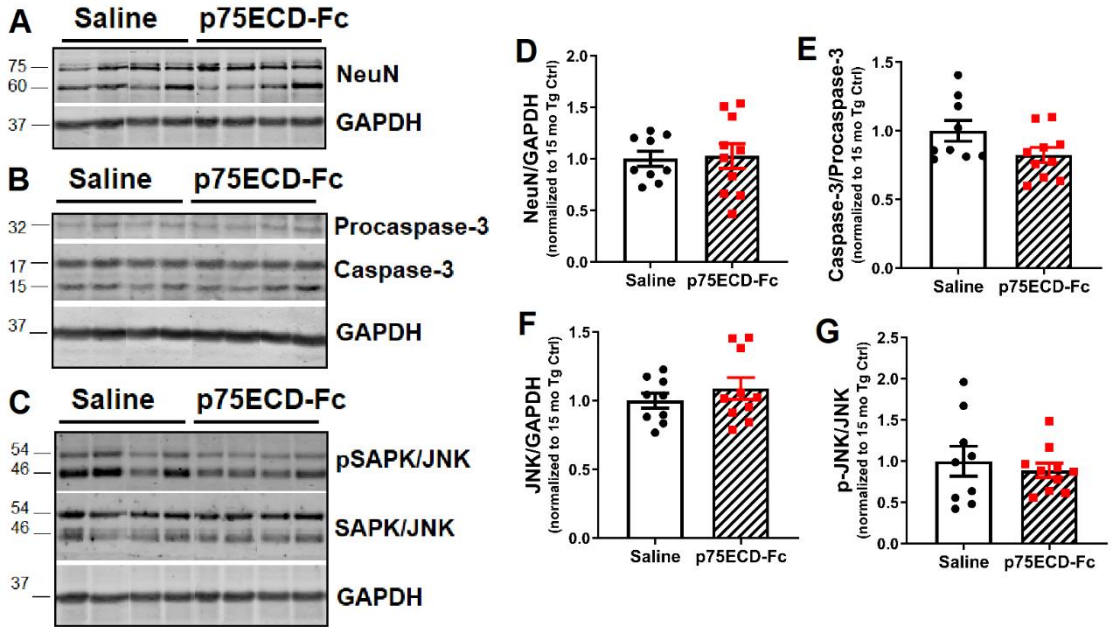


Figure 10 Effect of p75ECD-Fc treatment on apoptosis. (**A-C**) Western blotting of brain homogenates probed with NeuN and caspase-3 antibodies showing procaspase-3 and cleaved caspase-3 and antibodies against the total protein levels of SAPK/JNK and its phosphorylated form. (**D-G**) Quantification of the protein expression levels of NeuN, cleaved caspase-3 and JNK normalized to GAPDH. *p < 0.05, n = 9-10, Student t test, unpaired, two-tailed with Welch's correction. Results are presented as means ± SEM.

4.6. Effect of p75ECD-Fc on Tau phosphorylation and kinases involved in Aβ and Tau accumulation

Aberrant tau phosphorylation is a key pathologic feature of AD [54]. GSK-3β is a tau protein kinase that can phosphorylate tau at multiple sites in the paired helical filament leading to tangle formation [55]. Protein kinase B or termed Akt is a serine-threonine kinase, an upstream regulator of GSK-3, that can mediate tau phosphorylation through phosphorylating GSK-3β at its serine 9 residue thereby inactivating it [56]. Therefore, we examined the effect of p75ECD-Fc treatment on the levels of phosphorylated tau at serine 396 residue. We also performed western blotting to examine total proteins levels of GSk-3β, its inactivated form (phosphorylated at S9) as well as total Akt and its active phosphorylated form at S473.

Results showed no significant difference between control and treated mice in the levels of phosphorylated tau. Total protein levels of GSK-3β and Akt were not different between the two groups. While p75ECD-Fc did not significantly alter the levels of the phosphorylated form of either GSK-3β or Akt (**Figure 11**).

These results may suggest that p7ECD-Fc did not affect the signaling pathways involved in tau phosphorylation.

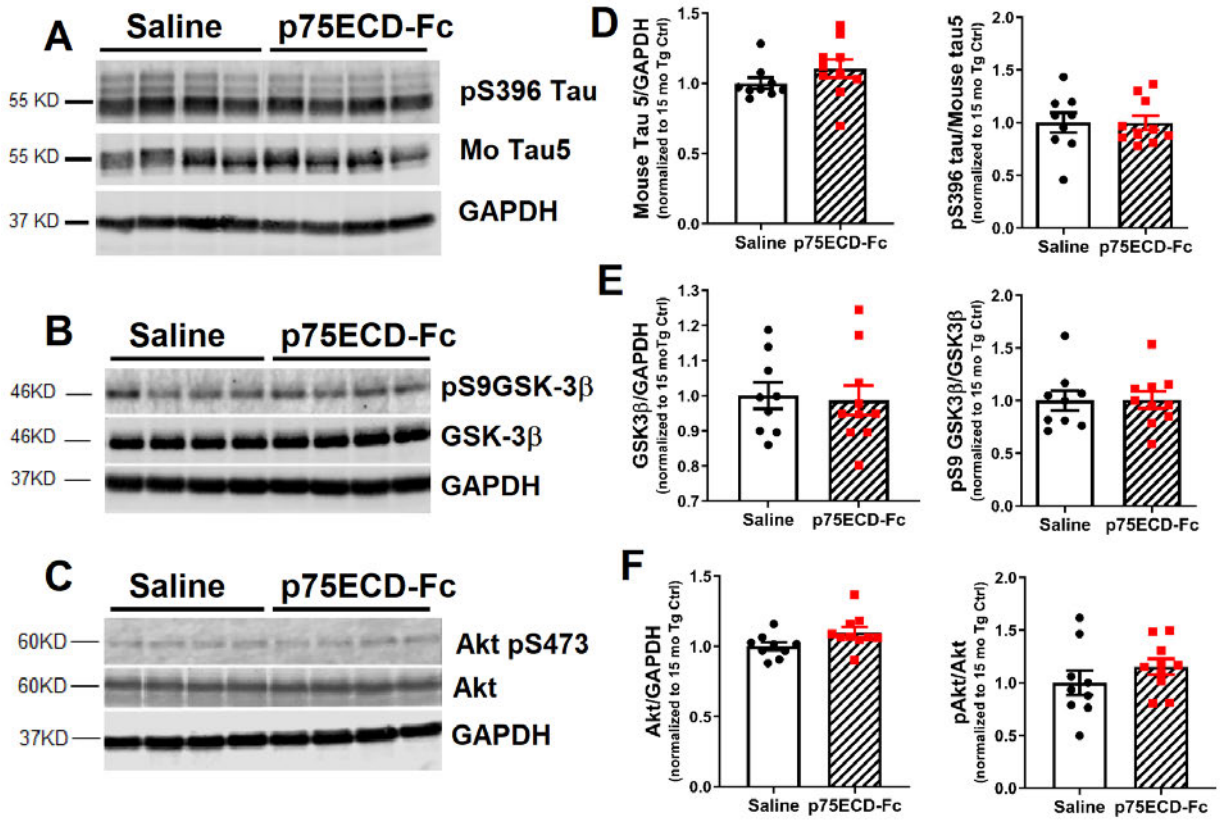


Figure 11 Effect of p75ECD-Fc treatment on Tau phosphorylation and expression levels of kinases involved in Aβ and phosphorylated Tau accumulation. (A) Immunoblot analysis showing the levels of phosphorylated tau at epitope serine 396 and total tau that was detected using Mouse tau5 antibody. **(B-C)** Immunoblot analysis showing the levels of total GSK-3β and Akt protein expression and their phosphorylated forms, GAPDH is used as loading control. **(D)** Quantification of the immunoblot bands of phosphorylated tau against total tau. **(E-F)**. Each graph displays quantification of the immunoreactivity of the specified phosphorylated form to the corresponding total protein level and expressed as relative intensity of the APP/PS1 Saline group, n = 9-10/group, Student t test, unpaired, two-tailed with Welch's correction. Results are presented as means ± SEM.

4.7. p75ECD-Fc did not generate significant increase in the endogenous antibodies.

Finally, we measured the levels of antibodies in serum against p75ECD-Fc in different groups. We found that there is no difference in the optical density and all groups generate low ELISA signals. These data suggest that p75ECD-Fc treatment did not induce significant increase in the production of endogenous antibodies against the protein (**Figure 12**).

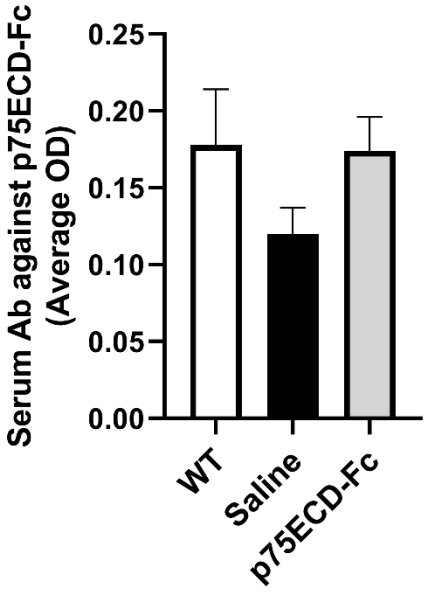


Figure 12 Comparison of serum antibodies to p75ECD-Fc among the WT, Saline treated APP/PS1 and p75ECD-Fc treated mice. n = 3-10, One-way ANOVA, Tukey's multiple comparison. Results are presented as means ± SEM.

5. Discussion

In the present study, we demonstrated that peripheral administration of p75ECD-Fc, a recombinant fusion protein of the extracellular domain of the human p75 neurotrophin receptor, can improve the cognitive function and reduce Aβ plaque load in AD mice and therefore, could represent a potential drug candidate for the treatment of Alzheimer's disease. Previous work by Wang et al. and Yao et al. discovered that p75ECD is a neuroprotective molecule against neurodegeneration in AD and that its shedding process from the full-length receptor is switched off in AD patients. Yao et al. found that intracranial delivery of AAV-p75ECD-Fc significantly reversed cognitive deficits and alleviated AD pathologies in APP/PS1 transgenic AD mice [14,12]. As brain delivery is quite invasive and mostly not appropriate in clinical settings, Wang et al. discovered that the intramuscular delivery of AAV-p75ECD-Fc was effective and able to reduce the plaque load in the brain [41]. In this study, we aimed to investigate the effectiveness of the peripheral delivery of the recombinant protein in AD mice as a safe alternative approach to the AAV gene delivery and to the brain delivery.

p75ECD-Fc, synthesized in cooperation with Fujian Tiantai and Wuxi APPtec in China, was delivered to 9-month-old APP/PS1 through intravenous injection at a dose of 10mg/kg once monthly for 6 consecutive months. Behavioral tests analysis revealed that p75ECD-Fc significantly improved the spatial reference memory of treated mice as shown by reduced escape latency in MWM test as well as increase in the number of platform site crossing in the probe trial. However, p75ECD-Fc treatment did not reduce the anxiety behavior in the open field test. We also did not find any difference among groups in the novel object recognition test, although WT and p75ECD-Fc treated APP/PS1 mice show higher preference to explore and interact with the novel object more frequently than the control APP/PS1 mice. Similarly, no difference was found between all groups in the Y maze novel arm or spontaneous alternation tests. Even though, control APP/PS1 showed more total arm entries compared to WT and

treated mice, but overall, the difference was not significant. In a previous study by Yao et al. [14], control APP/PS1 mice showed impairment in working memory in Y maze and novel object task, while AAV-ECD-Fc injection significantly reversed the memory impairment in these animals. Different findings could be attributed to different ages of the animals used and sex including both males and females in the current study, while in the aforementioned study only female mice were used. In our study, APP/PS1 mice showed increased activity in the Y maze novel arm task as indicated by higher number of total arm entries, which is consistent with previous study showing that APP/PS1 of age 15-17 months old displayed increased activity in the Y maze novel arm test, impaired acquisition and learning in MWM and similar behavior to WT mice in Y maze spontaneous alternation test [57].

Congo Red stain and total Aβ load immunohistochemistry showed that p75ECD-Fc significantly reduced the levels of Aβ plaques in the hippocampus and cortex of APP/PS1 by 25%. These results agree with previous studies reported that either intramuscular or brain delivery of the AAV-ECD-Fc reduced the plaque load in AD mice. Wang et al. reported that low levels of the protein were detected in the brain following peripheral delivery of AAV-p75ECD-Fc and majority of the expressed protein was localized in the liver and kidney [41]. The authors, therefore, concluded that the main site of action is the periphery. In consistency with these findings, our results showed that the protein is colocalized in the resident macrophages of peripheral organs specifically the liver and kidney, while small amounts were detected in the brain and CSF following IV and SC administration in Sprague Dawley rats. Taking into consideration that ~50% of toxic amyloid beta is cleared peripherally through the kidney and liver [58,59], and that amyloid beta can bind to p75 extracellular domain with high affinity [60]. Therefore, we assume that p75ECD-Fc could act through binding to amyloid beta in the periphery promoting its clearance, which as a result, would shift the equilibrium and would drive the efflux of these toxic proteins outside the CNS to the plasma via a “peripheral

sink mechanism" [61]. Since the protein was also detected in the CSF and brain following peripheral injection in rats [62], therefore, p75ECD-Fc might affect the amyloid pathology through central mechanism. Previous studies reported that soluble p7ECD can block the neurotoxic signaling and neurite collapse induced by full length p75 neurotrophin receptor through scavenging proneurotrophins and Aβ [12,7,63]. Interestingly, our results showed that p75ECD-Fc reduced the levels of CTFs significantly, as previously reported [14], while produced comparable effects on the levels of other APP fragments. It is reported that Aβ augment the expression and activation of BACE1 enzyme [64,65]. Therefore, reduction of Aβ in the brain may have resulted in inhibition of APP and BACE interaction and therefore reduction in β-secretase cleavage. However, we did not find significant difference in the expression levels of BACE1 enzyme between treated and control but, we found that p75ECD-Fc significantly increased the ratio of pBACE at S498 to total protein. BACE1 phosphorylation at S498 regulates its transport and recycling between TGN (trans Golgi network), cell surface, and endosomes through interactions with GGA proteins (Golgi-localized γ-ear containing ADP ribosylation factor-binding) [66]. Although, BACE1 phosphorylation at S498 site does not seem to significantly alter β-secretase activity, BACE1 trafficking may have a substantial impact on Aβ processing in the brain [46].

We did not find significant differences in GFAP and Iba-1 expression in western blotting, although we showed that the area fraction % of CD45 positive microglia was reduced in the neocortex and hippocampus of p75ECD-Fc treated APP/PS1 mice. Previous studies reported significant reduction in astrocytosis and microgliosis following AAV-p75ECD-Fc treatment, an effect that was explained to be secondary to Aβ reduction [14,41,67]. As we used whole brain homogenate for Western blotting, the homogenate may dilute the changes of GFAP and Iba-1 staining in the cortex and hippocampus seen by immunostaining.

However, we found that p75ECD-Fc significantly increased the density of dendritic spines in the hippocampus of APP/PS1 mice. Similarly, levels of presynaptic protein synaptophysin were significantly increased and we noticed slight increase in the levels of PSD-95 and VAMP-2. Reduction of brain Aβ levels might have impact on synaptic plasticity in AD [52].

Histomorphology showed no significant difference in % of area fraction of mature neurons between control and treated mice. Similarly, there was no difference between the two groups in the number of apoptotic cells observed with TUNEL staining. NeuN, caspase-3 expression and the levels of active (phosphorylated) JNK did not differ between groups although slight reduction in pJNK was observed.

We also found that p7ECD-Fc did not reduce tau phosphorylation in the brains of AD mice. Changes in the levels of inactive GSK-3β (S9) or Akt (pS473) which lie upstream in tau phosphorylation signaling was not different between control and treated AD mice.

Although this study did not show extensive beneficial effects of p75ECD-Fc on pathological key factors in AD such as neuroinflammation, apoptosis and Tau hyperphosphorylation, previous studies have already documented the phospho-tau reducing, neuroprotective and anti-inflammatory effects of AAV-p75ECD following either intracranial or intramuscular delivery [14,41]. The gene delivery of the protein could ensure constant and steady expression of the protein, which might not have been achieved with the protein delivery since only one dose was given once monthly. Therefore, optimizing the dose and frequency of administration might improve the efficiency of the peripheral delivery of the protein.

6. Conclusion

The neurotrophin imbalance theory of AD [6] besides the peripheral sink mechanism for the clearance of Aβ [61] have been suggested as novel concepts and objectives for understanding the pathophysiology of the disease and for therapeutic drug development. We have shown, in

this study, that peripheral administration of the extracellular domain of p75 neurotrophin receptor reduced Aβ plaque load and improved the synaptic plasticity in the brain of AD mice. These findings support the effectiveness of peripheral removal of brain Aβ, and possible outcomes for restoration of the p75ECD levels in brain. Owing to the complex pathophysiology of AD, further studies are required to develop multitarget therapeutic approach for the effective treatment of AD.

Table 1 Primary antibodies used in this study.

Antibody	Type/Host	Specificity	Phosph. site	Dilution	Source
AKT	Poly-/Rabbit	AKT		1:1000 WB	Cell signaling technology
pAKT (S473)	Poly-/Rabbit	pAKT	Ser 473	1:1000 WB	Cell signaling technology
SAPK/JNK	Poly-/Rabbit	pJNK (p46, p54)		1:1000 WB	Cell signaling technology
pSAPK/JNK	Poly-/Rabbit	JNK (p46, p54)	Thr183/Tyr185	1:1000 WB	Cell signaling technology
sAPPβ	Poly-/Rabbit	Soluble fragment cleaved N-terminus to the β-secretase cleavage of APP (human)		1:250 WB	BioLegend
sAPPα	Poly-/Mouse	soluble fragment resulting from the α-secretase cleavage of APP (human)		1:250 WB	BioLegend
Anti-APP A4 clone 22C11	Mono-/Mouse	mature APP~130kD immature APP~110kD sAPP~120kD		1:1000 WB	MERCK
APP-C terminal	Poly-/Rabbit	C-terminal fragment of APP		1:1000 WB	BioLegend
pAPP Thr 668	Poly-/Rabbit	pAPP T668	Thr668	1:1000 WB	Cell signaling technology
BACE-1	Mono-/Rabbit	beta-site APP cleaving enzyme (BACE)		1:1000 WB	Cell signaling technology
pBACE	Poly-/Rabbit	Phosphorylated beta-site APP cleaving enzyme (BACE)	S498	1:1000 WB	ThermoFisher
Caspase-3	Poly-/Rabbit	Cleaved caspase 3		1:500 WB	Sigma-Aldrich
CD45	Mono-/Rat	CD45		1:250 IHC	STEMCELL Technologies
GSK-3β	Mono-/Mouse	GSK-3β		1:3000 WB	Cell signaling technology

pGSK-3β	Poly-/Rabbit	pGSK-3β	Ser 9	1:3000 WB	Cell signaling technology
GAPDH	Poly-/Sheep	GAPDH		1:5000 WB	Osenses
GFAP	Poly-/Rabbit	GFAP		1:2000 WB 1:1000 IHC	Dako
Iba-1	Poly-/Rabbit	Iba-1		1:1000 WB	FUJIFILM Wako
MOAB-2, biotinylated	Mono-/Mouse	Aβ (1-40/42) peptides		1:500 IHC	Biosenses
NeuN	Mono-/Mouse Poly-/Rabbit	Neuronal nuclei		1:1000 WB 1:1000 IHC	Invitrogen
VAMP-2	Poly-/Rabbit	VAMP-2		1:3000 WB	Osenses
PSD-95	Mono-/Mouse	PSD-95		1:2000 WB	Sigma
pS396 Tau	Mono-/Rabbit	pTau	Ser 396	1:15,000 WB	Abcam
Tau 5	Mono-/Mouse	Mouse Tau		1:7500 WB	Life Technologies
Synaptophysin	Mono-/Mouse	Synaptophysin		1:4000 WB	Millipore

Phosph. site: phosphorylation site; Mono-: monoclonal; poly-: polyclonal; WB, Western blotting; IHC: immunohistochemistry.

References:

1. Alzheimer's Disease International: World Alzheimer Report 2018; The state of the art of dementia research: New frontiers.
2. Brown L, Hansnata E, HA. L (2017) Economic Cost of Dementia in Australia 2016-2056: Report prepared for Alzheimer's Australia. Australia : Alzheimer's Australia.
3. Hardy J, Selkoe DJ (2002) The Amyloid Hypothesis of Alzheimer's Disease: Progress and Problems on the Road to Therapeutics. Science 297 (5580):353-356. doi:10.1126/science.1072994
4. Cattaneo A, Calissano P (2012) Nerve Growth Factor and Alzheimer's Disease: New Facts for an Old Hypothesis. Molecular Neurobiology 46 (3):588-604. doi:10.1007/s12035-012-8310-9
5. Zhou X-F, Wang Y-J (2011) The p75NTR extracellular domain: A potential molecule regulating the solubility and removal of amyloid-β. Prion 5 (3):161-163. doi:10.4161/pri.5.3.16896
6. Zhou X-F (2016) The imbalance of neurotrophic signalling: an alternate hypothesis for the pathogenesis and drug development of Alzheimer's disease. Proc Neurosci 1 (1):13-18
7. Wang YJ, Valadares D, Sun Y, Wang X, Zhong JH, Liu XH, Majd S, Chen L, Gao CY, Chen S, Lim Y, Pollard A, Aguilar E, Gai WP, Yang M, Zhou XF (2010) Effects of proNGF on Neuronal Viability, Neurite Growth and Amyloid-beta Metabolism. Neurotoxicity Research 17 (3):257-267. doi:10.1007/s12640-009-9098-x
8. Ginsberg SD, Che S, Wuu J, Counts SE, Mufson EJ (2006) Down regulation of trk but not p75NTR gene expression in single cholinergic basal forebrain neurons mark the progression of Alzheimer's disease. Journal of Neurochemistry 97 (2):475-487. doi:10.1111/j.1471-4159.2006.03764.x
9. Yaar M, Zhai S, Pilch PF, Doyle SM, Eisenhauer PB, Fine RE, Gilchrest BA (1997) Binding of beta-amyloid to the p75 neurotrophin receptor induces apoptosis. A possible mechanism for Alzheimer's disease. Journal of Clinical Investigation 100 (9):2333-2340
10. Mangialasche F, Solomon A, Winblad B, Mecocci P, Kivipelto M (2010) Alzheimer's disease: clinical trials and drug development. The Lancet Neurology 9 (7):702-716. doi:http://dx.doi.org/10.1016/S1474-4422(10)70119-8
11. Sun Y, Lim Y, Li F, Liu S, Lu J-J, Haberberger R, Zhong J-H, Zhou X-F (2012) ProBDNF Collapses Neurite Outgrowth of Primary Neurons by Activating RhoA. PLOS ONE 7 (4):e35883. doi:10.1371/journal.pone.0035883
12. Wang YJ, Wang X, Lu JJ, Li QX, Gao CY, Liu XH, Sun Y, Yang M, Lim Y, Evin G, Zhong JH, Masters C, Zhou XF (2011) p75NTR regulates Abeta deposition by increasing Abeta production but inhibiting Abeta aggregation with its extracellular domain. The Journal of neuroscience : the official journal of the Society for Neuroscience 31 (6):2292-2304. doi:10.1523/JNEUROSCI.2733-10.2011
13. Rabizadeh S, Bitler CM, Butcher LL, Bredesen DE (1994) Expression of the low-affinity nerve growth factor receptor enhances beta-amyloid peptide toxicity. Proceedings of the National Academy of Sciences of the United States of America 91 (22):10703-10706
14. Yao XQ, Jiao SS, Saadipour K, Zeng F, Wang QH, Zhu C, Shen LL, Zeng GH, Liang CR, Wang J, Liu YH, Hou HY, Xu X, Su YP, Fan XT, Xiao HL, Lue LF, Zeng YQ, Giunta B, Zhong JH, Walker DG, Zhou HD, Tan J, Zhou XF, Wang YJ (2015) p75NTR ectodomain is a physiological neuroprotective molecule against amyloid-beta toxicity in the brain of Alzheimer's disease. Molecular Psychiatry 20 (11):1301-1310. doi:10.1038/mp.2015.49
15. Querfurth HW, LaFerla FM (2010) Alzheimer's Disease. New England Journal of Medicine 362 (4):329-344. doi:10.1056/NEJMra0909142

16. Allen SJ, Watson JJ, Dawbarn D (2011) The Neurotrophins and Their Role in Alzheimer's Disease. Current Neuropharmacology 9 (4):559-573. doi:10.2174/157015911798376190
17. Terry AV, Jr., Kutiyanawalla A, Pillai A (2011) Age-dependent alterations in nerve growth factor (NGF)-related proteins, sortilin, and learning and memory in rats. Physiol Behav 102 (2):149-157. doi:10.1016/j.physbeh.2010.11.005
18. Ernfors P, Lindefors N, Chan-Palay V, Persson H (1990) Cholinergic Neurons of the Nucleus basalis Express Elevated Levels of Nerve Growth Factor Receptor mRNA in Senile Dementia of the Alzheimer Type. Dementia and Geriatric Cognitive Disorders 1 (3):138-145. doi:10.1159/000107133
19. Verge V, Merlio J, Grondin J, Ernfors P, Persson H, Riopelle R, Hokfelt T, Richardson P (1992) Colocalization of NGF binding sites, trk mRNA, and low-affinity NGF receptor mRNA in primary sensory neurons: responses to injury and infusion of NGF. The Journal of Neuroscience 12 (10):4011-4022
20. Underwood CK, Coulson EJ (2008) The p75 neurotrophin receptor. The International Journal of Biochemistry & Cell Biology 40 (9):1664-1668. doi:https://doi.org/10.1016/j.biocel.2007.06.010
21. Ibanez CF, Simi A (2012) p75 neurotrophin receptor signaling in nervous system injury and degeneration: paradox and opportunity. Trends Neurosci 35 (7):431-440. doi:10.1016/j.tins.2012.03.007
22. Nykjaer A, Lee R, Teng KK, Jansen P, Madsen P, Nielsen MS, Jacobsen C, Kliemannel M, Schwarz E, Willnow TE, Hempstead BL, Petersen CM (2004) Sortilin is essential for proNGF-induced neuronal cell death. Nature 427 (6977):843-848. doi:10.1038/nature02319
23. Capsoni S, Ugolini G, Comparini A, Ruberti F, Berardi N, Cattaneo A (2000) Alzheimer-like neurodegeneration in aged antinerve growth factor transgenic mice. Proc Natl Acad Sci U S A 97 (12):6826-6831
24. Calissano P, Matrone C, Amadoro G (2010) Nerve growth factor as a paradigm of neurotrophins related to Alzheimer's disease. Developmental neurobiology 70 (5):372-383. doi:10.1002/dneu.20759
25. Zeng F, Lu JJ, Zhou XF, Wang YJ (2011) Roles of p75NTR in the pathogenesis of Alzheimer's disease: a novel therapeutic target. Biochemical pharmacology 82 (10):1500-1509. doi:10.1016/j.bcp.2011.06.040
26. Hu X-Y, Zhang H-Y, Qin S, Xu H, Swaab DF, Zhou J-N (2002) Increased p75NTR Expression in Hippocampal Neurons Containing Hyperphosphorylated τ in Alzheimer Patients. Experimental Neurology 178 (1):104-111. doi:10.1006/exnr.2002.8018
27. Sotthibundhu A, Sykes AM, Fox B, Underwood CK, Thangnipon W, Coulson EJ (2008) Beta-amyloid(1-42) induces neuronal death through the p75 neurotrophin receptor. J Neurosci 28 (15):3941-3946. doi:10.1523/JNEUROSCI.0350-08.2008
28. Perini G, Della-Bianca V, Politi V, Della Valle G, Dal-Pra I, Rossi F, Armato U (2002) Role of p75 neurotrophin receptor in the neurotoxicity by beta-amyloid peptides and synergistic effect of inflammatory cytokines. The Journal of experimental medicine 195 (7):907-918
29. Hashimoto Y, Kaneko Y, Tsukamoto E, Frankowski H, Kouyama K, Kita Y, Niikura T, Aiso S, Bredesen DE, Matsuoka M, Nishimoto I (2004) Molecular characterization of neurohybrid cell death induced by Alzheimer's amyloid-beta peptides via p75NTR/PLAIDD. J Neurochem 90 (3):549-558. doi:10.1111/j.1471-4159.2004.02513.x
30. Charalampopoulos I, Vicario A, Pediaditakis I, Gravanis A, Simi A, Ibanez CF (2012) Genetic dissection of neurotrophin signaling through the p75 neurotrophin receptor. Cell Rep 2 (6):1563-1570. doi:10.1016/j.celrep.2012.11.009

31. Longo FM, Massa SM (2013) Small-molecule modulation of neurotrophin receptors: a strategy for the treatment of neurological disease. Nat Rev Drug Discovery 12 (7):507-525. doi:10.1038/nrd4024

http://www.nature.com/nrd/journal/v12/n7/abs/nrd4024.html#supplementary-information
32. Urra S, Escudero CA, Ramos P, Lisbona F, Allende E, Covarrubias P, Parraguez JI, Zampieri N, Chao MV, Annaert W, Bronfman FC (2007) TrkA Receptor Activation by Nerve Growth Factor Induces Shedding of the p75 Neurotrophin Receptor Followed by Endosomal γ-Secretase-mediated Release of the p75 Intracellular Domain. Journal of Biological Chemistry 282 (10):7606-7615. doi:10.1074/jbc.M610458200
33. Wang Y-J, Wang X, Lu J-J, Li Q-X, Gao C-Y, Liu X-H, Sun Y, Yang M, Lim Y, Evin G, Zhong J-H, Masters C, Zhou X-F (2011) p75NTR Regulates Aβ Deposition by Increasing Aβ Production But Inhibiting Aβ Aggregation with Its Extracellular Domain. The Journal of Neuroscience 31 (6):2292-2304. doi:10.1523/jneurosci.2733-10.2011
34. Saadipour K, Yang M, Lim Y, Georgiou K, Sun Y, Keating D, Liu J, Wang Y-R, Gai W-p, Zhong J-h, Wang Y-J, Zhou X-F (2013) Amyloid beta1–42 (Aβ42) up-regulates the expression of sortilin via the p75NTR/RhoA signaling pathway. Journal of Neurochemistry 127 (2):152-162. doi:10.1111/jnc.12383
35. Costantini C, Rossi F, Formaggio E, Bernardoni R, Cecconi D, Della-Bianca V (2005) Characterization of the signaling pathway downstream p75 neurotrophin receptor involved in β-amyloid peptide-dependent cell death. Journal of Molecular Neuroscience 25 (2):141-156. doi:10.1385/jmn:25:2:141
36. Guglielmotto M., Monteleone D., Giliberto L., Fornaro M., Borghi R., Tamagno E., Tabaton M. (2011) Amyloid-β_{42} activates the expression of BACE1 through the JNK pathway. J Alzheimers Dis 27 (4):871-883
37. Pietri M, Dakowski C, Hannaoui S, Alleaume-Butaux A, Hernandez-Rapp J, Ragagnin A, Mouillet-Richard S, Haik S, Bailly Y, Peyrin J-M, Launay J-M, Kellermann O, Schneider B (2013) PDK1 decreases TACE-mediated [alpha]-secretase activity and promotes disease progression in prion and Alzheimer's diseases. Nat Med 19 (9):1124-1131. doi:10.1038/nm.3302

http://www.nature.com/nm/journal/v19/n9/abs/nm.3302.html#supplementary-information
38. Checler F (2013) Alzheimer's and prion diseases: PDK1 at the crossroads. Nat Med 19 (9):1088-1090. doi:10.1038/nm.3332
39. Matrone C, Marolda R, Ciafrè S, Ciotti MT, Mercanti D, Calissano P (2009) Tyrosine kinase nerve growth factor receptor switches from prosurvival to proapoptotic activity via Abeta-mediated phosphorylation. Proceedings of the National Academy of Sciences 106 (27):11358-11363. doi:10.1073/pnas.0904998106
40. Matrone C., Barbagallo APM, La Rosa LR, Florenzano F., Ciotti MT, Mercanti D., Chao MV, Calissano P., L. DA (2011) APP is phosphorylated by TrkA and regulates NGF/TrkA signaling APP regulates TrkA. J Neurosci August 17; 31 (33): 11756–11761
41. Wang Q-H, Wang Y-R, Zhang T, Jiao S-S, Liu Y-H, Zeng F, Li J, Yao X-Q, Zhou H-D, Zhou X-F, Wang Y-J (2016) Intramuscular delivery of p75NTR ectodomain by an AAV vector attenuates cognitive deficits and Alzheimer's disease-like pathologies in APP/PS1 transgenic mice. Journal of Neurochemistry 138 (1):163-173. doi:10.1111/jnc.13616
42. Borchelt DR, Ratovitski T, van Lare J, Lee MK, Gonzales V, Jenkins NA, Copeland NG, Price DL, Sisodia SS (1997) Accelerated amyloid deposition in the brains of transgenic mice coexpressing mutant presenilin 1 and amyloid precursor proteins. Neuron 19 (4):939-945. doi:10.1016/s0896-6273(00)80974-5
43. Morris RG, Garrud P, Rawlins JN, O'Keefe J (1982) Place navigation impaired in rats with hippocampal lesions. Nature 297 (5868):681-683. doi:10.1038/297681a0

44. Wolf A, Bauer B, Abner EL, Ashkenazy-Frolinger T, Hartz AM (2016) A Comprehensive Behavioral Test Battery to Assess Learning and Memory in 129S6/Tg2576 Mice. PLoS One 11 (1):e0147733. doi:10.1371/journal.pone.0147733
45. Groves TR, Wang J, Boerma M, Allen AR (2017) Assessment of Hippocampal Dendritic Complexity in Aged Mice Using the Golgi-Cox Method. JoVE (124):e55696. doi:doi:10.3791/55696
46. Cole SL, Vassar R (2007) The Alzheimer's disease β-secretase enzyme, BACE1. Molecular Neurodegeneration 2 (1):22. doi:10.1186/1750-1326-2-22
47. Song W-J, Son M-Y, Lee H-W, Seo H, Kim JH, Chung S-H (2015) Enhancement of BACE1 Activity by p25/Cdk5-Mediated Phosphorylation in Alzheimer's Disease. PLOS ONE 10 (8):e0136950. doi:10.1371/journal.pone.0136950
48. Sun M, Zhang H (2017) Par3 and aPKC regulate BACE1 endosome-to-TGN trafficking through PACS1. Neurobiol Aging 60:129-140. doi:10.1016/j.neurobiolaging.2017.08.024
49. Zhang T, Chen D, Lee TH (2019) Phosphorylation Signaling in APP Processing in Alzheimer's Disease. Int J Mol Sci 21 (1). doi:10.3390/ijms21010209
50. Moore AH, O'Banion MK (2002) Neuroinflammation and anti-inflammatory therapy for Alzheimer's disease. Adv Drug Deliv Rev 54 (12):1627-1656. doi:10.1016/s0169-409x(02)00162-x
51. Forloni G, Balducci C (2018) Alzheimer's Disease, Oligomers, and Inflammation. J Alzheimers Dis 62 (3):1261-1276. doi:10.3233/JAD-170819
52. Arendt T (2009) Synaptic degeneration in Alzheimer's disease. Acta Neuropathol 118 (1):167-179. doi:10.1007/s00401-009-0536-x
53. Shimohama S (2000) Apoptosis in Alzheimer's disease--an update. Apoptosis 5 (1):9-16. doi:10.1023/a:1009625323388
54. Pooler AM, Noble W, Hanger DP (2014) A role for tau at the synapse in Alzheimer's disease pathogenesis. Neuropharmacology 76 Pt A:1-8. doi:10.1016/j.neuropharm.2013.09.018
55. Ishiguro K, Shiratsuchi A, Sato S, Omori A, Arioka M, Kobayashi S, Uchida T, Imahori K (1993) Glycogen synthase kinase 3 beta is identical to tau protein kinase I generating several epitopes of paired helical filaments. FEBS Lett 325 (3):167-172. doi:10.1016/0014-5793(93)81066-9
56. Pei JJ, Khatoon S, An WL, Nordlinder M, Tanaka T, Braak H, Tsujio I, Takeda M, Alafuzoff I, Winblad B, Cowburn RF, Grundke-Iqbal I, Iqbal K (2003) Role of protein kinase B in Alzheimer's neurofibrillary pathology. Acta Neuropathol 105 (4):381-392. doi:10.1007/s00401-002-0657-y
57. Arendash GW, King DL, Gordon MN, Morgan D, Hatcher JM, Hope CE, Diamond DM (2001) Progressive, age-related behavioral impairments in transgenic mice carrying both mutant amyloid precursor protein and presenilin-1 transgenes. Brain Res 891 (1-2):42-53. doi:10.1016/s0006-8993(00)03186-3
58. Liu Y-H, Wang Y-R, Xiang Y, Zhou H-D, Giunta B, Manucat N, Tan J, Zhou X-F, Wang Y-J (2014) Clearance of Amyloid-Beta in Alzheimer's Disease: Shifting the Action Site from Center to Periphery. Molecular neurobiology 51. doi:10.1007/s12035-014-8694-9
59. Nalivaeva NN, Turner AJ (2019) Targeting amyloid clearance in Alzheimer's disease as a therapeutic strategy. British Journal of Pharmacology 176 (18):3447-3463. doi:10.1111/bph.14593
60. Yaar M, Zhai S, Fine RE, Eisenhauer PB, Arble BL, Stewart KB, Gilchrest BA (2002) Amyloid β Binds Trimers as Well as Monomers of the 75-kDa Neurotrophin Receptor and Activates Receptor Signaling. Journal of Biological Chemistry 277 (10):7720-7725. doi:10.1074/jbc.M110929200

61. DeMattos RB, Bales KR, Cummins DJ, Paul SM, Holtzman DM (2002) Brain to Plasma Amyloid-β Efflux: a Measure of Brain Amyloid Burden in a Mouse Model of Alzheimer's Disease. Science 295 (5563):2264-2267. doi:10.1126/science.1067568
62. Kelliny S, Lam HY, Parikh A, Wang Y, Bobrovskaya L, Upton R, Zhou X-F (2020) Preclinical Study of the Pharmacokinetics of p75ECD-Fc, a Novel Human Recombinant Protein for Treatment of Alzheimer's Disease, in Sprague Dawley Rats. Current Drug Metabolism 21:1-10. doi:http://dx.doi.org/10.2174/1389200221666200502015203
63. Yan J, Zhou X, Guo J-J, Mao L, Wang Y-J, Sun J, Sun L-X, Zhang L-Y, Zhou X-F, Liao H (2012) Nogo-66 inhibits adhesion and migration of microglia via GTPase Rho pathway in vitro. Journal of Neurochemistry 120 (5):721-731. doi:https://doi.org/10.1111/j.1471-4159.2011.07619.x
64. Guglielmotto M, Monteleone D, Giliberto L, Fornaro M, Borghi R, Tamagno E, Tabaton M (2011) Amyloid-β_{42} activates the expression of BACE1 through the JNK pathway. J Alzheimers Dis 27 (4):871-883. doi:10.3233/jad-2011-110884
65. Fukumoto H, Cheung BS, Hyman BT, Irizarry MC (2002) Beta-secretase protein and activity are increased in the neocortex in Alzheimer disease. Arch Neurol 59 (9):1381-1389. doi:10.1001/archneur.59.9.1381
66. Wahle T, Prager K, Raffler N, Haass C, Famulok M, Walter J (2005) GGA proteins regulate retrograde transport of BACE1 from endosomes to the trans-Golgi network. Mol Cell Neurosci 29 (3):453-461. doi:10.1016/j.mcn.2005.03.014
67. Herskowitz JH, Offe K, Deshpande A, Kahn RA, Levey AI, Lah JJ (2012) GGA1-mediated endocytic traffic of LR11/SorLA alters APP intracellular distribution and amyloid-β production. Mol Biol Cell 23 (14):2645-2657. doi:10.1091/mbc.E12-01-0014

CHAPTER 4: A Novel Oral Edaravone formulation partially alleviates Tau pathology and motor deficits in an animal model of Frontotemporal Dementia.

A Novel Oral Edaravone formulation partially alleviates Tau pathology and motor deficits in an animal model of Frontotemporal Dementia.

Sally Kelliny, Jing Xiong, Larisa Bobrovskaya, Xin-Fu Zhou

Publication status: To be Submitted

Author Contributions

Author	Wrote Manuscript	Revised Manuscript	Designed Research	Performed Research	Analysis of Data	Data Interpretation
Kelliny, S	✔	✔	✔	✔	✔	✔
Xiong, J		✔		✔		
Bobrovskaya, L		✔	✔			✔
Zhou, X. F		✔	✔			✔

Full name of co-author	Signature	Date
Sally Kelliny	[redacted]	20/04/2021
Jing Xiong	[redacted]	20/04/2021
Larisa Bobrovskaya	[redacted]	20/04/2021
Xin-Fu Zhou	[redacted]	20/04/2021

Title: A Novel Oral Edaravone formulation partially alleviates Tau pathology and motor deficits in an animal model of Frontotemporal Dementia

Sally Kelliny[1,3], Jing Xiong[2], Larisa Bobrovskaya[1], Xin-Fu Zhou[1*]

[1]Health and Biomedical Innovation, Clinical and Health Sciences, University of South Australia SA, 5000, Australia

[2]Department of Neurology, the Second Affiliated Hospital, Kunming Medical University, Kunming, Yunnan Province, China.

[3]Faculty of Pharmacy, Assiut University, Assiut, Egypt

[*]Corresponding author

XF Zhou: xin-fu.zhou@unisa.edu.au

Abstract

Oxidative stress (OS) is a key factor in the pathogenesis of several neurodegenerative disorders and is involved in the accumulation of amyloid beta plaques and Tau inclusions. Edaravone (EDR) is a free radical scavenger that is approved for motor neuron disease and acute ischemic stroke. EDR alleviates pathologies and cognitive impairment of AD via targeting multiple key pathways in transgenic mice. Herein, we aimed to study the effect of EDR on Tau pathology in P301L mice; an animal model of frontotemporal dementia (FTD) at two age time points representing the early and late stages of the disease. A novel EDR formulation was utilized in the study and the drug was delivered orally in drinking water for 3 months. Then, behavioral tests were conducted followed by animal sacrifice and brain dissection. Treatment with EDR improved the cognitive deficits as evaluated in Morris water maze, novel object recognition and significantly alleviated motor deficits in these mice. EDR also reduced the levels of 4-hydroxy-2-nonenal (4-HNE) and 3-nitrotyrosine (3-NT) adducts. In addition, immunohistochemistry showed that EDR reduced tau phosphorylation and neuroinflammation and partially rescued neurons against oxidative neurotoxicity. Moreover, EDR attenuated downstream pathologies involved in Tau hyperphosphorylation. These results suggest that EDR may be a potential therapeutic agent for the treatment of FTD.

Keywords: Frontotemporal dementia, Edaravone, P301L, oxidative stress, Tau.

Highlights:

- Oxidative stress is a key factor in the pathophysiology of neurodegenerative disorders.
- Oral Edaravone administration to P301L mice; a model of Frontotemporal dementia, improved recognition memory and alleviated motor deficits.
- Edaravone reduced oxidative stress, neuroinflammation and inhibited phosphorylated Tau accumulation in the hippocampus and amygdala.
- The FDA approved drug, Edaravone, for ischemic stroke and amyotrophic lateral sclerosis could be a potential candidate for treatment of dementia.

Abbreviations: 4-HNE, 4-hydroxy-2-nonenal; 3-NT, 3-nitrotyrosine; Edaravone, EDR; OS, oxidative stress; ROS and RNS, reactive oxygen species and reactive nitrogen species

1. Introduction

Tauopathies is a group of progressive neurological disorders that are characterized by intracellular accumulation of abnormal Tau inclusions in the brain and spinal cord [1]. Alzheimer's disease (AD) and frontotemporal dementia (FTD-tau) are the most common forms and account for majority of dementia cases among elderly people. Tauopathies also comprise other disorders including progressive supranuclear palsy, corticobasal degeneration, and Pick's disease [2]. The exact etiology of the disease is still unknown, but the majority of cases are sporadic [2]. Yet no disease-modifying therapy has been approved for treatment of tauopathies or AD. Therefore, understanding the underlying pathophysiology of these diseases and introducing a multitargeted therapeutic intervention is required.

The main hallmark of tauopathies is the intracellular accumulation of microtubule-associated protein Tau (MAPT) in certain brain regions involved in cognitive, behavior and motor functions [2]. In pathologic states, Tau undergoes aberrant hyperphosphorylation and self-aggregation to form neurotoxic oligomers and neurofibrillary tangles (NFT) which lead to dysfunction of axonal transport [3]. The driving force that stimulates misfolded Tau formation is multifactorial. Mutations in Tau gene [4], amyloid beta (Aβ) [5], brain injury [6], impaired insulin signaling [7] and chronic inflammation [8] are main risk factors.

Oxidative stress (OS) has been identified to be one of the cellular mechanisms that link pathogenic Tau to consequent neuron dysfunction and death [9-11]. It is defined as a state of imbalance between levels of oxidative stressors (reactive oxygen and nitrogen species; ROS and RNS) and antioxidant defence mechanisms in favor of oxidants [12] that are deleterious to cells and lead to apoptosis [13]. Multiple lines of evidence indicate that OS is a contributing factor in the neuropathology of ageing [14] and several neurodegenerative disorders [15-17]. In AD, the presence of OS is evident by accumulation of lipid peroxidation products, increased protein oxidation and mitochondrial dysfunction [18-20]. For instance, studies showed that OS and Tau hyperphosphorylation are strongly linked together in a vicious cycle that eventually leads to cell death [21]. OS could induce Tau pathology by upregulating key enzymes involved in tau phosphorylation [22,23]. In a feedback mechanism, misfolded Tau could further exacerbate OS via microglial activation and mitochondria dysfunction [24,25]. Therefore, therapeutic strategies being able to target OS could possibly provide better results than those directed towards the protein deposition. Thus, the use of antioxidants such as curcumin, coenzyme Q10 (CoQ10) and vitamins as vitamin E and C has been suggested and provided promising results in animal models of dementia in terms of reducing Tau and Aβ accumulation and alleviating behavioral deficits [26-28]. However, further studies are ongoing to support their clinical benefits and effectiveness in dementia [29].

Edaravone (3-methyl-1-phenyl-2-pyrazolin-5-one) is a potent free radical scavenger, developed by Mitsubishi Tanabe Pharma Corporation (Osaka, Japan). Currently, it is approved for treatment of acute ischemic stroke in Japan and other Asian countries and amyotrophic lateral sclerosis (ALS) by FDA. Clinical studies showed that EDR reduces neuronal damage following brain ischemia [30,31] and inhibits motor functional deterioration in ALS patients through its neuroprotective mechanisms [32]. EDR is considered the first disease modifying therapy to be approved and could hold great promise to alleviate several other neurodegenerative diseases. Recently, treatment of APP/PS1 AD mice with Edaravone injection reduced amyloid plaque pathology and ameliorated cognitive deficits [33]. In our previous studies, we have shown that the EDR novel oral formulation can dose-dependently reverse the cognitive deficits and mood disorders of very old APP/PS1 mice (17 months) [34]. Therefore, in this study, we aimed to investigate the effect of the novel Edaravone formulation on tau pathology of P301L mice, a model of frontotemporal dementia with parkinsonism linked

to chromosome-17 (FTDP-17). This animal model develops age dependent hyperphosphorylated Tau in the cortex, hippocampus, and amygdala, but NFT mainly confined to amygdala, and shows behavioral and motor deficits similar to that observed in certain tauopathies in humans [35-39]. This model also shows signs of mitochondrial dysfunction that becomes significant at advanced age [40]. The novel oral formulation of Edaravone was designed earlier in our laboratory by using self-nano micellizing solid dispersion strategy and proved to be safe and effective *in vitro* and in AD animal model [41,34].

2. Materials and methods

2.1. Materials

The novel Edaravone formulation was made by WuxiApptec and obtained from Suzhou Auzone Biotech, China. The vehicle control Soluplus [42] was provided as a gift from BASF Australia Ltd. Primary antibodies used in this study are listed in **Table 1** in supplementary material. Biotinylated IgG conjugated secondary antibodies for immunohistochemistry were obtained from Thermo Fisher Scientific, Australia. IRDye® 680RD and 800CW conjugated secondary antibodies for western blotting were obtained from LI-COR Millennium Science, Victoria, Australia. Protease and phosphatase cocktail inhibitors were purchased from Thermo Fisher Scientific, Australia (Roche Diagnostics GmbH, Mannheim, Germany). VECTASTAIN ABC kit was purchased from Vector laboratories, USA. Pierce™ BCA Protein Assay Kit was obtained from Thermo Fisher Scientific, Australia. Other chemicals were purchased from Sigma Aldrich, Australia.

2.2. Animals

The breeders of male and female P301L mutant mouse (pR5-183) mouse, bred on C57BL/6 X DBA/2 F2 genetic background, expressing the longest human MAPT brain isoform (Tau40) under the control of the murine Thy1.2 promoter and with parkinsonism linked to chromosome 17 [37], were obtained from Götz laboratory in Queensland Brain Institute and bred in the Core Animal Facility, University of South Australia. C57BL/6 (WT) mice were used as controls in behavioral experiments. Animals were kept under standard conditions of 22°C room temperature and a 12 h light/dark cycle with food and water provided ad libitum. All procedures were approved by the Animal Ethics Committee of the University of South Australia (U17/14 and U13/18) and compliant with the South Australian Animal Welfare Act and Regulations 1985.

2.3. Treatment Protocol

In order to evaluate the influence of oral EDR treatment on Tau pathology in P301L mice as the pathology progresses, we included two groups of animals **A** and **B**, one at the age of 9-10 months and an older cohort with an age of 21 months, respectively. **Group A**: n = 32, 18 P301L (11 males and 7 females) and 14 WT mice (4 males and 10 females), and **Group B**: n = 12, 8 P301L (4 males and 4 females) and 4 WT male mice. WT mice were used as controls for behavioral tests and have not received any treatments. P301L mice in both age categories were divided equally into two groups: a control group that was given the vehicle of drug (Soluplus) and a treatment group that received oral Edaravone formulation dissolved in drinking water at a dose of 24 mg/kg/day for 3 months as follows: **Group A**: Vehicle treated: n = 9 (3 females and 6 males) and EDR treated: n = 9 (4 females and 5 males), **Group B**: vehicle treated: n = 4 (2 males and 2 females), EDR treated: n = 4 (2 males and 2 females). Animals were then subjected to behavior and motor tests that lasted for 3 weeks while still receiving treatment. After that, animals were humanely killed by inhalation of overdose of CO_2 and transcardially perfused with ice cold saline. Brain tissues were harvested from each mouse and divided into two halves. The left hemisphere was snap frozen in liquid nitrogen and then stored at -80°C for

subsequent biochemical analysis while the right hemisphere was fixed in 4% paraformaldehyde in PBS for histological analysis. Schematic illustration of the study is shown in **scheme 1**.

2.4. Behavioral Tests

2.4.1. Morris Water Maze (MWM)

MWM was used to assess spatial reference learning and long-term memory [43]. The test was conducted in a black circular pool filled with water at 21 ±2°C that was made opaque using non-toxic white powder paint. The arena was divided into 4 quadrant zones using the ANY-maze software (Stoelting Co., USA). A white circular platform was placed in one of the four quadrants. The test was done over 6 consecutive days. On the 1st day, each animal was trained to find the visible platform within 60 seconds with the help of visual cues placed around the pool walls. In the next four days, the platform was submerged under water for 1-1.5 cm, and time required to find the hidden platform (escape latency) was calculated. Each animal was subjected to 4 trials/day (30-60 min interval), in each trial, the animal was placed at different starting point facing the pool side walls. If the animal failed to locate the platform, it was gently directed and allowed to sit on it for 30 seconds before being returned to the cage. In the last day, the platform was removed, and each animal was exposed to one probe trial for 60 seconds. Time spent in the target quadrant zone in which the platform was placed as well as number of platform site crossing were recorded using ANY-maze video tracking system v4.5. Escape latency during the hidden platform trials, swim speed and distance were also recorded.

2.4.2. Open field test and elevated plus maze test

To assess anxiety and exploratory behaviors, the open field and elevated plus maze tests were conducted as described previously [35]. In the open field test, each mouse was placed individually at the border of a square PVC arena (50 x 50 x 40 cm), and allowed to explore the arena freely for 5 min. The arena is divided into inner zone (central) and outer zone with the software tracking system. Anxiety and exploratory behaviors were assessed by measuring the number of rearing episodes, time immobile and time spent in central zone. Locomotor activity was assessed by measuring total distance travelled and number of zone transitions.

The elevated plus maze was used to assess amygdala related anxiety behavior. It is a runway consisted of 4 opposing arms each with 46 cm length and 5 cm width elevated to a height of 70 cm above the floor. Two opposing arms are open and the other two are closed. Each animal is placed at the end of a closed arm facing the wall and allowed to explore the maze freely for 5 min. The following parameters were measured: total distance travelled, number of zone transitions, total number of head dips, percentage of time spent in open arms and percentage of open arm entries to total arm entries.

2.4.3. Novel Object Recognition Test (NORT)

This test was conducted to evaluate recognition memory and preference to explore novel objects [44]. Following habituation to the test arena, the animal was exposed to two similar objects placed symmetrically away from the centre for a duration of 5 min (sample phase). 2-3 hours later, one of the objects is removed and replaced by a different one (novel) and then each animal was allowed to explore the two different objects for 5 min (test phase). Time spent exploring both objects was recorded. Recognition index (RI) was calculated by dividing the novel object exploration time by the total time spent to explore both objects and multiplied by 100.

2.4.4. Y maze spontaneous alternation and Y maze novel arm

These tests were used to evaluate working and short-term memory as described previously [44]. The test was carried out in a Y-shaped arena with 3 opaque arms placed at a 120° angle from each other. In Y-maze novel arm test, each animal can explore two open arms freely for 5 min while the third one is blocked. The blocked arm is then opened, and the animal again freely explores all the three arms for 5 min (test phase). Tendency to explore the novel arm was assessed by measuring the time spent in the novel arm and number of novel arm entries. Y maze spontaneous alternation test was carried out 1 week later in the same arena, but the arms were rotated 45° before starting. In this test, each animal explores the maze freely with all arms open for 5 min for a single trial. Percentage of spontaneous alternation and total number of arm entries were recorded. Subjects showing a total of less than 7 arm entries were excluded. Healthy animals should display tendency to visit a less recently visited arm, thus showing higher alternation percentage.

2.4.5. Hind Limb Clasping Test

Limb clasping is a motor test to evaluate deficits in the corticospinal function. Motor function deficits have been found in Tau transgenic animal models [45] and were observed in late stages of AD and FTD patients [46,47]. P301L mice start to show progressive hind limb retraction at 9-12 months of age. When the animal is suspended by the tail, normally it elicits escape response by spreading out the hind limbs and extending the toes. Deficits in this response is scored based on the severity from 0-4 depending on the ability to spread-out the hind limbs and extend the toes. The animal was suspended from the tail for 10 sec and the position of the hind limb is observed. If the hind limbs are steadily splayed outward away from the abdomen, it is given a score of 0. If one hindlimb is retracted and toes are normally splayed, it is given a score of 1. If both hindlimbs are partially retracted toward the abdomen, while the toes are normally splayed, it is given a score of 2. If its hindlimbs are totally retracted and touching the abdomen with curled toes and immobility, it is given a score of 3. If forelimbs and hind limbs are crossed and toes are curled and immobile, it is scored 4.

2.5. Immunohistochemical analysis (IHC)

Coronal brain sections were cut at 35 µm thickness using Leica cryostat (CM3050S, Germany) and stored in antifreeze solution (0.1M PBS containing 30% glycerol and 30% ethylene glycol) at -20°C till further immunostaining. Free floating brain sections were treated with 1% SDS in PBS (pH 7.4) for 10 min for antigen retrieval then incubated with 3% H_2O_2 in PBS for 15 min to inhibit endogenous peroxidases. After washing, sections were blocked with 20% normal horse serum (NHS) in PBS for 2 hours at room temperature (RT). Sections were incubated with the primary antibodies diluted in 1%NHS in PBS and 0.3% Triton-X 100 overnight at 4°C. Sections were then treated with biotinylated secondary antibody at RT for 2 hours followed by avidin/biotinylated horseradish peroxidase (ABC kit) and then developed with diaminobenzidine (DAB) for 5 min. Immuno-stained sections were mounted on slides and dehydrated, cleared with xylene and cover slipped for imaging and analysis. Slides were scanned with NanoZoomer S60 Automated Digital slide scanner (HAMAMATSU, Australia). Image analysis was done with Image J software (NIH, Bethesda, MD, USA). Primary antibodies and concentrations used in IHC are listed in **Table 1** supplement material.

2.6. Western Blotting analysis

Frozen hemi-brains were homogenized using liquid nitrogen and then sonicated with RIPA buffer (50mM Tris-HCl, 150mM NaCl, 2mM EDTA, 0.1% SDS, 1% Sodium deoxycholate and 1% Nonidet-40) (pH 7.4) at 4°C containing protease and phosphatase cocktail inhibitors. The homogenate was then centrifuged at 15000 rpm for 30 min and the supernatant (RIPA soluble extract) was collected. Total amount of protein was measured using BCA assay

(Bicinchoninic Acid) total protein assay kit. Samples with equal protein concentrations were separated on 10-12% SDS-PAGE and electro-transferred onto 0.2 µm nitrocellulose membranes (GE Healthcare, Life science, Germany). Blots were blocked with 5% milk in Tris-HCl buffer with 0.5% Tween 20 for 1 hour at RT then probed with primary antibodies overnight at 4°C. Blots were then incubated with IRDye conjugated secondary antibodies and imaged using Odyssey® CLx Infrared fluorescent scanner. Image analysis was then done using Image Studio Lite software (Li-COR Bioscience). Primary antibodies and concentrations used in western blotting are listed in **Table 1** supplement material.

2.7. Statistical analysis

Results were represented as mean ± SEM. One-way or two-way analysis of variance (ANOVA) when appropriate followed by Tukey's Multiple Comparison Test or Fisher LSD post-hoc tests were used to analyze behavioral test results between WT, control and treated groups. Unpaired two-tailed t test was used to compare means of two groups (control and treated P301L mice). Analysis was done using GraphPad Prism v 9.0.0 (GraphPad Software). p value < 0.05 was considered statistically significant for all comparisons.

3. Results

3.1. Edaravone improved spatial learning memory of P301L mice in MWM test

To assess the effect of EDR on spatial reference learning, vehicle and EDR treated mice with their WT littermates were tested in MWM. Results showed that the average escape latency during all hidden platform trials did not differ between groups. All groups learned to locate the hidden platform as evident by decrease in latency time during the acquisition phase {14 months (n = 9-14/group): time effect: $F(1.757, 15.81) = 0.9567$; $p = 0.3944$, treatment effect: $F(2, 9) = 0.2654$; $p = 0.7727$, treatment/time effect: $F(6, 27) = 0.3892$; $p = 0.8794$, {25 months [n = 4/group]: time effect: $F(2.748, 24.74) = 1.848$; $p = 0.1681$, treatment effect: $F(2, 9) = 3.746$; $p = 0.0655$, treatment/time effect: $F(6, 27) = 1.656$; $p = 0.1705$} (**Figure 1a** and **1b**). However, EDR treated mice and WT littermates showed reduced average escape latency compared to vehicle controls.

In the probe trial, 14 months old control P301L mice spent less time in the target quadrant zone compared to WT ($F(2,29) = 3.821$; $p = 0.033$) and showed the least number of platform site crossing ($F(2,29) = 0.8158$; $p = 0.452$). EDR treated mice performed better than vehicle controls as there was no difference in the time spent in the target zone between WT and EDR mice ($p = 0.6891$) (**Figure 1c, 1e**). No difference in the time spent in the target zone was found in 25-month-old mice ($F(2,9) = 0.1265$, $p = 0.8827$). However, EDR treated mice showed significantly higher number of platform site crossing compared to vehicle control group ($F(2, 9) = 7.929$; $p = 0.0236$), and nearly equal to WT group ($p = 0.943$). These results suggest that EDR improved acquisition and search accuracy of P301L mice (**Figure 1d, 1f**).

3.2. Edaravone altered the exploratory behavior of P301L mice in open field and elevated plus maze tests

Mice were tested in open field and elevated plus maze to evaluate the effect of Edaravone treatment on anxiety, exploratory and locomotor behavior. In open field test, control 14 months old P301L mice showed significantly longer immobility time % ($F(2,29) = 5.336$, $p = 0.0256$) compared to WT littermates. They also displayed less tendency to explore the central (anxious) zone (less time in central zone) ($F(2,29) = 7.576$, $p = 0.0139$), and travelled less distance ($F(2,29) = 7.307$, $p = 0.005$), with less average speed ($F(2,29) = 7.193$, $p = 0.0046$) compared to WT mice. They also showed less tendency of exploration as evident by reduced rearing behavior ($F(2,29) = 3.947$, $p = 0.038$). EDR treatment did not improve or reverse such behavior in the 14 months old group. The results of immobility time and the time spent in the central

zone were similar among younger mice and no difference was found between vehicle and EDR groups. At the old age group, both control and EDR treated P301L mice spent significantly less time in central zone compared to WT mice ($F(2, 9) = 9.201$; $p = 0.0089$ for control P301L vs WT, $p = 0.0175$ for EDR treated P301L vs WT). But there was no difference between vehicle and EDR treated mice ($p = 0.89$). Also, no significant difference was observed between P301L and WT mice for total distance, average speed, rearing episodes, number of zone transitions (line crossing) and immobility time %, possibly due to small sample size. (**Figure 2a-f**).

In the elevated plus maze task, no significant difference was found between WT and P301L mice at both age groups regarding time (14 months old group: $F(2, 29) = 1.742$; $p = 0.193$, 25 months old group: $F(2, 9) = 2.244$; $p = 0.1619$) and entries to open arms (14 months old group: $F(2, 29) = 2.162$; $p = 0.133$, 25 months old group: $F(2, 9) = 0.855$; $p = 0.457$), distance (14 months old group: $F(2, 29) = 0.5682$; $p = 0.5727$, 25 months old group: $F(2, 9) = 0.965$; $p = 0.417$), and total number of head dips (14 months old group: $F(2, 29) = 2.923$; $p = 0.0697$, 25 months old group: $F(2, 9) = 0.309$; $p = 0.742$). However, we observed that control P301L mice spent more time in the open arms and showed overall higher exportation and spontaneous locomotion. In contrast, EDR treated littermates tended to spend more time in the closed arms similar to WT littermates which may indicate that they can recognize their starting location with more protected head dips. We also found that EDR significantly increased the percentage of protected head dips of P301L mice at 25 months old group compared to vehicle controls ($F(2, 9) = 9.575$; $p = 0.011$ vs controls) (**Figure 2g-k)**.

3.3. Edaravone did not affect the working memory in Y maze novel arm test and spontaneous alternation test

In order to investigate the effect of EDR on spatial and short-term working memory, mice were tested in the Y maze test. In the spontaneous alternation task, all mice in the 14 months old group showed the same percentage of spontaneous alternation ($F(2, 29) = 0.7303$, $p = 0.4904$). However, in that group, WT mice showed more total arm entries compared to control ($F(2, 29) = 4.714$, $p = 0.08$) and significantly more than EDR treated mice ($p = 0.02$). Similarly, in the 25 months old age group, there was no significant difference in spontaneous alternation % among groups ($F(2, 9) = 2.928$, $p = 0.1048$), but control P301L mice showed the highest alternation (70%) while WT and EDR treated mice alternated between 50 and 55%. On the other hand, the total number of arm entries was significantly higher in WT mice compared to control P301L mice ($F(2, 9) = 4.344$, $p = 0.042$), while EDR treatment slightly increased it but the difference was not statistically significant compared to both WT ($p = 0.580$) and vehicle treated mice ($p = 0.199$) (**Figure 3a, b**). In the Y maze novel arm task, there was no significant difference in novel arm time (14 months old group: $F(2, 29) = 0.3917$; $p = 0.679$, 25 months old group: ($F(2, 9) = 1.145$, $p = 0.361$) or entries (14 months old group: $F(2, 29) = 0.08491$; $p = 0.919$, 25 months old group: $F(2, 9) = 0.3302$, $p = 0.727$) between WT and P301L mice in both age groups (**Figure 3c, d**).

3.4. EDR improved the recognition memory in P301L mice

Novel object recognition test was used to evaluate the effect of EDR on the animal tendency to explore novel objects over familiar ones. Results showed that there was no significant difference in the recognition index between groups in the 14 months old group ($F(2, 29) = 0.7909$, $p = 0.4630$). However, in the 25 months old group, control P301L mice showed less interaction with the novel object (RI = 35%) compared to WT mice (RI = 51%) , while EDR significantly improved the recognition memory of P301L treated mice ($F(2, 9) = 5.099$, $p = 0.0269$, RI = 70%) compared to their control littermates and performed even better than WT mice ($p = 0.2429$) (**Figure 4a**).

3.5. EDR attenuated motor deficits in P301L mice

In order to test the effect of EDR on the motor deficits observed in P301L mice, limb clasping test was carried out. In both age groups, control P301L mice showed significantly higher limb clasping score compared to WT (14 months old: $F(2, 29) = 15.20$, $p < 0.0001$, 25 months old: $F(2, 9) = 8.471$, $p = 0.007$) that agrees with previous findings observed in that model [48]. EDR reduced the limb clasping score compared to vehicle controls (14 months old: $p = 0.0217$, 25 months old: $p = 0.1541$) (**Figure 4b**). These results suggest that EDR rescued motor function in P301L mice.

3.6. Effect of EDR on phosphorylated Tau protein levels in P301L mice

To study the effect of EDR treatment on Tau pathology, we did immunostaining and western blotting of whole brain homogenate for epitope pS396 Tau and AT8 (an antibody for phosphorylated Tau at Ser202/Thr205). Given the initial characterization of P301L mice, Tau aggregates can be detected in several brain areas: early in the basolateral nucleus of amygdala (BLA) and later in the hippocampus (<18 months old) [37,35]. The expression of endogenous mouse tau and mutant human tau was detected by mouse tau 5 and HT7 antibodies, respectively. While neurons of WT littermates did not show any immunoreactivity towards HT7 antibody (data not shown). IHC revealed that EDR treatment significantly reduced the immunoreactivity of pS396 in the hippocampus (14 months old: $t(34) = 2.309$, $p = 0.027$; 25 months old: $t(14) = 3.681$, $p = 0.0025$) and amygdala (age = 14 months old: $t(35) = 1.692$, $p = 0.099$, age = 25 months old: $t(14) = 3.681$, $p = 0.0293$) compared to controls (**Figure 5A**, **Figure 7A**). In the same context, western blotting also showed modest reduction in the levels of pS396 and AT8 compared to total HT7, though, seemed to be less sensitive than IHC to detect any change in the total brain homogenate. The expression levels of total mouse tau and mutated human tau were not altered in control and treated mice. But, interestingly, HT7 expression level was significantly reduced in 25 months old EDR treated mice compared to their control littermates ($t(14) = 3.681$, $p < 0.0407$, **Figure 6a** and **Figure 8a**). We also performed two-way ANOVA to compare the hyperphosphorylated Tau protein levels between the two age groups. We found significant increase in levels of pS396 Tau and AT8 in the older age group compared to both vehicle and EDR treated 14 months old P301L mice, that indicated the build-up of the pathology with aging. Interestingly, EDR significantly reduced the levels of pS396 phosphorylated Tau ($F(3, 14) = 17.48$, $p < 0.0001$) and AT8 ($F(3, 14) = 17.12$, $p < 0.0001$) in the 25 months old P301L mice compared to the age matched vehicle controls (please refer to supplement figures 14,15 and 16 in supporting information).

3.7. EDR treatment altered GSK-mediated Tau phosphorylation

To assess the effect of EDR on the activity of Glycogen synthase kinase 3β (GSK-3β), we performed western blotting for the total protein level and its phosphorylated form at Ser9 (pS9-GSK3β). GSK-3β is a serine/threonine kinase and involved in aberrant Tau phosphorylation in neurodegenerative diseases [49,50]. Western blot revealed that P301L mice showed significantly reduced levels of the inactive pS9-GSK3β (inhibited) form to the total protein compared to age matched WT mice in the 14 months old group ($F(2, 23) = 14.38$, $p < 0.0001$), but no difference among all groups in the older age ($F(2, 8) = 0.1093$, $p = 0.8978$). However, total GSK-3β protein levels did not change. On the hand, EDR did not increase the levels of the phosphorylated form of GSK-3β in treated P301L mice compared to vehicle controls. This might indicate that the effect of EDR treatment on Tau hyperphosphorylation is mediated through different mechanisms but not mainly through altering the activity of GSK-3β (**Figure 6b** and **Figure 8b**). Performing Two-way ANOVA for samples run on same gel to compare the levels of pS9-GSK3β among groups of different ages, we found significant increase in the

levels of the phosphorylated form to the total protein levels in the EDR treated older P301L mice compared to age matched vehicle controls and to both vehicle and EDR treated younger P301L mice ($F(3, 14) = 14.74$, $p = 0.0001$ please refer to **supplement figure 19** in supporting information).

3.8. EDR treatment reduced neuroinflammation in the brains of P301L mice

In order to study effect of EDR on neuroinflammation, we examined the expression levels of glial fibrillary acidic protein (GFAP); a marker of astrocytosis and CD45; a leukocyte common antigen and Iba-1; both detect activated microglia. IHC showed that the density of GFAP-immunoreactive astrocytes was reduced in EDR treated mice from 9.4% to 4.7% ($t(6) = 3.760$, $p = 0.0094$) in the hippocampus and from 7.1% to 4.4% in the amygdala ($t(6) = 3.569$, $p = 0.0118$, **Figure 7C**) at 25 months old, and showed a trend towards reduction in the hippocampus of 14 months old group compared to controls ($t(16) = 0.8769$, $p = 0.393$, **Figure 5C**). In addition, EDR also significantly reduced CD45 positive microglia in the brains of old P301L mice ($t(6) = 2.576$, $p = 0.042$, **Figure 7E**). Western blotting of the whole brain homogenate showed subtle changes in GFAP expression levels in both age groups (**Figure 6c** and **Figure 8c**), and significant reduction in Iba-1 expression in 25 months age P301L group compared to age matched controls ($F(2,9) = 6.412$, $p = 0.0186$, **Figure 8c**). These results suggest that EDR oral formulation displayed some anti-inflammatory effects, which is more obvious in the older age group as Tau pathology progresses with aging.

3.9. EDR treatment attenuates loss of synaptic plasticity and protected neurons in the brain of P301L mice

Then, we studied the effect of EDR on the expression levels of some synaptic proteins including post synaptic density-95 (PSD-95), vesicle-associated membrane protein-2 (VAMP-2) and synaptophysin. Immunoblotting results showed that EDR oral formulation significantly increased the expression of synaptophysin in the 14 months old group ($F(3, 22) = 4.947$, $p = 0.0089$ vs age matched controls, two-way ANOVA, supplement Fig. 18), while slightly improved the expression levels of other synaptic proteins (**Figure 6d** and **Figure 8d**). To study the effect of EDR on neuron cell viability, we performed NeuN western blotting and IHC to detect nuclei of mature neurons in aged mice when massive neuron loss is evident. No significant difference was found in NeuN immunoreactivity (calculated as % of area fraction) in all regions of the hippocampus, dentate gyrus (DG) and neocortex of EDR treated P301L mice compared to controls (**Suppl. Fig. 2**), although data showed a trend towards improvement in EDR treated mice. Western blotting also showed no differences in NeuN protein expression between WT, controls and EDR treated in both age groups (**Figure 6c** and **Figure 8c**). These results might suggest that EDR oral formulation was able to improve synaptic function and, to some extent, inhibit neurotoxicity in aged P301L mice.

3.10. EDR alleviates oxidative stress in P301L mice.

4-hydroxynonenal (4-HNE) and 3-nitrotyrosine (3-NT) protein adducts are considered biomarkers of oxidative and nitrosative damage [51,52]. Results showed that EDR produced small but significant reduction in the levels of 4-HNE (**Figure 6t**, $t(16) = 6.728$, $p < 0.0001$, 14 months old) and 3-nitrotyrosin (3-NT) (**Figure 8t**, $t(6) = 5.979$, $p = 0.001$, 25 months old) in the brains P301L mice as evident by western blotting.

4. Discussion

OS is a key component of the pathophysiology of several neurodegenerative disorders [33,40,53]. Accumulation of OS markers and activation of antioxidant defences has been reported in patients and directly correlates with the age and disease progression [16,18]. Similar

findings were obtained from animal models of dementia [54]. Tau aggregate is a primary culprit in AD and tauopathies. Studies revealed that there is a strong relationship between OS and abnormal Tau aggregation [55]. *In vitro* studies showed that 4-HNE and lipid peroxide products could facilitate Tau polymerization and aggregation [56,57] and can alter the expression of kinases in favor of Tau hyperphosphorylation [22,58]. Also, nitro-tyrosine residues have been found colocalized with NFT in the brain of AD patients [59]. In addition, hyperphosphorylated Tau can provoke OS by altering the mitochonderial dynamics and microglial activation. This cycle results in cascade of events that eventually lead to cell death [60-62]. Therefore, it is assumed that targeting oxidative stress pathways could result in blocking multiple cascades involved in disease pathogenesis and therefore halt the disease progression.

EDR is a potent antioxidant and free radical scavenger. It can penetrate the blood brain barrier (BBB) where it acts centrally by reducing the oxidative injury in neurons through eliminating free radicals and lipid peroxidation products [63-66]. EDR also showed neuroprotective effects and suppressed proinflammatory responses following brain ischemia [67,68]. Thus, in the present work, we aimed to investigate if EDR treatment for a 3-months period could alleviate cognitive deficits and Tau pathology in P301L mice.

To achieve our goal, we used a novel oral formulation of Edaravone that was previously designed by Parikh et al [41]. Edaravone exhibits poor oral bioavailability (5.23%) [69] that requires its administration trough intravenous route. Parikh et al. developed a novel oral formulation using self-nano-micellizing solid dispersion of EDR and Soluplus as a drug carrier in a ratio of 1:5. EDR/Soluplus formulation displayed high aqueous solubility and enhanced oral bioavailability of EDR by 10.2-, 16.1-, and 14.8-fold compared to EDR suspension at 46, 138, and 414 µmol/kg doses in rats. Authors also reported that effective micellar encapsulation of EDR by Soluplus reduced the intestinal metabolic degradation of the drug and inhibited P-glycoprotein efflux, which could explain the improved oral bioavailability of this formulation. Furthermore, this formulation was assessed *in vivo* and was found to be able to alleviate cognitive deficits of 17 months old AD mice in a dose dependent manner [34].

Therefore, in this study, P301L mice were treated with the EDR formulation at a dose of 24 mg/kg/day dissolved in drinking water for 3 months. This approach was more acceptable than daily EDR injection or gavage in terms of animal welfare as it will not impact the animal behavior or cause any stress. P301L mice showed impaired spatial reference memory in MWM that deteriorate with aging. EDR improved the spatial learning by reducing the escape latency and significantly improved the accuracy to locate the platform in the probe trial as evident by increased number of platform site crossing in old P301L mice. This indicates that EDR preserved the cognitive function at that age. In line with these results, we found that EDR significantly increased the recognition index in NORT in old P301L mice, suggesting that EDR rescued the working memory in old mice when it is severely impaired. However, no difference was found between animals in the 14 months old group and may indicate intact working memory at that age.

In the open field test, P301L mice showed more anxiety and less exploratory behavior, however, EDR did not reduce such anxiety. Results from EPM were not consistent with those of the open field. In that test, control P301L mice seemed to be less anxious than WT and EDR treated littermates in both age groups. They visited the open arms more frequently and displayed more unprotected head dips. These results agree with previous findings showing that P301L mice exhibited modest disinhibition of exploratory behavior that becomes more pronounced with aging [35,70] and is accompanied by reduced anxiety levels. Such behavior

suggests the presence of abnormality in amygdala-dependent tasks and most likely due to Tau accumulation in this region of the brain. Interestingly, EDR treated mice behaved more similarly to WT littermates, which might suggest that EDR could partially reverse the amygdala dysfunction.

In Y maze spontaneous alternation, all animals alternated similarly, however, P301L mice showed fewer number of total arm entries than WT littermates. EDR significantly increased the number of total arm entries in old P301L mice. Similarly, no significant difference was found between animals in the Y maze novel arm test, that agrees with previous reports indicating intact spatial working memory in younger P301L mice (at 6 and 11 months of age) [35]. In line with previous reports, P301L mice showed minor motor impairment as evident by increased limb clasping score [37]. EDR treatment reduced the limb clasping score in both age groups, an indication of improved motor function following EDR treatment. This result is consistent with human studies in amyotrophic lateral sclerosis (ALS) which show the efficacy in the improvement of motor functions [32,71]. Our data in the present study suggest that the oral EDR formula may be more compliant to treat ALS patients than the injection formula.

EDR produced modest reduction in phosphorylation of both murine and mutant human Tau at different epitopes in CA1 region of the hippocampus and BLA of the amygdala. Further immunoblotting analysis revealed slightly increased levels of pS9-GSK3β which is the inactivated form of GSK-3β, a main kinase involved in abnormal Tau phosphorylation. Therefore, it is expected that Edaravone reduced Tau phosphorylation through inhibiting GSK-3β kinase activity. However, given that no significant difference was found in the levels of pS9-GSK between control and EDR treated mice, further investigation is required to study the effect of EDR on Tau phosphorylation and its mechanisms of action.

We also found a significant reduction in oxidative and nitrosative stress as evident by reduced levels of 4-HNE and 3-NT modified proteins in the brain of EDR treated mice. Therefore, it is likely that EDR suppresses tau hyperphosphorylation by attenuation of oxidative stress and OS-induced inflammation.

Activated astrocytes and microglia accompany Tau lesions [72] and directly correlate with the extent of cognitive decline [73]. EDR treatment reduced GFAP expression in different brain regions and microgliosis in old mice as evident in IHC and western blotting. We also found that EDR improved the levels of synaptic proteins in both age groups. Our results are supported by previous findings showing that EDR injection significantly attenuated neuroinflammation and improved synaptic plasticity in AD mice [33]. The anti-inflammatory effect of EDR could result from inhibition of abnormal Tau phosphorylation with subsequent improvement in synaptic function. In addition, the number of mature neurons in the brain of 25 months old treated mice showed a trend towards increase in all regions of the hippocampus, DG, and neocortex. These results might indicate the neuroprotective effect of EDR against oxidative neurotoxicity and agree with previous studies [68]. The neuroprotective activity of EDR could be attributed to its antioxidant and indirect anti-inflammatory effects.
In summary, we reported that treatment with oral Edaravone formulation was able to improve both memory and motor functions in P301L mice and reduce tau phosphorylation. We believe that the effect of EDR was significant at advanced ages in that model possibly because the OS and mitochondrial dysfunction become significant and obvious in P301L transgene as a result of Tau pathology aggravation as previously reported by David et. al [40]. These results clearly support the possible use of Edaravone to alleviate FTD.

However, this study has few limitations. First, the limited number of animals included in the old group. Second, only one therapeutic dose has been used although the maximal effect at the dose of 24 mg/kg/day was achieved in APP/PS1 mice in our previous study [34].

5. Conclusion

Herein, we highlighted the benefits of the anti-stroke drug Edaravone for the therapy of AD and other tauopathies by targeting multiple key pathways including OS, Tau phosphorylation and neuroinflammation. EDR as intravenous injection has proven to be clinically safe and effective for ALS and ischemic stroke, and our study further supports its efficacy in prevention and treatment of other neurodegenerative disorders. Besides, the oral drug administration is expected to be more convenient and safer than IV injection. Therefore, clinical trials are required to approve the efficacy of EDR and its effective doses in dementia and other oxidative stress-related diseases.

Acknowledgement

The authors would like to acknowledge the Research Training Program (RTP) scholarship (Australia) and Egyptian Ministry of Higher Education to support SK and NHMRC Fellowship grant to XFZ. The authors would like to acknowledge H Md Morshed Alam (BASF Australia Ltd) for providing samples of Soluplus, and Suzhou Auzone Biotech for the Edaravone formulation.

Conflict of interest

XFZ is one of the inventors of Chinese patent 200610149832.9. The authors report no other conflicts of interest in this work.

References:

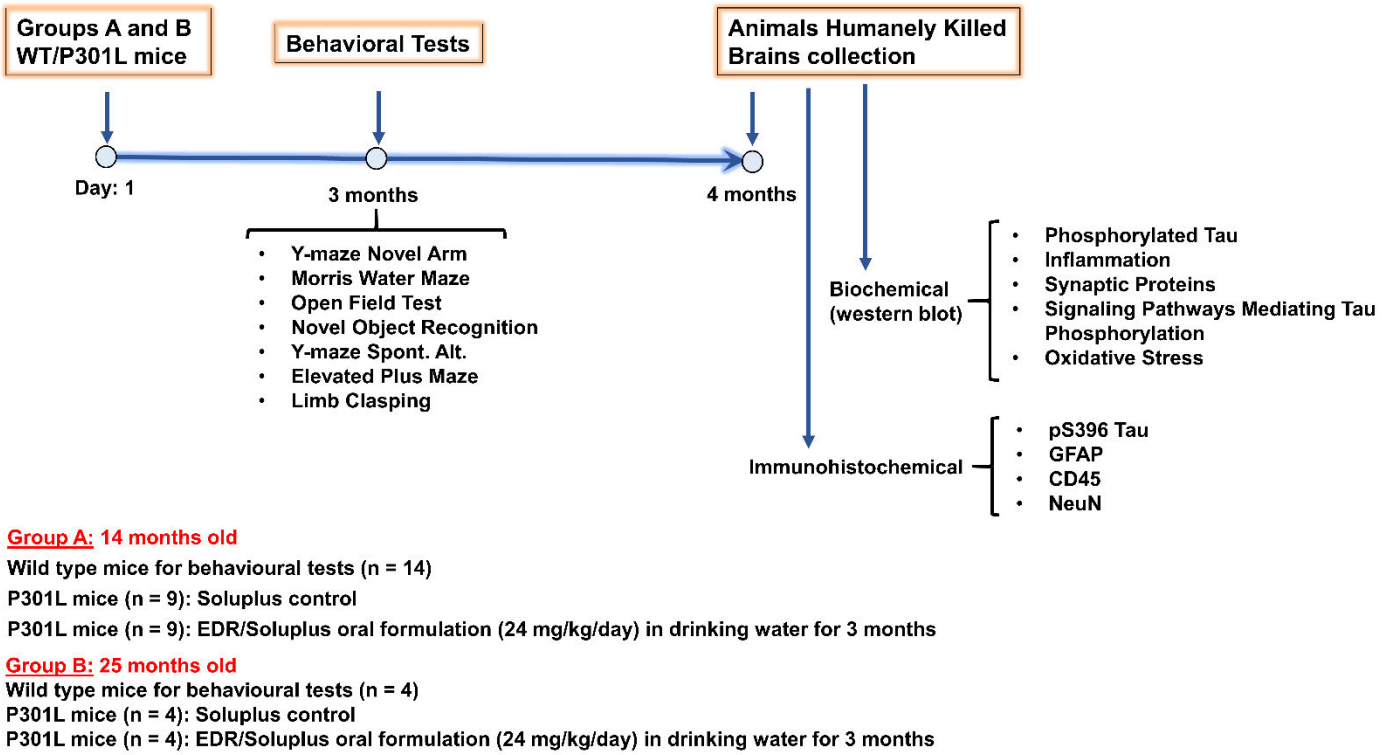
1. Orr ME, Sullivan AC, Frost B (2017) A Brief Overview of Tauopathy: Causes, Consequences, and Therapeutic Strategies. Trends Pharmacol Sci 38 (7):637-648. doi:10.1016/j.tips.2017.03.011
2. Götz J, Halliday G, Nisbet R (2019) Molecular Pathogenesis of the Tauopathies. Annual Review of Pathology: Mechanisms of Disease 14. doi:10.1146/annurev-pathmechdis-012418-012936
3. Wang Y, Mandelkow E (2016) Tau in physiology and pathology. Nature reviews Neuroscience 17 (1):5-21. doi:10.1038/nrn.2015.1
4. Poorkaj P, Bird TD, Wijsman E, Nemens E, Garruto RM, Anderson L, Andreadis A, Wiederholt WC, Raskind M, Schellenberg GD (1998) Tau is a candidate gene for chromosome 17 frontotemporal dementia. Ann Neurol 43 (6):815-825. doi:10.1002/ana.410430617
5. Rudenko LK, Wallrabe H, Periasamy A, Siller KH, Svindrych Z, Seward ME, Best MN, Bloom GS (2019) Intraneuronal Tau Misfolding Induced by Extracellular Amyloid-β Oligomers. Journal of Alzheimer's Disease 71:1125-1138. doi:10.3233/JAD-190226
6. Gabbita SP, Scheff SW, Menard RM, Roberts K, Fugaccia I, Zemlan FP (2005) Cleaved-tau: a biomarker of neuronal damage after traumatic brain injury. J Neurotrauma 22 (1):83-94. doi:10.1089/neu.2005.22.83
7. Yarchoan M, Toledo JB, Lee EB, Arvanitakis Z, Kazi H, Han L-Y, Louneva N, Lee VMY, Kim SF, Trojanowski JQ, Arnold SE (2014) Abnormal serine phosphorylation of insulin receptor substrate 1 is associated with tau pathology in Alzheimer's disease and tauopathies. Acta Neuropathol 128 (5):679-689. doi:10.1007/s00401-014-1328-5
8. Cherry JD, Tripodis Y, Alvarez VE, Huber B, Kiernan PT, Daneshvar DH, Mez J, Montenigro PH, Solomon TM, Alosco ML, Stern RA, McKee AC, Stein TD (2016) Microglial neuroinflammation contributes to tau accumulation in chronic traumatic encephalopathy. Acta neuropathologica communications 4 (1):112-112. doi:10.1186/s40478-016-0382-8
9. Dias-Santagata D, Fulga TA, Duttaroy A, Feany MB (2007) Oxidative stress mediates tau-induced neurodegeneration in Drosophila. J Clin Invest 117 (1):236-245. doi:10.1172/jci28769
10. Mecocci P, Polidori MC (2012) Antioxidant clinical trials in mild cognitive impairment and Alzheimer's disease. Biochimica et Biophysica Acta (BBA) - Molecular Basis of Disease 1822 (5):631-638. doi:https://doi.org/10.1016/j.bbadis.2011.10.006
11. Nakashima H, Ishihara T, Yokota O, Terada S, Trojanowski JQ, Lee VM, Kuroda S (2004) Effects of alpha-tocopherol on an animal model of tauopathies. Free radical biology & medicine 37 (2):176-186. doi:10.1016/j.freeradbiomed.2004.04.037
12. Sies H (1997) Oxidative stress: oxidants and antioxidants. Exp Physiol 82 (2):291-295. doi:10.1113/expphysiol.1997.sp004024
13. Martindale JL, Holbrook NJ (2002) Cellular response to oxidative stress: Signaling for suicide and survival*. Journal of Cellular Physiology 192 (1):1-15. doi:10.1002/jcp.10119
14. Stadtman ER (1992) Protein oxidation and aging. Science 257 (5074):1220-1224. doi:10.1126/science.1355616
15. Coyle JT, Puttfarcken P (1993) Oxidative stress, glutamate, and neurodegenerative disorders. Science 262 (5134):689-695. doi:10.1126/science.7901908
16. Albers DS, Augood SJ, Martin DM, Standaert DG, Vonsattel JPG, Beal MF (1999) Evidence for Oxidative Stress in the Subthalamic Nucleus in Progressive Supranuclear Palsy. Journal of Neurochemistry 73 (2):881-884. doi:10.1046/j.1471-4159.1999.0730881.x
17. Barber SC, Shaw PJ (2010) Oxidative stress in ALS: key role in motor neuron injury and therapeutic target. Free Radic Biol Med 48 (5):629-641. doi:10.1016/j.freeradbiomed.2009.11.018

18. Su B, Wang X, Nunomura A, Moreira PI, Lee Hg, Perry G, Smith MA, Zhu X (2008) Oxidative stress signaling in Alzheimer's disease. Current Alzheimer research 5 (6):525-532. doi:10.2174/156720508786898451
19. Smith CD, Carney JM, Starke-Reed PE, Oliver CN, Stadtman ER, Floyd RA, Markesbery WR (1991) Excess brain protein oxidation and enzyme dysfunction in normal aging and in Alzheimer disease. Proceedings of the National Academy of Sciences of the United States of America 88 (23):10540-10543. doi:10.1073/pnas.88.23.10540
20. Subbarao KV, Richardson JS, Ang LC (1990) Autopsy samples of Alzheimer's cortex show increased peroxidation in vitro. J Neurochem 55 (1):342-345. doi:10.1111/j.1471-4159.1990.tb08858.x
21. Alavi Naini SM, Soussi-Yanicostas N (2015) Tau Hyperphosphorylation and Oxidative Stress, a Critical Vicious Circle in Neurodegenerative Tauopathies? Oxidative Medicine and Cellular Longevity 2015:151979. doi:10.1155/2015/151979
22. Lovell MA, Xiong S, Xie C, Davies P, Markesbery WR (2004) Induction of hyperphosphorylated tau in primary rat cortical neuron cultures mediated by oxidative stress and glycogen synthase kinase-3. J Alzheimers Dis 6 (6):659-671; discussion 673-681. doi:10.3233/jad-2004-6610
23. Goedert M, Hasegawa M, Jakes R, Lawler S, Cuenda A, Cohen P (1997) Phosphorylation of microtubule-associated protein tau by stress-activated protein kinases. FEBS Letters 409 (1):57-62. doi:https://doi.org/10.1016/S0014-5793(97)00483-3
24. Mondragón-Rodríguez S, Perry G, Zhu X, Moreira PI, Acevedo-Aquino MC, Williams S (2013) Phosphorylation of tau protein as the link between oxidative stress, mitochondrial dysfunction, and connectivity failure: implications for Alzheimer's disease. Oxidative medicine and cellular longevity 2013:940603-940603. doi:10.1155/2013/940603
25. Wang L, Jiang Q, Chu J, Lin L, Li X-G, Chai G-S, Wang Q, Wang J-Z, Tian Q (2013) Expression of Tau40 Induces Activation of Cultured Rat Microglial Cells. Plos One 8 (10)
26. Rajasekar N, Dwivedi S, Tota SK, Kamat PK, Hanif K, Nath C, Shukla R (2013) Neuroprotective effect of curcumin on okadaic acid induced memory impairment in mice. Eur J Pharmacol 715 (1-3):381-394. doi:10.1016/j.ejphar.2013.04.033
27. Elipenahli C, Stack C, Jainuddin S, Gerges M, Yang L, Starkov A, Beal MF, Dumont M (2012) Behavioral Improvement after Chronic Administration of Coenzyme Q10 in P301S Transgenic Mice. Journal of Alzheimer's Disease 28:173-182. doi:10.3233/JAD-2011-111190
28. Sancheti H, Kanamori K, Patil I, Díaz Brinton R, Ross BD, Cadenas E (2014) Reversal of metabolic deficits by lipoic acid in a triple transgenic mouse model of Alzheimer's disease: a 13C NMR study. J Cereb Blood Flow Metab 34 (2):288-296. doi:10.1038/jcbfm.2013.196
29. Mecocci P, Polidori MC (2012) Antioxidant clinical trials in mild cognitive impairment and Alzheimer's disease. Biochim Biophys Acta 1822 (5):631-638. doi:10.1016/j.bbadis.2011.10.006
30. Yoshida H, Yanai H, Namiki Y, Fukatsu-Sasaki K, Furutani N, Tada N (2006) Neuroprotective Effects of Edaravone: a Novel Free Radical Scavenger in Cerebrovascular Injury. CNS Drug Reviews 12 (1):9-20. doi:10.1111/j.1527-3458.2006.00009.x
31. Feng S, Yang Q, Liu M, Li W, Yuan W, Zhang S, Wu B, Li J (2011) Edaravone for acute ischaemic stroke. Cochrane Database Syst Rev (12):Cd007230. doi:10.1002/14651858.CD007230.pub2
32. Yoshino H (2019) Edaravone for the treatment of amyotrophic lateral sclerosis. Expert Rev Neurother 19 (3):185-193. doi:10.1080/14737175.2019.1581610
33. Jiao S-S, Yao X-Q, Liu Y-H, Wang Q-H, Zeng F, Lu J-J, Liu J, Zhu C, Shen L-L, Liu C-H, Wang Y-R, Zeng G-H, Parikh A, Chen J, Liang C-R, Xiang Y, Bu X-L, Deng J, Li J, Xu J, Zeng Y-Q, Xu X, Xu H-W, Zhong J-H, Zhou H-D, Zhou X-F, Wang Y-J (2015) Edaravone

alleviates Alzheimer's disease-type pathologies and cognitive deficits. Proc Natl Acad Sci U S A 112 (16):5225-5230. doi:10.1073/pnas.1422998112
34. Parikh A, Kathawala K, Li J, Chen C, Shan Z, Cao X, Wang Y-J, Garg S, Zhou X-F (2018) Self-nanomicellizing solid dispersion of edaravone: part II: in vivo assessment of efficacy against behavior deficits and safety in Alzheimer's disease model. Drug Des Devel Ther 12:2111-2128. doi:10.2147/DDDT.S161944
35. Pennanen L, Wolfer DP, Nitsch RM, Götz J (2006) Impaired spatial reference memory and increased exploratory behavior in P301L tau transgenic mice. Genes, Brain and Behavior 5 (5):369-379. doi:10.1111/j.1601-183X.2005.00165.x
36. Ramsden M, Kotilinek L, Forster C, Paulson J, McGowan E, SantaCruz K, Guimaraes A, Yue M, Lewis J, Carlson G, Hutton M, Ashe KH (2005) Age-Dependent Neurofibrillary Tangle Formation, Neuron Loss, and Memory Impairment in a Mouse Model of Human Tauopathy (P301L). The Journal of Neuroscience 25 (46):10637-10647. doi:10.1523/jneurosci.3279-05.2005
37. Götz J, Chen F, Barmettler R, Nitsch RM (2001) Tau filament formation in transgenic mice expressing P301L tau. J Biol Chem 276 (1):529-534. doi:10.1074/jbc.M006531200
38. Dutschmann M, Menuet C, Stettner GM, Gestreau C, Borghgraef P, Devijver H, Gielis L, Hilaire G, Van Leuven F (2010) Upper airway dysfunction of Tau-P301L mice correlates with tauopathy in midbrain and ponto-medullary brainstem nuclei. J Neurosci 30 (5):1810-1821. doi:10.1523/jneurosci.5261-09.2010
39. Hampton AL, Hish GA, Aslam MN, Rothman ED, Bergin IL, Patterson KA, Naik M, Paruchuri T, Varani J, Rush HG (2012) Progression of ulcerative dermatitis lesions in C57BL/6Crl mice and the development of a scoring system for dermatitis lesions. J Am Assoc Lab Anim Sci 51 (5):586-593
40. David DC, Hauptmann S, Scherping I, Schuessel K, Keil U, Rizzu P, Ravid R, Dröse S, Brandt U, Müller WE, Eckert A, Götz J (2005) Proteomic and functional analyses reveal a mitochondrial dysfunction in P301L tau transgenic mice. J Biol Chem 280 (25):23802-23814. doi:10.1074/jbc.M500356200
41. Parikh A, Kathawala K, Tan CC, Garg S, Zhou X-F (2018) Self-nanomicellizing solid dispersion of edaravone: part I - oral bioavailability improvement. Drug Des Devel Ther 12:2051-2069. doi:10.2147/DDDT.S161940
42. Shamma RN, Basha M (2013) Soluplus®: A novel polymeric solubilizer for optimization of Carvedilol solid dispersions: Formulation design and effect of method of preparation. Powder Technology 237:406-414. doi:https://doi.org/10.1016/j.powtec.2012.12.038
43. Morris RG, Garrud P, Rawlins JN, O'Keefe J (1982) Place navigation impaired in rats with hippocampal lesions. Nature 297 (5868):681-683. doi:10.1038/297681a0
44. Wolf A, Bauer B, Abner EL, Ashkenazy-Frolinger T, Hartz AM (2016) A Comprehensive Behavioral Test Battery to Assess Learning and Memory in 129S6/Tg2576 Mice. PLoS One 11 (1):e0147733. doi:10.1371/journal.pone.0147733
45. Lewis J, McGowan E, Rockwood J, Melrose H, Nacharaju P, Van Slegtenhorst M, Gwinn-Hardy K, Paul Murphy M, Baker M, Yu X, Duff K, Hardy J, Corral A, Lin WL, Yen SH, Dickson DW, Davies P, Hutton M (2000) Neurofibrillary tangles, amyotrophy and progressive motor disturbance in mice expressing mutant (P301L) tau protein. Nature genetics 25 (4):402-405. doi:10.1038/78078
46. Burrell JR, Kiernan MC, Vucic S, Hodges JR (2011) Motor Neuron dysfunction in frontotemporal dementia. Brain 134 (9):2582-2594. doi:10.1093/brain/awr195
47. Aggarwal NT, Wilson RS, Beck TL, Bienias JL, Bennett DA (2006) Motor Dysfunction in Mild Cognitive Impairment and the Risk of Incident Alzheimer Disease. Archives of Neurology 63 (12):1763-1769. doi:10.1001/archneur.63.12.1763

48. Lewis J, McGowan E, Rockwood J, Melrose H, Nacharaju P, Van Slegtenhorst M, Gwinn-Hardy K, Murphy MP, Baker M, Yu X, Duff K, Hardy J, Corral A, Lin W-L, Yen S-H, Dickson DW, Davies P, Hutton M (2000) Neurofibrillary tangles, amyotrophy and progressive motor disturbance in mice expressing mutant (P301L) tau protein. Nature genetics 25 (4):402-405. doi:10.1038/78078
49. Hernandez F, Lucas JJ, Avila J (2013) GSK3 and tau: two convergence points in Alzheimer's disease. J Alzheimers Dis 33 Suppl 1:S141-144. doi:10.3233/jad-2012-129025
50. Köhler C, Dinekov M, Götz J (2013) Active glycogen synthase kinase-3 and tau pathology-related tyrosine phosphorylation in pR5 human tau transgenic mice. Neurobiol Aging 34 (5):1369-1379. doi:10.1016/j.neurobiolaging.2012.11.010
51. Ahsan H (2013) 3-Nitrotyrosine: A biomarker of nitrogen free radical species modified proteins in systemic autoimmunogenic conditions. Hum Immunol 74 (10):1392-1399. doi:10.1016/j.humimm.2013.06.009
52. Dalleau S, Baradat M, Guéraud F, Huc L (2013) Cell death and diseases related to oxidative stress:4-hydroxynonenal (HNE) in the balance. Cell Death & Differentiation 20 (12):1615-1630. doi:10.1038/cdd.2013.138
53. Dumont M, Stack C, Elipenahli C, Jainuddin S, Gerges M, Starkova NN, Yang L, Starkov AA, Beal F (2011) Behavioral deficit, oxidative stress, and mitochondrial dysfunction precede tau pathology in P301S transgenic mice. FASEB J 25 (11):4063-4072. doi:10.1096/fj.11-186650
54. Götz J, Ittner LM (2008) Animal models of Alzheimer's disease and frontotemporal dementia. Nature Reviews Neuroscience 9 (7):532-544. doi:10.1038/nrn2420
55. Haque MM, Murale DP, Kim YK, Lee J-S (2019) Crosstalk between Oxidative Stress and Tauopathy. Int J Mol Sci 20 (8):1959. doi:10.3390/ijms20081959
56. Gamblin TC, King ME, Kuret J, Berry RW, Binder LI (2000) Oxidative Regulation of Fatty Acid-Induced Tau Polymerization. Biochemistry 39 (46):14203-14210. doi:10.1021/bi001876l
57. Pérez M, Cuadros R, Smith MA, Perry G, Avila J (2000) Phosphorylated, but not native, tau protein assembles following reaction with the lipid peroxidation product, 4-hydroxy-2-nonenal. FEBS letters 486 (3):270-274. doi:10.1016/s0014-5793(00)02323-1
58. Lee K-Y, Koh S-H, Noh MY, Park K-W, Lee YJ, Kim SH (2007) Glycogen synthase kinase-3β activity plays very important roles in determining the fate of oxidative stress-inflicted neuronal cells. Brain Research 1129:89-99. doi:https://doi.org/10.1016/j.brainres.2006.10.055
59. Good PF, Werner P, Hsu A, Olanow CW, Perl DP (1996) Evidence of neuronal oxidative damage in Alzheimer's disease. Am J Pathol 149 (1):21-28
60. Stamer K, Vogel R, Thies E, Mandelkow E, Mandelkow E-M (2002) Tau blocks traffic of organelles, neurofilaments, and APP vesicles in neurons and enhances oxidative stress. Journal of Cell Biology 156 (6):1051-1063. doi:10.1083/jcb.200108057
61. Cente M, Filipcik P, Pevalova M, Novak M (2006) Expression of a truncated tau protein induces oxidative stress in a rodent model of tauopathy. European Journal of Neuroscience 24 (4):1085-1090. doi:10.1111/j.1460-9568.2006.04986.x
62. DuBoff B, Götz J, Feany MB (2012) Tau promotes neurodegeneration via DRP1 mislocalization in vivo. Neuron 75 (4):618-632. doi:10.1016/j.neuron.2012.06.026
63. Watanabe T, Yuki S, Egawa M, Nishi H (1994) Protective effects of MCI-186 on cerebral ischemia: possible involvement of free radical scavenging and antioxidant actions. J Pharmacol Exp Ther 268 (3):1597-1604
64. Yamamoto T, Yuki S, Watanabe T, Mitsuka M, Saito KI, Kogure K (1997) Delayed neuronal death prevented by inhibition of increased hydroxyl radical formation in a transient cerebral ischemia. Brain research 762 (1-2):240-242. doi:10.1016/s0006-8993(97)00490-3

65. Watanabe K, Tanaka M, Yuki S, Hirai M, Yamamoto Y (2018) How is edaravone effective against acute ischemic stroke and amyotrophic lateral sclerosis? J Clin Biochem Nutr 62 (1):20-38. doi:10.3164/jcbn.17-62
66. Yamamoto Y, Kuwahara T, Watanabe K, Watanabe K (1996) Antioxidant activity of 3-methyl-1-phenyl-2-pyrazolin-5-one. Redox Rep 2 (5):333-338. doi:10.1080/13510002.1996.11747069
67. Watanabe T, Tahara M, Todo S (2008) The Novel Antioxidant Edaravone: From Bench to Bedside. Cardiovascular Therapeutics 26 (2):101-114. doi:10.1111/j.1527-3466.2008.00041.x
68. Banno M, Mizuno T, Kato H, Zhang G, Kawanokuchi J, Wang J, Kuno R, Jin S, Takeuchi H, Suzumura A (2005) The radical scavenger edaravone prevents oxidative neurotoxicity induced by peroxynitrite and activated microglia. Neuropharmacology 48 (2):283-290. doi:10.1016/j.neuropharm.2004.10.002
69. Rong W-T, Lu Y-P, Tao Q, Guo M, Lu Y, Ren Y, Yu S-Q (2014) Hydroxypropyl-Sulfobutyl-β-Cyclodextrin Improves the Oral Bioavailability of Edaravone by Modulating Drug Efflux Pump of Enterocytes. Journal of Pharmaceutical Sciences 103 (2):730-742. doi:https://doi.org/10.1002/jps.23807
70. Cook C, Dunmore JH, Murray ME, Scheffel K, Shukoor N, Tong J, Castanedes-Casey M, Phillips V, Rousseau L, Penuliar MS, Kurti A, Dickson DW, Petrucelli L, Fryer JD (2014) Severe amygdala dysfunction in a MAPT transgenic mouse model of frontotemporal dementia. Neurobiol Aging 35 (7):1769-1777. doi:10.1016/j.neurobiolaging.2013.12.023
71. Sinha M, Hk A, Juyal R, Shukla R, Garg RK, Am D, Dm K (2009) Edaravone in acute ischemic stroke, An Indian experience. Neurology Asia 14
72. Thangavel R, Stolmeier D, Yang X, Anantharam P, Zaheer A (2012) Expression of glia maturation factor in neuropathological lesions of Alzheimer's disease. Neuropathology and Applied Neurobiology 38 (6):572-581. doi:10.1111/j.1365-2990.2011.01232.x
73. Kashon ML, Ross GW, O'Callaghan JP, Miller DB, Petrovitch H, Burchfiel CM, Sharp DS, Markesbery WR, Davis DG, Hardman J, Nelson J, White LR (2004) Associations of cortical astrogliosis with cognitive performance and dementia status. Journal of Alzheimer's Disease 6 (6):595-604. doi:10.3233/jad-2004-6604



Scheme 1: Schematic illustration of the study design showing animal groups, behavioral tests performed and different biochemical and immunohistochemical analysis.

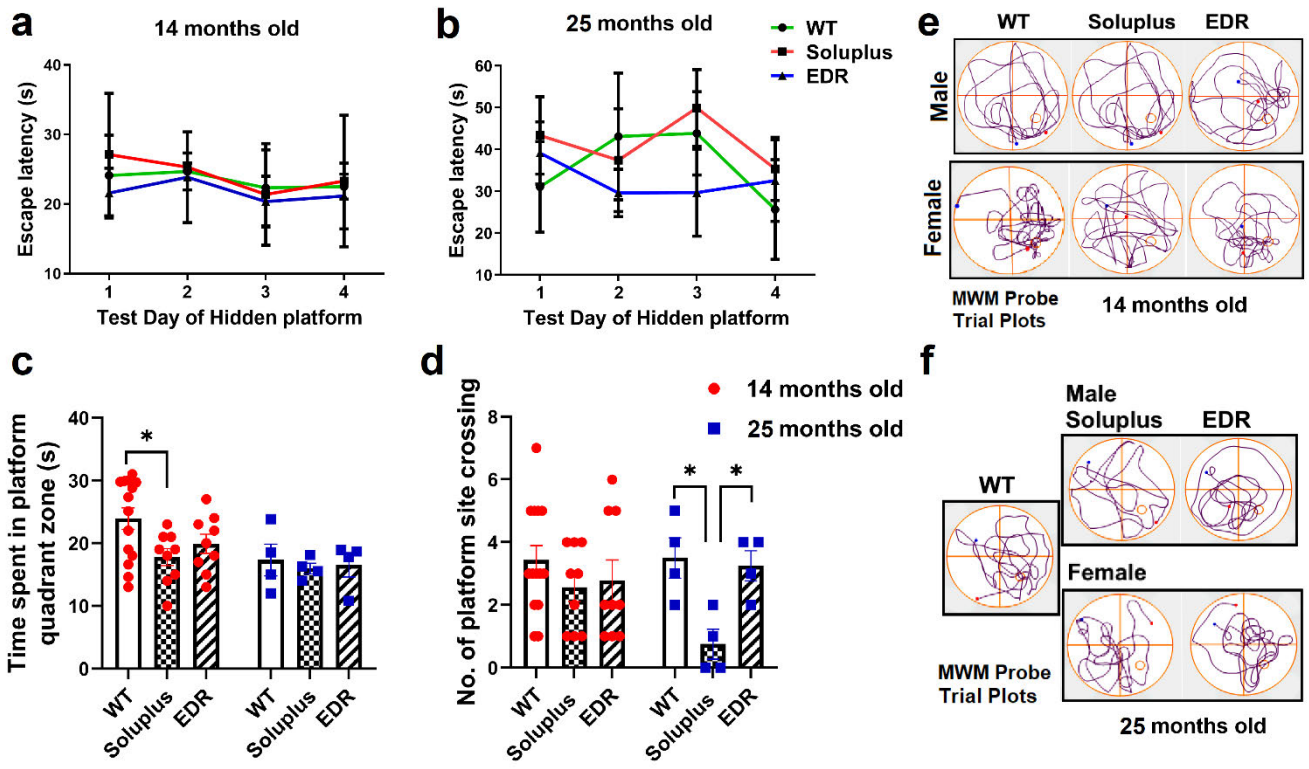


Figure 1 Acquisition learning and Probe trial in MWM test. (**a, b**) Hidden platform trials showing that both vehicle and EDR treated P301L mice in the 14 months old (**a**) and 25 months old group (**b**) learned to locate the hidden platform as shown by reduced escape latencies in the acquisition phase. Two-way ANOVA revealed no significant reduction of escape latency at day 4 compared to day 1 in all groups. In the 25 months old group (**b**), EDR treated mice showed more reduction in escape latency compared to WT and their control littermates, however, the difference was not significant. (**c, d**) (**e, f**) The track plots of the probe trial showing that EDR increased the time spent in the target quadrant zone, where the platform was previously hidden, and the number of platform site crossing. All data are presented as mean ± SEM. *means significant difference, $p < 0.05$ (one-way ANOVA), n = 9-14/group at 14 months; n = 4/group at 25 months. Two-way ANOVA was used to analyse data for the escape latency during hidden platform trials (Panel a, b).

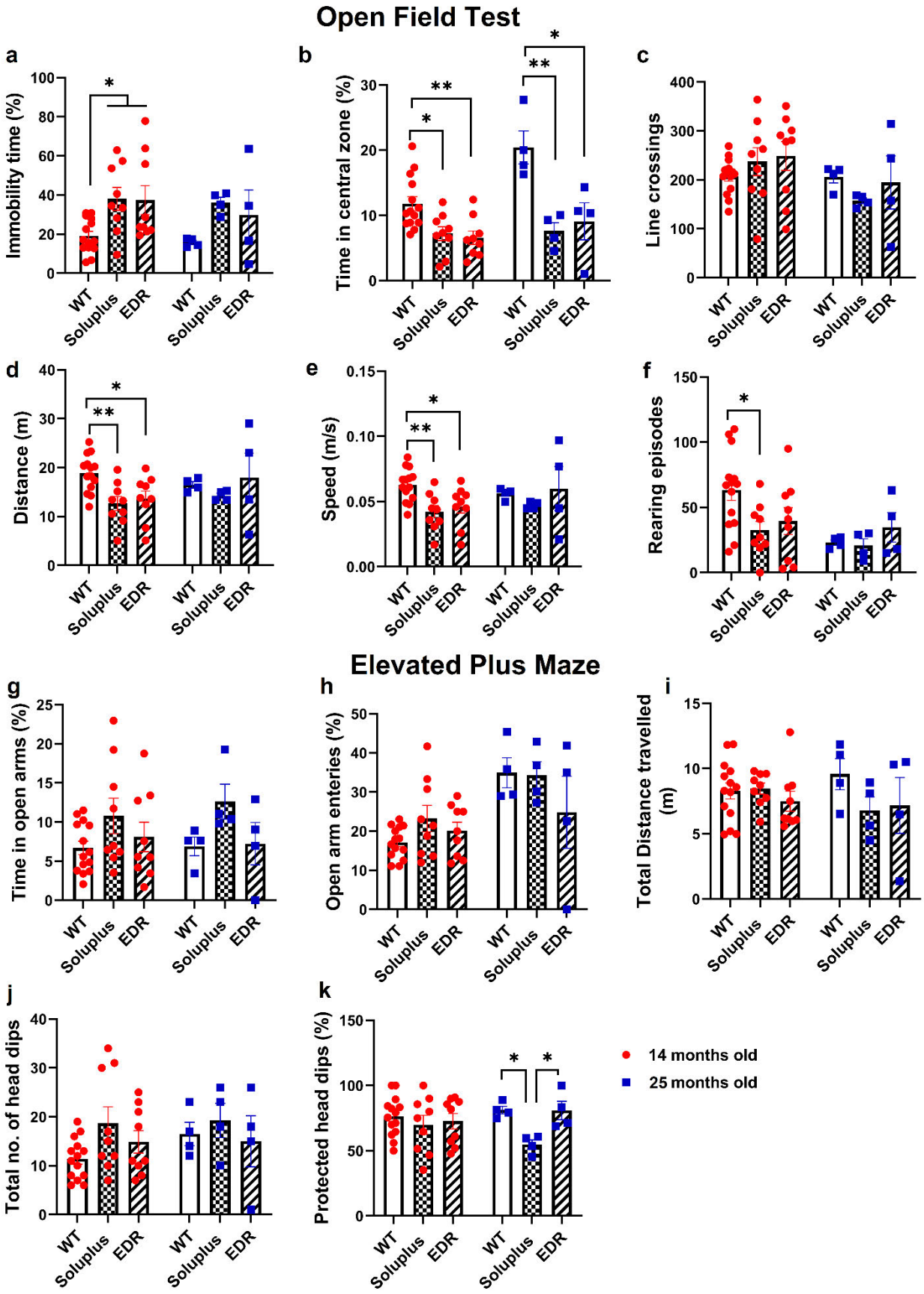

Open Field Test
a
Immobility time (%)
b
Time in central zone (%)
c
Line crossings
d
Distance (m)
e
Speed (m/s)
f
Rearing episodes
Elevated Plus Maze
g
Time in open arms (%)
h
Open arm enteries (%)
i
Total Distance travelled (m)
j
Total no. of head dips
k
Protected head dips (%)
WT
Soluplus
EDR
14 months old
25 months old

Figure 2 Open field and Elevated plus maze task. (**a-f**) Effect of EDR on anxiety and exploration of P301L mice in the open field task. Control P301L mice showed increased anxiety levels compared to WT littermates. EDR improved the exploratory behavior as evident by increasing the number of rearing episodes, and slightly improved the anxiety levels **(a)** Percentage of time spent immobile, **(b)** percentage of time spent in central (anxious) zone, **(c)** number of zone transitions or line crossing, **(d)** total distance travelled, **(e)** average speed and **(f)** total number of rearing episodes. **(g-k)** Effect of EDR on P301L mice in elevated plus maze task. Control P301L mice showed increased exploration compared to WT littermates. EDR treatment slightly reversed that behavior as evident by reduced open arms visits and increased percentage of protected head dips. **(g)** Percentage of time spent in open arms, **(h)** percentage of open arm entries, **(i)** total distance travelled, **(j)** total number of head dips and **(k)** percentage of protected head dips to total head dips. Data represent mean ± SEM, one-way ANOVA, * significant difference $p < 0.05$ n = 9-14/group at 14 months, n = 4/group at 25 months.

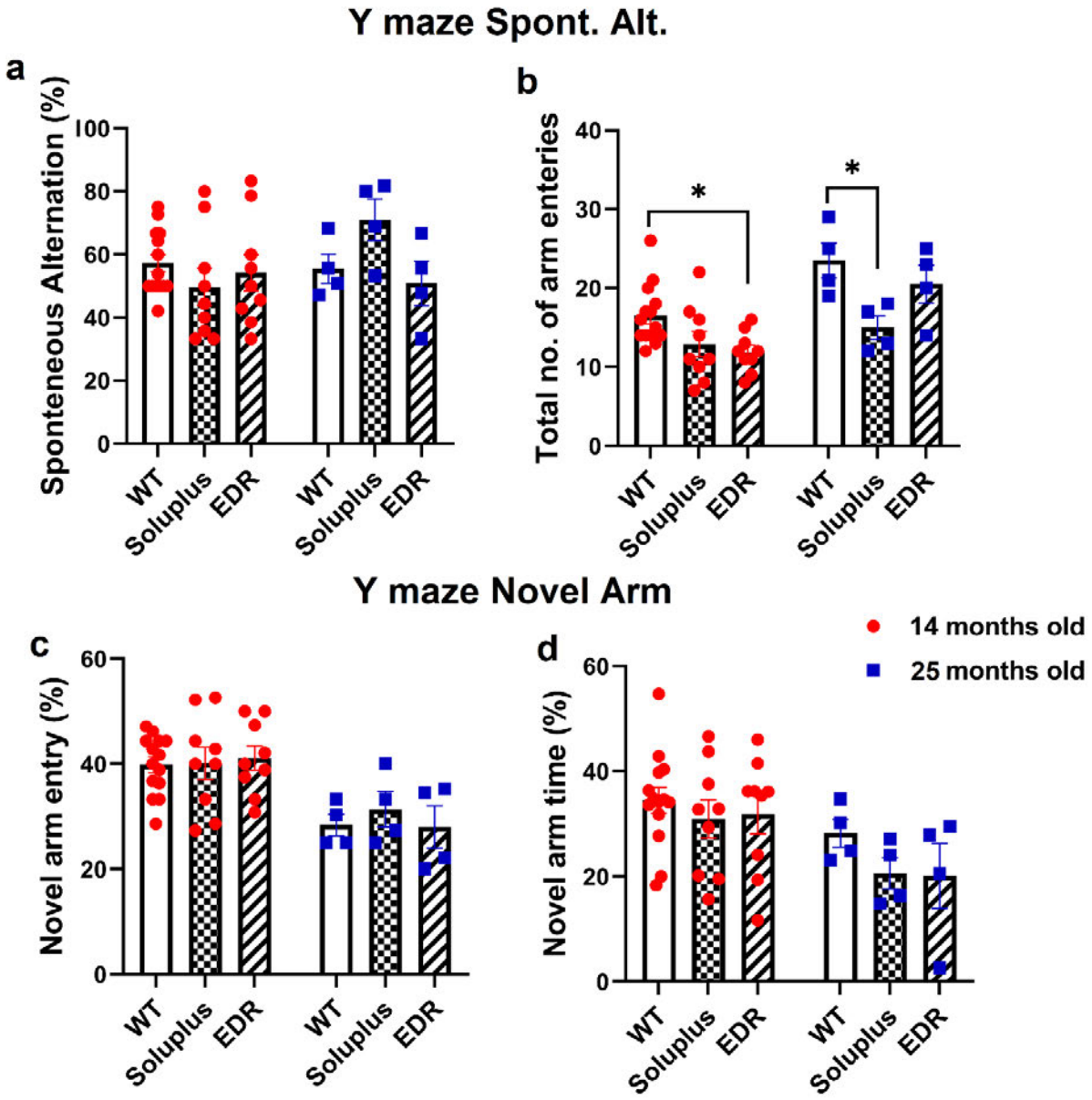


Figure 3 Y maze spontaneous alternation and Y maze novel arm tasks. (a-b) All groups showed the same percentage of alternation. But control P301L mice exhibited significantly lower number of total arm entries compared to WT mice in both age groups, which was slightly reversed by EDR in old age group. **(c-d)** No significant difference was observed between groups in Y maze novel arm test in 14 months old group. However, a trend towards impairment in the spatial working memory was noticed in P301L controls at 25 months, that was partially improved by EDR. Data represent mean ± SEM, one-way ANOVA, * significant difference $p < 0.05$ n = 9-14/group at 14 months old, n = 4/group at 25 months old.

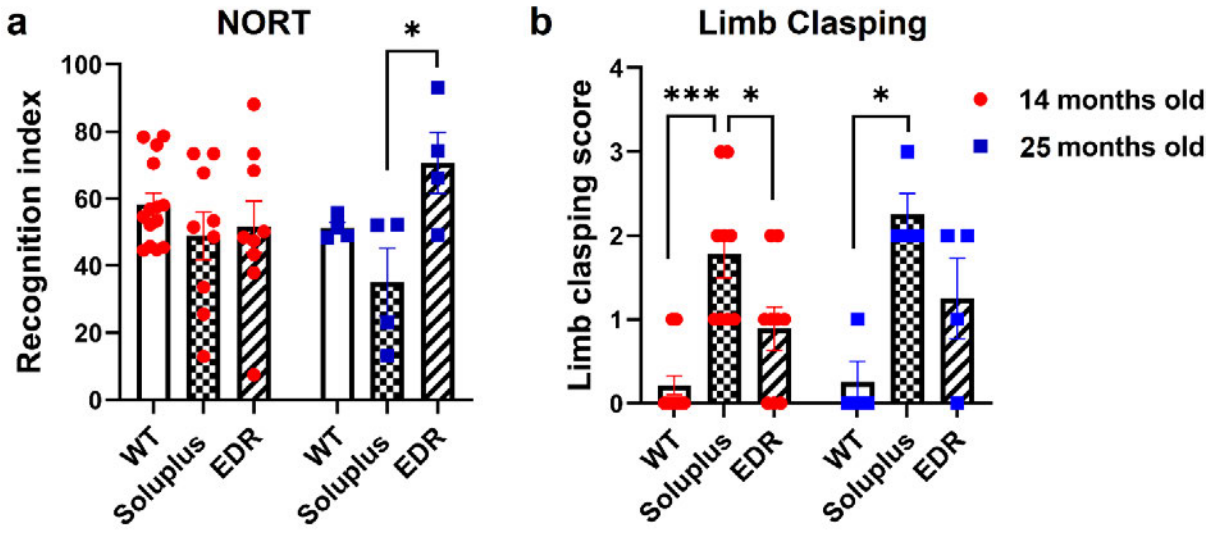


Figure 4 Effect of EDR on the recognition memory and motor function of P301L mice. (a) No significant difference was observed among groups at 14 months in the novel object recognition test, indicating that working memory is not impaired at that age. At 25 months old, control P301L mice showed less preference to explore the novel object. EDR significantly increased the recognition memory in old P301L that performed superior to WT littermates. **(b)** P301L mice showed minor motor impairment as evident by increased score in the limb clasping test. EDR significantly reduced the limb clasping score at 14 months of age and inhibited motor function deterioration in older mice. Data represent mean ± SEM, one-way ANOVA, * significant difference $p < 0.05$ n = 9-14/group at14 months, n = 4/group at 25 months.

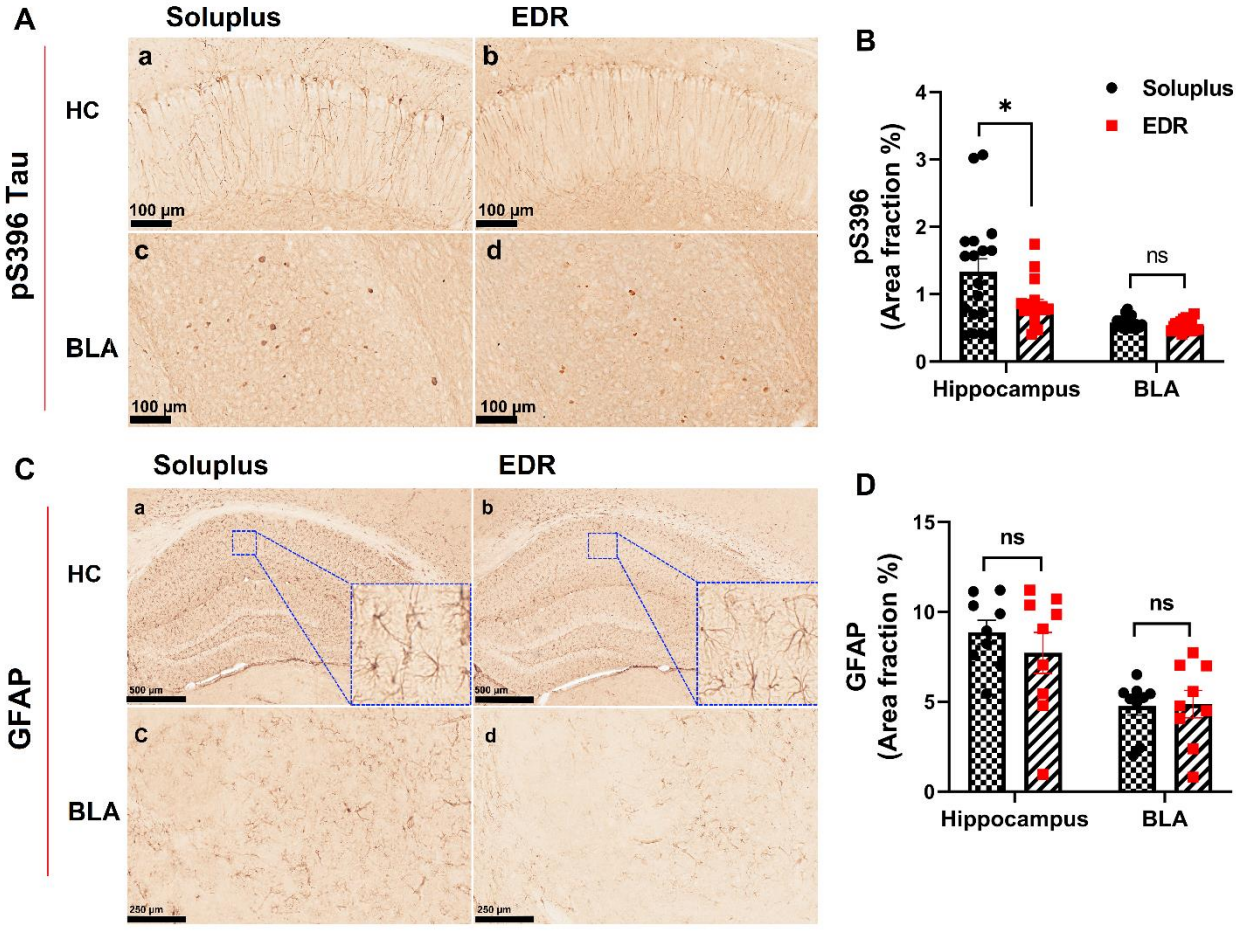


Figure 5 Immunostaining of coronal brain section from vehicle (Soluplus) and EDR-treated P301L mice (age = 14 months old) with anti-pS396 (A) and anti-GFAP (C). A (a and b) Images of hippocampus CA1 region and (c and d) of the amygdala region immunostained with pS396 tau antibody (Scale bar = 100 µm). **B** is a quantitative graph of pS396 positive neurons in vehicle and EDR treated mice showing the EDR treatment significantly reduced the levels of pS396 in the CA1 hippocampus regions and to some extent in the BLA. **C** (a and b) Images of the hippocampus and (c and d) of the amygdala region immunostained with GFAP antibody (Scale bar = 500 µm for the upper panel and 40x magnification of the image is shown in inset, Scale bar = 250 µm for the lower panel). **D** is a quantitative graph of GFAP positive astrocytes showing non-significant difference in GFAP positive astrocytes in the hippocampus, and in the amygdala of control and EDR treated animals. *p < 0.05 vs. Soluplus treated mice (unpaired two-tailed t test). Two sections were analyzed from each group for phosphorylated Tau (n = 2/animal). Results are presented as means ± SEM.

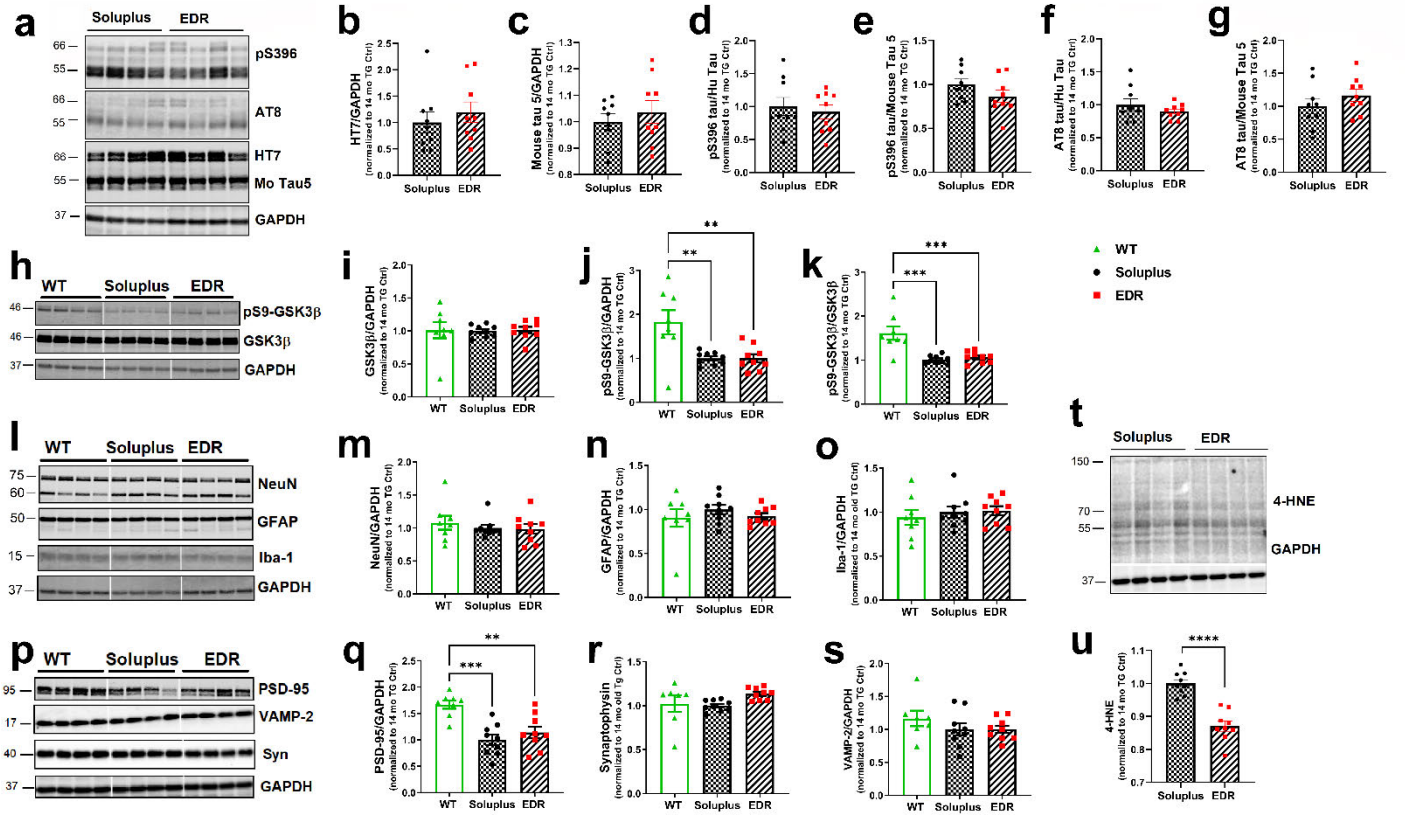


Figure 6 Western blot and their quantitative analysis of total brain homogenates of P301L mice at 14 months old probed with antibodies against **(a-g)** total and phosphorylated tau residues, **(h-k)** total GSK-3β, its phosphorylated form pS9, **(l-o)** NeuN, GFAP and Iba-1 **(p-s)** synapse-associated proteins including synaptophysin, PSD-95 and VAMP-2 and **(t-u)** 4-HNE modified protein levels. GAPDH was used as a loading control. Results showing the levels of proteins normalized to vehicle control P301L mice (age 14 months old). *p < 0.05, **p < 0.01, *** p < 0.0001vs. Soluplus treated mice (unpaired two-tailed t test and one-way ANOVA). Results are presented as means ± SEM.

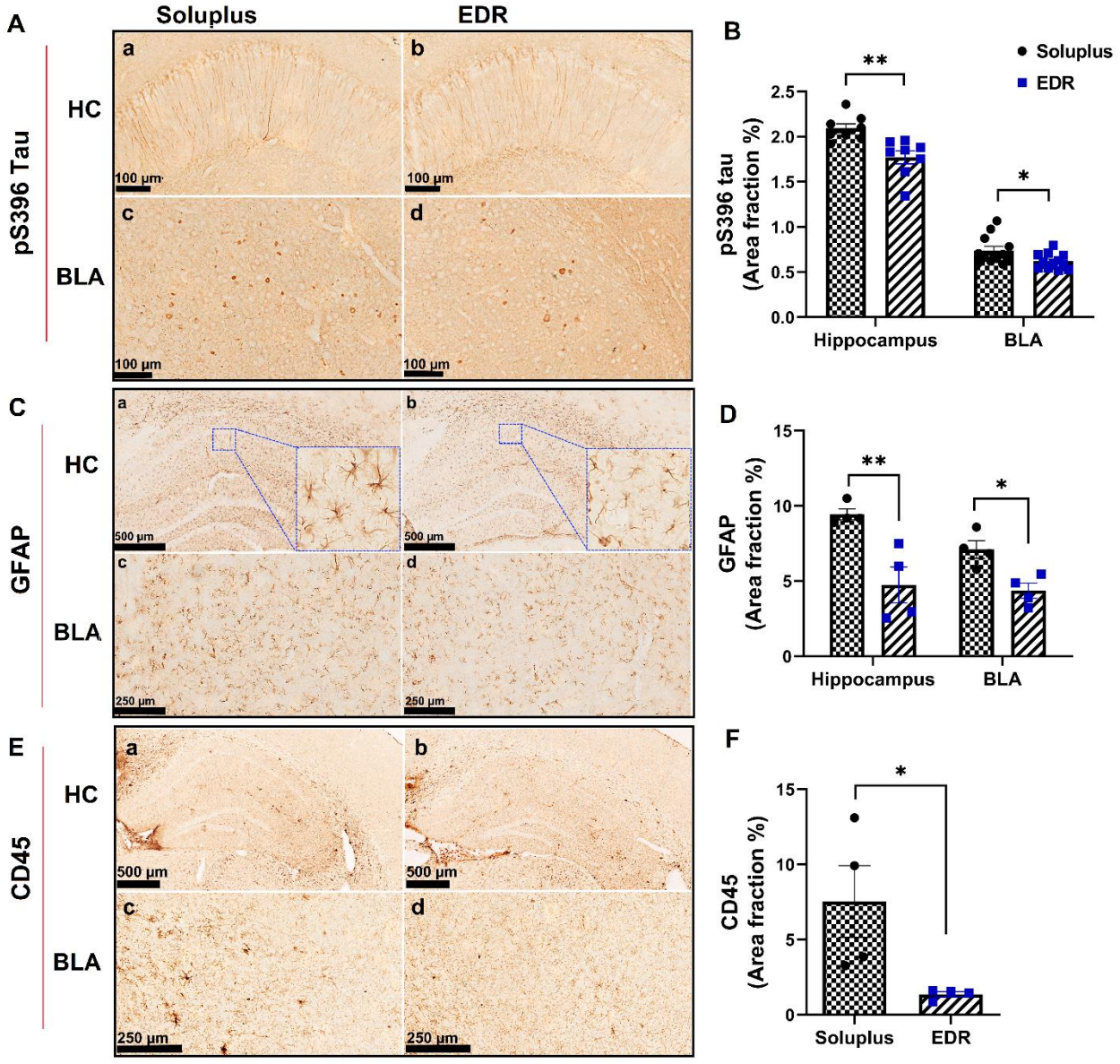


Figure 7 Immunostaining of coronal brain section from vehicle (Soluplus) and EDR-treated P301L mice (age = 25 months old) with anti-pS396 (A), anti-GFAP (C) and anti-CD45 (E). A (a and b) Images of CA1 region of the hippocampus (c and d) and amygdala region immunostained with pS396 tau antibody (Scale bar = 100 µm). **B** is the % of area fraction quantification of pS396 positive neurons in vehicle and EDR treated mice showing the EDR treatment significantly reduced the levels of pS396 in the CA1 hippocampus regions and BLA. **C** (a and b) Images of the hippocampus and (c and d) of the amygdala region immunostained with GFAP antibody (Scale bar = 500 µm for the upper panel and 40x magnification of the image is shown in inset, Scale bar = 250 µm for the lower panel; c and d). **D** is a quantitative graph of GFAP represented as % of area fraction showing significant reduction in GFAP positive astrocytes in both the hippocampus and amygdala of EDR treated mice compared to vehicle controls. **E** (a and b) Images of the hippocampus and (c and d) amygdala region immunostained with CD45 antibody (Scale bar = 500 µm; upper panel, and Scale bar = 250 µm for lower panel). **F** is a representative quantification (% of area fraction) of CD45 positive microglia showing that EDR treatment significantly reduced the overall expression levels of CD45 in the brain. Results are presented as mean ± SEM.*$p < 0.05$ vs. Soluplus treated mice (unpaired two-tailed t test).

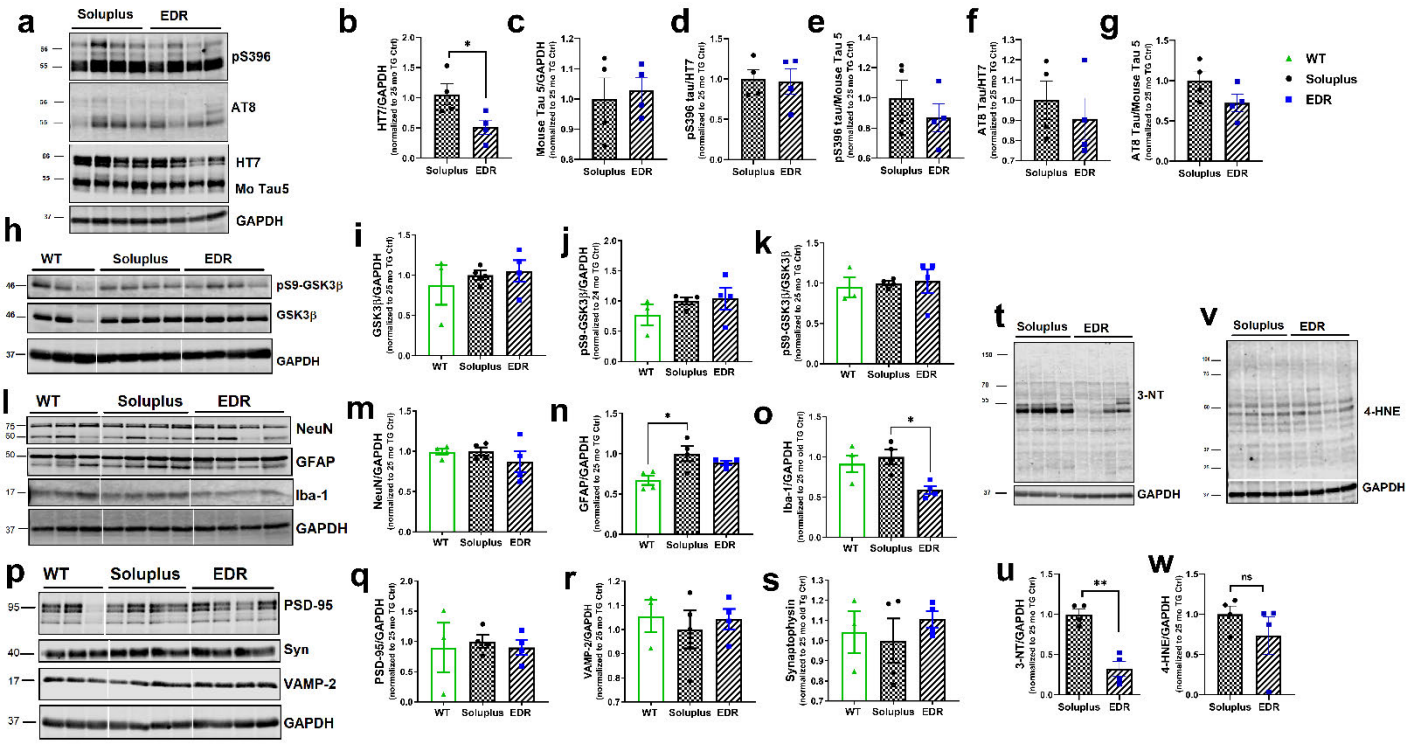


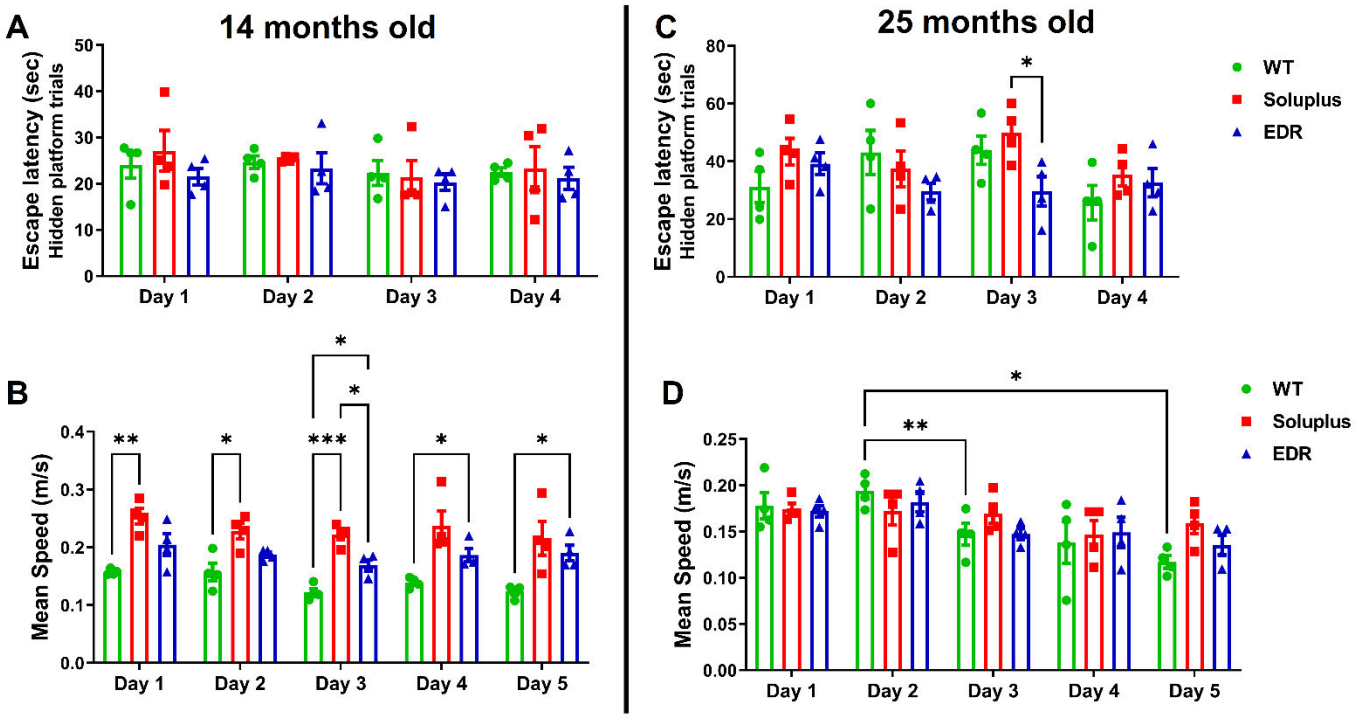
Figure 8 Western blot and their quantitative analysis of total brain homogenates of P301L mice at 25 months old probed with antibodies against **(a-g)** total and phosphorylated tau residues, **(h-k)** total GSK-3β, its phosphorylated form pS9 **(l-o)** NeuN, GFAP and Iba-1 **(p-s)** synapse-associated proteins including synaptophysin, PSD-95 and VAMP-2, **(t-u)** 3-NT modified protein levels and **(v-w)** 4-HNE modified proteins levels. GAPDH was used as a loading control. Results showing the expressions levels of proteins normalized to vehicle control P301L mice (age 25 months old). *p < 0.05, **p < 0.01 vs. Soluplus treated mice (unpaired two-tailed t test and one-way ANOVA). Results are presented as means ± SEM.

Supplementary Information

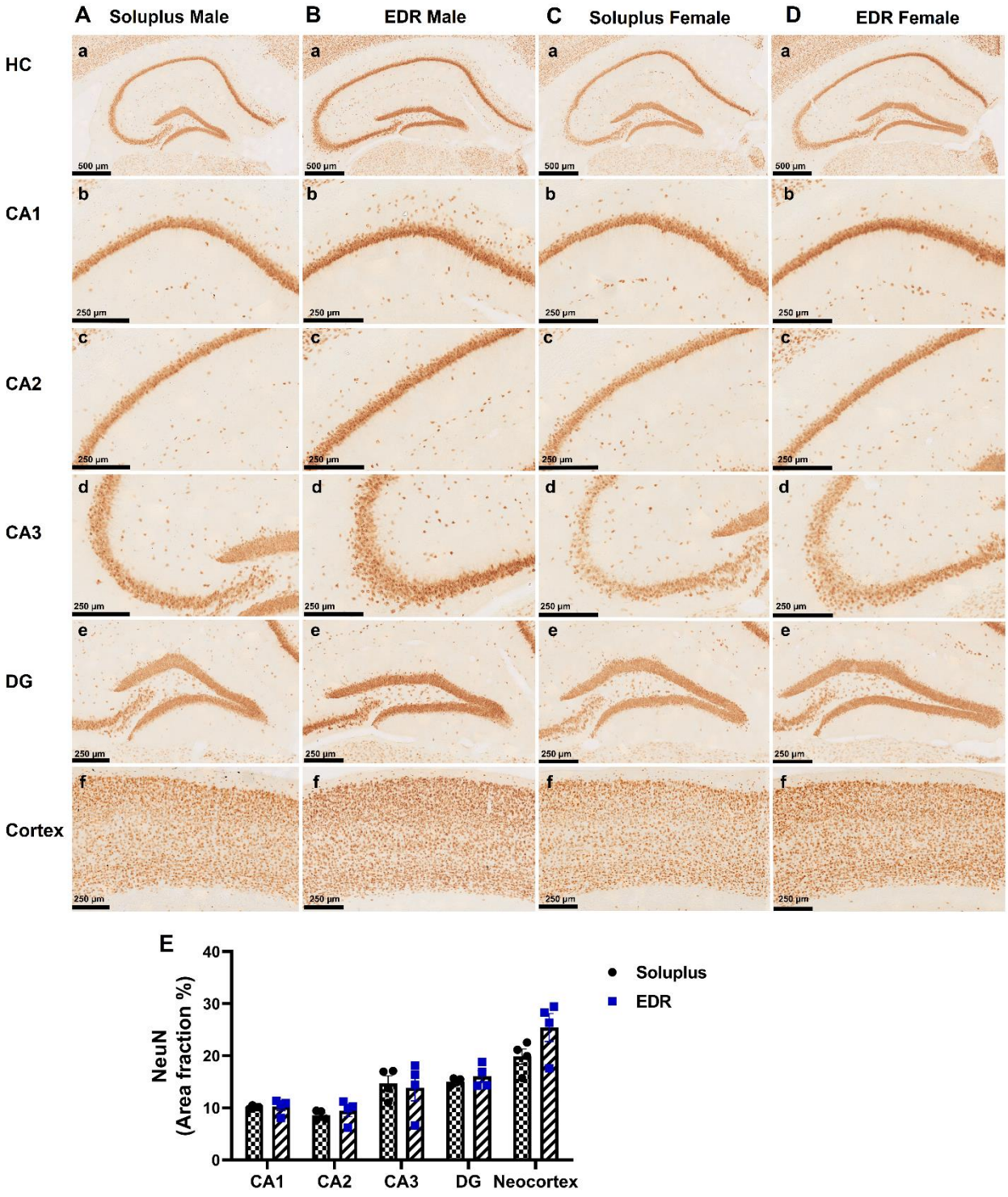
Suppl. Table 1 Primary antibodies used in this study

Antibody	Type/Host	Specificity	Phosph. site	Dilution	Source
3-NT	Mono-/Mouse	3 nitro tyrosine modified proteins		1:3000 WB	Abcam
4-HNE	Poly-/Rabbit	4-hydroxynonenal modified proteins		1:3000 WB	Abcam
AT8	Mono-/Mouse	pTau	Ser 202/ Thr 205	1:1000 WB	ThermoFisher
GSK-3β	Mono-/Mouse	GSK-3β		1:3000 WB	Cell signaling technology
pGSK-3β	Poly-/Rabbit	pGSK-3β	Ser 9	1:3000 WB	Cell signaling technology
GAPDH	Poly-/Sheep	GAPDH		1:5000 WB	Osenses
GFAP	Poly-/Rabbit	GFAP		1:2000 WB 1:1000 IHC	Dako
HT7 Tau	Mono-/Mouse	Human tau clone 7		1:10000 WB	Pierce Thermo Scientific
Iba-1	Poly-/Rabbit	Iba-1		1:750 WB	FUJIFILM Wako
NeuN	Mono-/Mouse	Neuronal nuclei		1:1000 IHC, WB	Invitrogen
VAMP-2	Poly-/Rabbit	VAMP-2		1:3000 WB	Osenses
PSD-95	Mono-/Mouse	PSD-95		1:2000 WB	Sigma
pS396 Tau	Mono-/Rabbit	pTau	Ser 396	1:15,000 WB 1:2000 IHC	Abcam
Synaptophysin	Mono-/Mouse	Synaptophysin		1:4000 WB	Millipore
Tau 5	Mono-/Mouse	Mouse Tau		1:7500 WB	Life Technologies

Phosph. site: phosphorylation site; Mono-: monoclonal; poly-: polyclonal; WB, Western blotting; IHC: immunohistochemical staining.

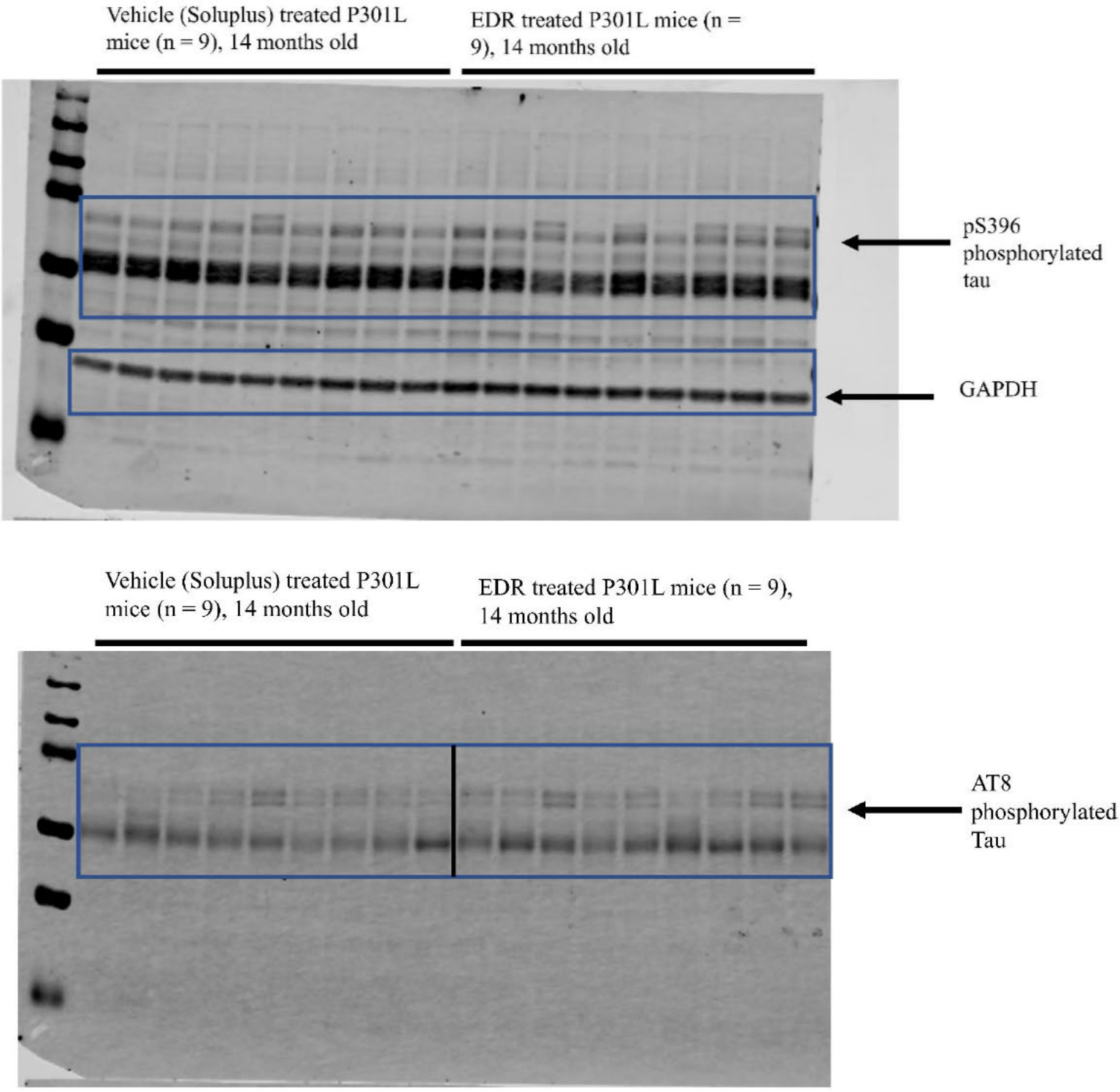


Supp. Figure 1 Morris Water Maze Test. Comparison of the average escape latency and speed across hidden platform trials between WT, control and EDR treated P301L mice. Two-way ANOVA revealed that all groups showed similar escape performance for the hidden platform at 14 months old group while showed significant reduction in EDR treated mice in day 3 compared to controls of the 25 months old group. Results also showed higher average speed of 14 months old P301L mice compared to age matched WT littermates that could reflect the higher tendency of exploration of that genotype, while no difference was found between groups in the 25 months old mice. For 14 months old: n = 14 for WT, n = 9 for control P301L mice, n = 9 for EDR treated P301L mice. For 25 months old: n = 4 for WT, n = 4 for control P301L and n = 4 for EDR treated P301L mice. Data represent mean ± SEM, two-way ANOVA, Tukey's test, *p < 0.05, **p < 0.01, ***p < 0.0001.

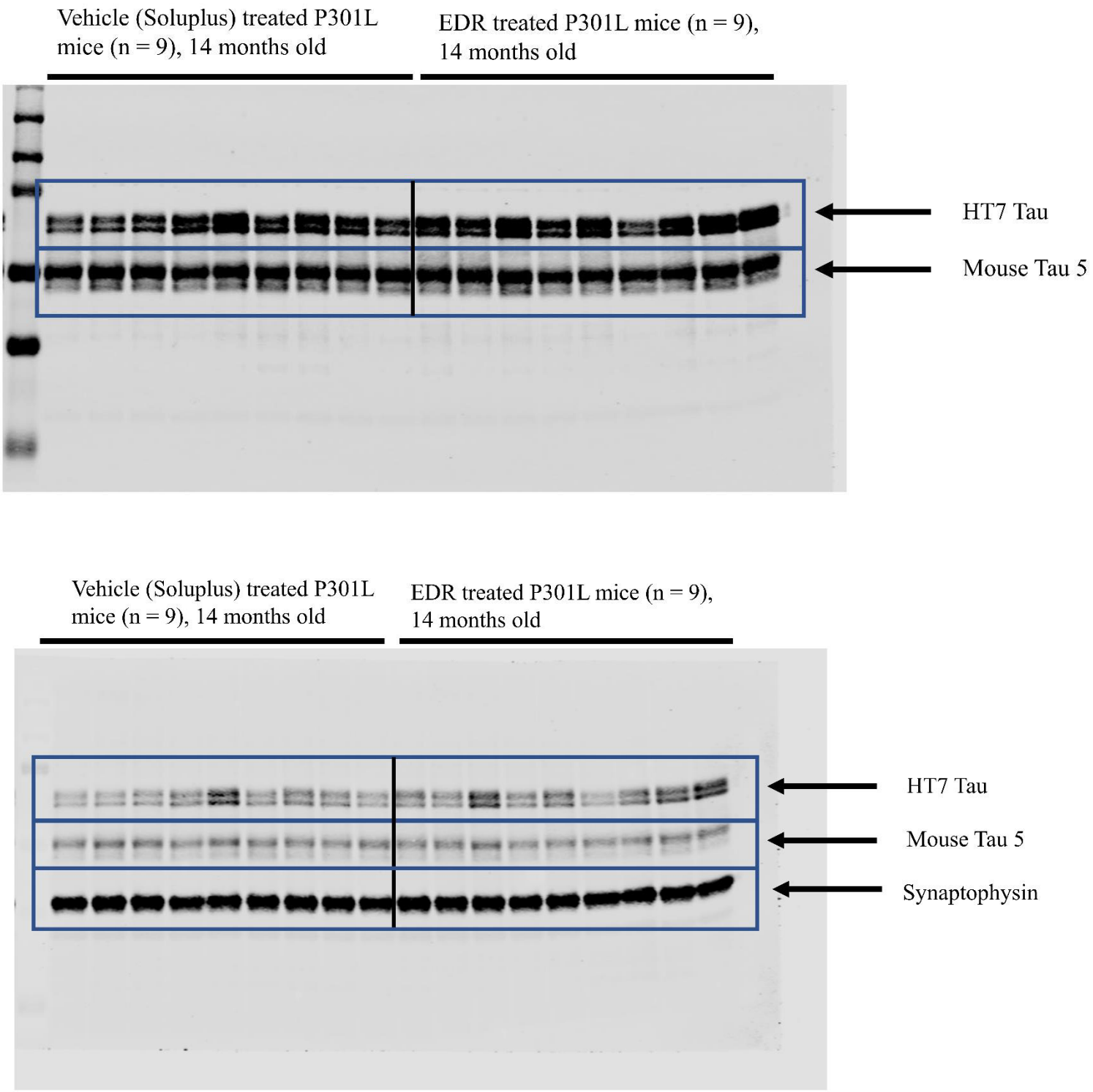


Suppl. Figure 2 Effect of EDR on neuronal viability against oxidative neurotoxicity in P301L mice at 25 months age. (A-D) Representative images of subregions of the hippocampus and neocortex immunostained with NeuN; a marker for mature neurons nuclei (Scale bar = 500 µm for upper panel [a], 250 µm for the rest of brain regions). **(E)** Quantification of area fraction% of NeuN positive staining in the cortex, whole hippocampus and its subregions. Results are presented as mean ± SEM (unpaired two-tailed t test).

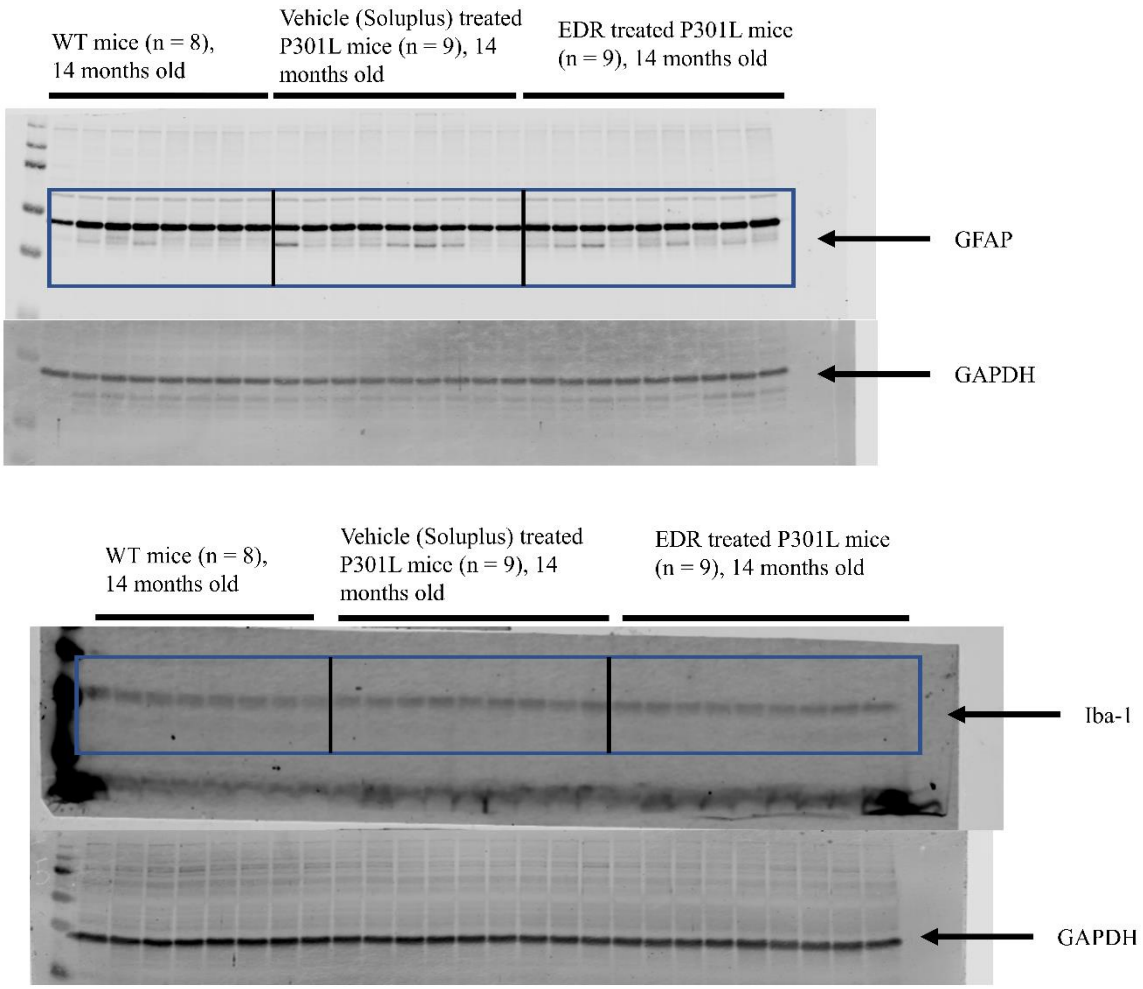
Original Western blots



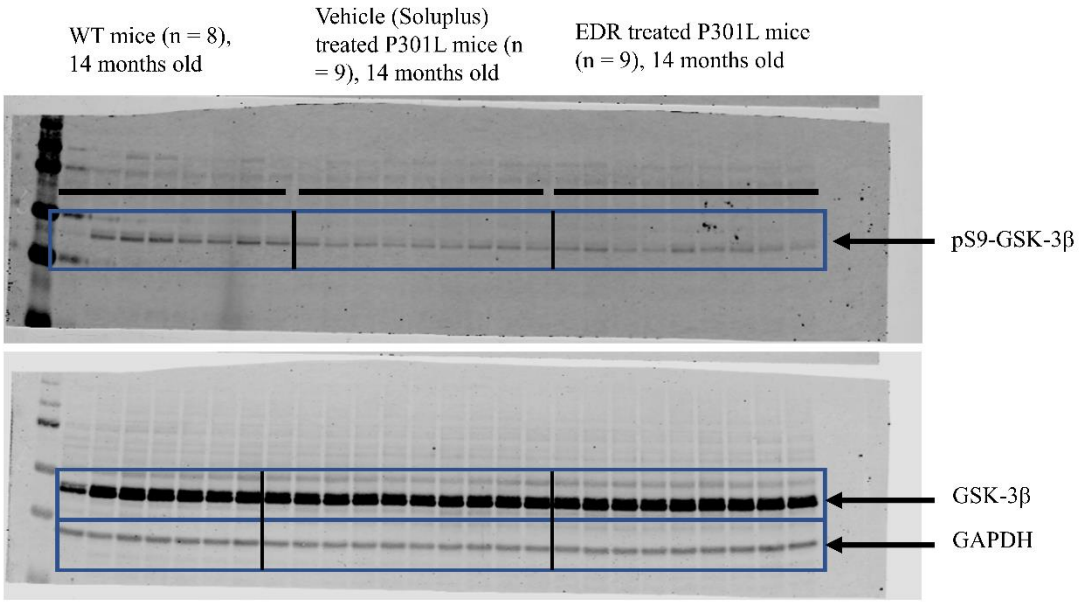
Suppl. Figure 3 Western blot of total brain homogenates of P301L mice at 14 months old probed with antibody against pS396 Tau (upper) and AT8 phosphorylated Tau (lower). GAPDH was used as a loading control.



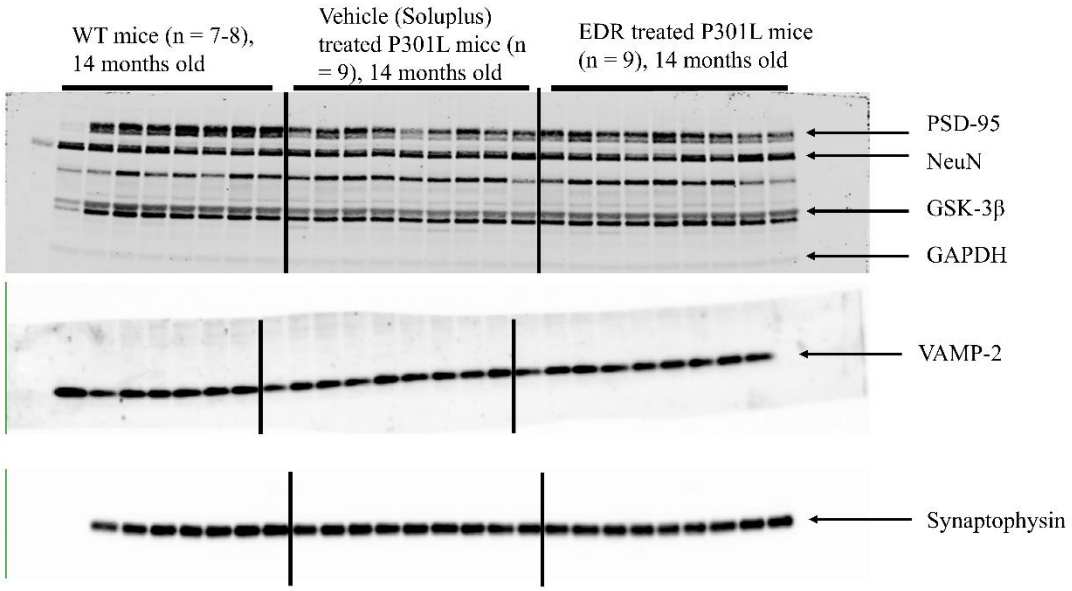
Suppl. Figure 4 Western blot of total brain homogenates of P301L mice at 14 months old probed with antibody against total human Tau (upper) and mouse Tau 5 and Synaptophysin (lower). GAPDH was used as a loading control.



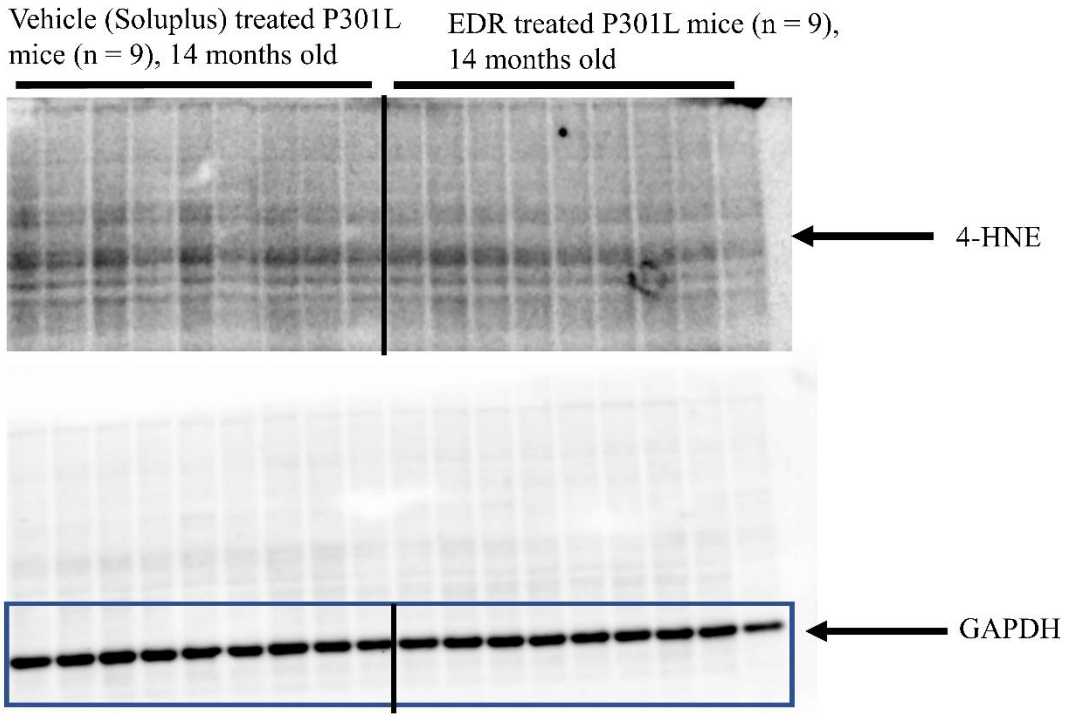
Suppl. Figure 5 The Whole Western blot of total brain homogenates of WT and P301L mice at 14 months old probed with antibody against GFAP (upper) and Iba-1 (lower). GAPDH was used as a loading control.



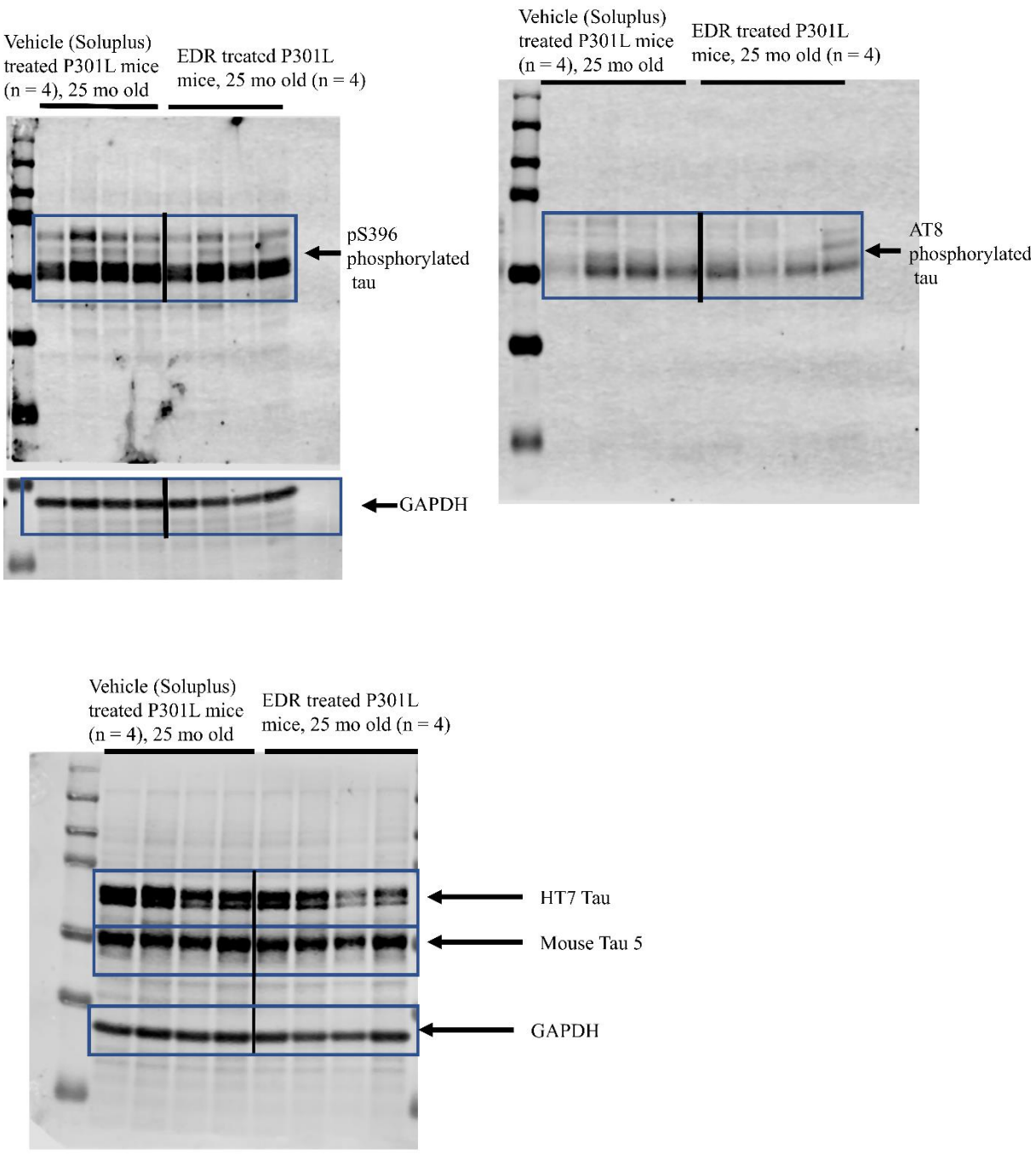
Suppl. Figure 6 The whole Western blot of total brain homogenates of WT and P301L mice at 14 months old probed with antibody against GSK-3β and its phosphorylated form pS9. GAPDH was used as a loading control.



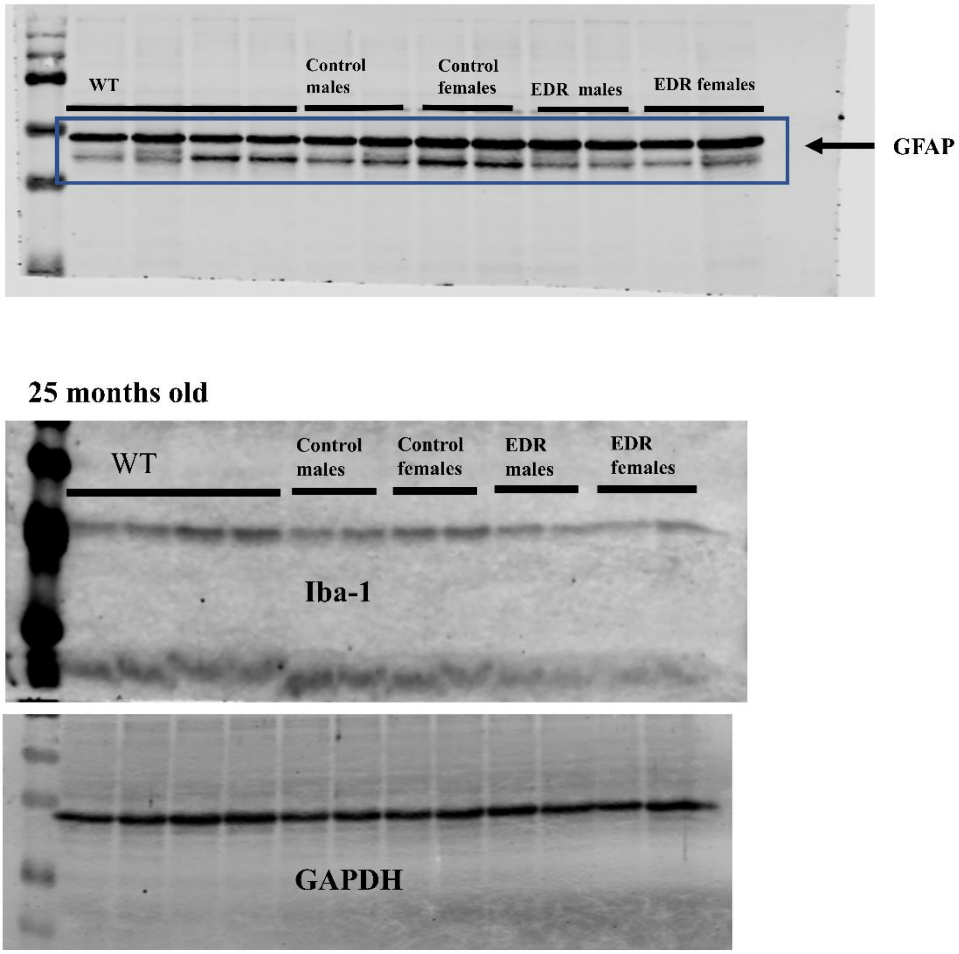
Suppl. Figure 7 The whole Western blot of total brain homogenates of WT and P301L mice at 14 months old probed with antibody against PSD-95, NeuN and VAMP-2. GAPDH was used as a loading control.



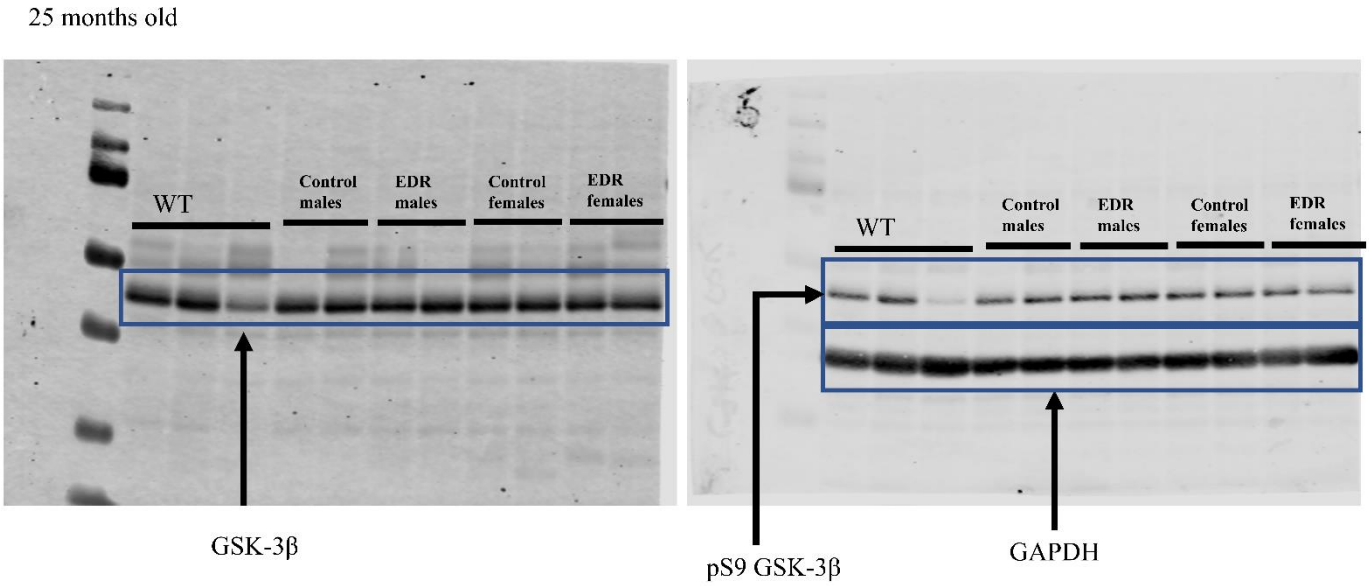
Suppl. Figure 8 Western blot of total brain homogenates of P301L mice at 14 months old probed with antibody against 4-HNE. GAPDH was used as a loading control.



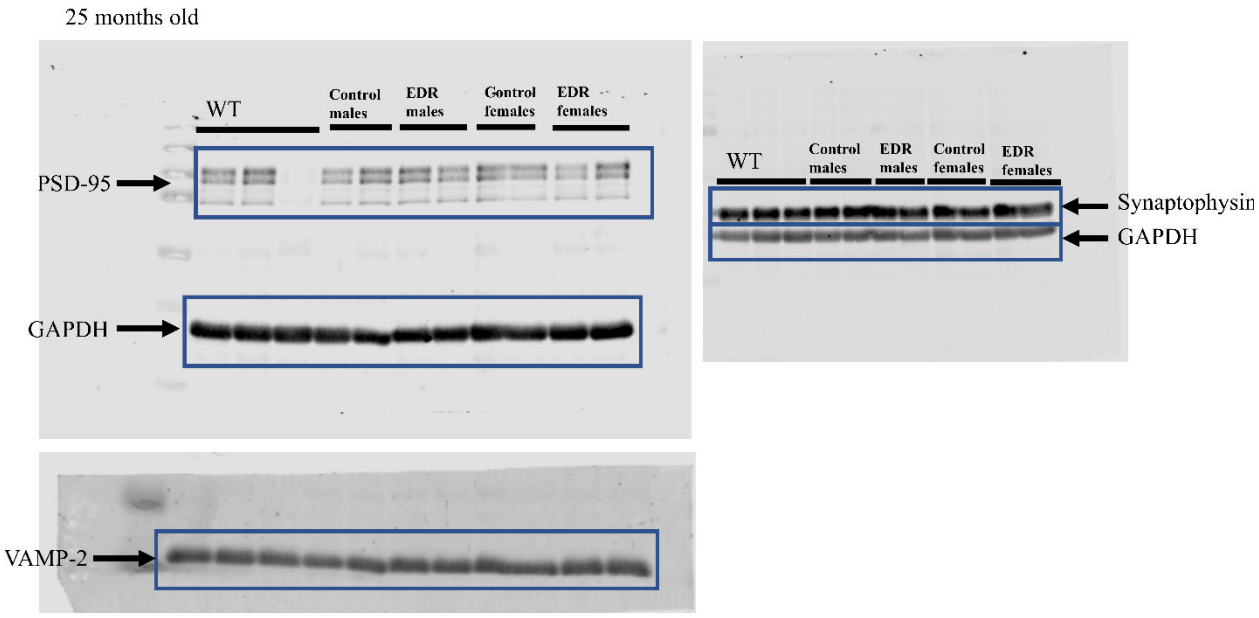
Suppl. Figure 9 Western blot of total brain homogenates of P301L mice at 25 months old probed with antibody against total human Tau, mouse Tau 5, pS396 and AT8 phosphorylated Tau. GAPDH was used as a loading control.



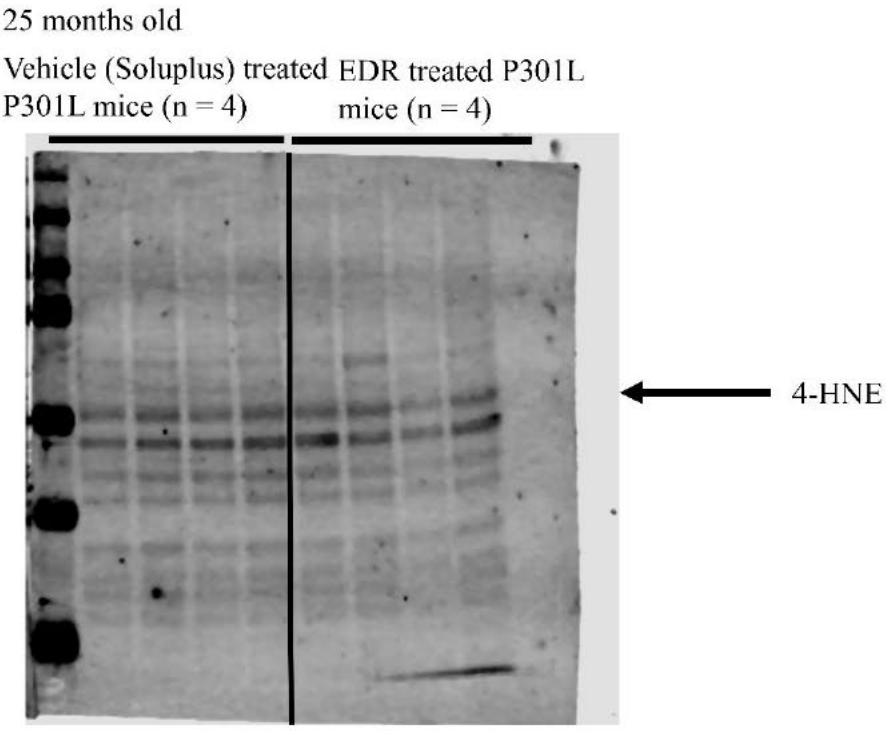
Suppl. Figure 10 The whole Western blot of total brain homogenates of WT and P301L mice at 25 months old probed with antibody against GFAP (upper) and Iba-1 (lower). GAPDH was used as a loading control.

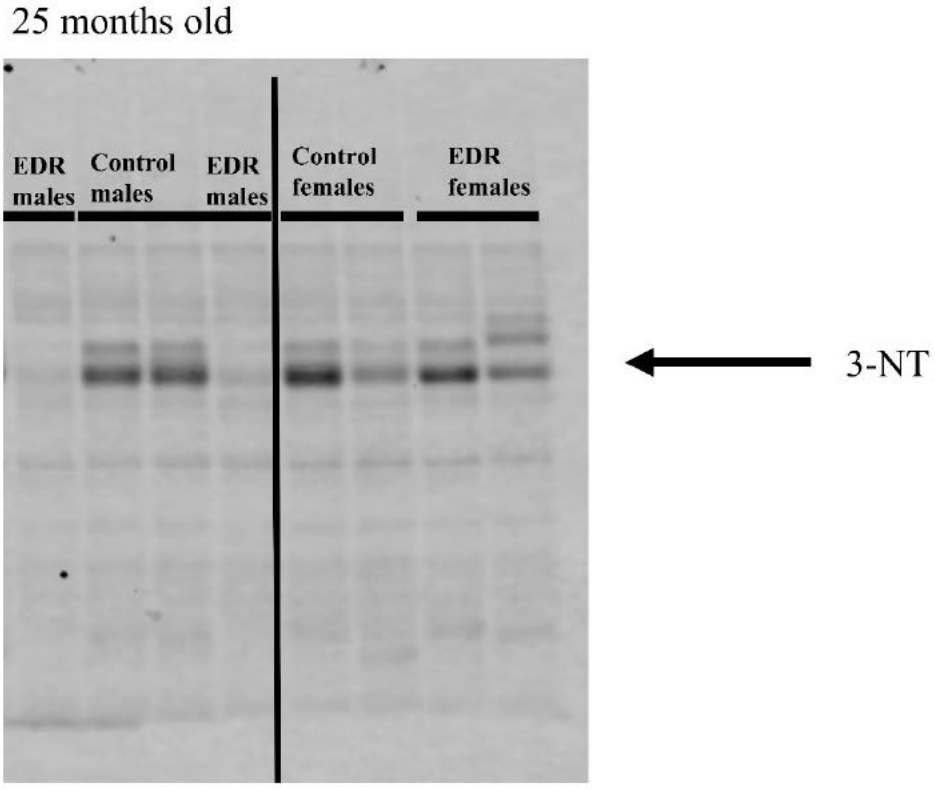


Suppl. Figure 11 The whole Western blot of total brain homogenates of WT and P301L mice at 25 months old probed with antibody against GSK-3β and its phosphorylated form pS9. GAPDH was used as a loading control.

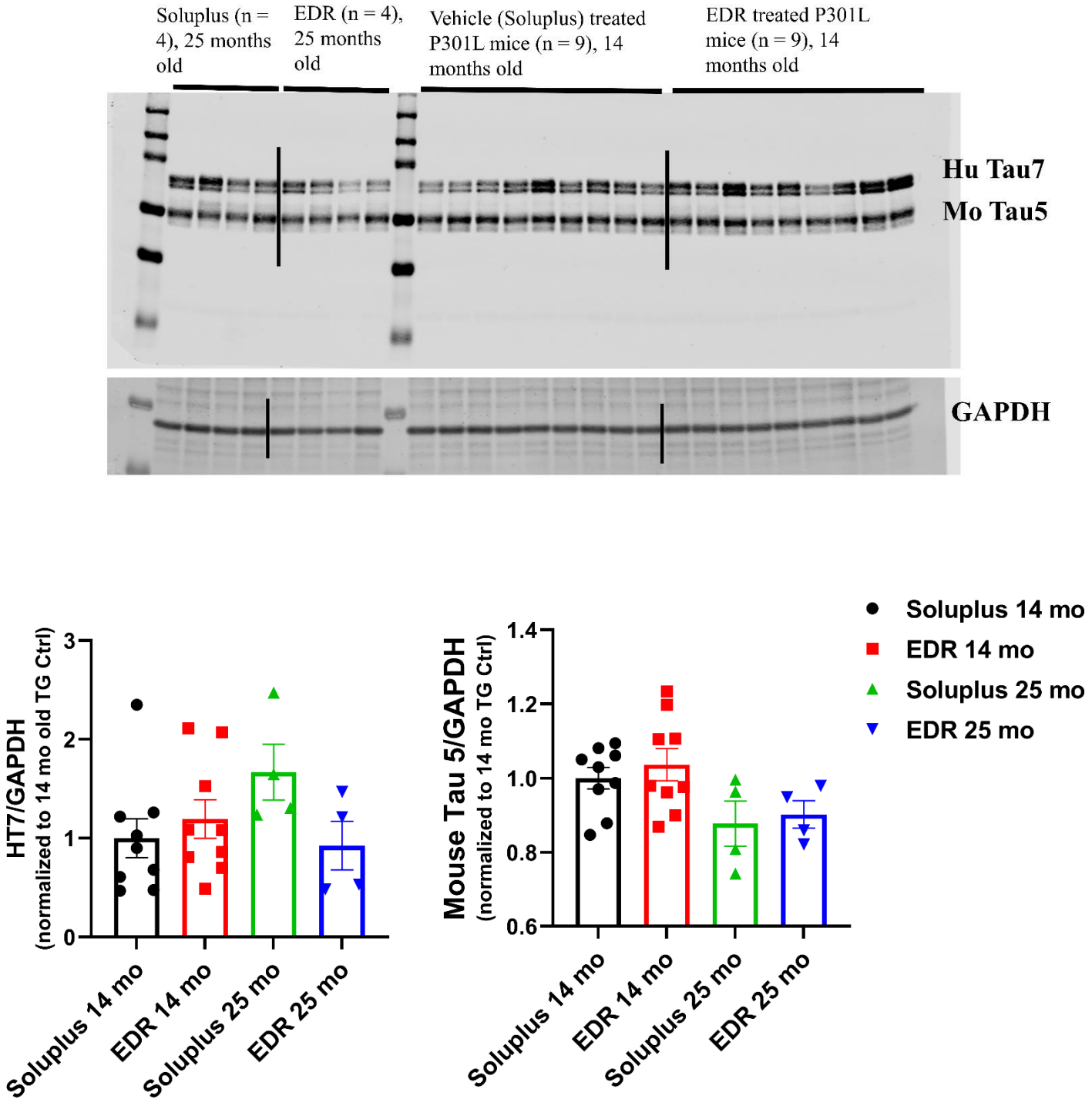


Suppl. Figure 12 Western blot of total brain homogenates of WT and P301L mice at 25 months old probed with antibody against PSD-95, VAMP-2 and Synaptophysin. GAPDH was used as a loading control.

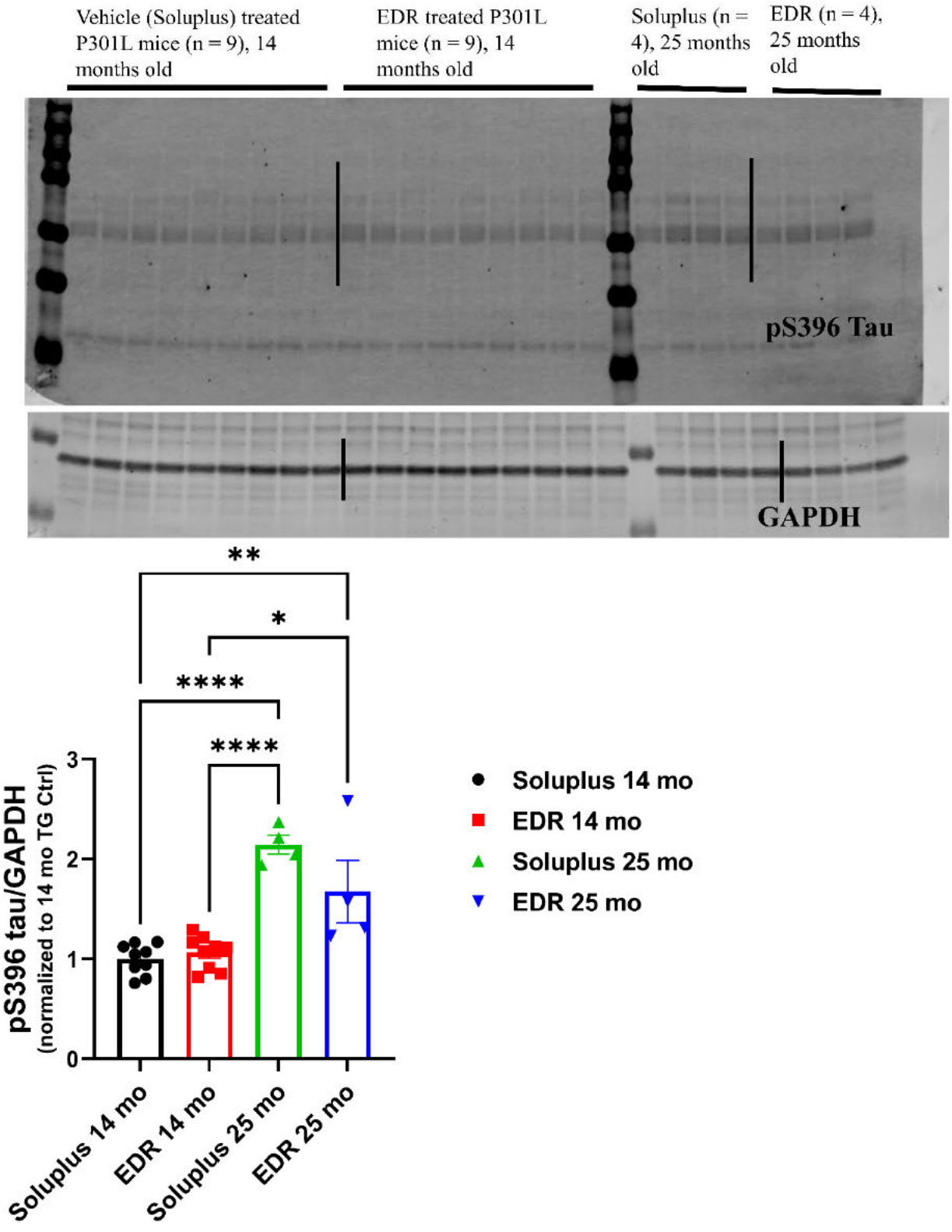




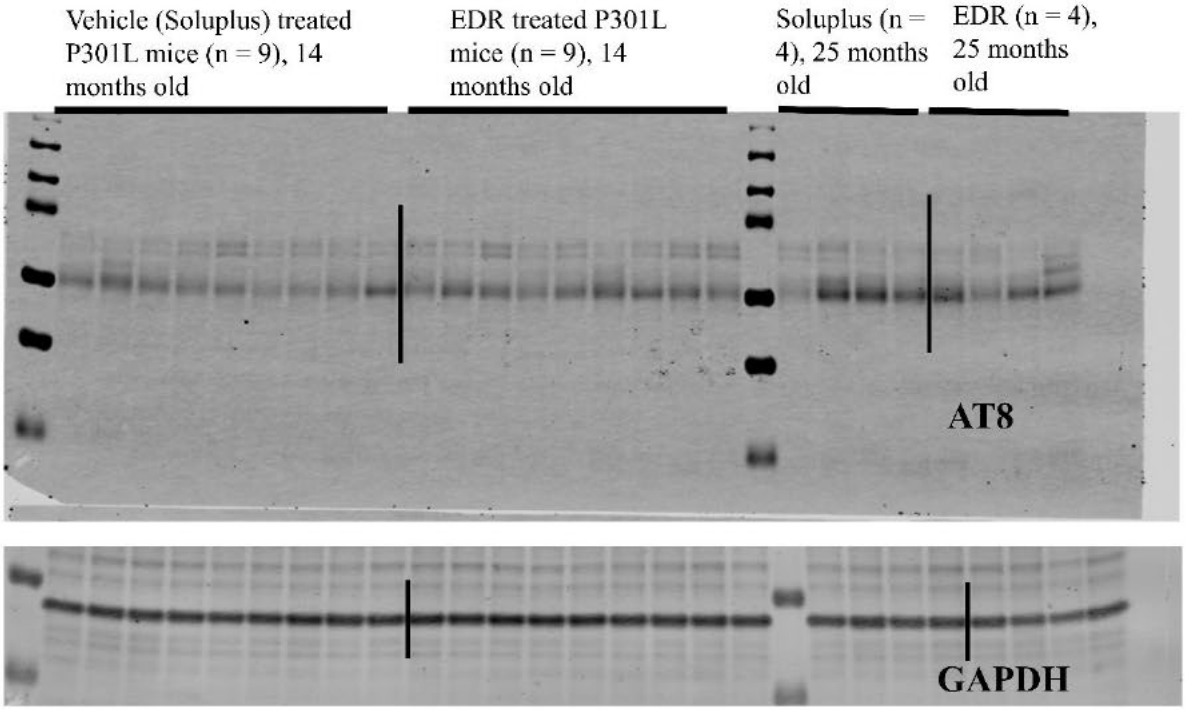
Suppl. Figure 13 Western blot of total brain homogenates of P301L mice at 25 months old probed with antibody against 4-HNE and 3-NT. GAPDH was used as a loading control.

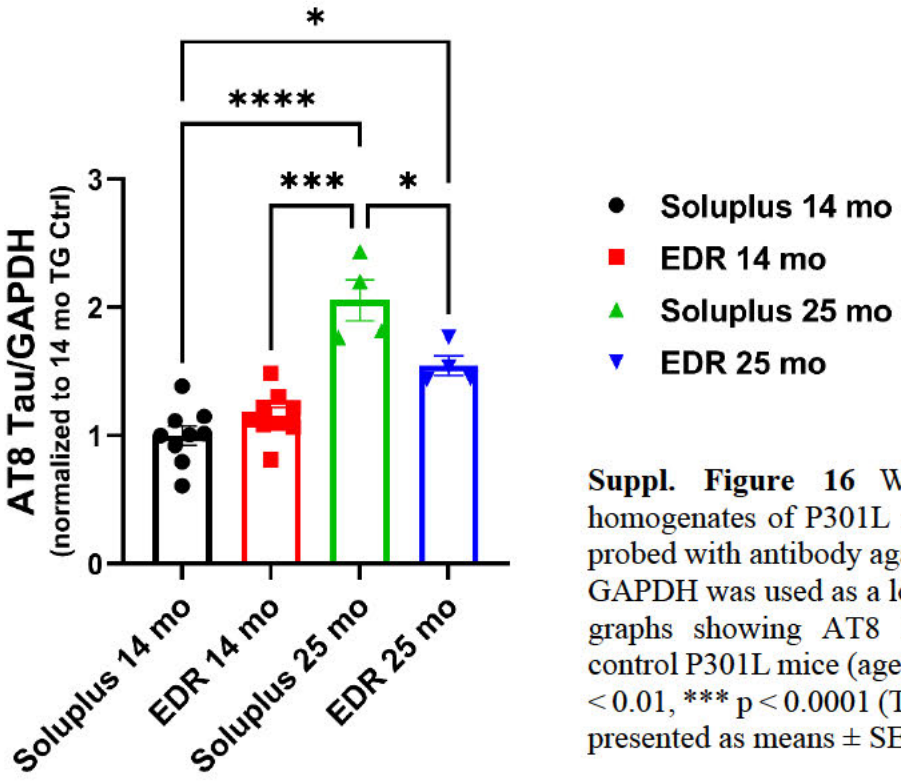


Suppl. Figure 14 Western blot of total brain homogenates of P301L mice at 14 and 25 months old probed with antibody against Total Human Tau7 and Mouse tau 5. GAPDH was used as a loading control and quantitative graphs showing the expressions levels normalized to vehicle control P301L mice (age 14 months old). *p < 0.05, **p < 0.01, *** p < 0.0001 (Two-way ANOVA). Results are presented as means ± SEM.

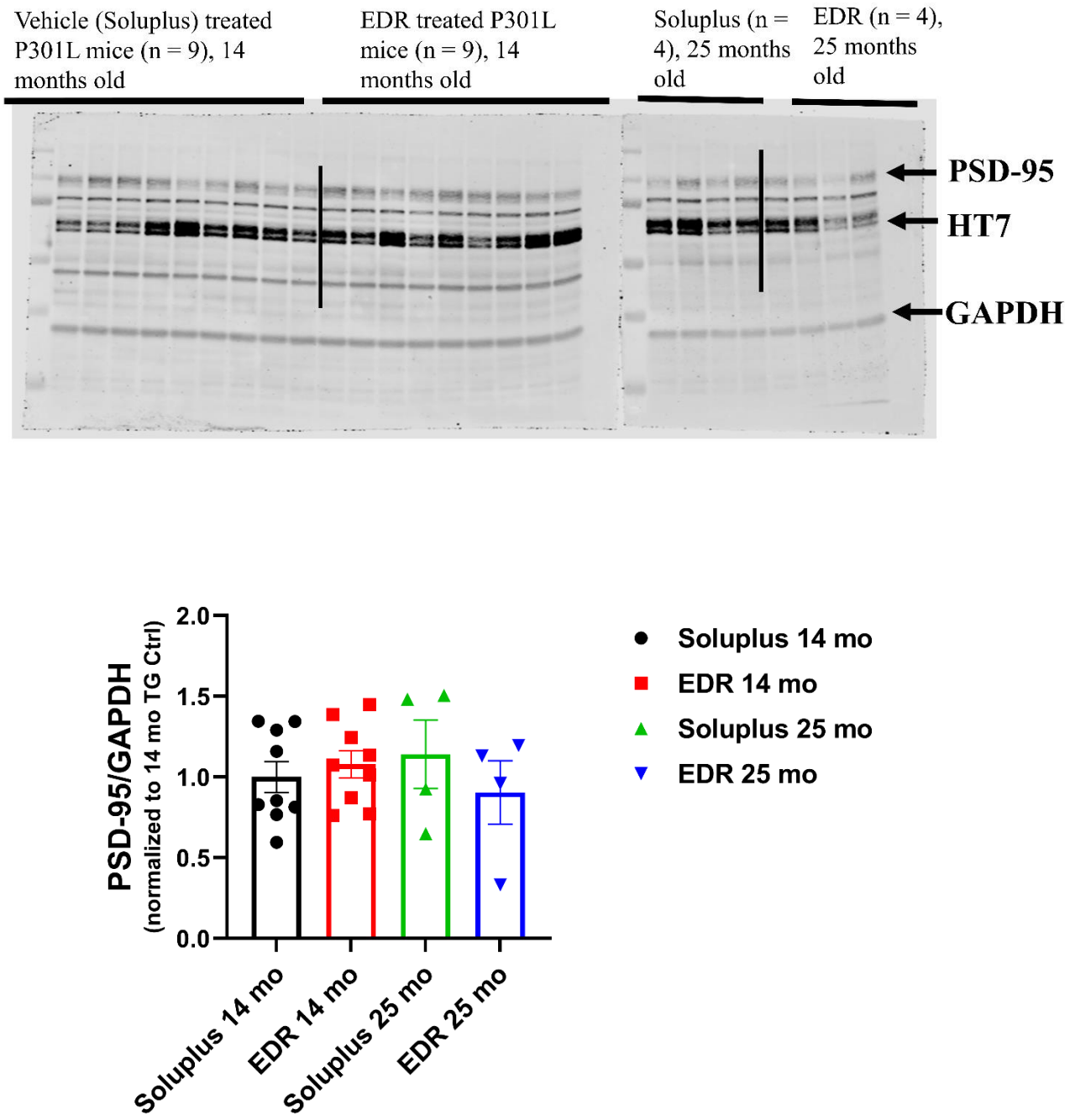


Suppl. Figure 15 Western blot of total brain homogenates of P301L mice at 14 and 25 months old probed with antibody against phosphorylated Tau pS396. GAPDH was used as a loading control and quantitative graphs showing pS396 tau levels normalized to vehicle control P301L mice (age 14 months old). *p < 0.05, **p < 0.01, *** p < 0.0001 (Two-way ANOVA). Results are presented as means ± SEM.

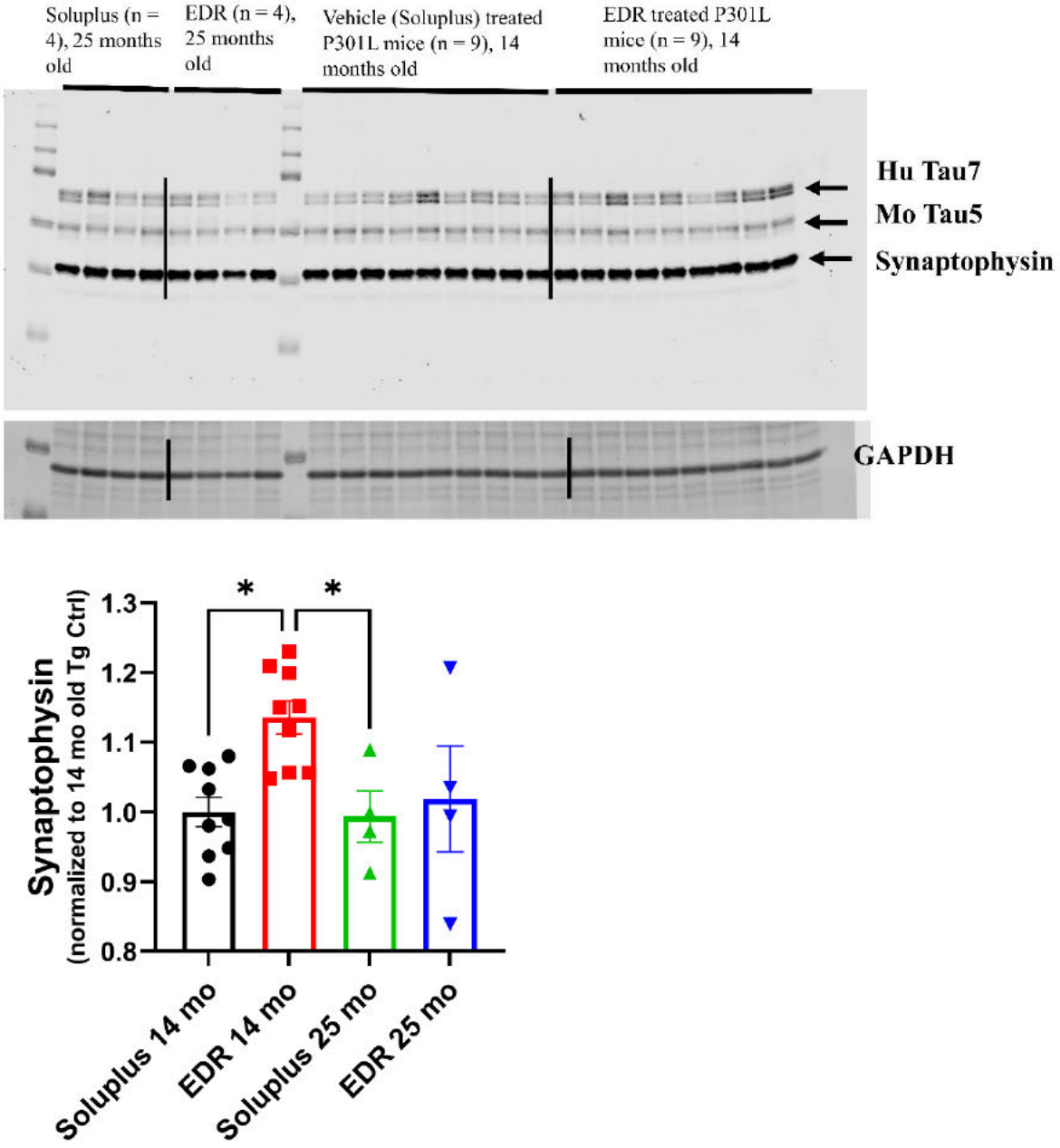




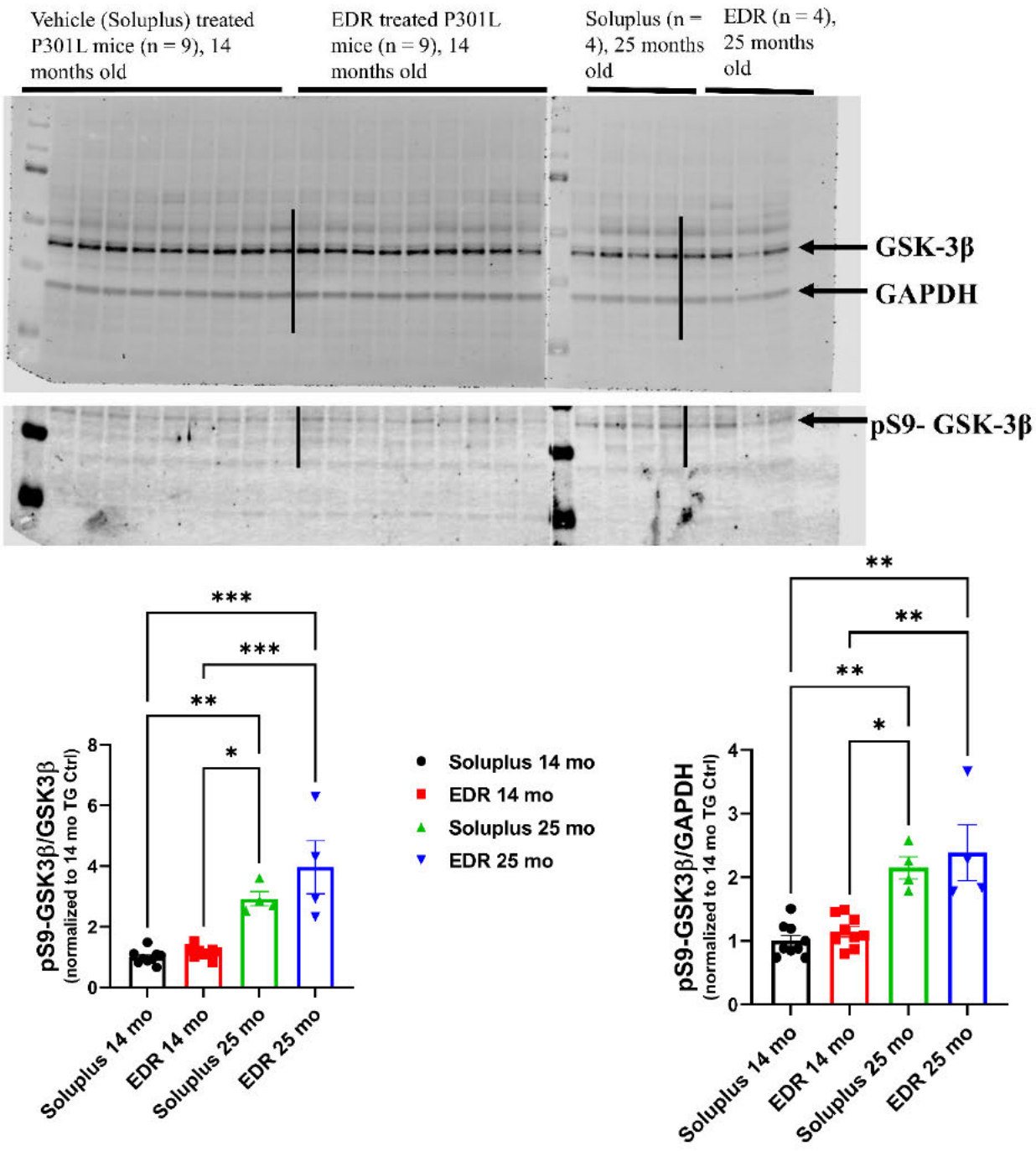
Suppl. Figure 16 Western blot of total brain homogenates of P301L mice at 14 and 25 months old probed with antibody against phosphorylated Tau AT8. GAPDH was used as a loading control and quantitative graphs showing AT8 levels normalized to vehicle control P301L mice (age 14 months old). *$p < 0.05$, **$p < 0.01$, *** $p < 0.0001$ (Two-way ANOVA). Results are presented as means ± SEM.



Suppl. Figure 17 Western blot of total brain homogenates of P301L mice at 14 and 25 months old probed with antibody against PSD-95. GAPDH was used as a loading control and quantitative graphs showing the expressions levels normalized to vehicle control P301L mice (age 14 months old). *p < 0.05, **p < 0.01, *** p < 0.0001 (Two-way ANOVA). Results are presented as means ± SEM.



Suppl. Figure 18 Western blot of total brain homogenates of P301L mice at 14 and 25 months old probed with antibody against Synaptophysin. GAPDH was used as a loading control and quantitative graphs showing the expressions levels normalized to vehicle control P301L mice (age 14 months old). *$p < 0.05$, **$p < 0.01$, *** $p < 0.0001$ (Two-way ANOVA). Results are presented as means ± SEM.



Suppl. Figure 19 Western blot of total brain homogenates of P301L mice at 14 and 25 months old probed with antibody against GSK-3β and its phosphorylated form pS9. GAPDH was used as a loading control and quantitative graphs showing the protein levels normalized to vehicle control P301L mice (age 14 months old). *p < 0.05, **p < 0.01, *** p < 0.0001 (Two-way ANOVA). Results are presented as means ± SEM.

CHAPTER 5: A New Approach to Model Sporadic Alzheimer's Disease by Intracerebroventricular Streptozotocin Injection in APP/PS1 Mice

Sally Kelliny, Liying Lin, Isaac Deng, Jing Xiong, Fiona Zhou, Mohammed Al-Hawwas, Larisa Bobrovskaya, Xin-Fu Zhou

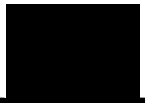
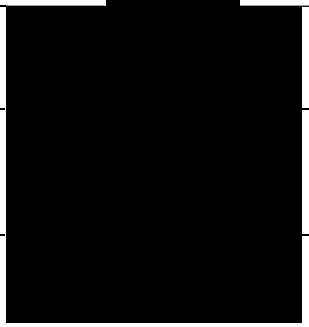
A New Approach to Model Sporadic Alzheimer's Disease by Intracerebroventricular Streptozotocin Injection in APP/PS1 Mice

Publication status: Published

The published version is available at: https://link.springer.com/article/10.1007/s12035-021-02338-5

Author Contributions

Author	Wrote Manuscript	Revised Manuscript	Designed Research	Performed Research	Analysis of Data	Data Interpretation
Kelliny, S	✔	✔	✔	✔	✔	✔
Lin, L. Y		✔		✔		
Deng, I		✔		✔		
Xiong, J		✔		✔		
Zhou, F		✔		✔		
Al-Hawwas, M		✔		✔		
Bobrovskaya, L		✔	✔			✔
Zhou, X. F		✔	✔	✔		✔

Full name of co-author	Signature	Date
Kelliny, S		15/03/2021
Lin, L. Y		16/03/2021
Isaac Deng		16/03/2021
Jing Xiong		16/03/2021
Fiona Zhou		16/03/2021

Mohammed Al-Hawwas	[redacted]	15/03/2021
Larisa Bobrovskaya		15/03/2021
Xin-Fu Zhou		16/03/2021

Molecular Neurobiology (2021) 58:3692–3711
https://doi.org/10.1007/s12035-021-02338-5

A New Approach to Model Sporadic Alzheimer's Disease by Intracerebroventricular Streptozotocin Injection in APP/PS1 Mice

Sally Kelliny[1,2] · Liying Lin[1] · Isaac Deng[1] · Jing Xiong[1,3] · Fiona Zhou[1] · Mohammed Al-Hawwas[1] · Larisa Bobrovskaya[1] · Xin-Fu Zhou[1]

Received: 15 August 2020 / Accepted: 22 February 2021 / Published online: 2 April 2021
© The Author(s), under exclusive licence to Springer Science+Business Media, LLC, part of Springer Nature 2021

Abstract

Alzheimer's disease (AD) is the most common cause of dementia among elderly people. Majority of AD cases are sporadic (SAD) with unknown cause. Transgenic animal models closely reflect the familial (genetic) aspect of the disease but not the sporadic type. However, most new drug candidates which are tested positive in transgenic animal models failed in clinical studies so far. Herein, we aim to develop an AD animal model that combines most of the neuropathological features seen in sporadic AD in humans with amyloid plaques observed in transgenic mice. Four-month-old wild-type and APP/PS1 AD mice were given a single intracerebroventricular (ICV) injection of 3 mg/kg streptozotocin (STZ), a diabetogenic agent. Three weeks later, their cognitive behavior was assessed, and their brain tissues were collected for biochemical and histological analysis. STZ produced cognitive deficits in both non-transgenic mice and AD mice. Biochemical analysis showed a severe decline in synaptic proteins, increase in tau phosphorylation, oxidative stress, disturbed brain insulin signaling with extensive neuroinflammation, and cell death. Significant increase was also observed in the level of the soluble beta amyloid precursor protein (APP) fragments and robust accumulation of amyloid plaques in AD mice compared to the control. These results suggest that STZ ICV treatment causes disturbance in multiple metabolic and cell signaling pathways in the brain that facilitated amyloid plaque accumulation and tau phosphorylation. Therefore, this animal model can be used to evaluate new AD therapeutic agents for clinical translation.

Keywords Streptozotocin · APP/PS1 mice · Cognitive deficits · Tau phosphorylation · Amyloid-β plaques · Neuroinflammation · Insulin signaling · Golgi stain

Introduction

Alzheimer's disease (AD) is the most common cause of dementia among elderly people. The main pathological hallmarks are the extracellular accumulation of amyloid plaques (consisting of amyloid beta peptides) and intracellular neurofibrillary tangles (NFT) (consisting of hyperphosphorylated tau protein) in certain brain regions. These manifestations are accompanied by reduced synaptic plasticity, neuroinflammation, and mitochondrial dysfunction that lead to widespread neurodegeneration and cognitive impairment [1]. Only 1–5% of all cases are familial that usually develop at early age and caused by mutations in the presenilin (PS-1, -2) or amyloid precursor protein (APP) genes [2], while most AD cases are sporadic and develop at old age (above 60 years; late-onset). The main cause of sporadic AD is still unknown; it may involve the interaction between several genetic and etiologic factors [2, 3]. While age is considered a main risk factor [4], other potential risk factors such as hypertension, head trauma, diabetes, and inflammation also contribute significantly to the disease pathogenicity [5]. As a result, development of an effective AD drug with multitargeted approach to prevent or symptomatically alleviate AD pathologies is highly demanded.

Many transgenic animal models of AD have been developed in the past two decades to evaluate potential novel therapeutic agents for AD. APP/PS1 mice, which harbor mutated human APP and PS1 genes, and the 3xTg which carries 3 mutated transgenes; APP, PS1, and tau_{P301L}, are examples

✉ Larisa Bobrovskaya
Larisa.Bobrovskaya@unisa.edu.au

✉ Xin Fu Zhou
xin fu.zhou@unisa.edu.au

[1] Health and Biomedical Innovation, Clinical and Health Sciences, University of South Australia, Adelaide, SA 5000, Australia

[2] Faculty of Pharmacy, Assiut University, Assiut, Egypt

[3] Department of Neurology, The Second Affiliated Hospital, Kunming Medical University, Kunming, Yunnan Province, China

of common transgenic AD mice [6]. Although these transgenic AD animal models are useful in understanding the disease pathology, they are not useful for testing AD drugs since they could only replicate part of the disease scenario [7]. This could explain why several novel AD drugs have worked in animal studies but failed to be effective in clinical settings [8]. It is worth mentioning that the exact distribution of amyloid beta plaques and tau tangles seen in the brains of AD patients has not been observed in any available transgenic model [9, 10]. Moreover, some of these models are lacking main features such as the tau pathology which is nearly absent in most APP/PS1 models [11] and extensive neuronal loss has not also been observed [12, 13].

Evidence indicates that inflammation of the nervous tissue is one of the earliest events of sporadic AD [14] which is accompanied by synaptic dysfunction [15] and mild cognitive impairment. Subsequently, accumulation of amyloid plaques, tangles, and nerve cell death occur [16]. Thus, we propose that the best model of sporadic AD should not only model the hallmarks of the disease but also model the natural sequential events of the disease progression.

Several studies showed that intraperitoneal (IP) or intracerebroventricular (ICV) injection of streptozotocin (STZ) in either wild-type or transgenic mice and rats could result in severe cognitive impairment. These animals developed AD-like features and in a sequence similar to that occurring in human AD [16–20]. STZ is a diabetogenic agent that was found to cause a state of insulin resistance or impaired insulin signaling in the brain of animals that led to AD-like symptoms [21–24].This insulin-resistant brain state has been identified to be one of the early events contributing to the onset of sporadic AD in humans and is involved in the chain leading to AD neuropathology [25, 26].

In this study, we aimed to develop an animal model of AD using APP/PS1 mouse that could replicate most of the main hallmarks of the disease such as neuro-inflammation, oxidative stress, and cell death, besides the plaques and tangles, and in a sequence, which resembles the disease progression of sporadic type in humans. We hypothesized that STZ could facilitate the development of amyloid plaques and tau pathology in transgenic mice as a possible consequence of the STZ-induced pathological changes and that would ultimately aggravate the cognitive deficits in these mice. Herein, APP/PS1 and wild-type (C57BL/6) mice received a single dose of STZ in one of the lateral ventricles. Three weeks later, the effect of STZ on the cognitive behavior and the pathological changes happening in the brain were investigated.

It is expected that this study will help to develop and characterize an animal model that can reflect sporadic AD in order to explore possible underlying mechanisms for the development of Aβ plaques and its relation to tauopathy in the brain for future research and the development of novel therapies.

Materials and Methods

Chemicals and Antibodies

Primary antibodies used in this study are listed in Table 1. Biotinylated anti-mouse and anti-rabbit IgG antibodies were obtained from Thermo Fisher Scientific, Australia. Donkey anti-rabbit IRDye® 680RD, Donkey anti-goat IRDye® 800CW, and Goat anti-mouse IRDye® 800CW were obtained from LI-COR Millennium Science, Victoria, Australia. Blood from adult normal horse was obtained from Abattoir/Slaughterhouse (Peterborough, South Australia) and serum was processed in our laboratory (house made). VECTASTAIN ABC kit was purchased from Vector laboratories, USA. Enhanced Golgi-cox stain kit was obtained from Bioenno Tech, LLC (Westminster Ave, CA, USA). Fluorometric TUNEL staining kit was purchased from Promega, Australia. Streptozotocin; STZ (2-Deoxy-2-(3-methyl-3-nitrosoureido)-D-glucopyranose)) was purchased from Sapphire, Bioscience, NSW, Australia. Pierce™ BCA Protein Assay Kit was obtained from Thermo Fisher Scientific, Australia. Oxidized Protein Western Blot Detection Kit was purchased from Abcam, Australia. Other chemicals and Congo red stain were purchased from Sigma Aldrich, Australia.

Animals

The APP/PS1 double transgenic mice expressing a chimeric mouse/human amyloid precursor protein (Mo/Hu K595N, M596L, Swedish mutation; APP695swe) and a mutant human presenilin 1 (PS1-dE9) [27] and the wild-type (WT) control mouse (C57BL/6 mice) were initially obtained from Jackson Laboratory (New Harbor, 124 ME, USA) and bred in the Core Animal Facility, University of South Australia. Mice were housed (4–5 animals per cage) with a 12/12 h light/dark cycle and food and water provided ad libitum. All procedures were compliant with the approved protocol (U26-15) from Animal Ethics Committee of the University of South Australia and the South Australia animal welfare act and the "Australian code of practice and use of animals for scientific purposes" [28]. 3Rs (Replacement, Reduction and Refinement) and proper strategies were practiced to ensure the maintenance of animal welfare through daily monitoring and recording, and detection and management of any pain or distress under the direction of the Animal Welfare Officer and Veterinary Surgeon.

The Experimental Protocol

A schematic diagram of the study design is shown in Fig. 1. Female APP/PS1 and WT (4 months old, average weight = 25 ± 2 g) were assigned randomly into 4 groups (n = 10–17/group). Two groups of WT and APP/PS1 mice received a

Table 1 Primary antibodies used in this study

Antibody	Type/host	Specificity	Phosph. site	Dilution	Source
AKT	Poly /Rabbit	AKT		1:1000 WB	Cell signaling technology
pAKT (S473)	Poly /Rabbit	pAKT	Ser 473	1:1000 WB	Cell signaling technology
SAPK/JNK	Poly /Rabbit	JNK (p46, p54)		1:1000 WB	Cell signaling technology
pSAPK/JNK	Poly /Rabbit	pJNK (p46, p54)	Thr183/Tyr185	1:1000 WB	Cell signaling technology
sAPPβ	Poly /Rabbit	Soluble fragment cleaved N terminus to the β secretase cleavage of APP (human)		1:250 WB	BioLegend
sAPPα	Poly /Mouse	soluble fragment resulting from the α secretase cleavage of APP (human)		1:250 WB	BioLegend
AT8	Mono /Mouse	pTau	Ser 202, Thr 205	1:1000 WB	ThermoFisher
Anti APP A4 clone 22C11	Mono /Mouse	mature APP~130kD immature APP~110kD sAPP~120kD		1:1000 WB	MERCK
APP C terminal	Poly /Rabbit	C terminal fragment of APP		1:1000 WB	BioLegend
pAPP Thr 668	Poly /Rabbit	pAPP T668	Thr668	1:1000 WB	Cell signaling technology
Caspase 3	Poly /Rabbit	Cleaved caspase 3		1:500 WB	Sigma Aldrich
CD45	Mono /Rat	CD45		1:250 IHC	STEMCELL Technologies
GSK 3β	Mono /Mouse	GSK 3β		1:3000 WB	Cell signaling technology
pGSK 3β	Poly /Rabbit	pGSK 3β	Ser 9	1:3000 WB	Cell signaling technology
GAPDH	Poly /Sheep	GAPDH		1:5000 WB	Osenses
GFAP	Poly /Rabbit	GFAP		1:2000 WB 1:1000 IHC	Dako
Iba 1	Poly /Rabbit	Iba 1		1:1000 WB	FUJIFILM Wako
MOAB 2, biotinylated	Mono /Mouse	Aβ (1 40/42) peptides		1:500 IHC	Biosenses
NeuN	Mono /Mouse	Neuronal nuclei		1:1000 IHC, WB	Invitrogen
VAMP 2	Poly /Rabbit	VAMP 2		1:3000 WB	Osenses
PSD 95	Mono /Mouse	PSD 95		1:2000 WB	Sigma
pS396 Tau	Mono /Rabbit	pTau	Ser 396	1:15,000 WB	Abcam
Tau 5	Mono /Mouse	Mouse Tau		1:7500 WB	Life Technologies
Synaptophysin	Mono /Mouse	Synaptophysin		1:5000 WB	Millipore

Phosph. site, phosphorylation site; *Mono* , monoclonal; *poly* , polyclonal; *WB*, western blotting; *IHC*, immunohistochemistry

single STZ intracerebroventricular (ICV) injection while the other two groups of WT and APP/PS1 received saline and served as control groups. Groups were allocated as follows: 10 WT mice (saline), 12 APP/PS1 mice (saline), 12 WT (STZ) and 17 APP/PS1 mice (STZ), aged 4 months old. At that age, no cognitive decline and Aβ deposition can be usually observed in APP/PS1 mice. Administering STZ at that point will help to study the effect of STZ on the cognitive abilities and Aβ load in these mice and to obtain a model that can mimic the sequential events in sporadic AD [29]. Female APP/PS1 animals were selected because they show more consistent and reliable results in behavioral tests that better reflect the AD pathology in the brain rather than age-matched male animals [30]. Mortality rate for APP/PS1 undergone surgery was set to be ≤ 10% as directed by the ethics approvals.

Intracerebroventricular STZ injection was done according to the procedure described previously [18]. Anesthesia was induced in animals by inhaled isoflurane at a flow rate of 3–3.5 mL/min delivered with an oxygen flow rate of 1–1.5 mL/min in a small cage. After deep anesthesia was confirmed, the animal was moved to the stereotaxic equipment and the head was fixed with screws under maintained isoflurane flow rate of 2–2.5 mL/min delivered through a nose tubing. The bregma point was exposed with 3% H_2O_2, then a hole was made according to the following stereotaxic coordinates: − 0.5 mm posterior, − 1 mm lateral, and 2.2 mm dorsoventral from the bregma point. The STZ group was given a single ICV

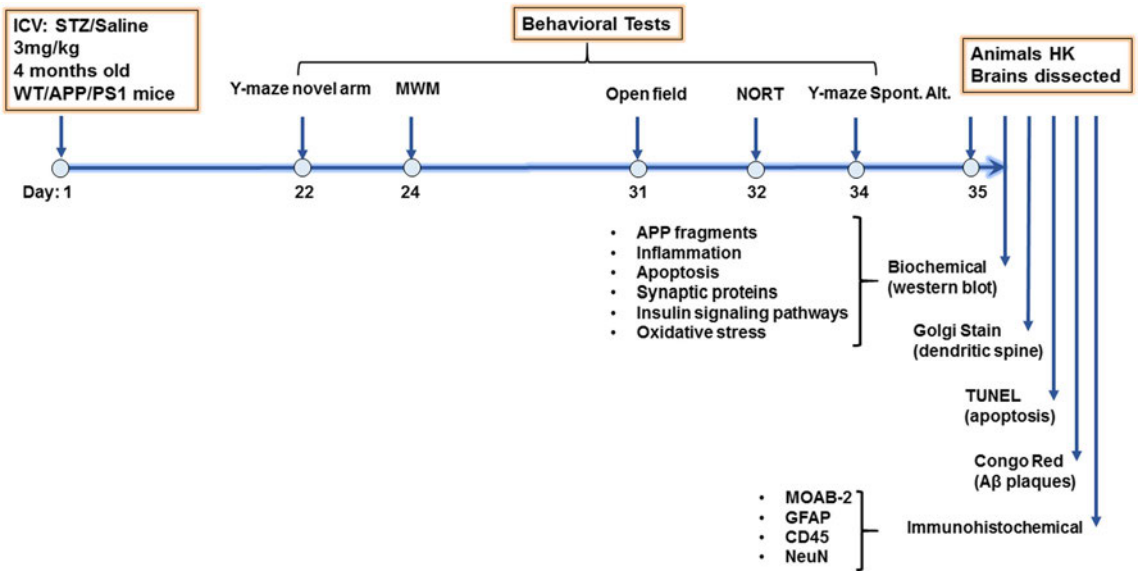


Fig. 1 Representative diagram of the study design

injection of 3 μL of STZ (3 mg/kg, dissolved in saline immediately before injection at a concentration of 25 mg/mL). Control WT and APP/PS1 mice underwent the same surgical procedures but received the same volume of saline instead of STZ. Three weeks after ICV injection, mice were exposed to a battery of behavior tests that lasted for 2 weeks. Finally, animals were humanely killed with deep CO_2 anesthesia and cervical dislocation, then perfused transcardially with ice cold saline and the brains were immediately harvested. Half of the brains were snap frozen in liquid nitrogen and stored at − 80 °C for further biochemical analysis. The other half was fixed in 4% paraformaldehyde in 0.1M PBS and kept in 4 °C for 1 day and then washed with PBS and kept in 30% sucrose in PBS prior to cryosection. Coronal sections of 35 μm thickness were obtained using Leica cryostat (CM3050S, Germany) and stored in antifreeze solution (0.1M PBS containing 30% glycerol and 30% ethylene glycol) at – 20 °C until further immunohistochemical staining. Two hemibrains from each group were carefully separated for further analysis of dendritic spines using Golgi-Cox method of staining.

Behavioral Tests

Morris Water Maze

Spatial reference learning and long-term memory were assessed by Morris Water Maze as described previously [31]. This test was conducted over 6 consecutive days including visible platform trials for 1 day followed by 4 days of hidden platform trials and finally 1 day of probe trial. The test was performed in a black pool filled with water at room temperature (21 ± 2 °C) that is made opaque by non-toxic white powder paint. A hidden platform is submerged 1–1.5 cm below water surface. The animal learns to escape from the water by locating the hidden platform with the help of visual cues placed around the pool walls. Each animal was subjected to 4 trials/day (with 30 min interval) for a period of 4 days. Each time, the animal was placed in a different starting location facing the side walls and allowed to find the platform within 60 s. If the animal failed to find it, it was gently guided and allowed to stay on the platform for 30 s. At the last day, the platform was removed, and the animal was placed in the pool for 60 s for a single probe trial. Time spent in the platform quadrant zone and number of platform zone crossing were recorded using ANY-maze video tracking system v4.5 (Stoelting Co., USA). Escape latency (time to find the platform during the hidden platform trials), swim distance, and speed were also recorded.

Open Field Test

Anxiety and exploratory behaviors were assessed by the open field test [18]. In this test, each animal was placed individually at the border of a PVC square arena (50 x 50 cm and 40 cm high) which is subdivided into inner (central) and outer zone using the software tracking system. Each animal was allowed to explore the arena freely for 5 min. The activity of the animals including rearing behavior, total distance travelled, time spent in inner zone, and % of time spent immobile was recorded using ANY-maze tracking software.

Novel Object Recognition Test

Recognition memory and tendency of mice to explore new objects was evaluated by the novel object recognition test [32]. Prior to testing, each animal was habituated to the testing

arena for 5 min. Following habituation, each animal was allowed to explore two identical objects placed symmetrically from the arena center for 5 min (sample phase). Two hours later, one of the familiar objects was replaced with a novel one and again each animal was allowed to explore the two objects (the sample and the novel objects) for 5 min (test phase). The time spent exploring both objects was recorded. Recognition index is calculated by dividing the time spent to explore the novel object by the total time spent to explore both objects.

Y Maze Spontaneous Alternation and Y Maze Novel Arm

Working memory and spontaneous alternation were evaluated by Y maze novel arm and alternation tests as described previously [32]. Testing occurred in a Y-shaped maze with three opaque arms at a 120° angle from each other. In novel arm test, one arm was blocked, and the animal was allowed to explore the two arms freely. Two hours later, the arm was opened, and the animal could explore all three arms freely. Willingness to explore new environment was evaluated by the time spent in the novel arm and the total number of novel arm visits. Y maze spontaneous alternation was performed few days later in the same maze but rotating it 45° prior to testing. The animal was allowed to explore the maze freely for 5 min. The number of arm entries and the number of triads were recorded to calculate the percentage of alternation. Over the course of several arm entries, healthy subject should show a tendency to enter a less recently visited arm thus displaying a higher alternation percentage. Mice with less than 7 arm total entries were excluded from analysis.

Immunohistochemical and TUNEL Staining

Free floating brain sections were treated with 1% SDS for 5 min for antigen retrieval followed by 3% H_2O_2 in PBS (pH 7.4) for 15 min to inhibit endogenous peroxidases. For total Aβ detection, antigen retrieval was done by 70% Formic acid for 30 min at RT. After washing with PBS, sections were blocked with 20% normal horse serum (NHS) in PBS for 2 h. Sections were then incubated with primary antibodies (diluted in 1% NHS in PBS and 0.3% Triton-X) overnight at 4 °C then with biotinylated secondary antibodies at RT followed by avidin/biotinylated horseradish peroxidase (ABC kit) and finally developed with DAB. Sections were gradually dehydrated with serial increasing ethanol concentrations, then xylene and finally mounted with Depex mounting media (Sigma Aldrich) and scanned with NanoZoomer S60 Automated Digital slide scanner (HAMAMATSU, Australia). Image analysis was performed with Image J software (NIH, Bethesda, MD, USA).

TUNEL staining was done according to the kit protocol provided. Sections were labeled with Terminal Deoxynucleotidyl Transferase/Nucleotide mixture for 1 h at 37 °C. Localized green, fluorescent apoptotic tissue was visualized using Olympus (CX40) fluorescence microscope and quantified with Image J software.

Congo Red Staining

Aβ plaques were visualized by Congo red staining. Briefly, brain sections were mounted on gelatin-coated slides and allowed to dry overnight at RT. For staining, sections were placed in a coplin jar and incubated with working sodium chloride solution (3% NaCl, 80% ethanol, and 0.01% NaOH) for 20 min at RT, followed by working Congo Red solution (0.2% in working sodium chloride solution) for 1 h at RT. Sections were then rinsed with distilled water, rapidly dehydrated twice in absolute ethanol and xylene then coverslip with Depex mounting media. Slides were scanned with NanoZoomer and 1–2 sections from each animal from similar region were analyzed using Image J software.

Golgi Staining

Freshly collected hemibrains (n = 2/group) were immediately impregnated with the potassium dichromate and mercuric chloride solution at room temperature in the dark for 11 days. Then, samples were washed thoroughly with deionized water and kept in post impregnation buffer for 2 days at room temperature. Prior to cryo-sectioning, half brains were immersed in 30% sucrose overnight at 4 °C. Subsequently, half brains were serially sectioned at a thickness of 100–150 μm using a Leica cryostat. Sections were washed in a collecting buffer and directly mounted on gelatin-coated slides and allowed to dry for few hours at room temperature. Before staining, sections were washed with 0.01 M PBS buffer (pH 7.4) with Triton X-100 (0.3%) and stained with ammonium hydroxide solution (as stated in the kit protocol). After staining and washing, sections were dehydrated in 100% ethanol 4 times, then cleared with xylene and finally mounted in Depex mounting media for imaging using Olympus BX53 microscope (cellSens imaging software and Olympus XC50 camera). Analysis of spine length and density was done using ImageJ software (NIH, Bethesda, MD, USA) according to the method described previously [33].

Western Blot Analysis

Frozen brain samples were pulverized with liquid nitrogen then sonicated with cold RIPA buffer (50 mM Tris-HCl, 2 mM EDTA, 150 mM NaCl, 0.1% SDS, 1% sodium deoxycholate, and 1% Nonidet-40) (pH 7.4) in a ratio of 10 mg tissue: 100 μL buffer containing protease and phosphatase cocktail inhibitors (Roche Diagnostics GmbH, Mannheim, Germany) at 4 °C. Samples were centrifuged at 20,000g for 30 min and the supernatant was collected and kept at – 80 °C. Protein concentrations

of the homogenates were measured by using BCA (Bicinchoninic Acid) total protein assay kit (Thermo Fisher). The samples were separated with 10% or 12% SDS-PAGE and electro-transferred onto 0.2 or 0.4 μm nitrocellulose membranes (GE Healthcare, Life science, Germany). Non-specific binding was blocked with 5% milk in Tris-HCl buffer with 0.5% Tween 20 for 1 h at RT. The blots were then probed with primary antibodies and developed with IRDye conjugated secondary antibodies. Blots were imaged using Odyssey® CLx Infrared fluorescent scanner and analyzed using Image Studio Lite software (Li-COR Bioscience).

For total oxidized protein assay, protein samples were treated with dinitrophenylhydrazine (DNPH) solution and neutralization buffer and then subjected to electrophoresis and finally detected with the 1ry and 2ry antibodies provided as described by kit protocol.

Statistical Analysis

Results were expressed as mean ± SEM. One-way analysis of variance (ANOVA), followed by Tukey's multiple comparison test or Fisher LSD post hoc tests, was used to analyze the data for more than two groups. Unpaired two-tailed *t* test with Welch's correction was used to compare means of two groups. Two-way ANOVA (two factors; time and treatment) followed by Tukey's multiple comparison test was used to analyze the escape latency data of the MWM test. The analysis was carried out using GraphPad Prism v9.0 (GraphPad Software). p value < 0.05 was considered statistically significant for all comparisons.

Results

Effect of STZ on Body Weight and Mortality

Following surgery, mice were monitored daily and their weight was recorded daily for the first week then once weekly. We observed that majority of the animals experienced different grades of weight loss which was more prominent in APP/PS1 and WT groups that received STZ (data not shown); however, all mice recovered their weight later. Three out of 17 APP/PS1 mice that received STZ died few days following surgery (fatality rate 17%) as seen in survival curve in Fig. 2 f. In contrast, no mortalities were reported in the WT groups that received saline or STZ nor with APP/PS1 mice that received saline.

STZ Exacerbates the Cognitive Decline in APP/PS1 Mice

Spatial Reference Memory (MWM)

Both WT and APP/PS1 STZ groups exhibited severe cognitive decline in spatial learning and acquisition. As shown in the learning curve, all groups learned to locate the platform across trials as evident by reduced escape latency (interaction: $F_{9,48} = 0.9565$, $p = 0.4868$, time factor: $F_{3,48} = 20.63$, $p < 0.0001$, treatment factor: $F_{3,48} = 79.58$, $p < 0.0001$, Fig. 2). However, STZ-treated mice spent more time to locate the hidden platform ($p < 0.0001$) indicating impaired ability of these mice to code and remember the spatial position of the platform. No significant difference was found between WT and APP/PS1 mice that received saline. In the probe trial, saline-treated mice spent approximately 50% of time in the target quadrant zone ($F_{3,\ 34} = 9.940$, $p < 0.0001$) and showed higher number of platform zone crossing ($F_{3,\ 34} = 11.32$, $p < 0.0001$) in contrast to STZ-treated mice which spent around 20% in the target zone and crossed the platform much less with some mice showed zero platform crossing number. These results indicated that STZ induced a cognitive decline in spatial reference and learning memory in WT mice and exacerbated the cognitive decline in APP/PS1 mice.

Anxiety, Locomotor and Exploratory Behavior (Open Field Test)

Both WT STZ and APP/PS1 STZ-treated mice seemed to be more anxious than their corresponding saline-treated groups as evident by less time spent in the central zone (4 vs. 9%, $F_{3,28} = 5.818$, $p = 0.0367$ {APP/PS1 STZ vs. saline controls}, $p = 0.0265$ {WT STZ vs. WT saline}). They also showed high immobility time % (25–42 vs. 18%, $F_{3,28} = 15.83$, $p = 0.0427$ {APP/PS1 STZ vs. saline controls}, $p = 0.0002$ {WT STZ vs. WT saline}). In addition, exploratory behavior was suppressed in STZ-treated mice as assessed by less distance travelled ($F_{3,28} = 9.844$, $p = 0.0469$ {APP/PS1 STZ vs. saline controls}, $p = 0.0212$ {WT STZ vs. WT saline}) and rearing episodes ($F_{3,\ 28} = 5.869$, $p = 0.045$ {APP/PS1 STZ vs. saline controls}, $p = 0.0242$ {WT STZ vs. WT saline}).

Results also showed that WT STZ mice exhibited higher immobility time % ($t(9.014) = 3.083$, $p = 0.0131$) and less total distance travelled ($t(13.22) = 3.727$, $p = 0.0025$) compared to APP/PS1 STZ (unpaired *t* test with Welch's correction). A representative track plot of the activity of mice in the open field test is shown in Fig. 3.

Working Memory (Y-Maze Novel Arm and Spontaneous Alternation)

As shown in Fig. 3 (f, g, and h), STZ produced significant reduction in number of novel arm entries in APP/PS1 mice

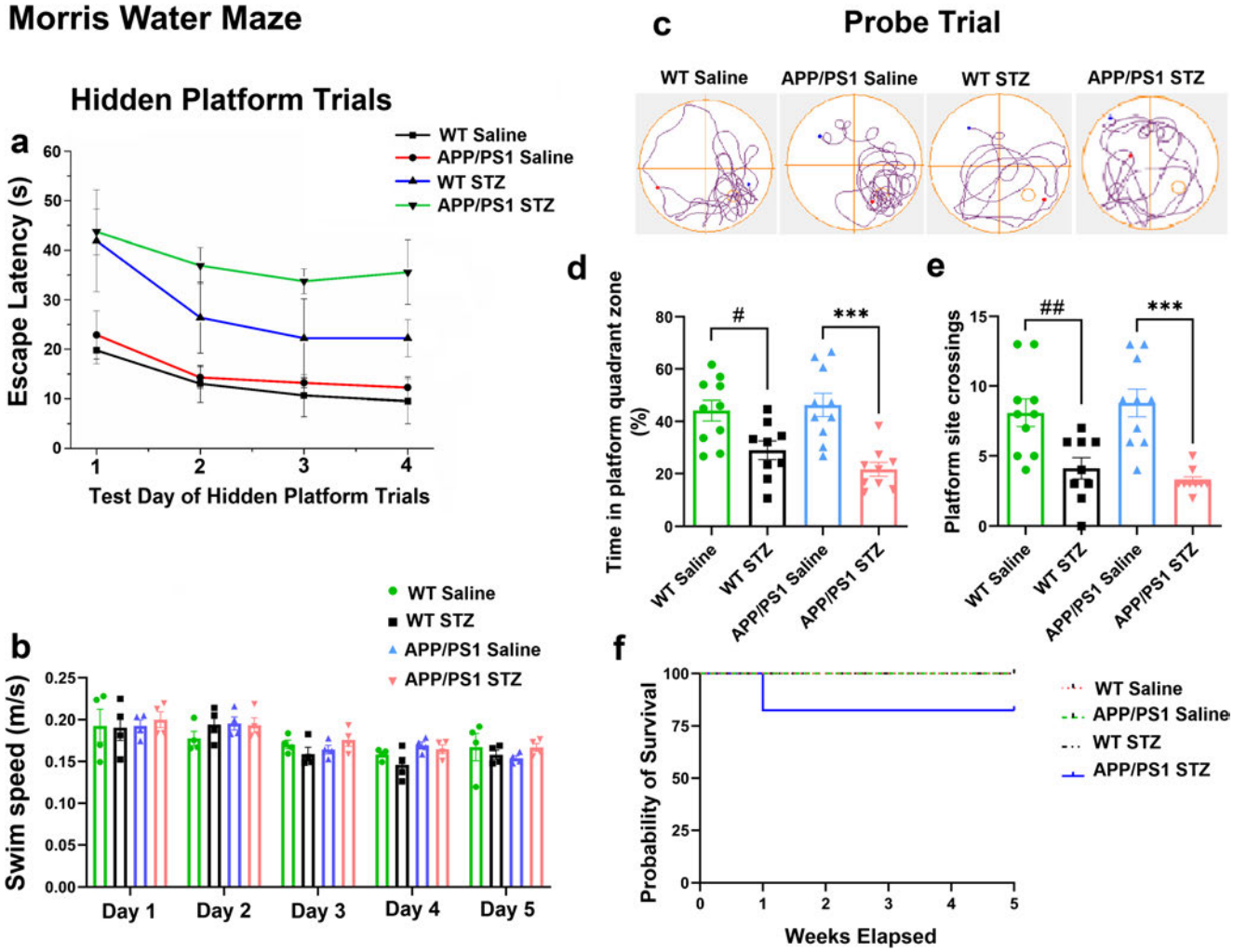


Fig. 2 Morris water maze. STZ treatment impairs spatial learning memory in WT and APP/PS1 mice. The test was conducted over 6 consecutive days, the 1st day is the visible platform training, 4 days of hidden platform testing, and a probe trial 24 h after the last hidden platform test. **a**, **b** The hidden platform trials showed that STZ significantly increased the escape latency but did not alter the swimming speed. Two way ANOVA revealed significant reduction in the escape latency at day 4 compared to day 1 in all groups indicating ability to spatial learning except for the APP/PS1 STZ group which showed no improvement in spatial learning. **c**, **d**, **e** The probe trial showing the track plots in which STZ significantly reduced the time that mice spent in the target quadrant zone, where the platform was previously hidden, and the number of platform site crossing. **f** Survival curve showing the dropout of animals along the experimental timeline. All data are presented as mean ± SEM. *means significant difference from APP/PS1 controls, #significant difference from WT controls. *, # $p < 0.05$, **, ## $p < 0.01$, *** and ### $p < 0.0001$ (one way ANOVA), $n = 7$ 10/group

($F_{3,\ 30} = 6.466$, $p = 0$ 0.0105) and in WT mice ($p = 0.0391$). Also, APP/PS1 STZ showed the least spontaneous alternation percentage (48.58 vs. 63.58% for APP/PS1 saline, $p = 0.0258$) and WT STZ showed a percentage of alternation of 49.45% ($p = 0.0271$ vs. WT saline), while saline-treated groups alternated between arms within a range of 63 and 65% ($F_{3,\ 30} = 6.006$, $p = 0.0025$).

Recognition Memory (NORT)

STZ caused significant decline in recognition memory in both WT ($p = 0.0157$, vs. saline controls) and APP/PS1 ($p = 0.0238$, vs. saline controls), ($F_{3,33} = 6.771$, $p = 0.0011$) as shown in Fig. 3 i. There was a significant reduction in the recognition index in those mice (39 vs. 68% for saline-treated mice). Thus, STZ-treated mice showed no preference towards the novel object over the familiar one, indicating a severe short-term memory impairment.

STZ Increases Aβ Plaques in APP/PS1 Mice

In order to study the effect of STZ on the plaque pathology in APP/PS1 mice, brain sections of STZ-treated and control groups were subjected to Congo Red stain and immunohistochemistry. Congo Red staining showed segregated congophilic deposits in mice brains of APP/PS1 after STZ

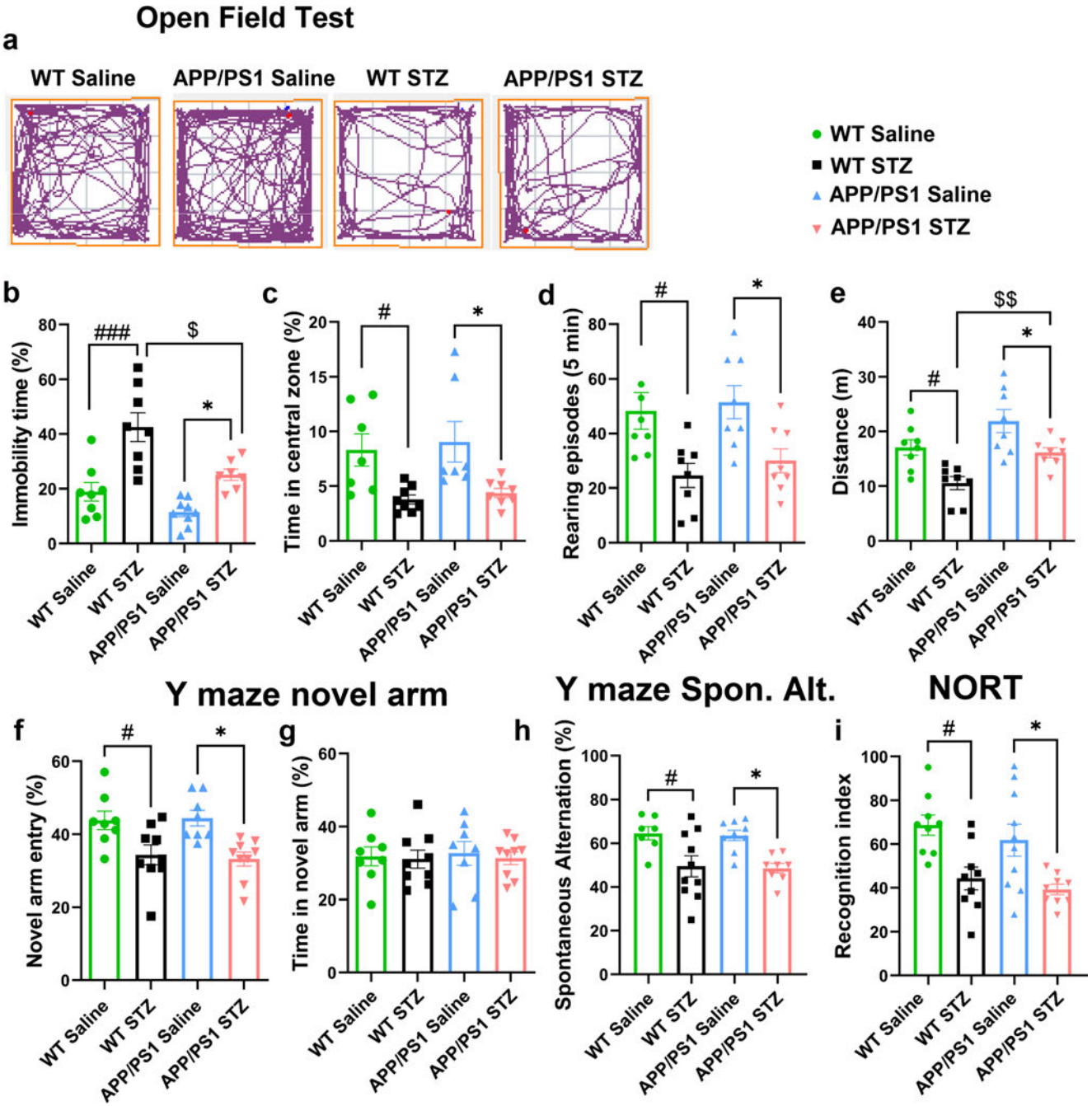


Fig. 3 Open field test, Y maze task, and novel object recognition test. **a** **e** STZ increased the anxiety like behavior and reduced exploratory behavior in both WT and APP/PS1 mice. **a** Representative plots showing the mice activity in the open field test, **b** the percentage of time spent by the animal immobile during the test, **c** % of time spent in the central (inner zone), **d** the number of rearing episodes that indicates the exploratory behavior of the animal, and **e** the total distance travelled (m) by the animal in the open field arena. **f** **i** STZ impairs short term working and recognition memory in both WT and APP/PS1 mice. **f**, **g** Y maze novel arm test; STZ significantly reduces the number of novel arm entries (expressed as % to the total number of arm entries) and to some extent reduces the % of time spent in the novel arm over the total time spent in the maze, **h** Y maze spontaneous alternation; STZ significantly reduces the % of spontaneous alternation between all arms compared to control mice, and **i** Novel object recognition test; STZ significantly reduces the time spent by the animal to explore the novel object to the total time of exploring both the both the familiar and novel objects during the test phase (recognition index). Data are presented as mean ± SEM. *means significant difference from APP/PS1 controls, #significant difference from WT controls. *, # $p < 0.05$, **, ## $p < 0.01$, (one way ANOVA), \$ $p < 0.05$ significant difference between WT STZ and APP/PS1 STZ (Student *t* test, unpaired, two tailed with Welch's correction), $n = 7$ 10/group

ICV injection. The plaque number and size were almost 2-fold higher than the control group (hippocampus: plaque number: $t(30) = 5.226$, $p < 0.0001$, area fraction (%): $t(21.55) = 3.425$, $p = 0.0025$); cortex: plaque number: $t(27.72) = 5.281$, $p < 0.0001$, area fraction (%): $t(14.25) = 3.889$, $p = 0.0016$). In order to confirm this result, total Aβ was stained with MOAB-2, a pan-specific antibody to Aβ peptides. Quantitative image analysis revealed significant increase in Aβ in the cortex (plaque number: $t(26.95) = 6.977$, $p < 0.0001$, area fraction (%): $t(17.23) = 3.596$, $p = 0.0010$) and in the hippocampus (plaque number: $t(26.54) = 5.11$, $p < 0.0001$, area fraction (%): $t(21.51) = 4.34$, $p = 0.0003$) of STZ-treated APP/PS1 compared to control APP/PS1 group, (Fig. 4a, b, and c).

To further elucidate whether the increase in Aβ pathology resulted from altered APP processing by STZ injection, western blot of full-length APP (APPfl), its phosphorylated form at Threonine 668 (T668) and its the cleavage fragments; APP C-terminal fragments (CTF-α and -β) and the N-terminus APP-β fragment (sAPPβ) was carried out. Results revealed a significant increase in the levels of sAPPβ by 39% ($t(8.344) = 2.618$, $p = 0.0297$), CTFs by 32% ($t(9.154) = 3.139$, $p = 0.0117$) and APPT668 by 33.6% ($t(11.38) = 2.717$, $p = 0.0195$) and reduction in sAPPα by 46% ($t(11.65) = 3.98$, $p = 0.0019$) (Fig. 4d, e) in APP/PS1 STZ relative to the control. Taken together, these findings suggest that STZ may enhance the amyloidogenic processing of APP in APP/PS1 mice brains.

STZ Increases Tau Phosphorylation in AD and WT Mice

Next, we investigated the effect of STZ ICV injection on tau pathology in the brains of WT and APP/PS1 mice. Western blot analysis of phosphorylated tau protein showed that STZ induced a significant increase in the levels of epitope pS396 in both WT ($F_{3,23} = 8.227$, $p = 0.046$ vs. WT saline) and APP/PS1 groups ($p = 0.018$ vs. APP/PS1 saline), but no change in the levels of total tau protein was observed (Fig. 5). The levels of AT8 (phosphorylated tau protein at serine 202 and threonine 205 residues) were significantly increased in WT STZ compared to saline-treated WT mice ($F_{3,23} = 17.44$, $p < 0.0001$). The same effect was observed in APP/PS1 mice ($F_{3,23} = 17.442$, $p = 0.048$). This result suggests that STZ

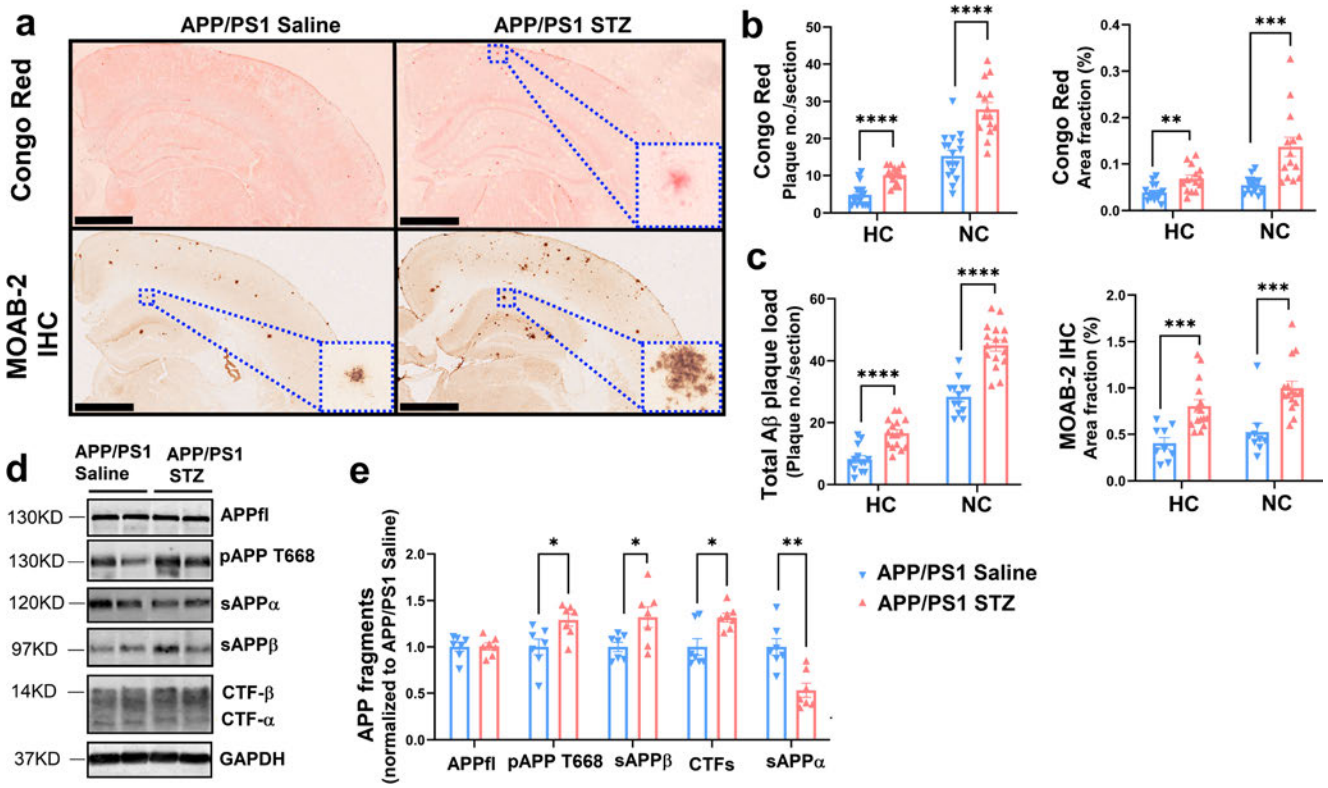


Fig. 4 STZ exacerbates the amyloid pathology in APP/PS1 mice. **a** Representative images of brain sections of vehicle and STZ treated transgenic mice showing Congo Red stain and MOAB 2 Aβ immunostaining 5 weeks after ICV STZ injection. Scale bar = 1 mm, insets show × 40 magnification of the pointed regions. **b**, **c** STZ significantly increased the number of congophilic plaques and the total plaque load in the cortex and hippocampus of the transgenic mice brains (n = 9 12; 1 2 sections were analyzed for each animal). **d** Representative blots showing the expression levels of APP fragments, levels are normalized to total full length protein (APPfl), GAPDH was used as a loading reference, $n = 5$ 7/group. **e** STZ treatment significantly reduced the levels of sAPPα while markedly increased the expression levels of the amyloidogenic pAPPT668, sAPPβ and CTFs. *$p < 0.05$, ** $p < 0.01$ (Student t test, unpaired, two tailed with Welch's correction). Results are presented as means ± SEM

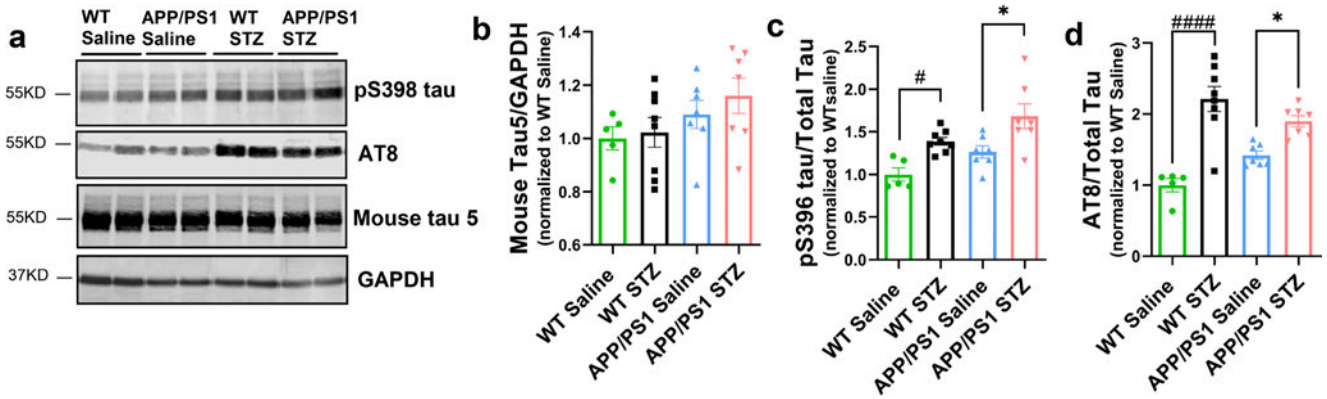


Fig. 5 STZ ICV induces tau hyperphosphorylation in the brains of WT and APP/PS1 mice. **a** Total brain lysates extracted with RIPA buffer from control and STZ treated mice were evaluated by western blots with the following antibodies: Mouse tau 5 antibody against total tau, pS396 and AT8 (pS202/pT205), (n = 5 8/group). **b** Quantification of the immunoblot bands of phosphorylated tau against total tau, normalized to GAPDH. *p < 0.05 vs. APP/PS1 saline. # p < 0.05 vs. WT saline (one way ANOVA). Results are presented as means ± SEM

may aggravate the tau pathology in the brains of AD and WT mice.

STZ Promotes Neuroinflammation in APP/PS1 and WT Mice

Neuroinflammation is currently identified as a key hallmark and a predisposing factor of AD [34]. We investigated the effect of STZ on neuroinflammation by measuring the levels of glial fibrillary acidic protein (GFAP), a marker for astrocyte activation, and ionized Ca^{2+}-binding adaptor molecule-1 (Iba-1), a marker for microglial activation in addition to CD45 which is a leukocyte common antigen that can detect activated microglial aggregates by using western blotting and IHC techniques. As previously reported, APP/PS1 showed higher microglial and astrocytic activation compared to WT animals. Western blotting showed that STZ further aggravated the neuroinflammation state in APP/PS1, by increasing GFAP ($F_{3,22}$ = 8.288, p = 0.009 vs. APP/PS1 saline) and Iba-1 expression ($F_{3,23}$ = 9.29, p = 0.0026 vs. APP/PS1 saline) as observed in western blotting. In case of WT mice, STZ increased GFAP ($F_{3,22}$ = 8.288, p = 0.016) and Iba-1 expression ($F_{3,23}$ = 9.29, p = 0.015) compared to their control littermates.

Immunohistochemistry of brain sections of APP/PS1 further showed that CD45 expression was significantly increased by STZ in the cortex ($F_{3,26}$ = 44.2, p < 0.0001) and hippocampus ($F_{3,26}$ = 23.19, p < 0.0001) indicating microglial overactivation. GFAP staining was elevated following STZ injection in APP/PS1 mice (cortex: $F_{3,29}$ = 18.33, p < 0.0001, hippocampus: $F_{3,29}$ = 19.3, p = 0.0001). The same response was observed in WT STZ mice in which GFAP expression was significantly elevated compared to saline-treated animals (cortex: $F_{3,29}$ = 18.33, p = 0.0072, hippocampus: $F_{3,29}$ = 19.3, p < 0.0001) and CD45 was also elevated (cortex: $F_{3,26}$ = 44.2, p < 0.0001, hippocampus: $F_{3,26}$ = 23.19, p < 0.0001). However, the pattern of microglial and astrocytic activation seen in APP/PS1 mice brain, shown as enlarged soma and thickened processes, was not observed by the same intensity in WT STZ (Fig. 6). Results also revealed that the expression levels of CD45 and GFAP (IHC immunoreactivity) are significantly higher in the cortex of APP/PS1 STZ mice compared to WT STZ mice (CD45: t(14.57) = 4.168, p = 0.0009, GFAP: t(16.96) = 3.047, p = 0.0073).

STZ Induces Oxidative Stress and Triggers Apoptotic Cell Death in APP/PS1 and WT Mice

Marked neuron loss is a prominent feature in AD [35]. To evaluate the effect of STZ on neuron cell viability, we performed NeuN IHC to detect mature neuron nuclei. TUNEL (terminal deoxynucleotidyl transferase mediated dUTP nick end labeling) staining was also performed for detection of DNA fragmentation, as marker of any possible apoptosis. In addition, western blotting of NeuN, caspase-3, a member of cysteine proteases family and JNK (c-Jun N-terminal kinase) activity, which plays a central role in proapoptotic signaling pathways, was conducted. Results showed that the number of TUNEL positive cells in CA3 region of the hippocampus has increased 4 times (assessed as % of area fraction) in both STZ-treated mice compared to control mice ($F_{3,\ 18}$ = 35.13, p < 0.0001 {APP/PS1 STZ vs. saline controls}, p = 0.0004 {WT STZ vs. saline controls}). This finding was further supported by NeuN IHC immunoreactivity results which was reduced significantly in Dentate Gyrus ($F_{3,\ 19}$ = 8.682, p = 0.0085 {WT STZ vs. saline controls}, p = 0.034 {APP/PS1 STZ vs. saline controls}) and in neocortex ($F_{3,\ 19}$ = 5.929, p = 0.03, {WT STZ vs. saline controls}, p = 0.04, {APP/PS1 STZ vs. saline controls}) while showed a trend towards reduction in CA1, CA2, and CA3 region of the hippocampus (Fig. 7a–d).

Western blotting analysis revealed significant decrease in NeuN expression in APP/PS1 STZ-treated mice ($F_{3,22}$ = 6.4, p = 0.009, Fig. 7e, f) and a significant increase in the ratio of

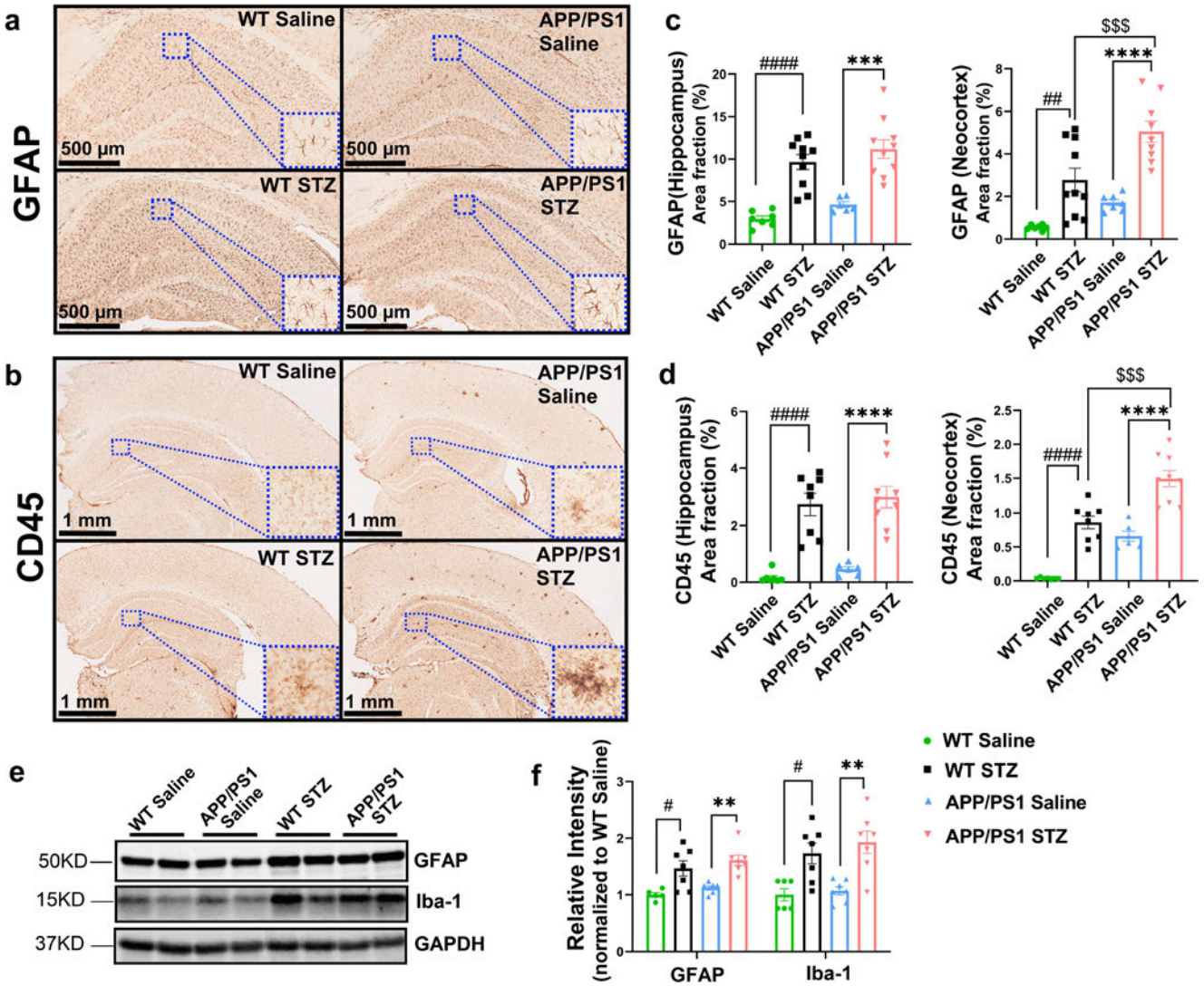
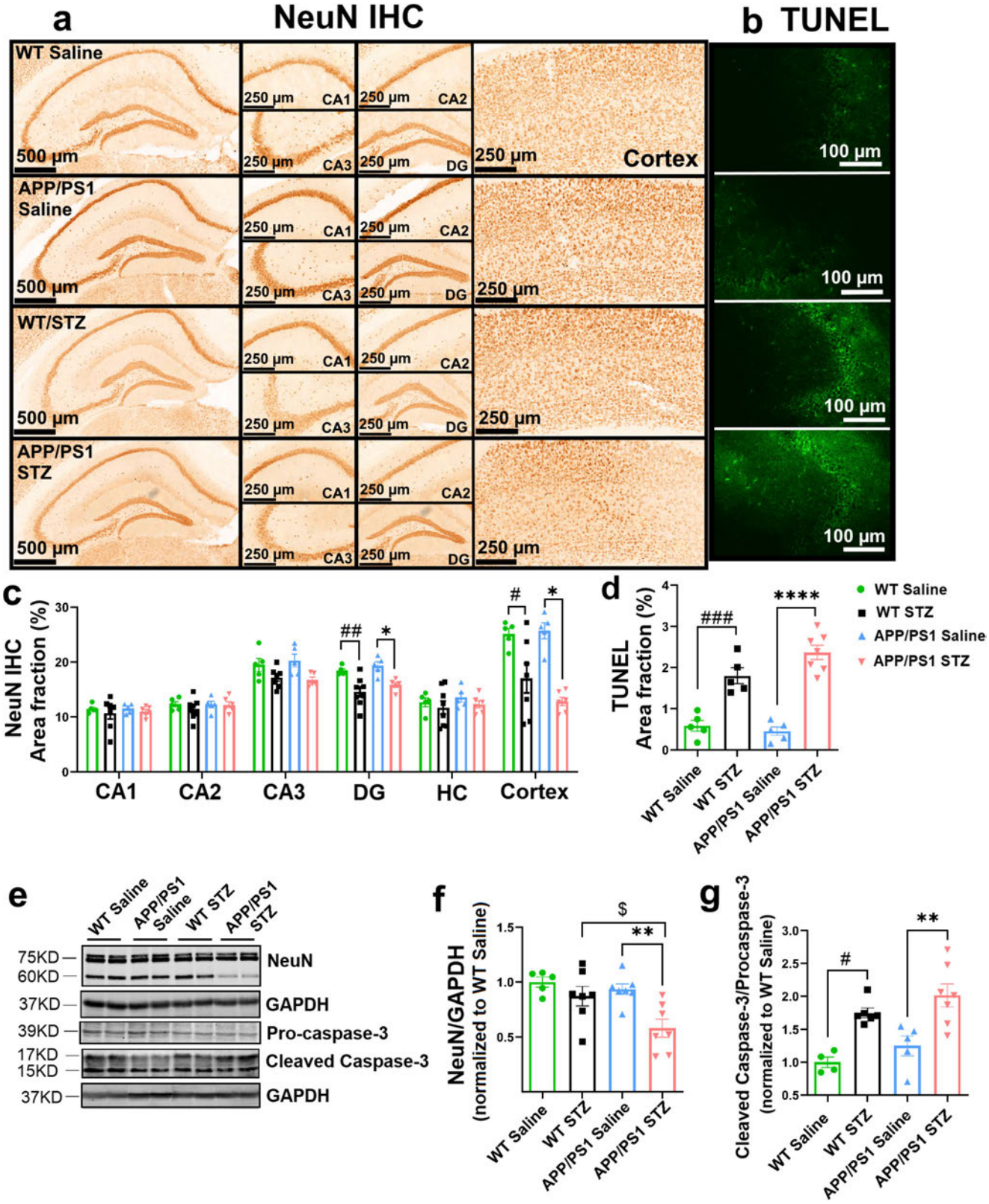


Fig. 6 STZ ICV promotes severe neuroinflammation in WT and APP/PS1 mice. **a** **d** Immunostaining and quantification of inflammation markers in the hippocampus and cortex of saline and STZ treated mice using (**a**) GFAP for astrocytosis and (**b**) CD45 for microgliosis (scale bar = 500 μm for **a**, 1 mm for **b**). Insets show × 40 magnification of the pointed regions, n = 5 13/group (1 2 sections/animal). **e** Whole brain homogenates of all groups were analyzed by western blots and probed with antibodies against GFAP and Iba 1. **f** Quantitative analysis of Iba 1 and GFAP protein expression normalized to GAPDH level, n = 5 7/group. *$p < 0.05$ vs. APP/PS1 saline. # $p < 0.05$ vs. WT saline (one way ANOVA), $ $p < 0.05$ significant difference between WT STZ and APP/PS1 STZ (Student t test, unpaired, two tailed with Welch's correction). Results are presented as means ± SEM

caspase-3 to procaspase-3 in both WT ($F_{3,18}$ = 10.38, p = 0.0118) and APP/PS1 STZ mice ($F_{3,18}$ = 10.38, p = 0.0046). STZ treatment led to activation of the JNK signaling pathway, and the ratio of p-JNK/JNK has increased in WT ($F_{3,23}$ = 16.69, p = 0.039) by 42% and 60.6% in APP/PS1 mice ($F_{3,23}$ = 16.69, $p < 0.0001$) compared to their matched controls (Fig. 9c, f). Compared to saline-treated mice, the levels of protein peroxidation products 2,4-dinitrophenylhydrazine (DNPH) were significantly elevated in the brain of STZ-treated ($F_{3,12}$ = 17.06, p = 0.0012, {WT STZ vs. saline controls}, p = 0.002, {APP/PS1 STZ vs. saline controls}), (Fig. 8a, b). Taken together, these results suggest that STZ activates oxidative stress markers and induces multiple signaling pathways mediated by phosphorylated active JNK and caspase-3 leading to apoptotic cell death and neurodegeneration.

STZ Alters Synaptic Proteins and Reduces Spine Density and Length in Hippocampus in AD and WT Mice

Synaptic dysfunction is an early event in AD pathogenesis [36] and directly correlates to the severity of cognitive decline [15]. Levels of synaptic proteins involved in structural plasticity were found to be dropped dramatically in aging [37]. Moreover, reduced synaptic density and loss of dendritic spine



were also reported in human AD brains [38]. Therefore, in this study, we measured the levels of synaptophysin (Syp), a presynaptic protein; postsynaptic density 95 (PSD95), a postsynaptic marker as well as VAMP-2, a vesicle-associated membrane protein which is a member of SNAREs family (soluble N-ethylmaleimide-sensitive factor attachment protein

◀ **Fig. 7** *STZ ICV induces neuronal apoptosis in WT and APP/PS1 mice.* **a** *Representative* images of the hippocampus and neocortex immunostained with NeuN; a marker for mature neurons nuclei (scale bar = 500 μm, 250 μm for focused regions). **b** A representative coronal section of the CA3 region of the mice hippocampus stained using a TUNEL assay to detect apoptotic cells in control and STZ treated groups (scale bar = 100 μm). **c**, **d** Quantification of area fraction% of NeuN and TUNEL positive staining in the cortex, whole hippocampus and its subregions. **e** Western blotting of brain homogenates probed with NeuN and caspase 3 antibodies showing procaspase 3 and cleaved caspase 3. **f**, **g** Quantification of the protein expression levels of NeuN, procaspase 3, and cleaved caspase 3, normalized to GAPDH, showing that STZ significantly reduced NeuN expression and elevated the levels of cleaved caspase 3 and reduced the mature procaspase 3 in WT and transgenic mice. *$p < 0.05$ vs. APP/PS1 saline. # $p < 0.05$ vs. WT saline (one way ANOVA), $ $p < 0.05$ significant difference between WT STZ and APP/PS1 STZ (Student t test, unpaired, two tailed with Welch's correction), $n = 4$ 8. Results are presented as means ± SEM

receptors) using western blotting. In addition, we performed Golgi stain to visualize the effect of STZ on dendritic spine length and density in hippocampus.

Results showed no significant difference in the level of synaptic proteins between control WT and APP/PS1 mice. STZ ICV injection produced a significant decline in the levels of PSD-95 ($F_{3,\ 19} = 8.120$, $p = 0.003$) and VAMP-2 ($F_{3,\ 19} = 7.345$, $p = 0.0013$) and synaptophysin ($F_{3,\ 19} = 3.576$, $p = 0.0376$) in APP/PS1 compared to their control littermates. In WT mice, STZ produced significant decline in the levels of PSD-95 ($p = 0.049$) compared to control WT mice, but the levels of VAMP-2 or synaptophysin were not significantly altered (Fig. 8c, d).

Second-order apical dendrites of the CA1 pyramidal neurons were analyzed using ImageJ software. Spine density represented as number of spines per μm of dendrite length as well as average spine length were assessed. Quantitative analysis of CA1 pyramidal neurons showed a significant reduction in the spine density for WT STZ and APP/PS1 STZ ($F_{3,76} = 20.2$, $p < 0.0001$) and average spine length ($F_{3,71} = 18.83$, $p < 0.0001$ for APP/PS1 STZ and $p = 0.047$ for WT STZ) compared to saline-treated groups (Fig. 8e, f).

Overall, these data suggest that STZ impaired synaptic plasticity in WT and APP/PS1 mice and decreased the dendritic spine complexity of the CA1 hippocampus pyramidal neurons. These changes might underlie the severe cognitive impairment observed in STZ-treated mice.

STZ Dysregulates Pathways Involved in Brain Insulin Signaling in APP/PS1 and WT Mice

Reduction of cerebral insulin levels [25] and impaired insulin transduction mechanisms [26] has been found in sporadic AD patients compared to age-matched controls, indicating that insulin resistance and sporadic AD are linked. To investigate the effect of STZ on insulin signaling mechanisms after 5 weeks of ICV administration, the levels of total Akt (protein kinase B) and GSK-3β (glycogen synthase kinase-3β) as well as their phosphorylated forms, as a downstream component of insulin signaling, were assessed by western blotting. Results showed that STZ increased the level of pS9-GSK3β in both WT STZ and APP/PS1, whereas the total protein level remained unchanged. When the phosphorylated form was normalized to the levels of the corresponding protein, we found that the ratio of pS9-GSK3β/GSK3β was significantly increased by > 50% in STZ-treated mice compared to controls ($F_{3,23} = 5.44$, WT STZ: $p = 0.045$, APP/PS1: $p = 0.038$) (Fig. 9a, d). Similarly, the expression level of p-Akt/Akt has increased significantly in APP/PS1 STZ ($F_{3,23} = 6.628$, $p = 0.027$) and WT ($F_{3,23} = 6.628$, $p = 0.02$) mice compared to their controls, while levels of the total protein were not altered (Fig. 9b, e). Taken together, these data suggest that STZ ICV caused disturbance in brain insulin signaling in these mice.

Discussion

Disturbance in brain insulin signaling has emerged as a main contributing factor of late onset AD [21, 39] confirming that diabetes and cognitive dysfunction are strongly linked [25]. Previously, clinical studies reported loss of insulin receptor activity [26], as well as disturbances of insulin levels in cerebrospinal fluid and plasma in patients with advanced AD. These changes were similar to age-matched healthy controls (age > 60), which means that aberrant insulin signaling is age-related and can precede any cognitive decline symptoms [40]. Therefore, the term "type 3 diabetes" has been proposed to describe the pathophysiology of sporadic AD [41]. In this perspective, animal studies further revealed that intraperitoneal or ICV injection of streptozotocin induces several metabolic changes and abnormalities that are quite similar and escalate in same pattern to those observed in the brain of sporadic AD [42, 43]. STZ is a diabetogenic agent that, if administered systemically in large doses, it induces type 1 diabetes by destroying the pancreatic insulin secreting cells [44], while, in small doses, it can cause insulin resistance by desensitizing insulin receptors through decreasing its autophosphorylation and activation [45, 46]. ICV STZ injection in very low doses does not cause systemic diabetes; however, it induces impaired insulin signaling and disturbance in cerebral glucose metabolism [42, 47]. Such energy disturbances, besides its direct neurotoxic damage of brain regions that are involved in learning and memory, could provide the basic initiative for the cascade of events that lead to marked cognitive decline in AD models [48, 49]. In the present study, we studied the effect of ICV injection of STZ into APP/PS1 and WT mice at 4

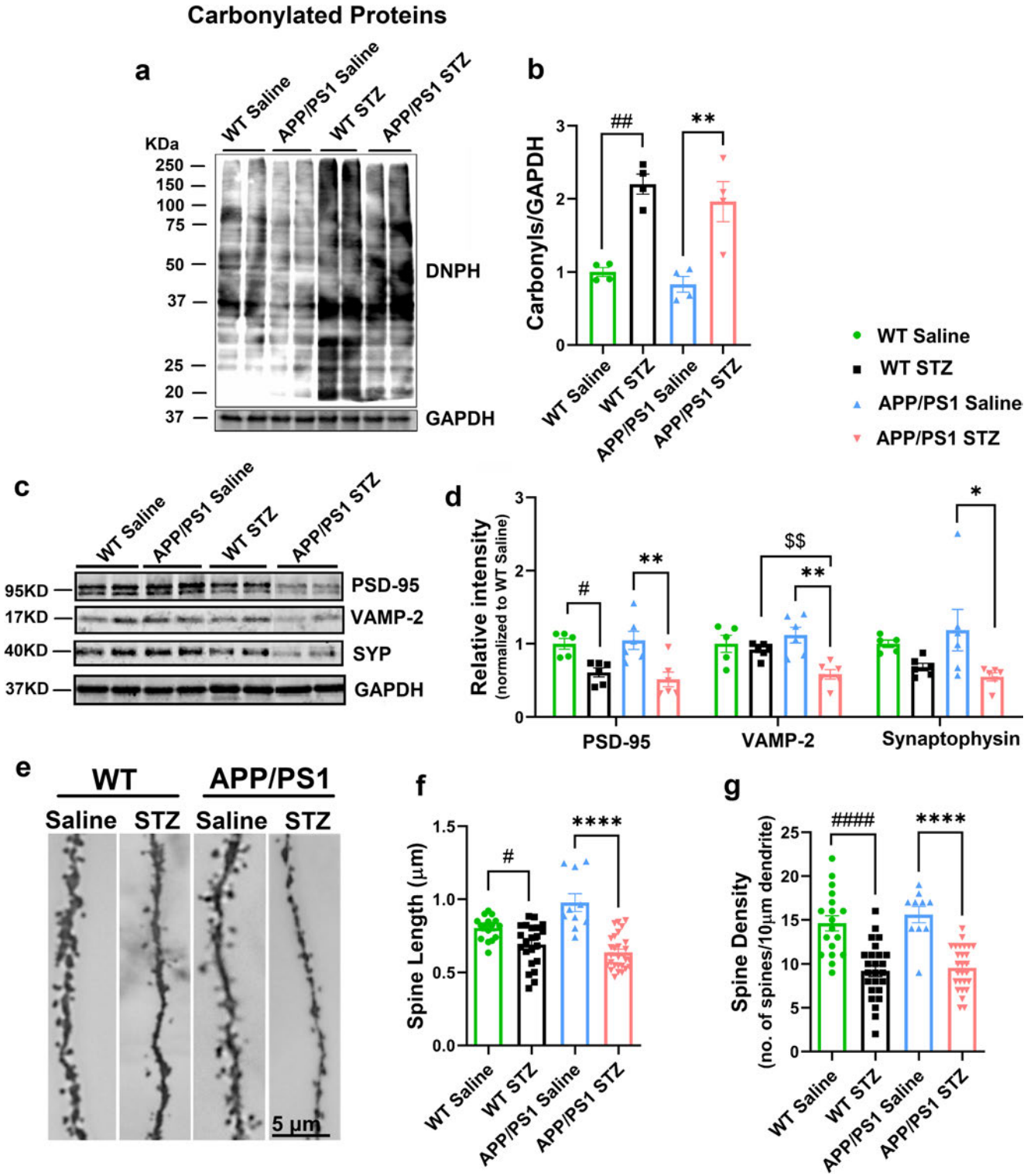


Fig. 8 **a**, **b** STZ ICV induces oxidative stress in the brains of WT and APP/PS1 mice. A representative Western blot image and quantification of protein peroxidation products DNPH (n = 4/group). **c** **f** STZ reduces synaptic plasticity in WT and APP/PS1 mice. **c**, **d** Immunoblot analysis and quantification for synapse associated proteins including PSD 95, VAMP 2, and synaptophysin in whole brain homogenates (n = 5 6/group). **e** **g** Representative image and quantification of average spine length and density of the apical dendrites of CA1 pyramidal neurons of the hippocampus (n = 2/group, 6 7 neurons per mouse, scale bar = 5 µm). *$p < 0.05$ vs. APP/PS1 saline. # $p < 0.05$ vs. WT saline (one way ANOVA), $ $p < 0.05$ significant difference between WT STZ and APP/PS1 STZ (Student t test, unpaired, two tailed with Welch's correction). Results are presented as means ± SEM

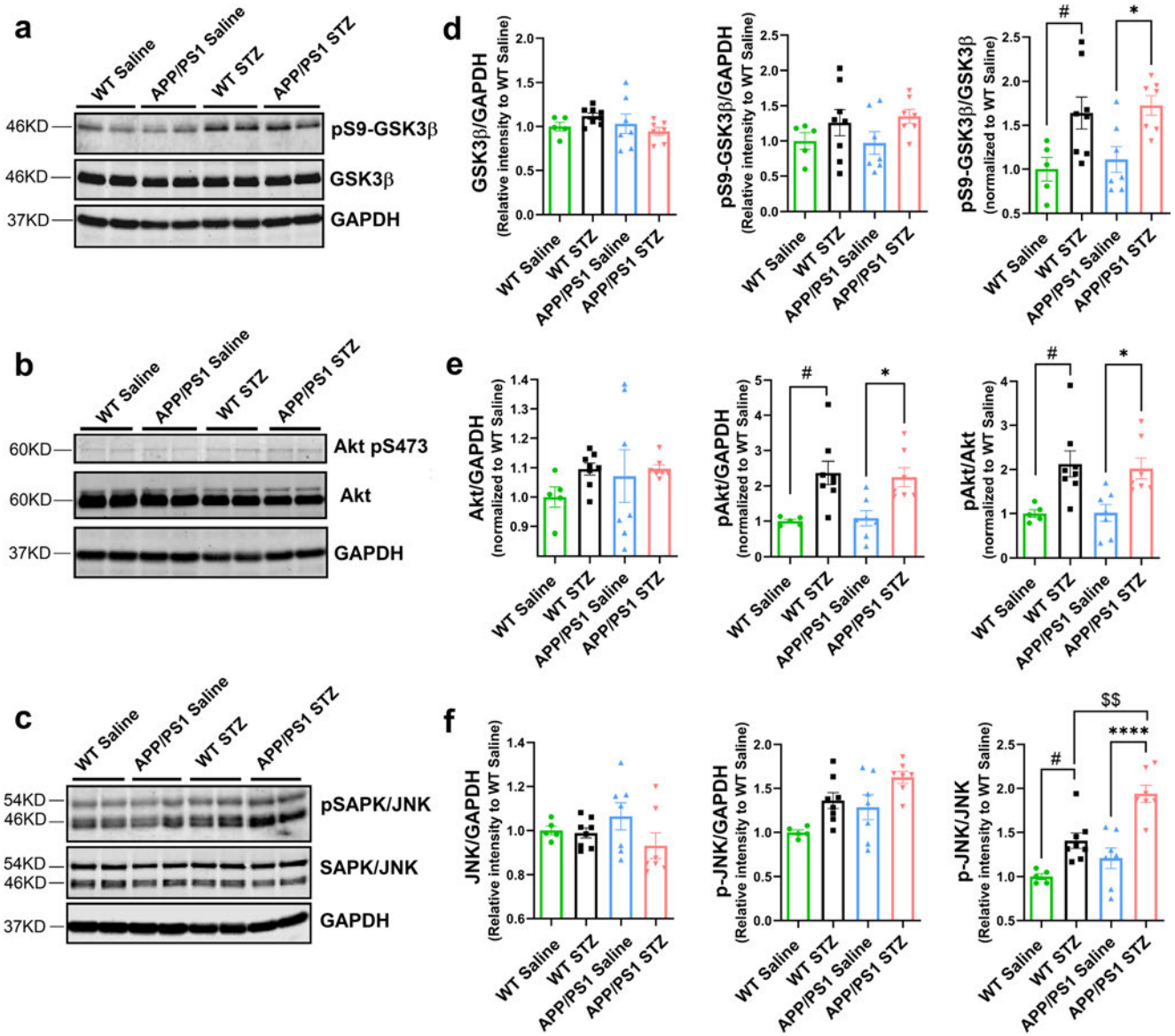


Fig. 9 Effects of ICV STZ on the expression levels of kinases involved in insulin signaling pathways and JNK phosphorylation in the WT and APP/PS1 mouse brain 5 weeks after injection. **a c** Immunoblot analysis showing the levels of total GSK 3β, Akt, and SAPK/JNK protein expression and their phosphorylated forms. **d f** Each graph displays quantification of the immunoreactivity of the specified phosphorylated form to the corresponding total protein level and expressed as relative intensity of the WT Saline which equals 1, GAPDH is used as loading control. STZ increased the levels of pS9 GSK 3β and thus the ratio of pS9/GSK 3β increased significantly. STZ also significantly increased Akt and SAPK/JNK phosphorylation and the ratio of pS473 Akt/Akt and pJNK/JNK increased significantly in STZ treated mice compared to controls. *$p < 0.05$ vs. APP/PS saline. #$p < 0.05$ vs. WT saline (one way ANOVA), $$p < 0.05$ significance difference between WT STZ and APP/PS1 STZ (Student *t* test, unpaired, two tailed with Welch's correction). Results are presented as means ± SEM, $n = 5$ 8

months old to evaluate the effect of brain insulin resistance on the plaque and tau pathology in transgenic AD mice.

In line with previous reports of STZ-induced cognitive deficits [18, 42, 43], ICV STZ decreased spatial learning and memory abilities in WT and APP/PS1 mice as examined by MWM. STZ-treated groups showed more escape latency time during the hidden platform trials and spent less time in the target quadrant zone in the probe trial compared to controls. STZ-treated mice also showed anxiety-like behavior in open field test as they displayed less tendency to visit the central zone and spent more time immobile compared to the controls. They also showed severe decline in working and short-term memory in Y maze and showed no preference towards the novel over the familiar object in novel object recognition test (NORT) test. Control APP/PS1 mice were not different from WT mice in these tests at the age of 5 months old. Our data indicate that STZ significantly facilitates the development of cognitive impairment in APP/PS1 mice whose cognitive decline can only be detected at 8 months old [50] .

We found that around 17% of APP/PS1 mice died post ICV STZ injection. However, STZ did not result in any deaths among WT mice and the surgery itself did not affect the control groups that received saline (data not shown). Therefore, it is speculated that transgenic mice could either be more sensitive to the neurotoxic insult of STZ, or likely died due to seizure which is a common feature of these mice [51].

Oxidative stress is one of the prominent features of AD which apparently precedes plaque and tangle deposition [52]. In this study, we found that STZ significantly elevated the levels of carbonylated proteins as detected by DNPH, a marker of oxidative stress, in the brains of WT and APP/PS1 mice as reported previously [43]. Upon degradation, STZ releases free radicles including reactive oxygen species (ROS) [53], which might be responsible for the oxidative stress observed in the current model. Also, impaired glucose metabolism might aggravate this condition.

Neuroinflammation is one of early key events that plays a role in accumulation of plaques and tau tangles [34]. Consistent with previous animal studies, we found that STZ promoted astrocytes and glial activation which is evident by the increase in GFAP and Iba-1 expression [18]. This is likely to be caused by STZ-induced oxidative stress [54, 55]. Although, activated astrocytes and microglia clustered around the amyloid plaques are already present in APP/PS1 at that age [50], STZ ICV further aggravated the pathology in transgenic mice as evident by IHC and immunoblotting.

In line with previous findings [16, 19], our results showed that STZ exacerbated the accumulation of Aβ in APP/PS1 transgenic mice. IHC and Congo Red stain revealed increased accumulation of congophilic plaques and higher immunoreactivity to Aβ antibody against total plaque load. Western blotting showed increased levels of CTFs which are substrates of γ-secretase cleavage and in sAPPβ level while the level of the sAPPα significantly decreased suggesting that the amyloidogenic processing of APP is favored [56]. Such increase in Aβ generation could be attributed to aggravation of inflammation in addition to energy failure and oxidative stress [57, 58].

Furthermore, we found that STZ elevated tau phosphorylation at epitope pS396 and at S202/Thr 205 (AT8) in the APP/PS1 and WT mice at the age of 5 months. It worth mentioning that the APP/PS1 mice show hyperphosphorylated tau-positive neuritic structures accompanying amyloid deposits only at 6–7 months old, with no tangles observed [50]. These results suggest that the ICV STZ may increase tau hyperphosphorylation in transgenic and WT mice. This finding agrees with previous reports showing an increase in tau phosphorylation after central and systemic administration of STZ in rodents [17, 20, 59].

To best understand the underlying molecular mechanisms that led to aggravation of Aβ and tau pathology, we investigated the effect of STZ on the two main pathways that lie downstream of insulin signaling including the PI3K/Akt/GSK-3 and MAPK/JNK pathways. These pathways were found to be involved in the formation of Aβ plaques [60], tau hyperphosphorylation [61], and neuronal apoptosis [62] that account for the main hallmarks of AD [63]. The levels of Akt (protein kinase B)/GSK-3 enzymes, that lie downstream in the insulin receptor-PI3 kinase signaling cascade [64], were altered. The ratio of phosphorylated GSK-3β at serine 9 (S9) (the inactive form) and Akt pS473 (the active form) to total protein levels were significantly upregulated 5 weeks after STZ ICV injection, while total protein levels were not changed. This finding is consistent with previous reports showing that the effect of STZ ICV on insulin signaling transduction system is time dependent. Salkovic-Petrisic et al. reported that the ratio of pGSK-3α/β and pAkt to total protein increased in rat hippocampus 1 month after ICV STZ injection followed by sharp decline after 3 months, while total proteins levels were unchanged [65]. Similar results were obtained by Clodfelder-Miller et al. following systemic STZ administration [20]. In line with these results, clinical studies showed that total protein levels of Akt/PKB and GSK-3 were unchanged in brains of AD patients at autopsy [41]. Either decrease or increase of the activity of Akt/PKB and GSK-3 pathway enzymes was observed in different post-mortem brain regions of AD patients [66–69]. In our experiments, we did not measure the activity of GSk-3β or Akt/PKB. However, we assume that the acute increase in pS9-GSk-3β observed in this study is a consequence of Akt activation (phosphorylation). Another possible explanation could be the role of protein phosphatase (PP2A). PP2A was found to be inhibited in sporadic AD [70, 71] and in STZ AD animal models [17, 18]. This enzyme negatively regulates the PI3K/Akt pathway by dephosphorylating Akt (i.e., inactivating) and slightly dephosphorylating GSK-3β (i.e., activating) [72]. Therefore, this initial upregulation in phosphorylated Akt and GSK-3β could be considered as a compensation for the enzyme activity followed by downregulation in later stages and possibly due to PP2A inhibition. Thus, our model of STZ in WT and APP/PS1 mice could mirror some of the pathological changes of sporadic AD in relation to the disease progression and severity.

GSK-3 that lies downstream of the insulin signaling pathway, is involved in APP processing through its α-isoform [73], and regulates tau protein phosphorylation through its β-isoform [74]. Therefore, it is presumed that the mismetabolism of APP and abnormal tau phosphorylation is a consequence of disturbed glucose metabolism and aberrant insulin signaling. Since we observed inhibition of GSK-3β rather than activation after STZ ICV injection, it is speculated that tau hyperphosphorylation could have resulted from other mechanisms. A previous study found that inhibition of PP2A is probably the principal factor in inducing tau hyperphosphorylation [75, 76] and accounts for the massive increase in tau phosphorylation at multiple sites following

systemic STZ administration [20, 77]. In addition, persistent inflammation could cause tau hyperphosphorylation and misfolding [78].

We found that STZ activated JNK signaling through increasing its phosphorylation levels, which agrees with previously published studies [19, 20]. JNK is a member of stress-activated protein kinase (SAPK) pathway that has been shown to be activated in AD as a response to cellular stress such as oxidative stress [79, 80]. JNK can further amplify the stress signal through modulating enzymes involved in formation of plaques and tangles [52, 57, 58]. Studies revealed that oxidative stress promotes amyloidogenic processing of APP by activation of BACE1 and APP phosphorylation (T668) through JNK signaling pathway [58, 81, 82]. We also detected a significant increase in the levels of phosphorylated APP (T668) in APP/PS1 STZ mice compared to their controls. These results are in line with Yoon et al. showing that JNK-3 is the main kinase for APP phosphorylation at T668 thereby, facilitating its endocytosis and subsequent processing [83].

JNK signaling pathway can also mediate neuronal apoptosis through caspase activation. In our study, the level of activated (cleaved) caspase-3 has increased compared to procaspase-3 following STZ ICV injection, as previously reported [55]. Caspases are activated as a result of metabolic and oxidative stress insult and has been found in brains of AD patients [84]. Reports also suggest caspase-3 plays a role in tau cleavage and hyperphosphorylation [85, 86], is involved in APP cleavage [87] and underlies early synaptic loss in AD [88].

STZ induced neuronal histopathologic alterations in the hippocampus and neocortex, as reflected by the increase in pre-apoptotic or apoptotic cells detected by TUNEL and NeuN IHC. In the STZ-treated group, the number of mature neurons was significantly reduced in DG and neocortex and showed a trend towards reduction in all regions of the hippocampus. This is explained as a result of the abnormality in insulin signaling pathways which could mediate apoptosis through JNK and caspase-3 [89].

STZ also induced severe synaptic dysfunction accompanied by reduction of PSD-95, synaptophysin, VAMP-2 levels, and reduction of average dendritic spine length and density. No prominent synaptic deficits are observed in APP/PS1 mice at that age compared to WT mice. These deficits are likely related to STZ-induced reduction of cerebral glucose metabolism and oxidative stress at synapses [90]. Soluble amyloid oligomers formed early in the disease could be involved in synaptic failure [15], and could ultimately explain severe synaptic deficits in APP/PS1-STZ compared to WT-STZ group.

Conclusion

To the best of our knowledge, this is the first study to report the comparative effects of ICV STZ injection in both WT and APP/PS1 mice. Our results indicated that STZ produced severe cognitive decline in WT and did facilitate the development of AD pathologies in APP/PS1 mice at 4 months old when they are usually normal in cognitive functions. The advantage of APP/PS1-STZ model is that we can obtain accelerated and severe cognitive decline. Also, Aβ pathology in that model correlates better with the synaptic and cognitive changes than that reported in the normal course of the disease in transgenic AD model [91]. Therefore, APP/PS1-STZ model at that age could reflect the interaction between genetic and etiologic factors of AD, and thus could be more effective and promising to test novel AD therapeutic approaches and their efficacy on the amyloid and tau pathology.

Acknowledgements The authors acknowledge the support provided to S. Kelliny by Commonwealth Research and Training scholarship and Egyptian Ministry of Higher Education. We would like to thank Dr Lewis Vaughan for technical assistance regarding the surgical procedure and Mr. Andrew Beck for suggestions regarding histological techniques and imaging.

Author Contribution Larisa Bobrovskaya and Xin Fu Zhou contributed to the study conception and design. Material preparation, experiments, data collection, and analysis were performed by Sally Kelliny. Liying Lin participated in tissue staining experiments; Isaac Deng, Jing Xiong, Fiona Zhou, and Mohammed Al Hawwas collaborated in animal studies. The first draft of the manuscript was written by Sally Kelliny and all authors commented on previous versions of the manuscript. Larisa Bobrovskaya and Xin Fu Zhou supervised the study. All the authors reviewed and approved the final version of the manuscript submitted.

Funding This study was supported by the National Health and Medical Research Council (NHMRC) grants (1020567, 1021409) and supporting grant from the University of South Australia.

Data Availability All of the data that was generated and analyzed in this study are included in this article.

Declarations

Ethics Approval All procedures were compliant with the approved pro tocol (U26 15) from the Animal Ethics Committee of the University of South Australia and the South Australia animal welfare act and the "Australian code of practice and use of animals for scientific purposes."

Consent to Participate Not applicable.

Consent for Publication Not applicable.

Conflict of Interest The authors declare no competing interests.

References

1. Alzheimer's Disease International: World Alzheimer Report 2018; The state of the art of dementia research: new frontiers (2018).

2. Blennow K, de Leon MJ, Zetterberg H (2006) Alzheimer's disease. Lancet (London, England) 368(9533):387 403. https://doi.org/10.1016/s0140 6736(06)69113 7
3. Zetterberg H, Mattsson Carlgren N (2014) Understanding the cause of sporadic Alzheimer's disease. Expert review of neurotherapeutics 14:621 630. https://doi.org/10.1586/14737175.2014.915740
4. Evans DA, Funkenstein HH, Albert MS, Scherr PA, Cook NR, Chown MJ, Hebert LE, Hennekens CH et al (1989) Prevalence of Alzheimer's disease in a community population of older persons. Higher than previously reported. Jama 262(18):2551 2556
5. Chakrabarti S, Khemka VK, Banerjee A, Chatterjee G, Ganguly A, Biswas A (2015) Metabolic risk factors of sporadic Alzheimer's disease: implications in the pathology, pathogenesis and treatment. Aging Dis 6 (4):282 299. https://doi.org/10.14336/AD.2014.002
6. Ribeiro FM, Camargos ER, de Souza LC, Teixeira AL (2013) Animal models of neurodegenerative diseases. Revista brasileira de psiquiatria (Sao Paulo, Brazil : 1999) 35 Suppl 2:S82 91. https://doi.org/10.1590/1516 4446 2013 1157
7. Li C, Ebrahimi A, Schluesener H (2013) Drug pipeline in neurodegeneration based on transgenic mice models of Alzheimer's disease. Ageing Research Reviews 12(1):116 140. https://doi.org/10.1016/j.arr.2012.09.002
8. Zahs KR, Ashe KH (2010) 'Too much good news' are Alzheimer mouse models trying to tell us how to prevent, not cure, Alzheimer's disease? Trends Neurosci 33(8):381 389. https://doi.org/10.1016/j.tins.2010.05.004
9. Götz J, Streffer JR, David D, Schild A, Hoerndli F, Pennanen L, Kurosinski P, Chen F (2004) Transgenic animal models of Alzheimer's disease and related disorders: histopathology, behavior and therapy. Mol Psychiatry 9(7):664 683. https://doi.org/10.1038/sj.mp.4001508
10. Calhoun ME, Wiederhold KH, Abramowski D, Phinney AL, Probst A, Sturchler Pierrat C, Staufenbiel M, Sommer B et al (1998) Neuron loss in APP transgenic mice. Nature 395(6704):755 756. https://doi.org/10.1038/27351
11. Metaxas A, Thygesen C, Kempf SJ, Anzalone M, Vaitheeswaran R, Petersen S, Landau AM, Audrain H et al (2018) Tauopathy in the $APP_{swe}/PS1_{\Delta E9}$ mouse model of familial Alzheimer's disease. bioRxiv:405647. https://doi.org/10.1101/405647
12. Jankowsky JL, Slunt HH, Gonzales V, Jenkins NA, Copeland NG, Borchelt DR (2004) APP processing and amyloid deposition in mice haplo insufficient for presenilin 1. Neurobiol Aging 25(7):885 892. https://doi.org/10.1016/j.neurobiolaging.2003.09.008
13. Götz J, Deters N, Doldissen A, Bokhari L, Ke Y, Wiesner A, Schonrock N, Ittner LM (2007) A decade of tau transgenic animal models and beyond. Brain pathology (Zurich, Switzerland) 17(1):91 103. https://doi.org/10.1111/j.1750 3639.2007.00051.x
14. Wyss Coray T (2006) Inflammation in Alzheimer disease: driving force, bystander or beneficial response? Nature Medicine 12(9):1005 1015. https://doi.org/10.1038/nm1484
15. Arendt T (2009) Synaptic degeneration in Alzheimer's disease. Acta Neuropathol 118(1):167 179. https://doi.org/10.1007/s00401 009 0536 x
16. Salkovic Petrisic M, Osmanovic Barilar J, Brückner MK, Hoyer S, Arendt T, Riederer P (2011) Cerebral amyloid angiopathy in streptozotocin rat model of sporadic Alzheimer's disease: a long term follow up study. Journal of neural transmission (Vienna, Austria : 1996) 118(5):765 772. https://doi.org/10.1007/s00702011 0651 4
17. Chen Y, Liang Z, Blanchard J, Dai CL, Sun S, Lee MH, Grundke Iqbal I, Iqbal K et al (2013) A non transgenic mouse model (icv STZ mouse) of Alzheimer's disease: similarities to and differences from the transgenic model (3xTg AD mouse). Mol Neurobiol 47(2):711 725. https://doi.org/10.1007/s12035 012 8375 5
18. Chen Y, Liang Z, Tian Z, Blanchard J, Dai C L, Chalbot S, Iqbal K, Liu F et al (2014) Intracerebroventricular streptozotocin exacerbates Alzheimer like changes of 3xTg AD mice. Mol Neurobiol 49(1):547 562. https://doi.org/10.1007/s12035 013 8539 y
19. Wang X, Zheng W, Xie JW, Wang T, Wang SL, Teng WP, Wang ZY (2010) Insulin deficiency exacerbates cerebral amyloidosis and behavioral deficits in an Alzheimer transgenic mouse model. Mol Neurodegener 5:46. https://doi.org/10.1186/1750 1326 5 46
20. Clodfelder Miller BJ, Zmijewska AA, Johnson GV, Jope RS (2006) Tau is hyperphosphorylated at multiple sites in mouse brain in vivo after streptozotocin induced insulin deficiency. Diabetes 55(12):3320 3325. https://doi.org/10.2337/db06 0485
21. Hoyer S (2000) Brain glucose and energy metabolism abnormalities in sporadic Alzheimer disease. Causes and consequences: an update. Experimental gerontology 35(9 10):1363 1372. https://doi.org/10.1016/s0531 5565(00)00156 x
22. Grieb P (2016) Intracerebroventricular streptozotocin injections as a model of Alzheimer's disease: in search of a relevant mechanism. Mol Neurobiol 53(3):1741 1752. https://doi.org/10.1007/s12035 015 9132 3
23. Hoyer S, Lannert H (2007) Long term abnormalities in brain glucose/energy metabolism after inhibition of the neuronal insulin receptor: implication of tau protein. Journal of neural transmission Supplementum 72:195 202. https://doi.org/10.1007/978 3 211 73574 9_25
24. Kamat PK, Kalani A, Rai S, Tota SK, Kumar A, Ahmad AS (2016) Streptozotocin Intracerebroventricular induced neurotoxicity and brain insulin resistance: a therapeutic intervention for treatment of sporadic Alzheimer's disease (sAD) like pathology. Mol Neurobiol 53(7):4548 4562. https://doi.org/10.1007/s12035 015 9384 y
25. Craft S, Peskind E, Schwartz MW, Schellenberg GD, Raskind M, Porte D Jr (1998) Cerebrospinal fluid and plasma insulin levels in Alzheimer's disease: relationship to severity of dementia and apolipoprotein E genotype. Neurology 50(1):164 168. https://doi.org/10.1212/wnl.50.1.164
26. Frölich L, Blum Degen D, Riederer P, Hoyer S (1999) A disturbance in the neuronal insulin receptor signal transduction in sporadic Alzheimer's disease. Ann N Y Acad Sci 893:290 293. https://doi.org/10.1111/j.1749 6632.1999.tb07839.x
27. Borchelt DR, Ratovitski T, van Lare J, Lee MK, Gonzales V, Jenkins NA, Copeland NG, Price DL et al (1997) Accelerated amyloid deposition in the brains of transgenic mice coexpressing mutant presenilin 1 and amyloid precursor proteins. Neuron 19(4):939 945. https://doi.org/10.1016/s0896 6273(00)80974 5
28. Health N, Medical Research Council (2013) Australian code for the care and use of animals for scientific purposes, 8th edition. Canberra: National Health and Medical Research Council. 2013
29. Krstic D, Knuesel I (2013) Deciphering the mechanism underlying late onset Alzheimer disease. Nature reviews Neurology 9(1):25 34. https://doi.org/10.1038/nrneurol.2012.236
30. Wang J, Tanila H, Puoliväli J, Kadish I, van Groen T (2003) Gender differences in the amount and deposition of amyloidbeta in APPswe and PS1 double transgenic mice. Neurobiol Dis 14(3):318 327. https://doi.org/10.1016/j.nbd.2003.08.009
31. Morris RG, Garrud P, Rawlins JN, O'Keefe J (1982) Place navigation impaired in rats with hippocampal lesions. Nature 297(5868):681 683. https://doi.org/10.1038/297681a0
32. Wolf A, Bauer B, Abner EL, Ashkenazy Frolinger T, Hartz AMS (2016) A comprehensive behavioral test battery to assess learning and memory in 129S6/Tg2576 mice. PloS one 11(1):e0147733 e0147733. https://doi.org/10.1371/journal.pone.0147733
33. Groves TR, Wang J, Boerma M, Allen AR (2017) Assessment of hippocampal dendritic complexity in aged mice using the Golgi Cox method. J Vis Exp 124:55696. https://doi.org/10.3791/55696
34. Moore AH, O'Banion MK (2002) Neuroinflammation and anti inflammatory therapy for Alzheimer's disease. Adv Drug Deliv

Rev 54(12):1627 1656. https://doi.org/10.1016/s0169 409x(02) 00162 x
35. Shimohama S (2000) Apoptosis in Alzheimer's disease an update. Apoptosis : an international journal on programmed cell death 5(1): 9 16. https://doi.org/10.1023/a:1009625323388
36. Masliah E, Mallory M, Hansen L, DeTeresa R, Alford M, Terry R (1994) Synaptic and neuritic alterations during the progression of Alzheimer's disease. Neurosci Lett 174(1):67 72. https://doi.org/10.1016/0304 3940(94)90121 x
37. Hatanpää K, Isaacs KR, Shirao T, Brady DR, Rapoport SI (1999) Loss of proteins regulating synaptic plasticity in normal aging of the human brain and in Alzheimer disease. J Neuropathol Exp Neurol 58(6):637 643. https://doi.org/10.1097/00005072 199906000 00008
38. DeKosky ST, Scheff SW, Styren SD (1996) Structural correlates of cognition in dementia: quantification and assessment of synapse change. Neurodegeneration 5(4):417 421. https://doi.org/10.1006/neur.1996.0056
39. Biessels GJ, Kappelle LJ (2005) Increased risk of Alzheimer's dis ease in Type II diabetes: insulin resistance of the brain or insulin induced amyloid pathology? Biochemical Society transactions 33(Pt 5):1041 1044. https://doi.org/10.1042/bst0331041
40. Hoyer S (2004) Glucose metabolism and insulin receptor signal transduction in Alzheimer disease. European Journal of Pharmacology 490(1):115 125. https://doi.org/10.1016/j.ejphar.2004.02.049
41. Steen E, Terry BM, Rivera EJ, Cannon JL, Neely TR, Tavares R, Xu XJ, Wands JR et al (2005) Impaired insulin and insulin like growth factor expression and signaling mechanisms in Alzheimer's disease is this type 3 diabetes? J Alzheimers Dis 7(1):63 80. https://doi.org/10.3233/jad 2005 7107
42. Lannert H, Hoyer S (1998) Intracerebroventricular administration of streptozotocin causes long term diminutions in learning and memory abilities and in cerebral energy metabolism in adult rats. Behavioral neuroscience 112(5):1199 1208. https://doi.org/10.1037//0735 7044.112.5.1199
43. Sharma M, Gupta YK (2001) Intracerebroventricular injection of streptozotocin in rats produces both oxidative stress in the brain and cognitive impairment. Life sciences 68(9):1021 1029. https://doi.org/10.1016/s0024 3205(00)01005 5
44. Szkudelski T (2001) The mechanism of alloxan and streptozotocin action in B cells of the rat pancreas. Physiological research 50(6): 537 546
45. Blondel O, Portha B (1989) Early appearance of in vivo insulin resistance in adult streptozotocin injected rats. Diabete & metabolisme 15(6):382 387
46. Kadowaki T, Kasuga M, Akanuma Y, Ezaki O, Takaku F (1984) Decreased autophosphorylation of the insulin receptor kinase in streptozotocin diabetic rats. J Biol Chem 259(22):14208 14216
47. Nitsch R, Hoyer S (1991) Local action of the diabetogenic drug, streptozotocin, on glucose and energy metabolism in rat brain cor tex. Neuroscience letters 128(2):199 202. https://doi.org/10.1016/0304 3940(91)90260 z
48. Shoham S, Bejar C, Kovalev E, Weinstock M (2003) Intracerebroventricular injection of streptozotocin causes neuro toxicity to myelin that contributes to spatial memory deficits in rats. Experimental Neurology 184(2):1043 1052. https://doi.org/10.1016/j.expneurol.2003.08.015
49. Weinstock M, Shoham S (2004) Rat models of dementia based on reductions in regional glucose metabolism, cerebral blood flow and cytochrome oxidase activity. Journal of neural transmission (Vienna, Austria : 1996) 111(3):347 366. https://doi.org/10.1007/s00702 003 0058 y
50. Radde R, Bolmont T, Kaeser SA, Coomaraswamy J, Lindau D, Stoltze L, Calhoun ME, Jäggi F et al (2006) Abeta42 driven cere bral amyloidosis in transgenic mice reveals early and robust pathology. EMBO Rep 7(9):940 946. https://doi.org/10.1038/sj.embor.7400784
51. Reyes Marin KE, Nuñez A (2017) Seizure susceptibility in the APP/PS1 mouse model of Alzheimer's disease and relationship with amyloid β plaques. Brain Res 1677:93 100. https://doi.org/10.1016/j.brainres.2017.09.026
52. Su B, Wang X, Nunomura A, Moreira PI, Lee H, Perry G, Smith MA, Zhu X (2008) Oxidative stress signaling in Alzheimer's dis ease. Current Alzheimer research 5(6):525 532. https://doi.org/10.2174/156720508786898451
53. Takasu N, Komiya I, Asawa T, Nagasawa Y, Yamada T (1991) Streptozocin and Alloxan induced H_2O_2 generation and DNA fragmentation in pancreatic islets: H_2O_2 as mediator for DNA frag mentation. Diabetes 40(9):1141 1145. https://doi.org/10.2337/diab.40.9.1141
54. Agrawal R, Tyagi E, Shukla R, Nath C (2009) A study of brain insulin receptors, AChE activity and oxidative stress in rat model of ICV STZ induced dementia. Neuropharmacology 56(4):779 787. https://doi.org/10.1016/j.neuropharm.2009.01.005
55. Rai S, Kamat PK, Nath C, Shukla R (2014) Glial activation and post synaptic neurotoxicity: the key events in Streptozotocin (ICV) induced memory impairment in rats. Pharmacology Biochemistry and Behavior 117:104 117. https://doi.org/10.1016/j.pbb.2013.11.035
56. Evin G, Zhu A, Holsinger RM, Masters CL, Li QX (2003) Proteolytic processing of the Alzheimer's disease amyloid precur sor protein in brain and platelets. Journal of neuroscience research 74(3):386 392. https://doi.org/10.1002/jnr.10745
57. Tong Y, Zhou W, Fung V, Christensen MA, Qing H, Sun X, Song W (2005) Oxidative stress potentiates BACE1 gene expression and Abeta generation. Journal of neural transmission (Vienna, Austria : 1996) 112(3):455 469. https://doi.org/10.1007/s00702 004 0255 3
58. Tamagno E, Guglielmotto M, Aragno M, Borghi R, Autelli R, Giliberto L, Muraca G, Danni O et al (2008) Oxidative stress acti vates a positive feedback between the gamma and beta secretase cleavages of the beta amyloid precursor protein. J Neurochem 104(3):683 695. https://doi.org/10.1111/j.1471 4159.2007.05072.x
59. Grünblatt E, Salkovic Petrisic M, Osmanovic J, Riederer P, Hoyer S (2007) Brain insulin system dysfunction in streptozotocin intracerebroventricularly treated rats generates hyperphosphorylated tau protein. J Neurochem 101(3):757 770. https://doi.org/10.1111/j.1471 4159.2006.04368 x
60. Savage MJ, Lin Y G, Ciallella JR, Flood DG, Scott RW (2002) Activation of c Jun N Terminal Kinase and p38 in an Alzheimer's disease model is associated with amyloid deposition. The Journal of Neuroscience 22(9):3376 3385. https://doi.org/10.1523/jneurosci.22 09 03376.2002
61. Liu SJ, Zhang AH, Li HL, Wang Q, Deng HM, Netzer WJ, Xu H, Wang JZ (2003) Overactivation of glycogen synthase kinase 3 by inhibition of phosphoinositol 3 kinase and protein kinase C leads to hyperphosphorylation of tau and impairment of spatial memory. J Neurochem 87(6):1333 1344. https://doi.org/10.1046/j.1471 4159.2003.02070.x
62. Beeler N, Riederer BM, Waeber G, Abderrahmani A (2009) Role of the JNK interacting protein 1/islet brain 1 in cell degeneration in Alzheimer disease and diabetes. Brain research bulletin 80(4 5): 274 281. https://doi.org/10.1016/j.brainresbull.2009.07.006
63. Yarza R, Vela S, Solas M, Ramirez MJ (2015) c Jun N terminal kinase (JNK) signaling as a therapeutic target for Alzheimer's dis ease. Front Pharmacol 6:321. https://doi.org/10.3389/fphar.2015.00321
64. Cross DA, Alessi DR, Cohen P, Andjelkovich M, Hemmings BA (1995) Inhibition of glycogen synthase kinase 3 by insulin

mediated by protein kinase B. Nature 378(6559):785 789. https://doi.org/10.1038/378785a0
65. Salkovic Petrisic M, Tribl F, Schmidt M, Hoyer S, Riederer P (2006) Alzheimer like changes in protein kinase B and glycogen synthase kinase 3 in rat frontal cortex and hippocampus after dam age to the insulin signalling pathway. J Neurochem 96(4):1005 1015. https://doi.org/10.1111/j.1471 4159.2005.03637 x
66. Pei JJ, Tanaka T, Tung YC, Braak E, Iqbal K, Grundke Iqbal I (1997) Distribution, levels, and activity of glycogen synthase kinase 3 in the Alzheimer disease brain. Journal of neuropathology and experimental neurology 56(1):70 78. https://doi.org/10.1097/00005072 199701000 00007
67. Pei JJ, Khatoon S, An WL, Nordlinder M, Tanaka T, Braak H, Tsujio I, Takeda M et al (2003) Role of protein kinase B in Alzheimer's neurofibrillary pathology. Acta Neuropathol 105(4): 381 392. https://doi.org/10.1007/s00401 002 0657 y
68. Preece P, Virley DJ, Costandi M, Coombes R, Moss SJ, Mudge AW, Jazin E, Cairns NJ (2003) Beta secretase (BACE) and GSK 3 mRNA levels in Alzheimer's disease. Brain research Molecular brain research 116(1 2):155 158. https://doi.org/10.1016/s0169 328x(03)00233 x
69. Rickle A, Bogdanovic N, Volkman I, Winblad B, Ravid R, Cowburn RF (2004) Akt activity in Alzheimer's disease and other neurodegenerative disorders. Neuroreport 15(6):955 959. https://doi.org/10.1097/00001756 200404290 00005
70. Vogelsberg Ragaglia V, Schuck T, Trojanowski JQ, Lee VM (2001) PP2A mRNA expression is quantitatively decreased in Alzheimer's disease hippocampus. Exp Neurol 168(2):402 412. https://doi.org/10.1006/exnr.2001.7630
71. Gong CX, Shaikh S, Wang JZ, Zaidi T, Grundke Iqbal I, Iqbal K (1995) Phosphatase activity toward abnormally phosphorylated tau: decrease in Alzheimer disease brain. J Neurochem 65(2):732 738. https://doi.org/10.1046/j.1471 4159.1995.65020732.x
72. Millward TA, Zolnierowicz S, Hemmings BA (1999) Regulation of protein kinase cascades by protein phosphatase 2A. Trends in bio chemical sciences 24(5):186 191. https://doi.org/10.1016/s0968 0004(99)01375 4
73. Phiel CJ, Wilson CA, Lee VM, Klein PS (2003) GSK 3alpha reg ulates production of Alzheimer's disease amyloid beta peptides. Nature 423(6938):435 439. https://doi.org/10.1038/nature01640
74. Kaytor MD, Orr HT (2002) The GSK3 beta signaling cascade and neurodegenerative disease. Current opinion in neurobiology 12(3): 275 278. https://doi.org/10.1016/s0959 4388(02)00320 3
75. Planel E, Yasutake K, Fujita SC, Ishiguro K (2001) Inhibition of protein phosphatase 2A overrides tau protein kinase I/glycogen synthase kinase 3 beta and cyclin dependent kinase 5 inhibition and results in tau hyperphosphorylation in the hippocampus of starved mouse. J Biol Chem 276(36):34298 34306. https://doi.org/10.1074/jbc.M102780200
76. Wang JZ, Grundke Iqbal I, Iqbal K (2007) Kinases and phospha tases and tau sites involved in Alzheimer neurofibrillary degenera tion. The European journal of neuroscience 25(1):59 68. https://doi.org/10.1111/j.1460 9568.2006.05226.x
77. Planel E, Tatebayashi Y, Miyasaka T, Liu L, Wang L, Herman M, Yu WH, Luchsinger JA et al (2007) Insulin dysfunction induces in vivo tau hyperphosphorylation through distinct mechanisms. J Neurosci 27(50):13635 13648. https://doi.org/10.1523/JNEUROSCI.3949 07.2007
78. Krstic D, Madhusudan A, Doehner J, Vogel P, Notter T, Imhof C, Manalastas A, Hilfiker M et al (2012) Systemic immune challenges trigger and drive Alzheimer like neuropathology in mice. Journal of Neuroinflammation 9(1):151. https://doi.org/10.1186/1742 2094 9 151
79. Zhu X, Raina AK, Rottkamp CA, Aliev G, Perry G, Boux H, Smith MA (2001) Activation and redistribution of c jun N terminal kinase/stress activated protein kinase in degenerating neurons in Alzheimer's disease. J Neurochem 76(2):435 441. https://doi.org/10.1046/j.1471 4159.2001.00046.x
80. Pei J J, Braak E, Braak H, Grundke Iqbal I, Iqbal K, Winblad B, Cowburn RF (2001) Localization of active forms of C jun kinase (JNK) and p38 kinase in Alzheimer's disease brains at different stages of neurofibrillary degeneration. Journal of Alzheimer's Disease 3:41 48. https://doi.org/10.3233/JAD 2001 3107
81. Yao M, Nguyen TV, Pike CJ (2005) Beta amyloid induced neuro nal apoptosis involves c Jun N terminal kinase dependent down regulation of Bcl w. J Neurosci 25(5):1149 1158. https://doi.org/10.1523/jneurosci.4736 04 2005
82. Quiroz Baez R, Rojas E, Arias C (2009) Oxidative stress promotes JNK dependent amyloidogenic processing of normally expressed human APP by differential modification of alpha , beta and gamma secretase expression. Neurochem Int 55(7):662 670. https://doi.org/10.1016/j.neuint.2009.06.012
83. Yoon SO, Park DJ, Ryu JC, Ozer HG, Tep C, Shin YJ, Lim TH, Pastorino L et al (2012) JNK3 perpetuates metabolic stress induced by Aβ peptides. Neuron 75(5):824 837. https://doi.org/10.1016/j.neuron.2012.06.024
84. Selznick LA, Holtzman DM, Han BH, Gökden M, Srinivasan AN, Johnson EM Jr, Roth KA (1999) In situ immunodetection of neu ronal caspase 3 activation in Alzheimer disease. Journal of neuro pathology and experimental neurology 58(9):1020 1026. https://doi.org/10.1097/00005072 199909000 00012
85. Rissman RA, Poon WW, Blurton Jones M, Oddo S, Torp R, Vitek MP, LaFerla FM, Rohn TT et al (2004) Caspase cleavage of tau is an early event in Alzheimer disease tangle pathology. J Clin Invest 114(1):121 130. https://doi.org/10.1172/JCI20640
86. Cotman CW, Poon WW, Rissman RA, Blurton Jones M (2005) The role of caspase cleavage of tau in Alzheimer disease neuropa thology. Journal of Neuropathology & Experimental Neurology 64(2):104 112. https://doi.org/10.1093/jnen/64.2.104
87. Gervais FG, Xu D, Robertson GS, Vaillancourt JP, Zhu Y, Huang J, LeBlanc A, Smith D et al (1999) Involvement of caspases in pro teolytic cleavage of Alzheimer's amyloid beta precursor protein and amyloidogenic A beta peptide formation. Cell 97(3):395 406. https://doi.org/10.1016/s0092 8674(00)80748 5
88. Mattson MP, Keller JN, Begley JG (1998) Evidence for synaptic apoptosis. Exp Neurol 153(1):35 48. https://doi.org/10.1006/exnr.1998.6863
89. Puro D, Agardh E (1984) Insulin mediated regulation of neuronal maturation. Science 225(4667):1170 1172. https://doi.org/10.1126/science.6089343
90. Van Der Heide LP, Kamal A, Artola A, Gispen WH, Ramakers GMJ (2005) Insulin modulates hippocampal activity dependent synaptic plasticity in a N methyl d aspartate receptor and phosphatidyl inositol 3 kinase dependent manner. Journal of Neurochemistry 94(4):1158 1166. https://doi.org/10.1111/j.1471 4159.2005.03269.x
91. Trinchese F, Liu S, Battaglia F, Walter S, Mathews P, Arancio O (2004) Progressive age related development of Alzheimer like pa thology in APP/PS1 mice. Annals of Neurology 55:801 814. https://doi.org/10.1002/ana.20101

Publisher's Note Springer Nature remains neutral with regard to jurisdic tional claims in published maps and institutional affiliations.

CHAPTER 6: GENERAL DISCUSSION AND FUTURE DIRECTIONS

1. Discussion

More than 50 million people worldwide, ~470,000 in Australia [1], suffer from Alzheimer's disease, a progressive neurodegenerative disorder, that accounts for 60-80% of dementia cases and leads to death within 3-9 years after diagnosis [2,3]. The pathophysiology of AD is complex and involves the interaction of several genetic and etiologic factors [4,5] . Current approved medications do not slow down or prevent the disease progression and thus are not effective on the long course [6]. Therefore, developing a disease-modifying therapy that can interfere with the underlying mechanisms of the disease and stop its progression is strongly needed. Novel therapeutic approaches have been developed that target Aβ disposition such as anti-Aβ antibodies, β-secretase inhibitors, and administration of Aβ degrading enzyme; neprilysin [6]. However, the incidence of severe adverse events [7,8] and failure to reduce Aβ levels in the brain [9,10] limited further clinical development of these agents.

The neurotrophin theory of AD has emerged as an alternative to the amyloid hypothesis, suggesting that imbalance in proneurotrophins and their receptors in the brain contributes significantly to the development of cognitive impairment during aging [11,12]. Besides, several pathological features in the brain have been identified as early events in the disease pathogenesis and may precede the appearance of plaques and tangles such as synaptic failure [13], neuroinflammation [14], oxidative stress [15] and aberrant insulin signalling in the brain [16,17]. Therefore, the aim of this thesis was to develop and characterize novel therapeutic approaches for treatment of AD. In this context, we used two different animal models of dementia: the APP/PS1 transgenic AD model that expresses human amyloid plaques to test the efficacy of p75 extracellular domain on plaque pathology. And the P301L a transgenic mouse model of FTD that develops Tau pathology with mitochondrial dysfunction and oxidative stress, but no amyloid plaques, to test the efficacy of a potent antioxidant compound; Edaravone on oxidative stress and subsequent Tau accumulation. In addition, we aimed to

develop a new animal model of AD that can replicate the features of sporadic AD in humans, and therefore would be used for testing the efficacy of aforementioned drug candidates and successful development of novel AD therapies.

Based on the aforementioned theories and hypothesis, we hypothesized that peripheral administration of the extracellular domain of p75 neurotrophin receptor could promote peripheral Aβ clearance and reverse cognitive deficits in AD mice through restoration of the abnormally low levels of the soluble ECD in the brain [18]. Results indicated that peripheral administration of p75ECD-Fc (a human recombinant fusion protein of p75 extracellular domain and Fc of IgG) improved the spatial reference memory and reduced the total plaque load in the brains of AD mice, besides, it improved the synaptic dysfunction. However, we failed to show any effects of the drug on Tau phosphorylation, inflammation, and neuron apoptosis. It is worth mentioning that previous studies reported that AAV-ECD-Fc brain or intramuscular injection reversed cognitive deficits in AD mice and displayed anti-inflammatory and antiapoptotic effects [19,18]. However, inherited variation between animals, number, age, and sex of mice used could influence the outcomes and results obtained.

To understand the mechanism of action of p75ECD-Fc in reducing brain Aβ, the pharmacokinetics of p75ECD-Fc, and its tissue distribution following peripheral administration were investigated. p75ECD-Fc was administered to Sprague Dawley rats either subcutaneously or intravenously at a single dose of 3mg/kg. Drug concentration in blood and tissue compartments was analysed using ELISA assay. The localization of the drug in tissues was investigated by double immunofluorescence staining. In addition, pharmacokinetic modelling was performed to show its distribution kinetics. Data showed that the drug exhibits long half-life of ~7 days following single IV injection with limited ability to cross the BBB. The drug was highly distributed in the liver and kidney where it was found colocalized in resident macrophages in these tissues. Pharmacokinetic modelling suggested a systemic two-

compartment model of p75ECD-Fc with linear elimination kinetics and further supported the tissue distribution findings. Therefore, we concluded that the drug main site of action is the periphery following systemic administration, which agrees with previous findings [19], even though small amounts were detected in CSF and the brain. Colocalization of the drug in resident macrophages may support our hypothesis that p75ECD-Fc could act through scavenging Aβ thus promoting its clearance in the periphery and subsequently reducing the levels in the brain. The data obtained from the p75ECD-Fc pharmacokinetic and pharmacologic study in AD mice supports the potential use of this novel protein in treatment of Alzheimer's disease.

Subsequently, we demonstrated that targeting oxidative stress could alleviate tau pathology and motor deficits in P301L mice. P301L mouse is an animal model of frontotemporal dementia linked with parkinsonism-17 (FTDP-17). It develops age-dependent hyperphosphorylated tau in different brain regions with behavioural and motor deficits similar to that observed in certain tauopathies in humans [20]. Administration of a novel Edaravone formulation orally in P301L mice at two different time points (ages) was able to improve cognitive and motor deficits in that model. Edaravone is a potent antioxidant that is approved for ischemic stroke and ALS [21,22]. Immunohistochemistry of the brain showed that EDR could reduce tau pathology in the hippocampus and amygdala of aged P301L mice, as well as reduction of oxidative stress and microgliosis was also found and confirmed by western blotting. These results suggest that targeting oxidative stress signalling represents a potential for treatment of neurodegeneration and agree with the hypothesis that oxidative stress contributes significantly to neurodegeneration [23]. We concluded that the effects of EDR on tau phosphorylation could be mediated mainly through its antioxidant effects, which could subsequently attenuate neuroinflammation and protect neurons against apoptosis and cell death. However, this study has few limitations. First, we could not confirm a direct effect of

EDR on GSK3β signalling pathway, a main kinase involved in abnormal Tau phosphorylation, although a previous study did show that EDR inhibited GSK signalling [24]. Western blotting results showed no significant difference in the levels of pS9-GSK3β, which is the inactivated form of GSK-3β, between control and age matched EDR treated mice, yet a trend towards increase was observed. When we performed two-way ANOVA between the two age groups, we found that EDR significantly increased pS9-GSK3β expression levels in aged, treated mice. Therefore, further investigation is required to establish the effects of EDR on GSK3β mediated tau phosphorylation signalling. Second, western blotting of synaptic proteins was not different between all groups including wild type mice and that of tau phosphorylation could not replicate the results from IHC. This might be caused by dilution effect of analysing whole brain homogenate instead of specific regions separately. However, when comparing between all groups, we found that EDR significantly reduced the expression levels of phosphorylated tau in the aged groups to levels close to the expression levels in the younger mice. One last limitation to this study is the limited number of animals used in the aged group and the use of single therapeutic dose of EDR in our experiments.

Finally, we have shown that intracerebroventricular injection of streptozotocin in young APP/PS1 mice could help to obtain an AD model that replicates most of the hallmarks of the disease and in a sequence similar to the disease progression in humans. APP/PS1 is the most common transgenic model used to study AD and novel treatments [25]. However, that model has many disadvantages, for example absence of some pathologic features such as Tau tangles and apoptosis [26,27]. In addition, that model could not represent the pathology of sporadic AD, because the plaque pathology starts to appear first followed by other events (i.e as inflammation, synaptic dysfunction) in a manner opposite to the normal course of the disease [28]. And finally, the most suitable age to use that model is 8-9 months old, when severe cognitive decline is obvious [29]. These drawbacks might explain the failure of most

therapeutic agents in clinical settings, while showing promising results in animal studies [30]. Data form the present study showed that STZ induced insulin resistance in the brain, that activates several upstream signalling pathways involved in tau phosphorylation and Aβ accumulation. STZ did facilitate the cognitive decline in APP/PS1 mice and boost the accumulation of Aβ pathology in a manner that correlates better with the synaptic and cognitive changes observed. Therefore, we believe that STZ APP/PS1 model is appropriate model to study the molecular mechanism of AD and to develop novel treatments, that could provide successful and hopeful results in clinical trials.

2. Conclusion

Overall, as summarized in **diagram 1**, this thesis has highlighted the possible benefits of the anti-stroke drug; Edaravone, and p75ECD-Fc for the therapy of AD and other tauopathies by targeting multiple key pathways including oxidative stress, Aβ, Tau phosphorylation and neuroinflammation. Combined use of these two agents could provide promising results in clinical trials. EDR as intravenous injection has proven to be clinically safe and effective for ALS and ischemic stroke. Findings from our animal studies further support its efficacy and suggest its potential benefits in prevention and treatment of other neurodegenerative disorders. Therefore, the oral drug administration is expected to be more convenient and safer than IV injection. On the other hand, the effect of p75ECD-Fc on brain Aβ, besides its reported efficacy and neuroprotective effects [18,31,32] support its possible use for treatment of AD. However, further thorough investigations are still required to confirm and approve the use of these potential disease-modifying therapies for treatment of AD and other forms of dementia. Finally, we have unveiled the advantages of STZ APP/PS1 animal model as a novel approach to study AD and new therapeutic approaches.

3. Future directions

While the results of p75ECD-Fc work in APP/PS1 mice showed that it was able to reduce Aβ in the brain, further investigations are required to understand the molecular mechanism of action. Pharmacokinetics and drug distribution analysis showed that the drug is colocalized in resident macrophages in peripheral organs and therefore, we assumed that it could scavenge peripheral Aβ and promote its efflux and clearance from the brain. However, we did not prove this assumption. Further experiments are required to detect Aβ peptides and p75ECD-Fc in peripheral organs and any possible colocalization or interaction between the two compounds to confirm this assumption. Besides, the levels of Aβ in blood should be analysed following acute and repeated administration to test the peripheral sink mechanism hypothesis following p75ECD-Fc treatment. Previous work by Wang et al. showed that the levels of Aβ in blood rises sharply following peritoneal injection of p75ECD-Fc, but then long-term peripheral expression of p75ECD following intramuscular AAV-ECD-Fc administration reduced Aβ levels both in periphery and the brain; likely a result of chronic clearance of Aβ in the brain and blood [19]. The same response was also observed in immunotherapies [33].

Furthermore, in our experiments, we showed that p75ECD-Fc reduced the levels of C-terminal fragments of APP and increased BACE1 phosphorylation at Ser498 site, that controls BACE trafficking and localization between TGN, cell surface and endosomes and subsequently its interaction with APP. However, we did not show how p75ECD-Fc affected BACE phosphorylation and activity. Previous study by Saadipour et al. revealed that $A\beta_{42}$ enhances the colocalization and phosphorylation of APP and BACE in cortical neurons expressing p75 neurotrophin receptor. They also found that treatment with p75ECD-Fc significantly reversed the toxic effects of $A\beta_{42}$ [34]. Although, our results on the effects of p75ECD-Fc on BACE1 phosphorylation at S498 seem to be in contrary and confusing, these findings could give us some insight on how p75ECD-Fc could act in APP/PS1 mice. Therefore, it is tempting to say that reduction of Aβ levels in the brain through p75ECD-Fc sequestering ability and peripheral

clearance [35] could indirectly reduce p75 neurotrophin signalling mediated by Aβ and consequently inhibit APP processing and interaction with BACE. However, to confirm this, we need to measure BACE enzymatic activity using fluorescence assay kit or homogeneous time-resolved fluorescence (HTRF) assay [36], instead of measuring the expression levels of total and phosphorylated form as BACE phosphorylation does not seem to significantly alter β-secretase activity [37]. Also, the effect of p75ECD-Fc on JNK and GSK3 signalling pathways needs further investigation. Finally, it is recommended to test different doses of p75ECD-Fc and comparing the efficacy of SC and IV route of administration with that of the intracranial injection of the protein.

While we showed that EDR oral formulation reduced cognitive deficits in P301L mice and displayed antioxidant and anti-inflammatory effects, further investigation is required to clearly elucidate the effect of EDR on GSK3 signalling pathways and synaptic plasticity using enzyme activity assay.

Furthermore, a combination therapy of p75ECD-Fc and EDR is worthwhile and could provide promising results in treatment of AD and tauopathies, as both agents could interfere with multiple underlying mechanisms of neurodegeneration. It is also suggested to investigate the effectiveness of this combined therapy on STZ APP/PS1 animal model. This model displayed the main hallmarks of AD such as neuroinflammation, apoptosis and oxidative stress together with Aβ and tau accumulation that in turn makes it appropriate and could provide true outcomes of the therapeutic value of these novel approaches and help pave the way for their clinical development. For example, STZ APP/PS1 model showed high oxidative stress signals and subsequent Aβ and Tau accumulation. Therefore, Edaravone would be an ideal candidate to be tested on that model and the obtained findings would clearly reveal if targeting oxidative stress pathway can stop AD pathologies accumulation and progression. Also, this would definitely provide clear answers about the effectiveness of these compounds in clinical settings and the

validity of that new model. Furthermore, studying the effects of p75ECD-Fc on STZ APP/PS1 model again would help us to understand the neurotrophin hypothesis in sporadic AD and if clearing Aβ from the brain could help alleviate other AD pathologies. Unfortunately, we were not able to test these drug candidates in STZ APP/PS1 model owing to the time frame of the whole study and the time required to initially establish the model and confirm the findings based on several biochemical and histological analysis. In conclusion, it is advised to investigate the efficacy of EDR and p75ECD-Fc in STZ APP/PS1 mice as a possible model of sporadic AD.

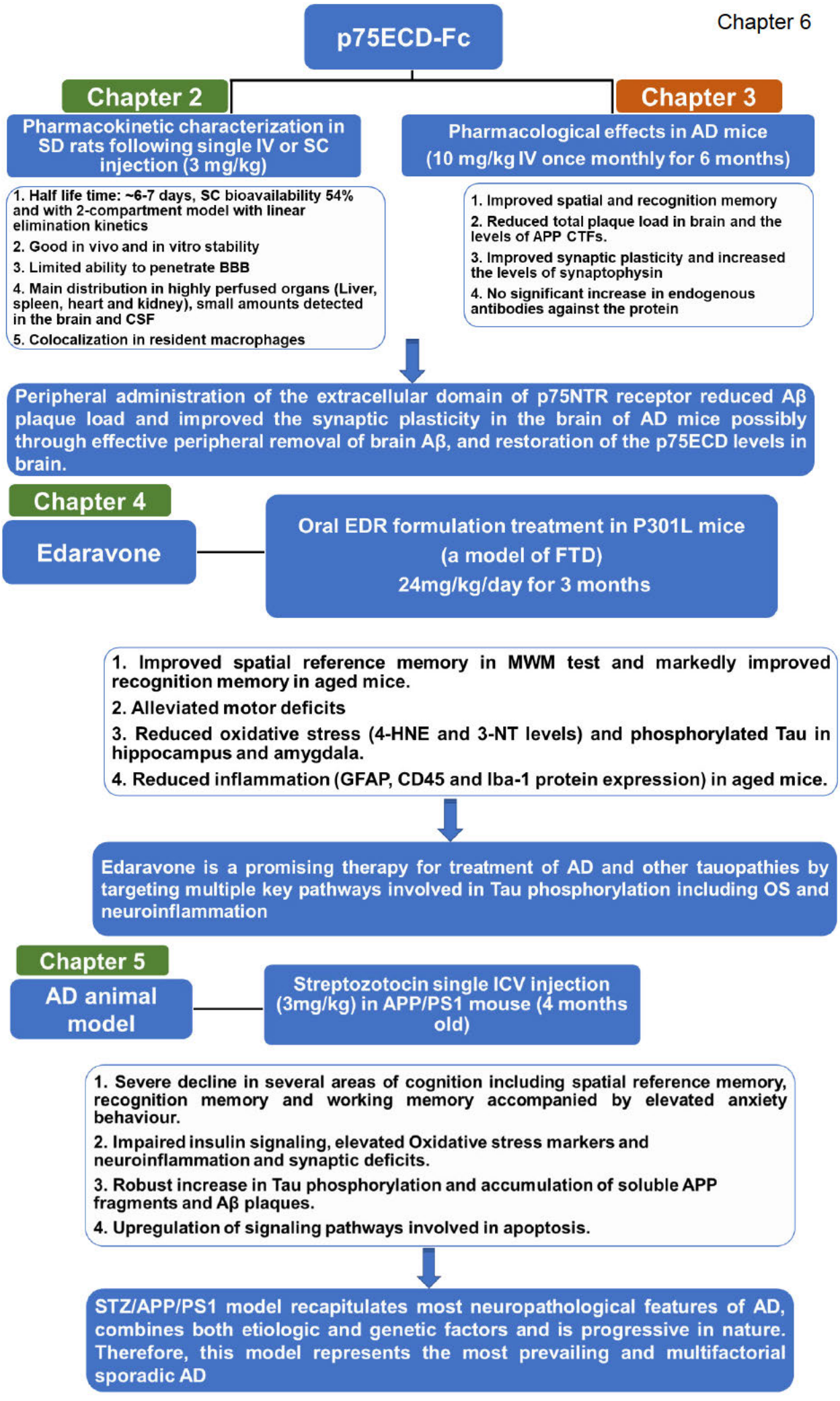


Diagram 1: A summary of the findings obtained throughout different chapters.

References:

1. DA 2020. Dementia statistics. Australia: DA.
2. 2020 Alzheimer's disease facts and figures. Alzheimer's & Dementia 16 (3):391-460. doi:https://doi.org/10.1002/alz.12068
3. Querfurth HW, LaFerla FM (2010) Alzheimer's Disease. New England Journal of Medicine 362 (4):329-344. doi:10.1056/NEJMra0909142
4. Zetterberg H, Mattsson-Carlgren N (2014) Understanding the cause of sporadic Alzheimer's disease. Expert review of neurotherapeutics 14:621-630. doi:10.1586/14737175.2014.915740
5. Blennow K, de Leon MJ, Zetterberg H (2006) Alzheimer's disease. Lancet 368 (9533):387-403. doi:10.1016/s0140-6736(06)69113-7
6. Yiannopoulou KG, Papageorgiou SG (2013) Current and future treatments for Alzheimer's disease. Ther Adv Neurol Disord 6 (1):19-33. doi:10.1177/1756285612461679
7. Carlson C, Estergard W, Oh J, Suhy J, Jack CR, Jr., Siemers E, Barakos J (2011) Prevalence of asymptomatic vasogenic edema in pretreatment Alzheimer’s disease study cohorts from phase 3 trials of semagacestat and solanezumab. Alzheimer's & Dementia: The Journal of the Alzheimer's Association 7 (4):396-401. doi:10.1016/j.jalz.2011.05.2353
8. Gilman S, Koller M, Black RS, Jenkins L, Griffith SG, Fox NC, Eisner L, Kirby L, Rovira MB, Forette F, Orgogozo J-M (2005) Clinical effects of Aβ immunization (AN1792) in patients with AD in an interrupted trial. Neurology 64 (9):1553-1562. doi:10.1212/01.wnl.0000159740.16984.3c
9. Walker JR, Pacoma R, Watson J, Ou W, Alves J, Mason DE, Peters EC, Urbina HD, Welzel G, Althage A, Liu B, Tuntland T, Jacobson LH, Harris JL, Schumacher AM (2013) Enhanced proteolytic clearance of plasma Aβ by peripherally administered neprilysin does not result in reduced levels of brain Aβ in mice. The Journal of neuroscience : the official journal of the Society for Neuroscience 33 (6):2457-2464. doi:10.1523/JNEUROSCI.3407-12.2013
10. Wang YJ (2014) Alzheimer disease: Lessons from immunotherapy for Alzheimer disease. Nat Rev Neurol 10 (4):188-189. doi:10.1038/nrneurol.2014.44
11. Cattaneo A, Calissano P (2012) Nerve Growth Factor and Alzheimer's Disease: New Facts for an Old Hypothesis. Molecular Neurobiology 46 (3):588-604. doi:10.1007/s12035-012-8310-9
12. Zhou X-F (2016) The imbalance of neurotrophic signalling: an alternate hypothesis for the pathogenesis and drug development of Alzheimer's disease. Proc Neurosci 1 (1):13-18
13. Arendt T (2009) Synaptic degeneration in Alzheimer's disease. Acta Neuropathol 118 (1):167-179. doi:10.1007/s00401-009-0536-x
14. Moore AH, O'Banion MK (2002) Neuroinflammation and anti-inflammatory therapy for Alzheimer's disease. Adv Drug Deliv Rev 54 (12):1627-1656. doi:10.1016/s0169-409x(02)00162-x
15. Quiroz-Baez R, Rojas E, Arias C (2009) Oxidative stress promotes JNK-dependent amyloidogenic processing of normally expressed human APP by differential modification of alpha-, beta- and gamma-secretase expression. Neurochemistry international 55 (7):662-670. doi:10.1016/j.neuint.2009.06.012
16. Bedse G, Di Domenico F, Serviddio G, Cassano T (2015) Aberrant insulin signaling in Alzheimer's disease: current knowledge. Frontiers in Neuroscience 9 (204). doi:10.3389/fnins.2015.00204
17. Frölich L, Blum-Degen D, Riederer P, Hoyer S (1999) A disturbance in the neuronal insulin receptor signal transduction in sporadic Alzheimer's disease. Annals of the New York Academy of Sciences 893:290-293. doi:10.1111/j.1749-6632.1999.tb07839.x
18. Yao XQ, Jiao SS, Saadipour K, Zeng F, Wang QH, Zhu C, Shen LL, Zeng GH, Liang CR, Wang J, Liu YH, Hou HY, Xu X, Su YP, Fan XT, Xiao HL, Lue LF, Zeng YQ, Giunta B, Zhong JH, Walker DG, Zhou HD, Tan J, Zhou XF, Wang YJ (2015) p75NTR ectodomain is a

physiological neuroprotective molecule against amyloid-beta toxicity in the brain of Alzheimer's disease. Molecular psychiatry 20 (11):1301-1310. doi:10.1038/mp.2015.49
19. Wang Q-H, Wang Y-R, Zhang T, Jiao S-S, Liu Y-H, Zeng F, Li J, Yao X-Q, Zhou H-D, Zhou X-F, Wang Y-J (2016) Intramuscular delivery of p75NTR ectodomain by an AAV vector attenuates cognitive deficits and Alzheimer's disease-like pathologies in APP/PS1 transgenic mice. Journal of Neurochemistry 138 (1):163-173. doi:10.1111/jnc.13616
20. Ramsden M, Kotilinek L, Forster C, Paulson J, McGowan E, SantaCruz K, Guimaraes A, Yue M, Lewis J, Carlson G, Hutton M, Ashe KH (2005) Age-dependent neurofibrillary tangle formation, neuron loss, and memory impairment in a mouse model of human tauopathy (P301L). J Neurosci 25 (46):10637-10647. doi:10.1523/jneurosci.3279-05.2005
21. Yoshida H, Yanai H, Namiki Y, Fukatsu-Sasaki K, Furutani N, Tada N (2006) Neuroprotective effects of edaravone: a novel free radical scavenger in cerebrovascular injury. CNS Drug Rev 12 (1):9-20. doi:10.1111/j.1527-3458.2006.00009.x
22. Feng S, Yang Q, Liu M, Li W, Yuan W, Zhang S, Wu B, Li J (2011) Edaravone for acute ischaemic stroke. Cochrane Database Syst Rev (12):Cd007230. doi:10.1002/14651858.CD007230.pub2
23. Stadtman ER (2006) Protein oxidation and aging. Free Radic Res 40 (12):1250-1258. doi:10.1080/10715760600918142
24. Jiao S-S, Yao X-Q, Liu Y-H, Wang Q-H, Zeng F, Lu J-J, Liu J, Zhu C, Shen L-L, Liu C-H, Wang Y-R, Zeng G-H, Parikh A, Chen J, Liang C-R, Xiang Y, Bu X-L, Deng J, Li J, Xu J, Zeng Y-Q, Xu X, Xu H-W, Zhong J-H, Zhou H-D, Zhou X-F, Wang Y-J (2015) Edaravone alleviates Alzheimer's disease-type pathologies and cognitive deficits. Proceedings of the National Academy of Sciences of the United States of America 112 (16):5225-5230. doi:10.1073/pnas.1422998112
25. Götz J, Streffer JR, David D, Schild A, Hoerndli F, Pennanen L, Kurosinski P, Chen F (2004) Transgenic animal models of Alzheimer's disease and related disorders: histopathology, behavior and therapy. Mol Psychiatry 9 (7):664-683. doi:10.1038/sj.mp.4001508
26. Metaxas A, Thygesen C, Kempf SJ, Anzalone M, Vaitheeswaran R, Petersen S, Landau AM, Audrain H, Teeling JL, Darvesh S, Brooks DJ, Larsen MR, Finsen B (2018) Tauopathy in the $APP_{swe}/PS1_{\Delta E9}$ mouse model of familial Alzheimer’s disease. bioRxiv:405647. doi:10.1101/405647
27. Götz J, Deters N, Doldissen A, Bokhari L, Ke Y, Wiesner A, Schonrock N, Ittner LM (2007) A decade of tau transgenic animal models and beyond. Brain Pathol 17 (1):91-103. doi:10.1111/j.1750-3639.2007.00051.x
28. Trinchese F, Liu S, Battaglia F, Walter S, Mathews PM, Arancio O (2004) Progressive age-related development of Alzheimer-like pathology in APP/PS1 mice. Ann Neurol 55 (6):801-814. doi:10.1002/ana.20101
29. Radde R, Bolmont T, Kaeser SA, Coomaraswamy J, Lindau D, Stoltze L, Calhoun ME, Jäggi F, Wolburg H, Gengler S, Haass C, Ghetti B, Czech C, Hölscher C, Mathews PM, Jucker M (2006) Abeta42-driven cerebral amyloidosis in transgenic mice reveals early and robust pathology. EMBO reports 7 (9):940-946. doi:10.1038/sj.embor.7400784
30. Zahs KR, Ashe KH (2010) 'Too much good news' - are Alzheimer mouse models trying to tell us how to prevent, not cure, Alzheimer's disease? Trends Neurosci 33 (8):381-389. doi:10.1016/j.tins.2010.05.004
31. Fang J, Wei Z, Zheng D, Ying T, Hong H, Hu D, Lin Y, Jiang X, Wu L, Lan T, Yang Z, Zhou X, Chen L (2020) Recombinant Extracellular Domain (p75ECD) of the Neurotrophin Receptor p75 Attenuates Myocardial Ischemia–Reperfusion Injury by Inhibiting the p‐JNK/Caspase‐3 Signaling Pathway in Rat Microvascular Pericytes. Journal of the American Heart Association 9 (13):e016047. doi:doi:10.1161/JAHA.119.016047

32. Lin L, Zhou X-F, Bobrovskaya L (2021) Blockage of p75NTR ameliorates depressive-like behaviours of mice under chronic unpredictable mild stress. Behavioural Brain Research 396:112905. doi:https://doi.org/10.1016/j.bbr.2020.112905
33. DeMattos RB, Bales KR, Cummins DJ, Paul SM, Holtzman DM (2002) Brain to Plasma Amyloid-β Efflux: a Measure of Brain Amyloid Burden in a Mouse Model of Alzheimer's Disease. Science 295 (5563):2264-2267. doi:10.1126/science.1067568
34. Saadipour K, Mañucat-Tan NB, Lim Y, Keating DJ, Smith KS, Zhong JH, Liao H, Bobrovskaya L, Wang YJ, Chao MV, Zhou XF (2018) p75 neurotrophin receptor interacts with and promotes BACE1 localization in endosomes aggravating amyloidogenesis. J Neurochem 144 (3):302-317. doi:10.1111/jnc.14206
35. Wang YJ, Wang X, Lu JJ, Li QX, Gao CY, Liu XH, Sun Y, Yang M, Lim Y, Evin G, Zhong JH, Masters C, Zhou XF (2011) p75NTR regulates Abeta deposition by increasing Abeta production but inhibiting Abeta aggregation with its extracellular domain. The Journal of neuroscience : the official journal of the Society for Neuroscience 31 (6):2292-2304. doi:10.1523/JNEUROSCI.2733-10.2011
36. Kennedy ME, Wang W, Song L, Lee J, Zhang L, Wong G, Wang L, Parker E (2003) Measuring human beta-secretase (BACE1) activity using homogeneous time-resolved fluorescence. Anal Biochem 319 (1):49-55. doi:10.1016/s0003-2697(03)00253-7
37. Cole SL, Vassar R (2007) The Alzheimer's disease β-secretase enzyme, BACE1. Molecular Neurodegeneration 2 (1):22. doi:10.1186/1750-1326-2-22

Appendices

Publications arising from this thesis.

Kelliny S, Lam HY, Parikh A, Wang Y, Bobrovskaya L, Upton R, et al. Preclinical Study of the Pharmacokinetics of p75ECD-Fc, a Novel Human Recombinant Protein for Treatment of Alzheimer's Disease, in Sprague Dawley Rats. Current Drug Metabolism. 2020; 21:1-10.

Kelliny S, Bobrovskaya L, Zhou X-F, Upton R. Pharmacokinetic Modelling of Human Recombinant Protein, p75ECD-Fc: A Novel Therapeutic Approach for Treatment of Alzheimer's Disease, in Serum and Tissue of Sprague Dawley Rats. European Journal of Drug Metabolism and Pharmacokinetics. 2021;46(2):235-48.

Kelliny S, Lin L, Deng I, Xiong J, Zhou F, Al-Hawwas M, et al. A New Approach to Model Sporadic Alzheimer's Disease by Intracerebroventricular Streptozotocin Injection in APP/PS1 Mice. Mol Neurobiol. 2021.

Kelliny S, Xiong J, Bobrovskaya L, Zhou X-F. A Novel Oral Edaravone Formulation Partially Alleviates Tau Pathology and Motor Deficits in an Animal Model of Frontotemporal Dementia. (To be submitted).

Other publications

Lin LY, Kelliny S, Liu LC, Al-Hawwas M, Zhou XF, Bobrovskaya L. Peripheral ProBDNF Delivered by an AAV Vector to the Muscle Triggers Depression-Like Behaviours in Mice. Neurotoxicity Research. 2020;38(3):626-39.

Xiong J, Deng I, Kelliny S, Lin LY, Bobrovskaya L and Zhou X-F. Long term high fat diet induces metabolic disorders and aggravates behavioral disorders and cognitive deficits in MAPT P301L transgenic mice (submitted to Metabolic Brain Disease).

Conference Abstracts

Investigating the Effects of Edaravone in an Animal Model of Frontotemporal Dementia. Sally Kelliny, Ankit Parikh, Larisa Bobrovskaya, Xin Fu Zhou

Awards and Scholarships

Commonwealth Research Training Program (RTP) Domestic Fee Offset and Domestic Stipend 2017

Egyptian Ministry of Higher Education 2016